JSCSEN 85(12)1507–1673(2020)

ISSN 1820-7421(Online)

Journal of the Serbian Chemical Society

Electronic version

VOLUME 85

No 12

BELGRADE 2020

Available on line at

www.shd.org.rs/JSCS/

The full search of JSCS is available through

DOAJ DIRECTORY OF OPEN ACCESS JOURNALS

www.doaj.org

The **Journal of the Serbian Chemical Society** (formerly Glasnik Hemijskog društva Beograd), one volume (12 issues) per year, publishes articles from the fields of chemistry. The **Journal** is financially supported by the **Ministry of Education, Science and Technological Development of the Republic of Serbia.**

Articles published in the **Journal** are indexed in **Clarivate Analytics products: Science Citation Index-Expanded™** – accessed *via* **Web of Science®** and **Journal Citation Reports®**.

Impact Factor announced 2020: **1.097; 5-year Impact Factor**: **1.023**.

Articles appearing in the **Journal** are also abstracted by: **Scopus, Chemical Abstracts Plus (CAplus℠), Directory of Open Access Journals, Referativnii Zhurnal (VINITI), RSC Analytical Abstracts, EuroPub, Pro Quest** and **Asian Digital Library.**

Publisher:	**Serbian Chemical Society**, Karnegijeva 4/III, P. O. Box 36, 1120 Belgrade 35, Serbia tel./fax: +381–11–3370–467, E-mails: **Society** – shd@shd.org.rs; **Journal** – jscs@shd.org.rs Home Pages: **Society** – http://www.shd.org.rs/, **Journal** – http://www.shd.org.rs/JSCS/
Internet Service:	Contents, Abstracts and full papers (from Vol 64, No. 1, 1999) are available in the electronic form at the Web Site of the **Journal** (http://www.shd.org.rs/JSCS/).
Former Editors:	**Nikola A. Pušin** (1930–1947), **Aleksandar M. Leko** (1948–1954), **Panta S. Tutundžić** (1955**–**1961), **Miloš K. Mladenović** (1962–1964), **Đorđe M. Dimitrijević** (1965–1969), **Aleksandar R. Despić** (1969–1975), **Slobodan V. Ribnikar** (1975–1985), **Dragutin M. Dražić** (1986–2006).
Editor-in-Chief:	BRANISLAV Ž. **NIKOLIĆ**, Serbian Chemical Society (E-mail: jscs-ed@shd.org.rs)
Deputy Editor:	DUŠAN **SLADIĆ**, Faculty of Chemistry, University of Belgrade
Sub editors:	
Organic Chemistry	DEJAN **OPSENICA**, Institute of Chemistry, Technology and Metallurgy, University of Belgrade JÁNOS **CSANÁDI**, Faculty of Science, University of Novi Sad
Biochemistry and Biotechnology	OLGICA **NEDIĆ**, INEP – Institute for the Application of Nuclear Energy, University of Belgrade
Inorganic Chemistry	MILOŠ **ĐURAN**, Serbian Chemical Society
Theoretical Chemistry	IVAN **JURANIĆ**, Serbian Chemical Society
Physical Chemistry	LJILJANA **DAMJANOVIĆ-VASILIĆ**, Faculty of Physical Chemistry, University of Belgrade
Electrochemistry	SNEŽANA **GOJKOVIĆ**, Faculty of Technology and Metallurgy, University of Belgrade
Analytical Chemistry	SLAVICA **RAŽIĆ**, Faculty of Pharmacy, University of Belgrade
Polymers	BRANKO **DUNJIĆ**, Faculty of Technology and Metallurgy, University of Belgrade
Thermodynamics	MIRJANA **KIJEVČANIN**, Faculty of Technology and Metallurgy, University of Belgrade
Chemical Engineering	TATJANA **KALUĐEROVIĆ RADOIČIĆ**, Faculty of Technology and Metallurgy, University of Belgrade
Materials	RADA **PETROVIĆ**, Faculty of Technology and Metallurgy, University of Belgrade
Metallic Materials and Metallurgy	NENAD **RADOVIĆ**, Faculty of Technology and Metallurgy, University of Belgrade
Environmental and Geochemistry	VESNA **ANTIĆ**, Faculty of Agriculture, University of Belgrade
History of and Education in Chemistry	DRAGICA **TRIVIĆ**, Faculty of Chemistry, University of Belgrade
English Language Editors:	LYNNE **KATSIKAS**, Serbian Chemical Society VLATKA **VAJS**, Serbian Chemical Society JASMINA **NIKOLIĆ**, Faculty of Technology and Metallurgy, University of Belgrade
Technical Editors:	VLADIMIR **PANIĆ**, ALEKSANDAR **DEKANSKI**, VUK **FILIPOVIĆ**, Institute of Chemistry, Technology and Metallurgy, University of Belgrade
Journal Manager & Web Master:	ALEKSANDAR **DEKANSKI,** Institute of Chemistry, Technology and Metallurgy, University of Belgrade
Office:	VERA **ĆUŠIĆ**, Serbian Chemical Society

Editorial Board

From abroad: **R. Adžić**, Brookhaven National Laboratory (USA); **A. Casini**, University of Groningen (The Netherlands); **G. Cobb**, Baylor University (USA); **D. Douglas**, University of British Columbia (Canada); **G. Inzelt**, Etvos Lorand University (Hungary); **N. Katsaros**, NCSR "Demokritos", Institute of Physical Chemistry (Greece); **J. Kenny**, University of Perugia (Italy); **Ya. I. Korenman**, Voronezh Academy of Technology (Russian Federation); **M. D. Lechner**, University of Osnabrueck (Germany); **S. Macura**, Mayo Clinic (USA); **M. Spiteller**, INFU, Technical University Dortmund (Germany); **M. Stratakis**, University of Crete (Grecce); **M. Swart**, University de Girona (Cataluna, Spain); **G. Vunjak-Novaković**, Columbia University (USA); **P. Worsfold**, University of Plymouth (UK); **J. Zagal**, Universidad de Santiago de Chile (Chile).

From Serbia: **B. Abramović**, **V. Antić, V. Beškoski**, **J. Csanadi**, **Lj. Damjanović-Vasilić**, **A. Dekanski**, **V. Dondur**, **B. Dunjić**, **M. Đuran, S. Gojković**, **I. Gutman**, **B. Jovančićević**, **I. Juranić**, **L. Katsikas**, **M. Kijevčanin**, **V. Leovac**, **S. Milonjić**, **V.B. Mišković-Stanković, O. Nedić**, **B. Nikolić**, **J. Nikolić, D. Opsenica**, **V. Panić**, **M. Petkovska**, **R. Petrović**, **I. Popović**, **B. Radak**, T. **Kaluđerović Radiočić, N. Radović**, **S. Ražić**, **D. Sladić**, **S. Sovilj**, **S. Šerbanović**, **B. Šolaja**, **Ž. Tešić**, **D. Trivić, V. Vajs**.

Subscription: The annual subscription rate is **150.00 €** including postage (surface mail) and handling. For Society members from abroad rate is **50.00 €**. For the proforma invoice with the instruction for bank payment contact the Society Office (E-mail: shd@shd.org.rs) or see JSCS Web Site: http://www.shd.org.rs/JSCS/, option Subscription.

Godišnja pretplata: Za članove SHD: **2.500,00 RSD**, za penzionere i studente: **1000,00 RSD**, a za ostale: **3.500,00 RSD**:za organizacije i ustanove: **16.000,00 RSD**. Uplate se vrše na tekući račun Društva: **205-13815-62**, poziv na broj **320**, sa naznakom "pretplata za JSCS".

Nota: Radovi čiji su svi autori članovi SHD prioritetno se publikuju.

Odlukom Odbora za hemiju Republičkog fonda za nauku Srbije, br. 66788/1 od 22.11.1990. godine, koja je kasnije potvrđena odlukom Saveta Fonda, časopis je uvršten u kategoriju međunarodnih časopisa (**M-23**). Takođe, aktom Ministarstva za nauku i tehnologiju Republike Srbije, 413-00-247/2000-01 od 15.06.2000. godine, ovaj časopis je proglašen za publikaciju od posebnog interesa za nauku. **Impact Factor** časopisa objavljen 2020. godine iznosi **1,097**, a petogodišnji **Impact Factor 1,023**.

INSTRUCTIONS FOR AUTHORS (2021)

GENERAL

The *Journal of the Serbian Chemical Society* (the *Journal* in further text) is an international journal publishing papers from all fields of chemistry and related disciplines. Twelve issues are published annually. The Editorial Board expects the editors, reviewers, and authors to respect the well-known standard of professional ethics.

Types of Contributions

Original scientific papers	(up to 15 typewritten pages, including Figures, Tables and References) report original research which must not have been previously published.
Short communications	(up to 8 pages) report unpublished preliminary results of sufficient importance to merit rapid publication.
Notes	(up to 5 pages) report unpublished results of short, but complete, original research
Authors' reviews	(up to 40 pages) present an overview of the author's current research with comparison to data of other scientists working in the field
Reviews[a]	(up to 40 pages) present a concise and critical survey of a specific research area. Generally, these are prepared at the invitation of the Editor
Surveys	(about 25 pages) communicate a short review of a specific research area.
Book and Web site reviews	(1 - 2 pages)
Extended abstracts	(about 4 pages) of Lectures given at meetings of the Serbian Chemical Society Divisions
Letters to the Editor	report miscellaneous topics directed directly to the Editor

[a]Generally, Authors' reviews, Reviews and Surveys are prepared at the invitation of the Editor.

Submission of manuscripts

Manuscripts should be submitted using the **OnLine Submission Form**, available on the JSCS Web Site (**http://www.shd-pub.org.rs/index.php/JSCS**). The manuscript must be uploaded as a Word.doc or .rtf file, with tables and figures (including the corresponding captions – above Tables and below Figures), placed within the text to follow the paragraph in which they were mentioned for the first time.

Please note that **Full Names (**First Name, Last Name), **Full Affiliation** and **Country** (from drop down menu) of **ALL OF AUTHORS** (written in accordance with English spelling rules - the first letter capitalized) must be entered in the manuscript Submission Form (Step 3). Manuscript Title, authors' names and affiliations, as well as the Abstract, **WILL APPEAR** in the article listing, as well as in **BIBLIOGRAPHIC DATABASES (WoS, SCOPUS...)**, in the form and in the order entered in the author details

Graphical abstract

Graphical abstract is a one-image file containing the main depiction of the authors work and/or conclusion and must be supplied along with the manuscript. It must enable readers to quickly gain the main message of the paper and to encourage browsing, help readers identify which papers are most relevant to their research interests. Authors must provide an image that clearly represents the research described in the paper. The most relevant figure from the work, which summarizes the content, can also be submitted. The image should be submitted as a separate file in **Online Submission Form - Step 2**.

Specifications: The graphical abstract should have a clear start and end, reading from top to bottom or left to right. Please omit unnecessary distractions as much as possible.

- **Image size:** minimum of 500×800 pixels (W×H) and a minimum resolution of 300 dpi. If a larger image is sent, then please use the same ratio: 16 wide × 9 high. Please note that your image will be scaled proportionally to fit in the available window in TOC; a 150x240 pixel rectangle. Please be sure that the quality of an image cannot be increased by changing the resolution from lower to higher, but only by rescanning or exporting the image with a higher resolution, which can be set in usual "settings" option.
- **Font:** Please use Calibri and Symbol font with a large enough font size, so it is readable even from the image of a smaller size (150 × 240 px) in TOC.
- **File type:** JPG and PNG only.

No additional text, outline or synopsis should be included. Please do not use white space or any heading within the image.

Cover Letter

Manuscripts must be accompanied by a cover letter (strictly uploaded in **Online Submission Step 2**) in which the type of the submitted manuscript and a warranty as given below are given. The Author(s) has(have) to warranty that the manuscript submitted to the *Journal* for review is original, has been written by the stated author(s) and has not been published elsewhere; is currently not being considered for publication by any other journal and will not be submitted for such a review while under review by the *Journal*; the manuscript contains no libellous or other unlawful statements and does not contain any materials that violate any personal or proprietary rights of any other person or entity. All manuscripts will be acknowledged on receipt (by e-mail).

Illustrations

Illustrations (Figs, schemes, photos…) in TIF or EPS format (JPG format is acceptable for colour and greyscale photos, only), must be additionally uploaded (Online Submission Step 2) as a separate file or one archived (.zip, .rar or .arj) file. Figures and/or Schemes should be prepared according to the **Artwork Instructions -** http://www.shd.org.rs/JSCS/jscs-pdf/Artwork_Instructions.pdf!

For any difficulties and questions related to **OnLine Submission Form -** https://www.shd-pub.org.rs/index.php/JSCS/submission/wizard, please refer to **User Guide -** https://openjournal-systems.com/ojs-3-user-guide/ , Chapter **Submitting an Article -** https://openjournalsystems.com/ojs-3-user-guide/submitting-an-article/. If difficulties still persist, please contact JSCS Editorial Office at **JSCS@shd.org.rs**

A manuscript not prepared according to these instructions will be returned for resubmission without being assigned a reference number.

Conflict-of-Interest Statement*: Public trust in the peer review process and the credibility of published articles depend in part on how well a conflict of interest is handled during writing, peer review, and editorial decision making. A conflict of interest exists when an author (or the author's institution), reviewer, or editor has financial or personal relationships that inappropriately influence (bias) his or her actions (such relationships are also known as dual commitments, competing interests, or competing loyalties). These relationships vary from those with negligible potential to those with great potential to influence judgment, and not all relationships represent true conflict of interest. The potential for a conflict of interest can exist whether or not an individual believes that the relationship affects his or her scientific judgment. Financial relationships (such as employment, consultancies, stock ownership, honoraria, paid expert testimony) are the most easily identifiable conflicts of interest and the most likely to undermine the credibility of the journal, the authors, and of science itself. However, conflicts can occur for other reasons, such as personal relationships, academic competition, and intellectual passion.

Informed Consent Statement*: Patients have a right to privacy that should not be infringed without informed consent. Identifying information, including patients' names, initials, or hospital numbers, should not be published in written descriptions, photographs, and pedigrees unless the information is essential for scientific purposes and the patient (or parent or guardian) gives written informed consent for publication. Informed consent for this purpose requires that a patient who is identifiable be shown the manuscript to be published. Authors should identify Individuals who provide writing assistance and disclose the funding source for this assistance. Identifying details should be omitted if they are not essential. Complete anonymity is difficult to achieve, however, and informed consent should be obtained if there is any doubt. For example, masking the eye region in photographs of patients is inadequate protection of anonymity. If identifying characteristics are altered to protect anonymity, such as in genetic pedigrees, authors should provide assurance that alterations do not distort scientific meaning and editors should so note. The requirement for informed consent should be included in the journal's instructions for authors. When informed consent has been obtained it should be indicated in the published article.

Human and Animal Rights Statement* When reporting experiments on human subjects, authors should indicate whether the procedures followed were in accordance with the ethical standards of the responsible committee on human experimentation (institutional and national) and with the Helsinki Declaration of 1975, as revised in 2000 (5). If doubt exists whether the research was conducted in accordance with the Helsinki Declaration, the authors must explain the rationale for their approach, and demonstrate that the institutional review body explicitly approved the doubtful aspects of the study. When reporting experiments on animals, authors should be asked to indicate whether the institutional and national guide for the care and use of laboratory animals was followed.

---

*International Committee of Medical Journal Editors ("Uniform Requirements for Manuscripts Submitted to Biomedical Journals"), February 2006

PROCEDURE

All contributions will be peer reviewed and only those deemed worthy and suitable will be accepted for publication. The Editor has the final decision. To facilitate the reviewing process, authors are encouraged to suggest up to three persons competent to review their manuscript. Such suggestions will be taken into consideration but not always accepted. If authors would prefer a specific person not be a reviewer, this should be announced. The Cover Letter must be accompanied by these suggestions. Manuscripts requiring revision should be returned according to the requirement of the Editor, within 60 days upon reception of the reviewing comments by e-mail.

The *Journal* maintains its policy and takes the liberty of correcting the English as well as false content of manuscripts **provisionally accepted** for publication in the first stage of reviewing process. In this second stage of manuscript preparation by JSCS Editorial Office, the author(s) may be required to supply some **additional clarifications and corrections**. This procedure will be executed during copyediting actions, with a demand to author(s) to perform corrections of unclear parts before the manuscript would be published OnLine as **finally accepted manuscript (OLF Section of the JSCS website)**. Please note that the manuscript can receive the status of **final rejection** if the author's corrections would not be satisfactory.

When finally accepted manuscript is ready for printing, the corresponding author will receive a request for proof reading, which should be performed within 2 days. Failure to do so will be taken as the authors agree with any alteration which may have occurred during the preparation of the manuscript for printing.

Accepted manuscripts of active members of the Serbian Chemical Society (all authors) have publishing priority.

MANUSCRIPT PRESENTATION

Manuscripts should be typed in English (either standard British or American English, but consistent throughout) with 1.5 spacing (12 points Times New Roman; Greek letters in the character font Symbol) in A4 format leaving 2.5 cm for margins. For Regional specific, non-standard characters that may appear in the text, save documents with Embed fonts Word option: *Save as -> (Tools) -> Save Options… -> Embed fonts in the text.*

The authors are requested to seek the assistance of competent English language expert, if necessary, to ensure their English is of a reasonable standard. The Serbian Chemical Society can provide this service in advance of submission of the manuscript. If this service is required, please contact the office of the Society by e-mail (jscs-info@shd.org.rs).

Tables, figures and/or schemes must be embedded in the main text of the manuscript and should follow the paragraph in which they are mentioned for the first time. **Tables** must be prepared with the aid of the **WORD table function**, without vertical lines. The minimum size of the font in the tables should be **10 pt**. Table columns must not be formatted using multiple spaces. Table rows must not be formatted using any returns (enter key; ↵ key) and are **limited to 12 cm width**. Tables should not be incorporated as graphical objects. **Footnotes to Tables** should follow them and are to be indicated consequently (in a single line) in superscript letters and separated by semi-column.

Table caption must be placed above corresponding Table, while **Captions of the Illustrations** (Figs. Schemes...) must follow the corresponding item. **The captions, either for Tables or Illustrations**, should make the items comprehensible without reading of the main text (but clearly referenced in), must follow numerical order (Roman for Tables, Arabic for Illustrations), and should not be provided on separate sheets or as separate files.

High resolution Illustrations (named as Fig. 1, Fig. 2… and/or Scheme 1, Scheme 2…) in **TIF or EPS format** (JPG format is acceptable for photos, only) **must be additionally uploaded as a separate files or one archived (.zip, .rar) file.**

Illustrations should be prepared according to the ARTWORK INSTRUCTIONS - http://www.shd.org.rs/JSCS/jscs-pdf/Artwork_Instructions.pdf. **!**

All pages of the manuscript must be numbered continuously.

DESIGNATION OF PHYSICAL QUANTITIES AND UNITS

IUPAC recommendations for the naming of compounds should be followed. SI units, or other permissible units, should be employed. The designation of physical quantities must be in italic throughout the text (including figures, tables and equations), whereas the units and indexes (except for indexes having the meaning of physical quantities) are in upright letters. They should be in Times New Roman font. In graphs and tables, a slash should be used to separate the designation of a physical quantity from the unit

(example: p / kPa, j / mA cm^{-2}, t / °C, T_0 / K, τ / h, ln (j / mA cm^{-2})…). Designations such as: p (kPa), t [min]…, are not acceptable. However, if the full name of a physical quantity is unavoidable, it should be given in upright letters and separated from the unit by a comma (example: Pressure, kPa; Temperature, K; Current density, mA cm^{-2}…). Please do not use the axes of graphs for additional explanations; these should be mentioned in the figure captions and/or the manuscript (example: "pressure at the inlet of the system, kPa" should be avoided). The axis name should follow the direction of the axis (the name of y-axis should be rotated by 90°). Top and right axes should be avoided in diagrams, unless they are absolutely necessary.

Latin words, as well as the names of species, should be in *italic*, as for example: *i.e.*, *e.g.*, *in vivo*, *ibid*, *Calendula officinalis* L., *etc*. The branching of organic compound should also be indicated in *italic*, for example, *n*-butanol, *tert*-butanol, *etc*.

Decimal numbers must have decimal points and not commas in the text (except in the Serbian abstract), tables and axis labels in graphical presentations of results. Thousands are separated, if at all, by a comma and not a point.

Mathematical and chemical equations should be given in separate lines and must be numbered, Arabic numbers, consecutively in parenthesis at the end of the line. All equations should be embedded in the text Complex equations (fractions, integrals, matrix…) should be prepared with the aid of the **Microsoft Equation 3.0** (or higher) or **MathType** (Do not use them to create simple equations and labels). **Using the Insert -> Equation option, integrated in MS Office 2010 and MS Office 2013, as well as insertion of equation objects within paragraph text IS NOT ALLOWED.**

ARTICLE STRUCTURE

- TITLE PAGE;
- MAIN TEXT – including Tables and Illustrations with corresponding captions;
- SUPPLEMENTARY MATERIAL (optional**)**

Title page

- **Title** in bold letters, should be clear and concise, preferably 12 words or less. The use of non-standard abbreviations, symbols and formulae is discouraged.
- AUTHORS' NAMES in capital letters with the full first name, initials of further names separated by a space and surname. Commas should separate the author's names except for the last two names when 'and' is to be used. In multi-affiliation manuscripts, the author's affiliation should be indicated by an Arabic number placed in superscript after the name and before the affiliation. Use * to denote the corresponding author(s).
- *Affiliations* should be written in italic. The e-mail address of the corresponding author should be given after the affiliation(s).
- *Abstract:* A one-paragraph abstract written of 150 – 200 words in an impersonal form indicating the aims of the work, the main results and conclusions should be given and clearly set off from the text. Domestic authors should also submit, on a separate page, an Abstract - Izvod, the author's name(s) and affiliation(s) in Serbian (Cyrillic letters). (Домаћи аутори морају доставити Извод (укључујући имена аутора и афилијацију) на српском језику, исписане ћирилицом, иза Захвалнице, а пре списка референци.) For authors outside Serbia, the Editorial Board will provide a Serbian translation of their English abstract.
- *Keywords:* Up to 6 keywords should be given. Do not use words appearing in the manuscript title
- RUNNING TITLE: A one line (maximum five words) short title in capital letters should be provided.

Main text – should have the form:

- **INTRODUCTION,**
- **EXPERIMENTAL (RESULTS AND DISCUSSION),**
- **RESULTS AND DISCUSSION (EXPERIMENTAL),**
- **CONCLUSIONS,**
- **NOMENCLATURE (optional) and**
- ***Acknowledgements*: If any.**
- REFERENCES (Citation of recent papers published in chemistry journals that highlight the significance of work to the general readership is encouraged.)

The sections should be arranged in a sequence generally accepted for publication in the respective fields. They subtitles should be in capital letters, centred and NOT numbered.

- The INTRODUCTION should include the aim of the research and a concise description of background information and related studies directly connected to the paper.
- The EXPERIMENTAL section should give the purity and source of all employed materials, as well as details of the instruments used. The employed methods should be described in sufficient detail to enable experienced persons to repeat them. Standard procedures should be referenced and only modifications described in detail. On no account should results be included in the experimental section.

Chemistry

Detailed information about instruments and general experimental techniques should be given in all necessary details. If special treatment for solvents or chemical purification were applied that must be emphasized.

Example: Melting points were determined on a Boetius PMHK or a Mel-Temp apparatus and were not corrected. Optical rotations were measured on a Rudolph Research Analytical automatic polarimeter, Autopol IV in dichloromethane (DCM) or methanol (MeOH) as solvent. IR spectra were recorded on a Perkin-Elmer spectrophotometer FT-IR 1725X. ^{1}H and ^{13}C NMR spectra were recorded on a Varian Gemini-200 spectrometer (at 200 and 50 MHz, respectively), and on a Bruker Ultrashield Advance III spectrometer (at 500 and 125 MHz, respectively) employing indicated solvents (*vide infra*) using TMS as the internal standard. Chemical shifts are expressed in ppm (δ / ppm) values and coupling constants in Hz (J / Hz). ESI-MS spectra were recorded on Agilent Technologies 6210 Time-Of-Flight LC-MS instrument in positive ion mode with CH_3CN/H_2O 1/1 with 0.2 % HCOOH as the carrying solvent solution. Samples were dissolved in CH_3CN or MeOH (HPLC grade purity). The selected values were as follows: capillary voltage = 4 kV, gas temperature = 350 °C, drying gas flow 12 L min^{-1}, nebulizer pressure = 310 kPa, fragmentator voltage = 70 V.The elemental analysis was performed on the Vario EL III- C,H,N,S/O Elemental Analyzer (Elementar Analysensysteme GmbH, Hanau-Germany). Thin-layer chromatography (TLC) was performed on precoated Merck silica gel 60 F254 and RP-18 F254 plates. Column chromatography was performed on Lobar LichroPrep Si 60 (40-63 μm), RP-18 (40-63 μm) columns coupled to a Waters RI 401 detector, and on Biotage SP1 system with UV detector and FLASH 12+, FLASH 25+ or FLASH 40+ columns pre packed with KP-SIL [40-63 μm, pore diameter 6 nm (60 Å)], KP-C18-HS (40-63 μm, pore diameter 9 nm (90 Å) or KP-NH [40-63 μm, pore diameter 10 nm (100 Å)] as adsorbent. Compounds were analyzed for purity (HPLC) using a Waters 1525 HPLC dual pump system equipped with an Alltech, Select degasser system, and dual λ 2487 UV-VIS detector. For data processing, Empower software was used (methods A and B). Methods C and D: Agylent Technologies 1260 Liquid Chromatograph equipped with Quat Pump (G1311B), Injector (G1329B) 1260 ALS, TCC 1260 (G1316A) and Detector 1260 DAD VL+ (G1315C). For data processing, LC OpenLab CDS ChemStation software was used. For details, see Supporting Information.

1. Synthesis experiments

Each paragraph describing a synthesis experiment should begin with the name of the product and any structure number assigned to the compound in the Results and Discussions section. Thereafter, the compound should be identified by its structure number. Use of standard abbreviations or unambiguous molecular formulas for reagents and solvents, and of structure numbers rather than chemical names to identify starting materials and intermediates, is encouraged.

When a new or improved synthetic method is described, the yields reported in key experimental examples, and yields used for comparison with existing methods, should represent amounts of isolated and purified products, rather than chromategraphically or spectroscopically determined yields. Reactant quantities should be reported in weight and molar units and for product yields should be reported in weight units; percentage yields should only be reported for materials of demonstrated purity. When chromatography is used for product purification, both the support and solvent should be identified.

2. Microwave experiments

Reports of syntheses conducted in microwave reactors must clearly indicate whether sealed or open reaction vessels were used and must document the manufacturer and model of the reactor, the method of monitoring the reaction mixture temperature, and the temperature-time profile. Reporting a wattage rating or power setting is not an acceptable alternative to providing temperature data. Manuscripts describing work done with domestic (kitchen) microwave ovens will not be accepted except for studies where the unit is used for heating reaction mixtures at atmospheric pressure.

3. Compound characterization

The Journal upholds a high standard for compound characterization to ensure that substances being added to the chemical literature have been correctly identified and can be synthesized in known yield and purity by the reported preparation and isolation methods. For **all new** compounds, evidence adequate to establish both **identity** and **degree of purity** (homogeneity) must be provided.

Identity *- Melting point.* All homogeneous solid products (*e.g.* not mixtures of isomers) should be characterized by melting or decomposition points. The colors and morphologies of the products should also be noted.

Specific rotations. Specific rotations based on the equation $[\alpha]^t; D = (100\ \alpha) / (l\ c)$ should be reported as unitless numbers as in the following example: $[\alpha]^{20}$; D = -25.4 (c 1.93, $CHCl_3$), where c / g mL^{-1} is concentration and l / dm is path length. The units of the specific rotation, (deg mL) / (g dm), are implicit and are not included with the reported value.

Spectra/*Spectral Data.* Important IR adsorptions should be given.

For all new diamagnetic substances, NMR data should be reported (^1H, ^{13}C, and relevant heteronuclei). ^1H NMR chemical shifts should be given with two digits after the decimal point. Include the number of protons represented by the signal, signal multiplicity, and coupling constants as needed (*J* italicized, reported with up to one digit after the decimal). The number of bonds through which the coupling is operative, ^xJ, may be specified by the author if known with a high degree of certainty. ^{13}C NMR signal shifts should be rounded to the nearest 0.01 ppm unless greater precision is needed to distinguish closely spaced signals. Field strength should be noted for each spectrum, not as a comment in the general experimental section. Hydrogen multiplicity (C, CH, CH_2, CH_3) information obtained from routine DEPT spectra should be included. If detailed signal assignments are made, the type of NOESY or COSY methods used to establish atom connectivity and spatial relationships should be identified in the Supporting Information. Copies of spectra should also be included where structure assignments of complex molecules depend heavily on NMR interpretation. Numbering system used for assignments of signals should be given in the Supporting Information with corresponding general structural formula of named derivative.

HPLC/LCMS can be substituted for biochemistry papers where the main focus is not on compound synthesis.

HRMS/*elemental analysis.* To support the molecular formula assignment, HRMS data accurate within 5 ppm, or combustion elemental analysis [carbon and hydrogen (and nitrogen, if present)] data accurate within 0.5 %, should be reported for new compounds. HRMS data should be given in format as is usually given for combustion analysis: calculated mass for given formula following with observed mass: (+)ESI-HRMS *m*/*z*: [molecular formula + H]$^+$ calculated mass, observed mass. Example: (+)ESI-HRMS *m*/*z*: calculated for [$C_{13}H_8BrCl_2N + H^+$] 327.92899, observed 327.92792.

NOTE: in certain cases, a crystal structure may be an acceptable substitute for HRMS/elemental analysis.

Biomacromolecules. The structures of biomacromolecules may be established by providing evidence about sequence and mass. Sequences may be inferred from the experimental order of amino acid, saccharide, or nucleotide coupling, from known sequences of templates in enzyme-mediated syntheses, or through standard sequencing techniques. Typically, a sequence will be accompanied by MS data that establish the molecular weight.

Example: Product was isolated upon column chromatography [dry flash (SiO_2, eluent EA, EA/MeOH gradient 95/5 → 9/1, EA/MeOH/NH_3 gradient 18/0.5/0.5 → 9/1/1, and flash chromatography (Biotage SP1, RP column, eluent MeOH/H_2O gradient 75/25 → 95/5, N-H column, eluent EA/Hex gradient 6/3 → EA). was obtained after flash column chromatography (Biotage SP NH column, eluent hexane/EA 4:6 → 2:6). Yield 968.4 mg (95 %). Colorless foam softens at 96-101 °C. $[\alpha]^{20}$; D = +0,163 (c =2.0×10^{-3} g/mL, CH_2Cl_2). IR (ATR): 3376w, 2949m, 2868w, 2802w, 1731s, 1611w, 1581s, 1528m, 1452m, 1374s, 1331w, 1246s, 1171m, 1063w, 1023m, 965w, 940w, 881w, 850w, 807w, cm^{-1}. ^1H NMR (500 MHz, $CDCl_3$, δ): 8.46 (*d*, 1H, J = 5.4, H-2'), 7.89 (*s*, 1H, J = 2.0, H-8'), 7.71 (*d*, 1H, J = 8.9, H-5'), 7.30 (*dd*, 1H, J_1 = 8.8, J_2 = 2.1, H-6'), 6.33 (*d*, 1H, J = 5.4, H-3'), 6.07 (*s*, HN-Boc, exchangeable with D_2O), 5.06 (*s*, 1H, H-12), 4.92-4.88 (*m*, 1H, H-7), 4.42 (*bs*, H-3), 3.45 (*s*,CH_3-N), 3.33 (*bs*, H-9'), 3.05-2.95 (*m*, 2H, H-11'), 2.70-2.43 (*m*, 2H, H-24) and HN, exchangeable with D_2O), 2.07 (*s*, CH_3COO), 2.04 (*s*, CH_3COO), 1.42 (*s*, 9H, $(CH_3)_3$C-N(Boc)), 0.88 (*s*, 3H, CH_3-10), 0.79 (*d*, 3H,J = 6.6, CH_3-20), 0.68 (*s*, 3H, CH_3-13). ^{13}C NMR (125 MHz, $CDCl_3$, δ): 170.34, 170.27, 151.80, 149.92, 148.87, 134.77, 128.36, 125.11, 121.43, 117.29, 99.98, 75.41, 70.82, 50.43, 49.66, 47.60, 47.33, 44.97, 43.30, 41.83, 41.48, 37.65, 36.35, 35.44, 34.89,

34.19, 33.23, 31.24, 28.79, 28.35, 27.25, 26.45, 25.45, 22.74, 22.63, 21.57, 21.31, 17.85, 12.15. (+)ESI-HRMS (*m/z*): calculated for $[C_{45}H_{67}ClN_4O_6 + H]^+$ 795.48219, observed 795.48185. Combustion analysis for $C_{45}H_{67}ClN_4O_6$: Calculated. C 67.94, H 8.49, N 7.04; found C 67.72, H 8.63, N 6.75. HPLC purity: method A: RT 1.994, area 99.12 %; method C: RT 9.936, area 98.20 %.

Purity **-** Evidence for documenting compound purity should include one or more of the following:

a) Well-resolved high field 1D ^{1}H NMR spectrum showing at most only trace peaks not attributable to the assigned structure and a standard 1D proton-decoupled ^{13}C NMR spectrum. Copies of the spectra should be included as figures in the Supporting Information.
b) Quantitative gas chromatographic analytical data for distilled or vacuum-transferred samples, or quantitative HPLC analytical data for materials isolated by column chromatography or separation from a solid support. HPLC analyses should be performed in two diverse systems. The stationary phase, solvents (HPLC), detector type, and percentage of total chromatogram integration should be reported; a copy of the chromatograms may be included as a figure in the Supporting Information.
c) Electrophoretic analytical data obtained under conditions that permit observing impurities present at the 5 % level.

HRMS data may be used to support a molecular formula assignment **but cannot be used as a criterion of purity**.

4. Biological Data

Quantitative biological data are required for all tested compounds. Biological test methods must be referenced or described in sufficient detail to permit the experiments to be repeated by others. Detailed descriptions of biological methods should be placed in the experimental section. Standard compounds or established drugs should be tested in the same system for comparison. Data may be presented as numerical expressions or in graphical form; biological data for extensive series of compounds should be presented in tabular form. Tables consisting primarily of negative data will not usually be accepted; however, for purposes of documentation they may be submitted as supporting information. Active compounds obtained from combinatorial syntheses should be resynthesized and retested to verify that the biology conforms to the initial observation.

Statistical limits (statistical significance) for the biological data are usually required. If statistical limits cannot be provided, the number of determinations and some indication of the variability and reliability of the results should be given. References to statistical methods of calculation should be included. Doses and concentrations should be expressed as molar quantities (*e.g.*, mol/kg, μmol/kg, M, mM). The routes of administration of test compounds and vehicles used should be indicated, and any salt forms used (hydrochlorides, sulfates, *etc.*) should be noted. The physical state of the compound dosed (crystalline, amorphous; solution, suspension) and the formulation for dosing (micronized, jet-milled, nanoparticles) should be indicated. For those compounds found to be inactive, the highest concentration (*in vitro*) or dose level (*in vivo*) tested should be indicated.

- The RESULTS AND DISCUSSION should include concisely presented results and there significance discussed and compared to relevant literature data. The results and discussion may be combined or kept separate.
- The inclusion of a CONCLUSION section, which briefly summarizes the principal conclusions, is recommended.
- NOMENCLATURE is optional but, if the authors wish, a list of employed symbols may be included.
- REFERENCES should be numbered sequentially as they appear in the text. Please note that any reference numbers appearing in the Illustrations and/or Tables and corresponding captions must follow the numbering sequence of the paragraph in which they appear for the first time. When cited, the reference number should be superscripted in Font 12, following any punctuation mark. In the reference list, they should be in normal position followed by a full stop. Reference entry must not be formatted using Carriage returns (enter key; ↵ key) or multiple space key. The formatting of references to published work should follow the *Journal'*s style as follows:

Journals[a]:	A. B. Surname1, C. D. Surname2, *J. Serb. Chem. Soc.* **Vol** (Year) first page Number (https://doi.org/doi)[b]
Books:	A. B. Surname1, C. D. Surname2, *Name of Book*, Publisher, City, Year, pp. 100-101 (https://doi.org/doi)[b]
Compilations:	A. B. Surname1, C. D. Surname2, in *Name of Compilation*, A. Editor1, C. Editor2, Ed(s)., Publisher, City, Year, p. 100 (https://doi.org/doi)[b]
Proceedings:	A. B. Surname1, C. D. Surname2, in *Proceedings of Name of the Conference or Symposium*, (Year), Place of the Conference, Country, *Title of the Proceeding*, Publisher, City, Year, p. or Abstract No. 100
Patents:	A. B. Inventor1, C. D. Inventor2, (Holder), Country Code and patent number (registration year)
Chemical Abstracts:	A. B. Surname1, C. D. Surname2, *Chem. Abstr*. CA 234 567a; For non-readily available literature, the Chemical Abstracts reference should be given in square brackets: [C.A. 139/2003 357348t] after the reference
Standards:	EN ISO 250: *Name of the Standard* (Year)
Websites:	Title of the website, URL in full (date accessed)

[a] When citing Journals, the International Library Journal abbreviation is required. Please consult, *e.g.*, https://images.webofknowledge.com/WOK46/help/WOS/A_abrvjt.html

[b] doi should be replaced by doi number of the Article, for example: http://dx.doi.org/10.2298/JSC161212085B (as active link). If doi do not exist, provide the link to the online version of the publication.

Only the last entry in the reference list should end with a full stop.

The names of all authors should be given in the list of references; the abbreviation *et al.* may only be used in the text. The original journal title is to be retained in the case of publications published in any language other than English (please denote the language in parenthesis after the reference). Titles of publications in non-Latin alphabets should be transliterated. Russian references are to be transliterated using the following transcriptions:

ж→zh, х→kh, ц→ts, ч→ch, ш→sh, щ→shch, ы→y, ю→yu, я→ya, э→e, й→i, ь→’.

Supplementary material

Authors are encouraged to presentthe information and results non-essential to the understanding of their paper as SUPPLEMENTARY MATERIAL (can be uploaded inStep 4 of Online Submission). This material may include as a rule, but is not limited to, the presentation of analytical and spectral data demonstrating the identity and purity of synthesized compounds, tables containing raw data on which calculations were based, series of figures where one example would remain in the main text, etc. The Editorial Board retain the right to assign such information and results to the Supplementary material when deemed fit. Supplementary material does not appear in printed form but can be downloaded from the web site of the JSCS.

Mathematical and chemical equations should be given in separate lines and must be numbered, Arabic numbers, consecutively in parenthesis at the end of the line. All equations should be embedded in the text Complex equations (fractions, integrals, matrix…) should be prepared with the aid of the Microsoft Equation 3.0 (or higher) or MathType (Do not use them to create simple equations and labels). Using the Insert -> Equation option, integrated in MS Office 2010 and MS Office 2013, as well as insertion of equation objects within paragraph text IS NOT ALLOWED.

Deposition of crystallographic data

Prior to submission, the crystallographic data included in a manuscript presenting such data should be deposited at the appropriate database. Crystallographic data associated with organic and metal-organic structures should be deposited at the Cambridge Crystallographic Data Centre (CCDC) by e-mail to **deposit@ccdc.cam.ac.uk**

Crystallographic data associated with inorganic structures should be deposited with the Fachinformationszentrum Karlsruhe (FIZ) by e-mail to **crysdata@fiz-karlsruhe.de**. A deposition number will then be provided, which should be added to the reference section of the manuscript.

For detailed instructions please visit the JSCS website:
https://www.shd-pub.org.rs/index.php/JSCS/Instructions

ARTWORK INSTRUCTIONS

JSCS accepts only **TIFF** or **EPS** formats, as well as **JPEG** format (only for colour and greyscale photographs) for electronic artwork and graphic files. **MS files** (Word, PowerPoint, Excel, Visio) **NOT acceptable**. Generally, scanned instrument data sheets should be avoided. Authors are responsible for the quality of their submitted artwork. Every single Figure or Scheme, as well as any part of the Figure (A, B, C…) should be prepared according to following instructions (every part of the figure, A, B, C…, must be submitted as an independent single graphic file):

TIFF

Virtually all common artwork and graphic creation software is capable of saving files in TIFF format. This 'option' can normally be found under 'the 'Save As...' or 'Export...' commands in the 'File' menu.

TIFF (Tagged Image File Format) is the recommended file format for bitmap, greyscale and colour images.

- Colour images should be in the RGB mode
- When supplying TIFF files, please ensure that the files are supplied at the correct resolution:
    1. Line artwork: minimum of 1000 dpi
    2. RGB image: minimum of 300 dpi
    3. Greyscale image: minimum of 300 dpi
    4. Combination artwork (line/greyscale/RGB): minimum of 500 dpi
- Images should be tightly cropped, without frame and any caption.
- If applicable please re-label artwork with a font supported by JSCS (Arial, Helvetica, Times, Symbol) and ensure it is of an appropriate font size.
- Save an image in TIFF format with LZW compression applied.
- It is recommended to remove Alpha channels before submitting TIFF files.
- It is recommended to flatten layers before submitting TIFF files.

Please be sure that quality of an image cannot be increased by changing the resolution from lower to higher, but only by rescanning or exporting the image with higher resolution, which can be set in usual "settings" facilities.

EPS

Virtually all common artwork creation software, such as Canvas, ChemDraw, CorelDraw, SigmaPlot, Origin Lab…, are capable of saving files in EPS format. This 'option' can normally be found under the 'Save As...' or 'Export...' commands in the 'File' menu.

For vector graphics, EPS (Encapsulated PostScript) files are the preferred format as long as they are provided in accordance with the following conditions:

- when they contain bitmap images, the bitmaps should be of good resolution (see instructions for TIFF files)
- when colour is involved, it should be encoded as RGB
- an 8-bit preview/header at a resolution of 72 dpi should always be included
- embed fonts should always included and only the following fonts should be used in artwork: Arial, Helvetica, Times, Symbol
- the vertical space between the parts of an illustration should be limited to the bare necessity for visual clarity
- no data should be present outside the actual illustration area
- line weights should range from 0.35 pt to 1.5 pt
- when using layers, they should be reduced to one layer before saving the image (Flatten Artwork)

JPEG

Virtually all common artwork and graphic creation software is capable of saving files in JPEG format. This 'option' can normally be found under 'the 'Save As...' or 'Export...' commands in the 'File' menu.

JPEG (Joint Photographic Experts Group) is the acceptable file format **only for colour and greyscale photographs**. JPEG can be created with respect to photo quality (low, medium, high; from 1 to 10), ensuring file sizes are kept to a minimum to aid easy file transfer. Images should have a minimum resolution of 300 dpi. Image width: minimum 3.0 cm; maximum 12.0 cm.

Please be sure that quality of an image cannot be increased by changing the resolution from lower to higher, but only by rescanning or exporting the image with higher resolution, which can be set in usual "settings" facilities.

SIZING OF ARTWORK

- JSCS aspires to have a uniform look for all artwork contained in a single article. Hence, it is important to be aware of the style of the journal.
- Figures should be submitted in black and white or, if required, colour (charged). If coloured figures or photographs are required, this must be stated in the cover letter and arrangements made for payment through the office of the Serbian Chemical Society.
- As a general rule, the lettering on an artwork should have a finished, printed size of 11 pt for normal text and no smaller than 7 pt for subscript and superscript characters. Smaller lettering will yield a text that is barely legible. This is a rule-of-thumb rather than a strict rule. There are instances where other factors in the artwork, (for example, tints and shadings) dictate a finished size of perhaps 10 pt. Lines should be of at least 1 pt thickness.
- When deciding on the size of a line art graphic, in addition to the lettering, there are several other factors to address. These all have a bearing on the reproducibility/readability of the final artwork. Tints and shadings have to be printable at the finished size. All relevant detail in the illustration, the graph symbols (squares, triangles, circles, *etc*.) and a key to the diagram (to explain the explanation of the graph symbols used) must be discernible.
- The sizing of halftones (photographs, micrographs,...) normally causes more problems than line art. It is sometimes difficult to know what an author is trying to emphasize on a photograph, so you can help us by identifying the important parts of the image, perhaps by highlighting the relevant areas on a photocopy. The best advice that can be given to graphics suppliers is not to over-reduce halftones. Attention should also be paid to magnification factors or scale bars on the artwork and they should be compared with the details inside. If a set of artwork contains more than one halftone, again please ensure that there is consistency in size between similar diagrams.

General sizing of illustrations which can be used for the Journal of the Serbian Chemical Society:

- Minimum fig. size: 30 mm width
- Small fig. size - 60 mm width
- Large fig. size - 90 mm width
- Maximum fig. size - 120 mm width

Pixel requirements (width) per print size and resolution for bitmap images:

	Image width	A	B	C
Minimal size	30 mm	**354**	**591**	**1181**
Small size	60 mm	**709**	**1181**	**2362**
Large size	90 mm	**1063**	**1772**	**3543**
Maximal size	120 mm	**1417**	**2362**	**4724**

A: 300 dpi > RGB or Greyscale image
B: 500 dpi > Combination artwork (line/greyscale/RGB)
C: 1000 dpi> Line artwork

The designation of physical quantities and graphs formatting

The designation of physical quantities on figures must be in italic, whereas the units are in upright letters. They should be in Times New Roman font. In graphs a slash should be used to separate the designation of a physical quantity from the unit (example: p / kPa, t °C, T_0 / K, τ / h, ln (j / mA cm^{-2})…). Designations such as: p (kPa), t [min]…, are not acceptable. However, if the full name of a physical quantity is unavoiable, it should be given in upright letters and separated from the unit by a comma (example: Pressure, kPa, Temperature, K…). Please do not use the axes of graphs for additional explanations; these should be mentioned in the figure captions and/or the manuscript (example: "pressure at the inlet of the system, kPa" should be avoided). The axis name should follow the direction of the axis (the name of y-axis should be rotated by 90°). Top and right axes should be avoided in diagrams, unless they are absolutely necessary. Decimal numbers must have decimal points and not commas in the axis labels in graphical presentations of results. Thousands are separated, if at all, by a comma and not a point.

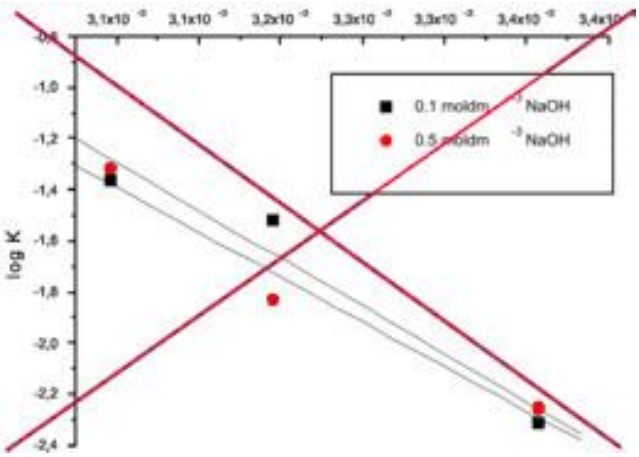

INCORRECT

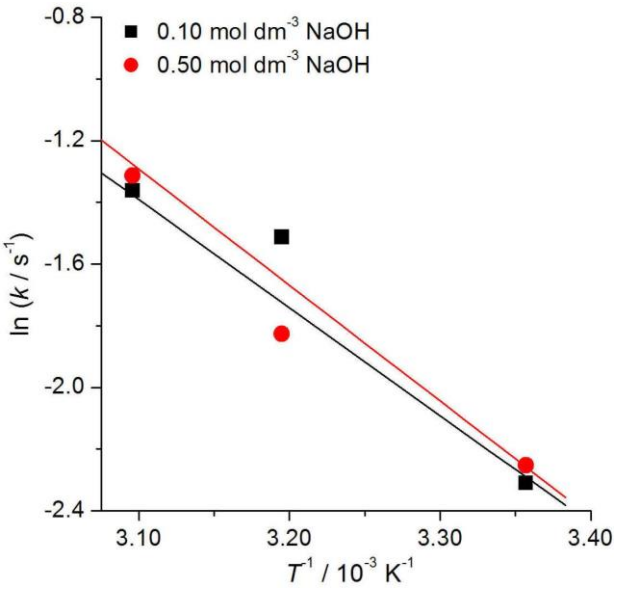

CORRECT

Journal of the Serbian Chemical Society
JSCS-info@shd.org.rs • www.shd.org.rs/JSCS

J. Serb. Chem. Soc. Vol. 85, No. 12 (2020)

CONTENTS*

Published by the Serbian Chemical Society
Karnegijeva 4/III, P. O. Box 36, 11120 Belgrade, Serbia
Printed by the Faculty of Technology and Metallurgy
Karnegijeva 4, P. O. Box 35-03, 11120 Belgrade, Serbia

* For colored figures in this issue please see electronic version at the Journal Home Page: http://www.shd.org.rs/JSCS/

Journal of the Serbian Chemical Society
JSCS-info@shd.org.rs • www.shd.org.rs/JSCS
J. Serb. Chem. Soc. *85* (12) 1507–1538 (2020)
JSCS–5390
UDC 577.11:766.092.000.57:620.28:502
Survey

SURVEY

Understanding bioplastic materials – Current state and trends

SANJA JEREMIC[1], JELENA MILOVANOVIC[1], MARIJA MOJICEVIC[2], SANJA SKARO BOGOJEVIC[1] and JASMINA NIKODINOVIC-RUNIC[1]*

[1]*Institute of Molecular Genetics and Genetic Engineering, Vojvode Stepe 444a, 11042 Belgrade 152, Serbia and* [2]*Athlone Institute of Technology, Dublin Road, Athlone, Co. Westmeath, Ireland*

(Received 20 July, revised 31 August, accepted 4 September 2020)

Abstract: Plastic pollution is now considered one of the largest environmental threats facing humans and animals globally. Development of bioplastic materials may offer part of the solution as bioplastics include both nondegradable and biodegradable materials with both being important for sustainability. Bioplastic materials are currently being designed to encompass minimal carbon footprint, high recycling value and complete biodegradability. This review examines recent developments and trends in the field of bioplastic materials. A range of the most utilized bioplastic materials is presented (poly(lactic acid) (PLA), polyhydroxyalkanoate (PHA), starch, cellulose, bio-based poly(butylene succinate) (bio-PBS) and bio-polyethylene (bio-PE)) including their production, application and degradation options.

Keywords: bioplastics; biopolymers; biodegradation; poly(lactic acid); sustainability polyhydroxyalkanoates.

CONTENTS

* Corresponding author. E-mail: jasmina.nikodinovic@imgge.bg.ac.rs
https://doi.org/10.2298/JSC200720051J

1. INTRODUCTION

"Plastics" as synthetic polymers were introduced about 100 years ago and today they are one of the most produced, used, and versatile materials.[1] Nevertheless, their biggest advantage, namely durability, turned out to be their biggest problem, as their degradation rate does not match their intended service life and so their build-up in the environment is inevitable. Environmental pollution from plastic is a vast issue, given that in 2018 alone the worldwide production of plastics from fossil resources reached almost 360 million tons, while in Europe it reached 62 million tones.[2] This translates that each person consumes 50 kg of plastic per year in the European Union and 68 kg per year in the United States.[3] Approximately half of the synthetic polymers are used in single-use or short-lived products, which mostly end up on landfills and in oceans, where they become fragmented over time into 'microplastics' that harm and kill various organisms, finally ending up on our plates.[4] In January 2018, the EU released its vision for a more sustainable plastics industry to be achieved by 2030. The new plastics strategy states that 100 % of plastics should either be reusable or recyclable by 2030.[2]

Environmental concerns over plastic pollution coupled with a growing debate over crude oil dependence and depletion have sparked and fuelled interest in bioplastics. Bioplastics include both nondegradable and biodegradable plastics (Fig. 1) and both are important for sustainable solutions. The production and use of bioplastics are generally regarded as more sustainable activities when compared with plastic production from petroleum (petrochemical plastics; petroplastics) because they rely less on fossil fuels as the carbon source. They also introduce fewer, net-new greenhouse emissions if they biodegrade.[5] Bioplastics also significantly reduce hazardous waste caused by oil-derived plastics. However, the manufacture of bioplastic materials is still often reliant on petroleum as a source of energy and materials.[6,7]

1.1. Bioplastics – definitions

The term "bioplastic" is often used by the public and in scientific literature. However, the term "bioplastic" refers to either to the bio-based origin of the plastic or the biodegradable character of the plastic. These two aspects of plastic are not synonymous, and therefore, the term 'bioplastic' is confusing. In this review, a clear distinction is made between bio-based and biodegradable plastics (Fig. 1). According to the International Union of Pure and Applied Chemistry (IUPAC), a bioplastic is derived from ''biomass or monomers derived from biomass and which, at some stage in its processing into finished products, can be shaped by flow''.[8]

It is also important to make the distinction between degradable, biodegradable and compostable. These terms are often incorrectly used interchangeably. Degradable plastic is a plastic that will undergo some significant structural

change in some definite environment. The "environment" may as well be an industrial process instead of some naturally occurring microbial one. According to the IUPAC, biodegradable polymers are defined as "polymers, susceptible to degradation by biological activity, with the degradation accompanied by a lowering of its mass".[9] Some other definitions require a biodegradable material to be mineralized into carbon dioxide, water, and biomass during biodegradation (standard CEN/TR 15351:2006).[10]

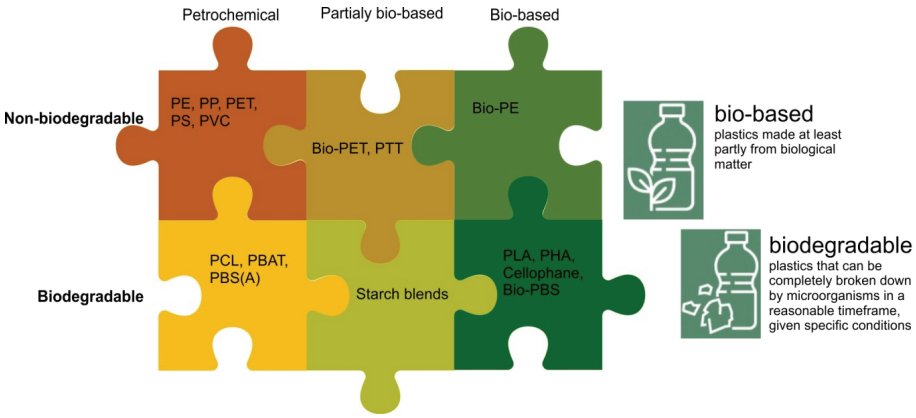

Fig. 1. Not all bio-based plastics are biodegradable, and not all biodegradable plastics are bio-based. PE=polyethylene; PP=polypropylene; PET=poly(ethylene terephthalate); PS=polystyrene; PVC=poly(vinyl chloride); PTT=poly(1,3-propylene terephthalate); PCL=poly(caprolactone); PBAT= poly(butylene adipate terephthalate); PBS(A)= =poly(butylene succinate(adipate)); PLA=polylactide; PHA=polyhydoxyalkanoate.

Compostable plastic is a plastic "capable of undergoing biological decomposition in a compost site as part of an available program, such that the plastic is not visually distinguishable and breaks down to carbon dioxide, water, inorganic compounds, and biomass, at a rate consistent with known compostable materials (*e.g.*, cellulose) and leaves no toxic residue..." defined by the American Society for Testing and Materials.[11] Unfortunately, the term "biodegradable plastic" has also been used by producers of specially modified petrochemical-based plastics that appear to biodegrade. This is the case with the plastics to which a degradation initiator has been added to achieve a controlled UV/oxidation disintegration process. This type of plastic may be referred to as degradable plastic or oxy-degradable plastic or photodegradable plastic as the process is not initiated by microbial action. However, plastic bag manufacturers often misrepresent the degradability of their products by misleading the use of the terms biodegradable or compostable. It has been shown that even biodegradable plastics might not biodegrade in every environment.[12]

1.2. Historic perspective of bioplastics

Natural plastic materials (plant gum, shellac, starch) have been used for thousands of years.[1] The first plastics in the modern sense were celluloid and cellophane and they were bio-based. Cellophane, commercialized in 1912, is still in use today.[13] In the early 1950s, amylomaize (>50 % amylose content corn) was successfully bred and commercial bioplastics applications started to be explored. Modern bioplastics started emerging in the 1980s when the environmental effects of plastic waste became obvious. The first bioplastics were blends of starch with conventional polymers so that certain biodegradability and the use of natural feedstock were partly achieved.

In 1982, Biopol (poly(hydroxybutyrate), PHB) was introduced as the first fully biodegradable plastic, but costing nearly 20 times its non-biodegradable competitors. In 2004, NEC developed a flame-retardant plastic, poly(lactic acid) (PLA), without the employment of halogens and phosphorus compounds. In 2005, Fujitsu became one of the first technology companies to make personal computer cases from bioplastics, which were featured in their FMV-BIBLO NB80K line. In 2007, Braskem of Brazil announced it had developed a route to manufacture high-density polyethylene (HDPE) using ethylene derived from sugar cane.[1,14]

There are three ways to produce bioplastics that include: *i*) using natural bio-based polymers such as starch with partial modifications to meet the requirements; *ii*) producing monomers by fermentation followed by polymerization (PLA, poly(butylene succinate) (PBS), bio-based polyethylene, bio-PE); *iii*) producing them by bacteria directly (polyhydroxyalkanoates, PHAs).[15] The first generation technologies focused on feedstock such as corn, starch, or rice to produce bioplastics, which were deemed unacceptable in the food *vs*. fuel debate, so the focus shifted towards various waste streams from wood and paper as well as food industries or to third generations from micro-algae, marine bacteria, sewage sludge).[15–17]

In the last decade, the production of bioplastics has been accelerated and reached substitution alternatives for major petrochemical plastics (Table I).

TABLE I. Bioplastics alternatives for major petrochemical plastics; source: Chemical Market Resources Inc.; substitution potential: +++ - high; ++ - medium; + - low; – - not foreseen

Bioplastic	LDPE[a]	HDPE[a]	PP[a]	PS[a]	PVC[a]	PET[a]	PUR[a]
PLA[a]	+	++	++	++	–	++	–
PHA[a]	++	+++	+++	++	+	++	++
Starch blends	++	++	++	+	–	++	–
Bio-PE	+++	+++	–	–	–	–	–

[a]LDPE = low-density polyethylene; HDPE = high-density polyethylene; PS = polystyrene; PP = polypropylene; PVC = poly(vinyl chloride); PET = poly(ethylene terephthalate); PUR = polyurethane; PLA = polylactide; PHA = polyhydoxyalkanoate

In most cases, they exhibit similar properties and can even exceed the performances of conventional plastics: *e.g.*, PLA can replace fossil-based polystyrene (PS), and can be modified to replace conventional PE or polypropylene (PP); PHA can gradually substitute PP and low-density polyethylene (LDPE) with similar physicochemical, thermal, and mechanical properties; poly(hydroxybutyrate) (PHB) possesses better physical properties than PP for food packaging applications and is completely nontoxic. In addition, bio-based polyesters have the potential to avoid the release of micro-plastics if they are formulated to be biodegradable or compostable. On the other hand, the cost of bioplastics is currently still not competitive with that of petroplastics. Bioplastics do not yet reach fossil fuel parity of fossil fuel-derived energy for their manufacture, reducing the cost advantage over petroleum-based plastics.[5]

2. DESCRIPTION OF IMPORTANT BIOPLASTICS

Bioplastics contribute less than one percent to the overall plastics production, but the market is growing. About half (44.5 % in 2019) of all bioplastics on the market are bio-based and not biodegradable (Fig. 2). Bio-PE, bio-based PET (bio-PET) and bio-based PTT (bio-PTT) account for the majority of these so-called drop-in materials. They are more or less equivalent to their fossil-based counterparts, so they are very convenient for the industry. Producers and recyclers can drop them into their existing infrastructure, however, they cause the same kind of pollution as petrochemical plastics. Besides PLA, which accounts for 14 % of the global production capacity for bioplastics (biodegradable and non-biodegradable), mainly starch blends (21 %), other biodegradable polyesters including PBS (4 %) and PHAs (1 %) are produced on the industrial scale (Fig. 2).

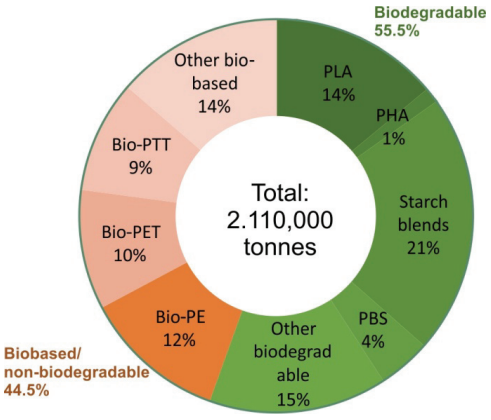

Fig. 2. Global production capacities of bioplastics in 2019 (data adapted from European Bioplastics[18]).

Five commercial bioplastics have been chosen for this review based on the volume of their production and the wide range of applications that they cover (Table II).

TABLE II. Biobased polymers described in this study (adapted from Hatti-Kaul and co-workers[19])

Polymer	Structure	Biobased content, %[a]	Annual production, t[b]	Trademarks/Company	Application
Bio-PE	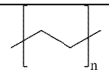	100	200 000	I'm green/Braskem	Packaging films and bags
Bio-PBS	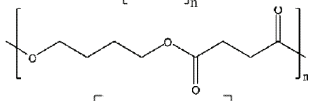	Up to 100	97 000	Bionolle 1000/Showa Denko, BioPBS/PTT MCC Biochem	Films and sheets for food packaging, fishing nets, the automotive industry
Starch	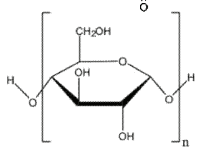	100	384 000	MaterBi/Novamont	Food packaging, compostable films and bags, disposable utensils
PHA	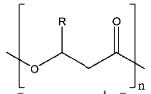	100	30 000	Minerv-PHA/Bio-On, PHBH/Kaneka, Nodax/Danimer Sci.	Packaging, compost bags, tissue engineering
PLA	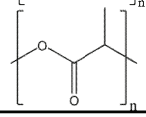	100	217 000	Ingeo/ NatureWorks, Lumony/ TotalCorbion, Lacty/Shimadzy, Vyloecol/Toyobo	Packaging, medical implants, 3D printing polymers, electronics, textiles

[a]The biobased content of the polymers is based on current information about commercially available products; [b]the annual production volume of the polymers was obtained from www.european-bioplastics.org/market/

2.1. Poly(lactic acid) (PLA)

PLA is a biobased and biodegradable aliphatic polyester that represented 13.9 % of global bioplastic production capacities in 2019 (Fig. 2[20]). Lactic acid (2-hydroxy propionic acid) is the basic monomer of PLA produced either by bacterial fermentation of basic carbohydrates or by chemical synthesis. Industrial lactic acid producers, such as NatureWorks and Total Corbion, utilize the lactic fermentation process rather than synthesis.[21] The use of corn starch, cassava roots, sugar cane, or potato as the carbohydrate source makes the industrial process of lactic acid production sustainable and renewable.[22] PLA is one of the most efficient biopolymers, yielding 1 kg of polymer from 1.6 kg of the fermented amount of carbohydrate feedstock, while other biopolymers require 2–3 times more feedstock for production. PLA and PLA-blends generally come in the form of granulates with various properties and are used in the plastics processing industry for the production of foil, moulds, cups, bottles and mulch films used in agricultural fields. On the other hand, due to the relatively low glass transition temperature of PLA, PLA cups cannot hold hot liquids, so much research is devoted to the development of a heat resistant PLA. Additional research is also ongoing to find even more eco-friendly and economical methods for producing lactic acid by using crop residues, such as stems, straw, husks, and leaves as carbohydrate sources.[23] Lactic acid can be used to produce PLA of variable molecular weights, however, usually, only high *M*w PLA has major commercial value in various industries.

There are three routes for PLA production:

1) direct condensation polymerization: esterification of lactic acid monomers and free water removal using progressive vacuum and high temperatures, resulting in a less-desired low *Mw* PLA;

2) direct polycondensation in an azeotropic solution: PLA production by direct condensation and continuous removal of condensation water by azeotropic distillation;

3) polymerization through lactide formation (ring-opening method): industrially accomplished for high Mw PLA production using lactide as an intermediate state. This process results in a metal catalyst combining with a lactide to form larger PLA molecules.

PLA has versatile applications in the food-packing industry, medical and cosmetics industry, textile industry, structural applications and 3D printing (Table II). The global PLA market was valued at USD 673.88 million in 2018 and it is estimated that it will generate a net revenue of approximately USD 2277.57 million by 2027. The PLA market is dominated by 1–5 major players, *i.e.*, NatureWorks, Total Corbion, Synbra Technology BV, Futerro and Sulzer Ltd., with NatureWorks and Total Corbion being the major producers, with a

capacity of 1.5×10^5 and 0.75×10^5 metric t per year, respectively (Table S-I of the Supplementary material paper to this paper).[24]

In the past 10 years, the vast majority of patents regarding PLA production are related to methods of processing PLA into materials for specific applications, such as 3D printing wires, fibbers, sheets, *etc*., or the modification of available PLA in order to improve the properties (CN108705753A, CN106738783A, CN104138310A, US2015337097A1 and CN104356365A). When it comes to patents concerning the production of raw material, they are mainly focused on methods of obtaining high molecular weight PLA (US9023953B2, US9062006B2 and CN106750199A). Additionally, two patents should be emphasized since they deal with the production of lactic acid using agricultural feedstock and sideline products, thus making PLA production process ecologically and environmentally even more viable (US7507561B2, CN104592500A).

As mentioned, PLA has some significant shortcomings, such as low melt strength, poor processability, high brittleness, low toughness, and slow biodegradation rate, which hamper specific PLA applications.[25] Therefore, PLA is often blended/combined with a range of different polymers, additives, and fillers in order to improve material properties, reduce costs and open up new opportunities for PLA application.[26] Some of the most studied PLA blends with other polymers are listed below:

- The development of PLA blends with biobased and biodegradable thermoplastic starch (TPS) is of great interest for food packaging applications and could also be considered in biomedical applications, due to achieved improvements in toughness;[27]
- Addition of biobased and biodegradable PHB to PLA enhances its crystallinity, which is important for food packaging applications in order to increase the barrier performance of PLA based materials;[28]
- PLA blends with biodegradable PCL have improved ductility and toughness compared to neat PLA, and increased tensile strength compared to neat PCL, and as such, they are utilized in tissue engineering and grafts, as well as in packaging applications with easy-open peelable feature;[29]
- PLA and biodegradable PBS blends exhibit ductile behaviour with gradual losses of strength and modulus during biodegradation, so they have potential in food packaging applications. In addition, PBS/PLA blends have excellent mechanical properties and suitability as materials for 3D printing;[30,31]
- PLA and synthetic, non-degradable PEG blends have decreased viscoelasticity, and increased hydrophilicity and degradation rate, and often are used for drug delivery and scaffolds. Recently, 3D-printed scaffolds have also been produced using PLA/PEG blends.[32]

Recycling, as one of the possible disposal routes for plastic, has been extensively studied on PLA. Currently, only 10 % of PLA waste is returned to the

PLA production process.[33] PLA can undergo mechanical or chemical recycling. An easy and the cost-effective way to recycle post-consumer PLA is mechanical recycling, which involves recovering, sorting, regrinding, and reprocessing the waste plastic, has become common practice in the industry.[34] However, this method has limitations affecting the PLA quality, thus limiting the range of products in which it could be used, and reducing the economic viability.[35] An alternative is chemical recycling, during which PLA is hydrolyzed at a high temperature to yield lactic acid, which could be readily polymerized to high Mw PLA. NatureWorks is an example of successful off-grade Ingeo™ recycling using a chemical method, while Galactic started a pilot unit to produce recycled PLA using a chemical recycling process (Loopla). However, chemical recycling is still a complex and expensive process. Although PLA is potentially recyclable, no separate recycling stream for PLA yet exists.[36] The presence of PLA in the current plastic recycling infrastructure, even at low concentrations, causes contamination of the recycling stream and production of inferior recycled material. Thus, it is crucial to remove PLA from other plastics and to establish single streams for materials such as PLA in order to recycle them. In addition, PLA is assigned the Resin Identification Code (RIC) number "7-OTHER" (ASTM D7611), with several other, rather new, polymers, and that is not considered accurate for the identification and (pre)sorting of PLA from a waste mixture.[35]

Another end-life scenario for PLA and the natural way of recycling is biodegradation. Numerous literature data deal with PLA degradability in soil and compost. The majority of these studies used industrially produced PLA for testing, and polymer weight loss or molecular weight loss as methods to assess degradability. PLA degradation upon disposal in the environment is very challenging due to the resilience of PLA to the actions of microorganisms in soil or sewage under ambient conditions.[21] No significant PLA degradation was observed when the polymer was buried in a real soil environment, or in soil under controlled temperatures of 25 and 37 °C, even after 24 months of exposure.[37–40] However, PLA – including commercially available PLA bottles and PLA deli containers, could be degraded in the compost after only 45–60 days, but high temperatures of 50–60 °C are required to hydrolyze the polymer into smaller molecules, which are then degraded by microorganisms to CO_2 and H_2O.[41,42] A search of patents from the previous decade revealed a large number of patented microorganisms and corresponding enzymes with PLA degrading activity (Table III).

Since PLA must first be hydrolyzed at elevated temperatures to reduce the molecular weight before biodegradation can commence,[38] it is more accurate to say that PLA is compostable, but due to a specific temperature and moisture conditions necessary for proper PLA composting, the path to zero waste is complicated and unattainable at this moment. In contrast to soil and compost, only a few studies deal with PLA biodegradation in aquatic environments. Since after 10

weeks no evidence of microbial degradation was found, the authors suggested that marine microbes have a limited ability to degrade PLA.[43,44]

TABLE III. Examples of patented microorganisms for PLA degradation

Patent number	Year	PLA-degrading microorganism (enzymes)
CN110317762A	2019	*Pseudomonas* sp. LXM88/protease
WO2017198786A1	2017	–
CA2937569A1	2017	*Alcanivorax borkumensis*, *Rhodopseudomonas palustris* /hydrolase
WO2016146540 A1	2016	*Micromonospora* sp./hydrolase
WO2016062695A1	2016	*Actinomadura keratinilytica* T16-1/hydrolase
AU2014325231A1	2016	protease
EP2483429A1	2012	*Ochrobactrum* sp.
CN102380180A	2012	*Lentzea waywayandensis*, *Tritirachium album*, *Amycolatopsis orientalis*
CN102181378 (A)	2011	*Pseudomonas* sp. DS1001
JP4273504B2	2009	*Aspergillus oryzae*, *Aspergillus soya* /serine hydrase

2.2. Polyhydroxyalkanoates (PHA)

PHAs are a family of natural biodegradable polyesters, usually produced by prokaryotes as cytoplasmatic water-insoluble storage compounds of carbon and energy.[45]

Since the discovery of the simple PHB homopolymer by Lemoigne in the 1920s, a family of over 150 different aliphatic polyesters of the same general structure was revealed. As a result, the polymer properties demonstrated by this family are very broad.[46] Although their shape, size, structure, and physical properties depend on the producing organism and cultivation conditions, all polyesters are thermoplastic, water-insoluble, non-toxic, relatively resistant to hydrolytic degradation, biocompatible and biodegradable.[47] PHAs are classified into two major subdivisions by the carbon chain length of their monomeric units: short-chain-length-3-hydroxyalkanoates (scl-3HA) have 3–5 carbon atoms and medium-chain-length-3-hydroxyalkanoates (mcl-3HA) with 6–16 carbon atoms.[45]

PHB was the first bacterial PHA identified. The unique properties of PHAs are recognized as better oxygen barrier than PP and PET, better water vapour barrier (than PP), and fat/odour barrier. Such superior physicochemical properties of PHA (*e.g.*, in reference to PP) have promoted their usage in various fields, including food packaging.[48] However, the poor mechanical performance and melt processing behaviour of PHB, *i.e.*, high brittleness, low thermal stability and difficult processing, along with insufficient barrier properties, limits its widespread use.[49]

Several companies have developed PHA copolymers in order to improve the properties of PHAs. The incorporation of secondary different hydroxy acid (HA) monomers other than PHB, such as 3-hydroxyvalerate (3HV), 3-hydroxyhexa-

noate (3HH), 3-hydroxypropionate (3HP) and 4-hydroxybutyrate (4HB), into the polymer chain to form copolymers is a common strategy.[47]

One of the first copolymers to be manufactured in the industry was Biopol®, poly(3-hydroxybutyrate-*co*-3-hydroxyvalerate) (PHBV). This copolymer is a thermoplastic and has a melting temperature in the range of 140–180 °C. It has a range of uses, such as packaging, shampoo bottles, disposable razors, disposable cups, surgical stitches, surgical pins, disposable knives and forks, woven medical patches and nappy linen.[47] The mole percentage of 3HV is important in determining the properties of the copolymer since the composition of P(3HB-*co*-3HV) can range from 0 to 30 mol. % 3HV. Li *et al.* found better tensile strength and Young's modulus of P(3HB-*co*-3HV-*co*-3HHp) in comparison to P(3HB).[50] The P(3HB-*co*-4HB) copolymer exhibits a broad array of morphologies, such as highly crystalline to elastomeric based on the concentration of 4HB.[51]

PHB has a comparable melting temperature to PLA, and thus allows for the blending of both polymers in their molten state.[52] Blends of PHAs with natural raw materials from sustainable resources are well discussed.[53] The most common are PHA blends with starch, lignin and cellulose derivatives.[54,55]

Many years of research efforts have led to the large-scale production of PHA and its copolymers. Procter and Gamble have developed Nodax® (Table II), PHA polymer consisting of PHB and a comparatively small quantity of medium chain length (mcl) monomers. The mcl units used include 3HH, 3-hydroxyoctanoate (3HO) and 3-hydroxydecanoate (3HD). Tianan's biopolymer Enmat® is a PHBV copolymer containing about 5 % 3HV, which improves the flexibility of the polymer. The USA based company Newlight Technologies chose methane as the carbon source for fermentation with a planned capacity of 43,000 t per year within the next 20 years. Other commercial PHAs are produced by Bio-on (MINERV®), Metabolix (Mvera®, Mirel®) and PHB Industrial (BIOCYCLE®) among other manufacturers (Table S-II). Worldwide, more than 20 companies are known to be engaged in PHA production and applications. China, Italy, the USA and Brazil represent the main producers of PHAs using corn, cassava, sugar beet juice and sugarcane.[56]

PHA has been produced with limited success on the market mostly due to the high production costs and instability of thermo-mechanical properties resulting from changing molecular weights and structures, which are related to varying the PHA synthase activity.[57] The mechanical properties and biocompatibility of PHA can also be changed by blending, modifying the surface or combining PHA with other polymers, enzymes and inorganic materials, allowing a wider range of applications.

Although 300 types of natural PHA producers have been identified, only a few bacteria have been adopted for commercial production of PHA. Such bacteria, including *Alcaligenes latus*, *Bacillus megaterium*, *Cupriavidus necator* and

Pseudomonas oleovorans, are found to convert different kinds of carbon sources into PHA.[48] The main carbon sources are glucose, fructose and fatty acids, such as lauric acid. In particular, the feedstock cost for PHA production represents half of the overall production cost.[58] An enormous number of studies have been conducted to find low-cost feedstock for PHA production on the industrial scale. Although food waste is a good initial feedstock for the production of bioplastics, it must be pre-treated to improve or modify the physicochemical and biological properties.[59]

Gerngross and co-workers reported for the first time the *in vitro* production of PHB.[60] This finding brought a new perspective and insight into economical processes for the synthesis of PHAs using enzymes as a catalyst and will offer the possibility of carrying out reactions in aqueous solution, which is a cheaper and more environmentally benign medium. Unusual PHAs can be synthesized from a wide range of substrates mediated by commercially available enzymes, such as lipases and cutinases. Major disadvantages of this approach include high consumption of organic solvents, a progressive increase of medium viscosity over time and relatively low Mw of the obtained polymers.[61] To commercialize the enzymatic process, the production and purification costs of the enzyme need to be reduced.[62] Today industries are still using the more robust and conventional way to synthesize PHAs, which is microbial fermentation.

Three techniques have been investigated, including mechanical, chemical and biological recycling.[63] PHAs can be mechanically recycled with some loss of molecular weight and mechanical properties.[64] Recently, PHBV was mechanically recycled by Zaverl *et al.*,[65] showing that PHBV is recyclable for up to five cycles because the reprocessing cycles did not significantly affect the mechanical properties (tensile and flexural testing, and impact toughness). The main disadvantage of mechanical recycling is that it is not applicable for the collected bioplastics from waste, which is expected to be heterogeneous. Chemical recycling of PHAs by thermal degradation has resulted in a transformation of PHAs into vinyl monomers.[66] Ariffin and co-workers used alkali earth compound catalysts (CaO and $Mg(OH)_2$) to enforce smooth and selective degradation of the polymer at a lower temperature. The obtained monomers, crotonic acid and 2-pentenoic acid, were then used as feedstock for the production of poly (crotonic acid-*co*--acrylic acid) through copolymerization.

PHAs are an appropriate candidate for biological recycling as their biodegradation can occur under both aerobic and anaerobic conditions.[67,68] Numerous bacteria, streptomycetes, and fungi isolated from different terrestrial and aquatic environments produce extracellular PHA depolymerases in order to hydrolyze solid PHA into water-soluble monomers or oligomers to be used as nutrients.[69] In this sense, many scl-PHA depolymerases have been purified and characterized in contrast to a limited number of mcl-PHA depolymerases. It is very difficult to

compare the activities of PHB depolymerases because of the various set of conditions used in the tests. Martinez-Tobon and co-workers compared the activity of strains with proven and predicted PhaZ activity for PHB film degradation, which helped to identify strains displaying high degradation activity. The strains *Crupriavidus* sp. and *Comamonas testosteroni* 31A showed the highest percentage weight loss after 7 days, 90 and 53 %, respectively.[70] There are some examples of highly tolerant enzymes in harsh conditions such as PhaZs depolymerases from *C. testosteroni* YM1004, *Schlegelella* sp. KB1a, *Schlegelella thermodepolymerans*, *Streptomyces* sp. IN1 and *Thermus thermophilus* HB8. These biocatalysts could be employed in the degradation of polymers from industrial wastes that may require high pH and/or temperatures since polymer solubility is increased and microbial contamination is reduced.[71]

Several factors can influence the time needed for total biodegradation, including polymer characteristics, surrounding conditions, and the type of degrading organisms. The "real-life tests" separate composting, soil burial and field-testing.[68] In a study by Hablot *et al.*, the degradation of PLA/PHA non-woven mulches was performed using simulated weathering. At 63 °C, the repetition of UV irradiation and the water spray system promoted the degradation of the PLA/PHA blend and molecular weight loss of 90 % was achieved after 180 days.[72] When the PHB films were immersed in the sea at a depth of 1.5 m, their weight loss after 4 weeks was about 90 %. On the contrary, the biodegradation in seawater by the laboratory test method for 4 weeks was around 50 %.[73] Biodegradation tests performed in artificial environments lack transferability to real conditions and, therefore, there is the necessity of environmentally authentic and relevant field-testing conditions.

In the patent base for the last 10 years, a great number of innovations related to the advancement of the PHA production process have been described (Table S-III). Many inventions are focused on downstream feedstock costs (WO2014032633A1, US20190360008A1). The microbial production of PHA copolymers from two raw materials (sugar cane and sugar beet) containing sucrose is disclosed (EP2780461A1). Isolation of new PHA-producing microorganisms and genetic modification of existing ones is also the purpose of many inventions. In WO2012149162, the organisms are engineered to efficiently utilize ethanol (or in some cases xylose) as the carbon source to produce a range of PHA copolymers in a cost-effective yield.

The process of producing monomers from PHA by depolymerisation is the focus of many inventions (CN104328062A, WO2016085396A1). A method for efficiently decomposing PHA and converting it to biogas containing methane as the main component, particularly under anaerobic conditions, was disclosed by Kaneka (WO2015122190A1). Additionally, major PHA producers disclosed several patents related to the improvement of the production process, processing,

and functional modification of PHAs (US2017369908A1, WO2018021046A1, and US2020109423A1).

2.3. Starch and cellulose

The interest in polysaccharides as biomaterials has been increasing continuously during the past decade owing to their applications in pharmaceuticals, biomedical use, food supplements, and cosmetics. The fact that these polymers, such as cellulose and starch, are extracted from natural resources has led to the impression of good biocompatibility and biodegradability.[74]

Starch is a well-known, versatile, inexpensive and primary energy reserve polysaccharide in plants. Generally, the native starch isolated from different plants tends to have limited shear resistance, thermal resistance, thermal decomposition, and a high tendency toward retrogradation. Additionally, starch dissolves in the aqueous media, and it shows low mechanical and shapes stabilities in liquids. To overcome these limitations, starch can be combined with stable, synthetic, thermoplastic polymers.[75] For example, pairing starch with PCL resulted in improved processability of starch, reduced high stiffness, and overcome high moisture sensitivity of starch, which is one of the greatest weaknesses of starch as a biomaterial. On the other hand, starch improves the biodegradability of PCL and, as the cheapest biomaterial on the planet, starch can substantially lower the high cost of the final product.[76,77] Development of starch blending techniques tends to be more interesting while potential applications are extensive and they can be able to substitute an older material that exhibits the same properties. Among its tissue-engineering applications, starch is most famous for its use in generating scaffolds for bone regeneration due to its bone-bonding behaviour when reinforced with hydroxyapatite, good mechanical properties, non-cytotoxic and biocompatible nature, excellent support for cell adhesion, and thermoplastic behaviour when combined with thermoplastic polymers.[78,79]

The plant material is grounded in water, the debris is filtered from the slurry, and starch granules are obtained after centrifugation from the suspension.[80] The content of amylose and amylopectin in starch varies and largely depends on the starch source. Typically, the amylose content is between 18–28 %. The ratio of amylose and amylopectin in the starch may affect starch behaviour during processing and the properties of the end product. As the amylose content increases, the crystallinity of starch-based products increases as well, resulting in texture firming.[81] Several techniques may be applied to develop starch-based biomaterials with improved properties: thermoplasticization, cross-linking, esterification and blending with different polymers.

Most of the starch produced worldwide is derived from corn but other types, such as cassava, sweet potato, potato and wheat starch, are also produced in large amounts.[82] Italy-based Novamont is a manufacturer of starch-based plastic called Mater-Bi used to make BioBag branded certified compostable bags (Table II).

BioBag® is the world's largest brand of certified compostable bags and films made from Mater-Bi. SpudWare® was one of the first bioplastic starch-based cutleries brought to the market. It stood out for its ability to withstand high heat. BioMass Packaging® uses TSP to manufacture water-soluble packing (http://www.biomasspackaging.com/education/bioplastics/). Some fishing hooks are also made from starch-based polymers. Since corn starch can absorb 1000 times its weight in moisture, it is used for disposable diapers (Tethis™), fuel filters to remove water (Super Absorbent Co.), and as a treatment for burns (Sonett).[83]

Cellulose is the most abundant renewable resource on the planet and the major structural component in plant cell walls. Besides plants, some species of bacteria and algae produce cellulose. In general, cellulose, regardless of the source, is a highly crystalline and high molecular weight biopolymer and is, usually, fibrous, tough and hydrophilic but insoluble in water and other common solvents. The chemical structure of cellulose makes it suitable to form hydrogels, which are used in tissue engineering, cartilage modelling, bone implantation, cell culture scaffolds, enhanced drug delivery, heavy metal absorbance and for retaining soil water and efficient fertilizer release for agricultural efficiency. Due to its abundance, cellulose can serve as a virtually inexhaustible source of raw material in the production of sustainable bioproducts.[84,85] Nanocomposites of cellulose have revolutionized the medical field and are being used in tissue engineering, ligament engineering and wound healing. In addition, cellulose-based ethanol production helps to reduce the pressure on conventional energy sources.[86,87] As its anhydroglucopyranose unit contains reactive hydroxyl groups, cellulose has potential use in the design of advanced polymeric materials. So far, most of the industrial modifications of cellulose to improve its properties have been cellulose esters, ethers and graft copolymers, obtained by exchange of the hydroxyl groups of the cellulose molecules.[88]

Cellulose can be produced by two means: natural synthesis procedures including plant photosynthesis and microbial synthesis.[89] Cellulose is present in small quantities in all brown algae, and most of red and golden algae. The most effective producers of bacterial cellulose (BC) are *A. xylinum*, *A. hansenii* and *A. pasteurianus.*[90–92] BC is chemically pure, free of lignin, hemicellulose and pectin. Current methods of BC production include static culture, submerged fermentation through aerated or agitated cultivation and airlift bioreactors.[93] In static cultures, BC is formed at the liquid–air interface as hydrogel-like membranes, with thickness from millimetres to centimetres. The microfibrillar structure of BC is responsible for most of its properties, such as high tensile strength, high crystallinity index and higher degree of polymerization.[94,95] The modification of BC can be performed during its biogenesis by the introduction of different substances into the BC-producing growth medium or by modification of bacterial cells. The other approaches for modification of cellulose (plant or bacterial) inc-

lude the use of physical factors, such as ultrasound irradiation (or sonication), static magnetic field (SMF), or rotating magnetic field (RMF) exposure. BC can be modified by cultivation with an $AgNO_3$ solution, which results with the BC membrane containing silver nanoparticles. The new properties of BC can also be achieved by incorporating reinforcing particles into the membrane structure.[96,97]

It is challenging to estimate the time that cellulosic material will be available to microbial degradation because of the limited number of microbial organisms able to degrade solid cellulose and due to different crystalline forms of cellulose. As a result, microbial degradation of solid cellulose can often be the rate-limiting step. The deconstruction of cellulose contained in the plant cell wall requires the action of specific enzymes able to release degradation products from this substrate.[98] Enzymatic degradation of cellulose is generally performed by hydrolases. Biodegradation of cellulose wastes by fungal or bacterial enzymatic activities represents a large area of research experiments concerning the influence of different physical and biochemical factors.[99]

NatureFlex™ by Futamura (Japan) is a major source of renewable cellophane film (natural biopolymer made of cellulose from plants). Nature Flex bags generally degrade in several weeks in a home compost pile or a commercial compost facility. BioMass Packaging carries cellophane products made with Nature Works LLC, a 100 % cellulose biopolymer with excellent oxygen, grease, oil and moisture barrier characteristics. They are used as packaging films for bakery product wraps, other food wraps, and food-grade transparent bags. Bioprocess®, XCell® and Biofill® are bacterial cellulose-based products already available commercially for topical application in wound healing,[100] http://www.biomass-packaging.com/education/bioplastics/). BC is extensively used in the food industry, packaging and acoustic diaphragms for audio speakers and headphones. Large surface area and great absorbance properties enable the use of very low BC concentrations/amounts to form excellent binding, thickening and coating agents. Papers that are coated with BC are extremely strong and smooth as the coating protects the underlying fibres from moisture.[101]

The biodegradation of starch-based materials depends on the starch processing method used as well as on the biodegradability of other components. The main elements in biodegradability testing are the incubation of the sample under conditions conducive to microbial attack and/or their enzymes, and evaluation of the degree of degradation. Polyvinyl alcohol (PVA) and starch are biodegradable in some microbial environments: they are compatible and their blends present good film properties. Several wheat starch/PVA/glycerol blends prepared using the solution casting technique under ISO 14855 were examined by composting for 45 days. Starch and glycerol were absolutely degraded while PVA appeared practically intact.[102] The biodegradation of co-extruded starch/PLA films was studied in liquid, inert solid, and composting media using experimental ISO

methods. The percentage of mineralization in the compounds was higher than the minimum required 60 % that allows a compound to be classified as biodegradable. Researchers found that the addition of starch enhanced the biodegradation of the PLA component, especially in liquid media.[103] Studies also showed that ternary blends composed of PLA, PCL, and starch buried in soil degraded rapidly in the first 8 weeks.[104]

Biodegradability of cellulose is dependent on the degree of crystallinity, structure, functional groups, cross-linking and molecular weight of the cellulose.[105] Two general types of substrates were used to measure the biodegradation of cellulose: relatively unaltered natural substrates (pure crystalline cellulose or biomass) and modified cellulosic substrates (substituted or dyed celluloses). Studies showed that PHB/BC composite biodegraded at a greater rate and extent than those of PHB alone, reaching 80 % degradation after 30 days, whereas PHB did not reach this level of degradation until close to 50 days of composting.[106,107] Even though the biodegradation of some cellulose samples have been studied, there is still a lack of a comprehensive study on the biodegradability of a variety of cellulose-based packaging materials that could potentially replace synthetic packaging films.[108]

A list of patents related to starch and cellulose is presented in Table S-IV of the Supplementary material. The process described in WO2017130106A1 relates to the production of starch from microalgae, which is more efficient in comparison to the conventional production. Method of producing a starch-based biodegradable polymer, using processed cannabis waste as the carbon source, is described in WO2020037394A1, while the process for producing biodegradable plastic from renewable resource-based agricultural by-products is covered in WO2019155398A1. Patent WO2018125897A1 is related to the production of material formed from one or more starches, a plasticizer and water, resulting in improved sustainability, biodegradability and increased strength. CN102585485B relates to the preparation of a composite material (starch combined with thermoplastic polyurethane). This material has the advantages of high mechanical property, low cost, biodegradability and the preparation process is simple. WO2016138593A1 also covers the potential of starch to combine with one or more biodegradable polymers (PCL, PBS, PLA, and PHA) in order to obtain biocomposites with tailored properties. WO2018041779A1 and WO2020034958A1 describes the application of starch and its modifications in food packaging using low tensile strength products, while WO2017091463A1 provides methods for making coated particles using different kinds of starch. Patent WO2019209834A1 relates to new additive materials that are physically blended with polymeric materials, such as starch, to impart biodegradability to polymers that are not otherwise biodegradable. Patent WO2020014762A1 relates to the production of a nanocellulosic material based on fractioning a cellulosic pulp stream originating

from pre-treatment or mechanical defibrillation. WO2019221535A1 presents a method for the manufacture of crystal nanocellulose and WO2020015884A1 describes a device and a method for producing nanocellulose from natural raw materials. WO2017160218A1 also relates to a method of manufacturing a cellulose product from cellulose fibres. On the other hand, bacterial cellulose production on cassava bagasse as a suitable feedstock and its processing is covered in WO2016029432A1. Methods for the production and processing of multi-phase biomaterials based on bacterially synthesized nanocellulose are presented in WO2016113400A1. WO2017192476A1 presents an invention that provides a pulp product with nanocellulose as a tool for improving the strength properties. Cellulose derivative with excellent thermoplasticity, waterproofness, elastic modulus and impact strength and its production method are presented in WO2017061190A1. Patent WO2018187782A1 provides a method for the modification of the surface of polymer-based materials (bacterial nanocellulose, nanocellulose and a cellulose derivative) and compositions generated thereby. WO2016174104A1 relates to the use of a bacterial nanocellulose composite in chip technology and material engineering, and furthermore, for medical purposes (skin, tissue or neuro transplant). WO2020035734A1 is also connected with medical usage of cellulose nanofibrils describing a method of producing a three-dimensional autologous fat graft.

2.4. Poly(butylene succinate) (PBS)

PBS is an aliphatic biodegradable polyester produced by polycondensation from two raw materials: succinic acid (SA) and 1,4-butanediol (BDO). The mechanical properties of PBS are similar to those of low-density polyethylene (LDPE) or polypropylene (PP)[109,110] but it can be biodegraded in contrast to LDPE and PP.[111] Beside the production of PBS by polycondensation, recently, a lipase-catalysed synthesis of PBS was developed.[112] PBS synthesized by lipase has a narrower polydispersity index than that synthesized by polycondensation, but the remaining lipase may cause a problem in the subsequent thermal processing.[112]

In the beginning, PBS was a biodegradable but petro-based polyester, while currently, large plants for producing renewably sourced SA have been developed and Mitsubishi commercializes bio-based PBS (bio-PBS) that is obtained using bio-based SA (bio-SA). Furthermore, bio-based BDO (bio-BDO) can also be produced on an industrial scale. Nowadays, products of 100 % bio- PBS can be found on the markets. Bio-PBS is produced in various demo and pilot plants, mainly from sugarcane and cassava monomers.[113] The production of bio-PBS includes the productions of BDO and SA, and the production of BDO includes the production of bio-ethanol and SA (Argonne National Laboratory, 2014).[113] The production of bio-ethanol using sugarcane is separated into three major stages: the sugarcane plantation, the conversion of sugarcane into molasses by

sugar milling and refining, and the processing of molasses into bio-ethanol by fermentation.[113] In a more recent study, a novel, nonphosphorylative pathway was used to convert biomass sugars to BDO with a 100 % theoretical maximum molar yield.[114] In this pathway, assimilation of sugars into the TCA cycle is allowed and afterward built of artificial biosynthetic pathways to BDO using the enzymes 2-ketoacid decarboxylases and alcohol dehydrogenases.[114] Bio-SA is mainly produced by several microorganisms as a fermentation product. In 2008, Bioamber built the first plant that uses *Escherichia coli* as the host microorganism and wheat-derived glucose as the substrate for SA production. Four years later, Reverdia, a joint venture between DSM and Roquette, started production of bio-SA from starch using low-pH yeast technology, and Myriant Technologies set up a SA plant with a production capacity of 30 million pounds from unrefined sugars as feedstock using *E. coli* as the host organism.[115] Derived from natural resources, such as sugarcane, cassava and corn, bio-PBS is compostable into biomass, carbon dioxide and water. There are already several producers with existing commercial capacities for the production of bio-PBS and additional dedicated and non-dedicated capacities are expected to start up in the coming years (Table S-V). Bio-PBS is currently being employed in a wide range of industries, such as packaging, agriculture, pharmaceutical, consumer goods, electronics and electrical, textile, automotive and interiors.[116] It is also utilized to produce bowls, plates, plastic utensils, and diapers.[116] Amongst others biopolymers, bio-PBS has strengths in flexibility, natural fibre compatibility, heat resistance and biodegradability under specific conditions (according to DIN EN 13432). It was found that PBS polymer was more ductile if some adipic acid/lactic acid or some other monomer was added during the standard polymerization of SA and BDO.[117] These results indicate that copolymerization of PBS is essential for improving its characteristics. Depending on the monomer and the stereochemical nature of the monomer, different PBS (bio-PBS) copolymers have been registered, such as: PBSA (poly(butylene succinate-*co*-adipate)), PBST (poly(butylene succinate-*co*--terephthalate)), PBSF (poly(butylene succinate-*co*-fumarate)), PBS-DLS (poly-(butylene-succinate-dilinoleic succinate), P(BS-BMS) poly(butylene succinate-*co*-butylene 2-methylsuccinate), PBS-PLA blends, *etc*. Amongst the different possibilities for PBS copolymers, PBSA, PBST and PBS-PLA blends are the most commonly mentioned in the literature. PBSA copolymer is better degraded than PBS due to its lower crystallinity and glass transition temperature,[118] and together with PBS it was manufactured under the trademark Bionolle® (series 1000 and 3000, respectively) by Showa Highpolymer Co., Ltd. for application as trash bags, plant pots, filaments, bottles, gloves, containers, laminated paper, trays, *etc.*[71] PBST copolymer has a lower crystallinity than PBS, but biodegrades more slowly in contrast to PBSA.[111] PBST like other aliphatic-aromatic copolymers may be used as a film or coating in disposable food packaging. PBS–PLA

blends with low toxicity have potential in food packaging, biomedicine and agricultural markets.[119] Commercial PBS-PLA blends have been utilized for production of food service ware by NatureWorks LLC.[64] Based on extensive research, PBS-PLA blends have been successfully modified and processed into fibres, blown films, flat films, and sheets.[25] PBS and its copolymers are biodegradable in lipase solution, soil burial, water, activated sludge and compost.[120–122]

Currently, about 75 % of plastic waste is disposed in sanitary landfills and about 25 % is recycled.[123] In general, bioplastics can degrade under anaerobic conditions in landfills releasing methane, but with a proper composting facility, bioplastics can be converted to compost and recycled.[124] Recycling of plastic waste and bio-based waste, such as bio-PBS, may be realised through several processes: mechanical, chemical and organic processes. Chemical recycling of bio-based PBS and its copolymers is environmentally harmful, thus the use of polyester-degrading enzymes is an eco-friendly alternative. Many hydrolases from several fungi and bacteria have been discovered and successfully evaluated for their activity against different aliphatic and aromatic PBS polymers and copolymers.[71,125] Bio-PBS produced by PTT MCC Biochem has industrially compostable and home compostable grades, but the current grade used for paper coating is only industrially compostable.[126] Bio-PBS can be easily separated from paper when soaking under water without damaging the paper pulp, which can be recycled to produce paper again, or as backyard compost, or in the case of a leak to the environment, it will degrade eventually in a limited time.[126] Testing the degradation phenomena of bio-PBS plastics in the environment can be classified into three categories: field tests, simulation tests, and laboratory tests.[127] The performed degradation studies of a commercially available PBS and PBSA copolymer in various environments have shown that the most favourable degradation environment was compost, which contains microorganisms and natural enzymes that support degradation.[128] In these studies, degradation after four to six weeks was observed, followed by a strong mass loss in the compost, due to interaction with enzymes. In addition, the strength of polymers was significantly reduced. Biodegradation test in soil gave the same results as biodegradation in compost, but the changes in the molecular parameters were less intense because of the lower concentration of microorganisms, enzymes and lower temperature of the process.[128]

According to the patents base, in the last 10 years, most patents are based on bio-PBS biodegradability. Mostly, patents deal with the promotion of methods for preparing new bio-PBS materials having improved mechanical properties, compatibility, control of degradation rate, and effective reduction of the cost of bio-PBS production (CN109608835A, CN103709688A, CN110240788A, CN109867921A, CN106589854B and CN105670248A). Bio-PBS materials with improved properties have been used through patents in the last 10 years mainly in

the form of coated paper, synthetic fibre, trash bag, coffee capsule cutlery, *etc.* (US20180058010A1, US20140021574A1, WO2010151798A2 and WO2016105217A1).

2.5. Bio-polyethylene (Bio-PE)

PE consists of long chains of ethylene and it is produced as either HDPE or LDPE, or linear low density polyethylene (LLDPE).[129] PE is chemically synthesized by polymerization of ethane.[129] Bio-based PE (bio-PE) is chemically identical to fossil-based PE, it has the same technical properties and is not biodegradable.[130] Bio-PE is used to produce high value products using low pollution processes and contributing to the global environmental balance. The process involves: pre-treatment, enzymatic scarification, fermentation, dehydration and polymerization.[131] The ethanol produced by fermentation from renewable resources can be used as a raw material for polyethylene production. Production of bio-PE from renewable resources consists of three steps:[130]

1) synthesis of ethanol by a fermentation process from sugars, extracted from natural materials, *e.g.*, sugarcane;

2) chemical dehydration reaction transforming of ethanol into ethylene;

3) "classical" reaction of polymerization of ethylene into polyethylene to make the various grades of PE (HDPE, LDPE, LLDPE).

Bio-based PE produced this way is used in packaging applications, such as carrying bags, plastic films and bottles, automotive fuel tanks, injection melded parts, tubes.[132] The most used PE copolymer is HDPE. HDPE is a rigid polymer with polymer chains packed closer one to other resulting in greater intermolecular forces. The presence of a strong intermolecular forces results in a dense, highly crystalline material form. It is a relatively tough and resistant polymer that can withstand high temperatures, up to 120 °C, without any effect on the properties of the material. Furthermore, HDPE is an extremely resistant material to many chemicals, hence its widespread use in healthcare and laboratory environments. It is resistant to many acids, alcohols, aldehydes, esters, bases and oils. The Braskem Company is the world-leading supplier of bio-PE (HDPE, LDPE and LLDPE) and the current Braskem bio-PE grades are mainly targeted towards food packaging, cosmetics, personal care, automotive parts and toys, but there are many other companies in the world producing bio-PE (Table S-VI.). Bio-PE is a bio-based polymer but it is not biodegradable. It is well known that polyethylene is resistant to degradation due to its chemical and biological inertness, which is the result of its high molecular weight, three-dimensional structure and hydrophobic nature, all of which interfere with polyethylene availability for the action of microorganisms, light, water, *etc*. According to some research,[133,134] the addition of antioxidants and stabilizers protects polyethylene against oxidation at the production stage, which further increases its resistance to degradation.

The degradation of a commercial environmentally degradable PE was investigated in two stages: firstly, by abiotic oxidation in an air oven to simulate the effect of the compost environment and secondly, in the presence of selected microorganisms.[135,136] It was observed that microbial growth occurred in the presence of PE samples that had been compression moulded to thick sections but had not been deliberately pre-oxidized. Changes in the molecular weight distribution occurred after preheating in air at 60 °C and not at ambient temperatures, but colonization of microorganisms occurred on all samples.[135] Also, erosion of the film surface was observed in the vicinity of the microorganisms and the decay of oxidation products on the surface of the polymer film was found to be associated with the formation of protein and polysaccharides, due to the growth of microorganisms (*Rhodococcus rhodochrous* ATCC 29672, *Cladosporium cladosporoides* ATCC 20251, *Nocardia asteroides* GK 911).[135,136] Nowadays, bio-PE is accepted for recycling in many recycling centres, especially HDPE. The recycling process consists of the collection and separation of the plastic using sink–float separation or Near-Infrared Radiation (NIR) techniques, then homogenization and melting of the plastic, and finally cooling the plastic into pellets that can be reused for the production of, for example, toys, rope, piping *etc*.[137] Recycling HDPE has many benefits, such as cost-efficiency of the manufacture of a product from recycled HDPE instead of producing "virgin" plastic.

According to the base of patents in the last 10 years, most patents are based on PE biodegradability and recycling. Patents are focused on improving PE materials (HDPE, LDPE) in terms of advancing their mechanical properties and production of materials with a simple structure that is easy to recycle. Many patents have marketed products, such as blow moulding, injection moulding and foam products, which showed that new materials of excellent quality and biodegradability can be produced from recycled PE materials (CN207467268U, US9593177, US9637626B2 and US2016/0108217A1). Analysing the commercial application of patents over the last decade, it has been shown that bio-PE has found application in bags, boxes, bottles, toys, pipes, *etc.* (Table S-VI).

3. (BIO)DEGRADATION AND RECYCLING OF BIOPLASTICS

In January 2018, the EU released its vision for a more sustainable plastics industry to be achieved by 2030. The new plastics strategy states that 100 % of plastics should be either reusable or recyclable by 2030. Prevention, re-use, collection and recycling should always be the first choice in efforts to achieve some of these goals. As mentioned, to overcome both oil dependence, price fluctuations and enhance resource efficiency, bioplastic materials constitute an applicable route that has to be explored as a part of the solution. Plastics that are currently marketed as "biodegradable" will themselves contribute to plastic pollution if they are lost or littered. They do not break down as quickly and completely

in the environment and can thus harm wildlife and ecosystems. To reinforce the positive impact of bioplastics, successful recycling strategies also need to be clearly proposed and applied. In general, the purpose of recycling is to convert the production of postconsumer waste into building blocks for the production of new polymers.

The degree of biodegradation varies with temperature, polymer stability, and available oxygen content. Consequently, most bioplastics will only degrade in the tightly controlled conditions of industrial composting units. Apart from starch-based bioplastics, in compost piles or simply in the soil/water, most bioplastics will not degrade.[138] Bioplastics are still plastics and being made from plants or having the potential to biodegrade under limited conditions does not make them "planet-safe". Presently, there is a need for more transparency about environmental claims of bioplastic products. A ban on labelling plastic products as "biodegradable" or as "compostable", unless they meet strict standards, is urgently needed. There are currently few international organizations that have established standards and testing methods for compostability,[139] namely:

- American Society for Testing and Materials – ASTM-6400-99,
- European Standardization Committee (CEN) – EN13432,
- International Standards Organization (ISO) – ISO14855 (only for biodegradation),
- German Institute for Standardization (DIN) – DIN V49000.

The ASTM, CEN and DIN standards specify the criteria for biodegradation, disintegration and eco-toxicity in order for a plastic to be called compostable.

Biodegradability is determined by measuring the amount of CO_2 produced over a certain period by the biodegrading plastic. The standards require 60 % conversion of carbon into carbon dioxide within 180 days for resins made from single polymer and 90 % conversion of carbon into carbon dioxide for copolymers or polymer mixes.

Disintegration is measured by sieving the material to determine the biodegraded size and less than 10 % should remain on a 2 mm screen within 120 days.

Eco-toxicity is measured by having concentrations of heavy metals below the limits set by the standards and by testing plant growth by mixing the compost with soil in different concentrations and comparing it with controlled compost.

The EN 13432 industrial standard is arguably the most international in scope and compliance with this standard is required to claim a product be compostable in the European market. In summary, it requires biodegradation of 90 % of the materials in a laboratory within 180 days. The ASTM-6400 standard is the regulatory framework for the United States and sets a less stringent threshold of 60 % biodegradation within 180 days, again within commercial composting conditions.

The most accurate standard test method for anaerobic environments is the ASTM D5511 – 02 Standard Test Method for Determining Anaerobic Biodeg-

radation of Plastic Materials under High-Solids Anaerobic-Digestion Conditions. Another standard test method for testing in anaerobic environments is the ASTM D5526 – 94(2002) Standard Test Method for Determining Anaerobic Biodegradation of Plastic Materials under Accelerated Landfill Conditions. However, this latter test has proven extremely difficult to perform. Both of these tests are used for the ISO DIS 15985 on determining anaerobic biodegradation of plastic materials.

It should be born in mind that none of the standards for plastics labelled as biodegradable or compostable today makes them suitable for disposal in the open environment. However, currently, the most likely destination of many biodegradable products is the landfill as numerous composting facilities focus on food scraps and either will not accept biodegradable packaging or will still frequently screen it along with other plastics for shipment to a landfill. The environmental consequences of land filled biodegradable materials have led some researchers and advocates to push for more universal access to compost collection, as well as to the development of altogether new materials.[7,140]

As mentioned, PLA needs industrial composting conditions for biodegradation, including temperatures above 58 °C. It needs to be properly managed and routed to specialized industrial composting or recycling facilities. Under the right circumstances, microorganisms can turn the material into carbon dioxide and water within a couple of weeks. However, if it becomes littered or dumped, PLA remains for much longer. When pure PLA ends up in seawater, it does not seem to biodegrade at all. Other kinds of bioplastics are known to better biodegrade in marine environments.[141] However, whether that really happens in a specific case, and how long it will take, is highly unpredictable.

Improved recycling strategies have to be developed for bioplastics. In particular, bio-based polyesters (PLA, PHA/B and PBS) have demonstrated the potential for either mechanical or biochemical recycling.[63] Ongoing research includes bio-upcycling efforts[142] as well as improvement of chemical recycling processes.[143] On the other hand, research is intensive on the side of material design, where molecular triggers are explored.[19]

4. CONCLUSIONS

Bioplastics are a large family of materials with widely varying properties. As with conventional plastics, the end-of-life options depend entirely on the application, the way the product is disposed of by its user, and the available infrastructure in the region where the product is being disposed. Therefore, “biodegradable”, a magic word for environmentally minded consumers, is not always a green magic bullet. Claims that bioplastics reduce environmental impact still lack sufficient evidence.[140] Whether bio-based plastics are more sustainable than fossil-based ones, and what contribution they could have as a building block for

sustainable development of an innovative bioeconomy, still cannot be answered conclusively due to insufficient data.[140] It is evident that there is a lot of branding around biodegradability and that a demand for biodegradables continues to climb – with packaging, take-out containers, even designer jeans and athletic shoes now carrying this designation. It is important that consumers do not allow biodegradable marketing tactics to influence their purchasing decisions and to trade one set of environmental problems with another. It is evident that bioplastics will not solve the plastic waste crisis, so tackling consumption remains the key.

ABBREVIATIONS

3HH	3-hydroxyhexanoate
3HD	3-hydroxydecanoate
3HO	3-hydroxyoctanoate
3HP3	hydroxypropionate
3HV	3-hydroxyvalerate
4HB4	hydroxybutyrate
BC	bacterial cellulose
BDO	1,4-butanediol
bio-BDO	bio-based 1,4-butanediol
bio-PBS	bio-based poly(butylene succinate)
bio-PE	bio-based polyethylene
bio-PET	bio-based poly(ethylene terephthalate)
bio-PTT	bio-based poly(1,3-propylene terephthalate)
bio-SA	bio-based succinic acid
HDPE	high-density polyethylene
IUPAC	International Union of Pure and Applied Chemistry
LDPE	low-density polyethylene
LLDPE	linear low density polyethylene
mcl-3HA	medium-chain - length 3-hydroxyalkanoates
NIR	near-infrared radiation
PBAT	poly(butylene adipate terephthalate)
PBA	poly(butylene adipate)
PBS	poly(butylene succinate)
PBSA	poly(butylene succinate-*co*-adipate)
PBST	poly(butylene succinate-*co*-terephthalate)
PBSF	poly(butylene succinate-*co*-fumarate)
PBS-DLS	poly(butylene-succinate-dilinoleic succinate)
P(BS-BMS)	poly(butylene succinate-*co*-butylene 2-methylsuccinate)
PCL	poly(caprolactone)
PE	polyethylene
PET	poly(ethylene terephthalate)
PHA	polyhydoxyalkanoate
PHB	poly(hydroxybutyrate)
PHBV	poly(3-hydroxybutyrate-*co*-3-hydroxyvalerate)
PLA	poly(lactic acid)
PP	polypropylene

PS	polystyrene
PTT	poly(1,3-propylene terephthalate)
PUR	polyurethane
PVA	poly(vinyl alcohol)
PVC	poly(vinyl chloride)
SA	succinic acid
scl-3HA	short-chain-length 3-hydroxyalkanoates
TPS	thermoplastic starch

SUPPLEMENTARY MATERIAL

Additional data are available electronically at the pages of journal website: https://www.shd-pub.org.rs/index.php/JSCS/index, or from the corresponding author on request.

Acknowledgements. This project has received funding from the European Union's Horizon 2020 research and innovation programme under grant agreement No. 870292 (BioICEP).

ИЗВОД

РАЗУМЕВАЊЕ БИОПЛАСТИЧНИХ МАТЕРИЈАЛА: ТРЕНУТНО СТАЊЕ И ТРЕНДОВИ

САЊА ЈЕРЕМИЋ[1], ЈЕЛЕНА МИЛОВАНОВИЋ[1], МАРИЈА МОЈИЋЕВИЋ[2], САЊА ШКАРО БОГОЈЕВИЋ[1] и ЈАСМИНА НИКОДИНОВИЋ-РУНИЋ[1]

[1]*Институт за молекуларну генетику и генетичко инжењерство, Војводе Степе 444а, 11042 Београд и* [2]*Атлон технолошки институт, Dublin Road, Athlone, Co. Westmeath, Ireland*

Загађење пластиком сада се сматра једном од највећих претњи по животну средину по људе. Развој биополимерних материјала може бити део решења јер биопластика укључује и неразградиве и биоразградиве материјале, а обе су важне за одрживи развој. Биопластични материјали се у овом моменту дизајнирају тако да имају минималан угљенични отисак, високу могућност рециклирања и потпуну биоразградивост. Овај преглед приказује недавна дешавања и трендове у области биопластичних материјала. Представљен је низ биопластичних материјала који се најчешће користе: (поли-(млечна киселина) (PLA), поли(хидроксиалканоат) (PHA), скроб, целулоза, поли(бутилен-сукцинат) на бази обновљивих материјала (био-PBS) и полиетилен од обновљивих сировина (био-PE)), укључујући њихову производњу, могућности примене и деградацију.

(Примљено 20. јула, ревидирано 31. августа, прихваћено 4. септембра 2020)

REFERENCES

1. M. Lackner, *Bioplastics*, Kirk-Othmer Encyclopedia of Chemical Technology, John Wiley & Sons, New York, 2015 (https://doi.org/10.1002/0471238961.koe00006)
2. PlasticsEurope, *Plastics – the Facts 2019: An analysis of European plastics production, demand and waste data*, Düsseldorf, 2019
3. T. Thiounn, R. C. Smith, *J. Polym. Sci.* **58** (2020) 1347 (https://doi.org/10.1002/pol.20190261)
4. L. Lu, T. Luo, Y. Zhao, C. Cai, Z. Fu, Y. Jin, *Sci. Total Environ.* **667** (2019) 94 (https://doi.org/10.1016/j.scitotenv.2019.02.380)
5. H. Karan, C. Funk, M. Grabert, M. Oey, B. Hankamer, *Trends Plant Sci.* **24** (2019) 237 (https://doi.org/10.1016/j.tplants.2018.11.010)
6. M. Rujnić-Sokele, A. Pilipović, *Waste Manage. Res.* **35** (2017) 132 (https://doi.org/10.1177/0734242X16683272)

7. S. Spierling, E. Knüpffer, H. Behnsen, M. Mudersbach, H. Krieg, S. Springer, S. Albrecht, C. Herrmann, H.-J. Endres, *J. Cleaner Prod.* **185** (2018) 476 (https://doi.org/10.1016/j.jclepro.2018.03.014)
8. M. Vert, Y. Doi, K.-H. Hellwich, M. Hess, P. Hodge, P. Kubisa, M. Rinaudo, F. Schué, *Pure Appl. Chem.* **84** (2012) 377 (https://doi.org/10.1351/PAC-REC-10-12-04)
9. A. McNaught, A. Wilkinson, *Compendium of Chemical Terminology: IUPAC Recommendations*, Blackwell Science, Malden, MA, 1997 (ISBN 0865426848)
10. P*D CEN/TR 15351: Guide for vocabulary in the field of degradable and biodegradable polymers and plastic items*, 2006
11. G. Kale, T. Kijchavengkul, R. Auras, M. Rubino, S. E. Selke, S. P. Singh, *Macromol. Biosci.* **7** (2007) 255 (https://doi.org/10.1002/mabi.200600168)
12. T. Narancic, S. Verstichel, S. Reddy Chaganti, L. Morales-Gamez, S. T. Kenny, B. De Wilde, R. Babu Padamati, K. E. O'Connor, *Environ. Sci. Technol.* **52** (2018) 10441 (https://doi.org/10.1021/acs.est.8b02963)
13. M. P. Groover, *Fundamentals of Modern Manufacturing: Materials, Processes, and Systems*, Wiley & Sons, New York, 2011 (ISBN: 978-1-118-231463)
14. K. Nehra, P. Jamdagni, P. Lathwal, in *Plant Biotechnology: Recent Advancements and Developments*, S. K. Gahlawat, R. K. Salar, P. Siwach, J. S. Duhan, S. Kumar, P. Kaur (Eds.), Springer, Singapore, 2017, pp. 297 (ISBN 978-981-10-4732-9)
15. R. P. Babu, K. O'Connor, R. Seeram, *Prog. Biomater.* **2** (2013) 8 (https://doi.org/10.1186/2194-0517-2-8)
16. J. E. G. van Dam, B. de Klerk-Engels, P. C. Struik, R. Rabbinge, *Ind. Crops Prod.* **21** (2005) 129 (https://doi.org/10.1016/j.indcrop.2004.02.003)
17. S. Ramesh Kumar, P. Shaiju, K. E. O'Connor, P. Ramesh Babu, *Current Op. Green Sustain. Chem.* **21** (2020) 75 (https://doi.org/10.1016/j.cogsc.2019.12.005)
18. *European Bioplastics* (https://www.european-bioplastics.org/market, accessed July 30th 2020)
19. R. Hatti-Kaul, L. J. Nilsson, B. Zhang, N. Rehnberg, S. Lundmark, *Trends Biotechnol.* **38** (2020) 50 (https://doi.org/10.1016/j.tibtech.2019.04.011)
20. *Bioplastics Market Development Update 2019*, European Bioplastics, 2019
21. M. Jamshidian, E. A. Tehrany, M. Imran, M. Jacquot, S. Desobry, *Compr. Rev. Food Sci. Food Saf.* **9** (2010) (https://doi.org/10.1111/j.1541-4337.2010.00126.x)
22. Y. Wang, Y. Tashiro, K. Sonomoto, *J. Biosci. Bioeng.* **119** (2015) 10 (https://doi.org/10.1016/j.jbiosc.2014.06.003)
23. E. T. H. Vink, K. R. Rábago, D. A. Glassner, B. Springs, R. P. O'Connor, J. Kolstad, P. R. Gruber, *Macromol. Biosci.* **4** (2004) 551 (https://doi.org/10.1002/mabi.200400023)
24. C. Castro-Aguirre, F. Iñiguez-Franco, H. Samsudin, X. Fang, R. Auras, *Adv. Drug Delivery Rev.* (2016) (https://dx.doi.org/10.1016/j.addr.2016.03.010)
25. S. Su, R. Kopitzky, S. Tolga, S. Kabasci, *Polymers* **11** (2019) 1193 (https://doi.org/10.3390/polym11071193)
26. O. Martin, L. Averous, *Polymer* **42** (2001) 6209 (https://doi.org/10.1016/S0032-3861(01)00086-6)
27. R. Turco, R. Ortega-Toro, R. Tesser, S. Mallardo, S. Collazo-Bigliardi, A. Boix, M. Malinconico, M. Rippa, M. Di Serio, G. Santagata, *Coatings* **9** (2019) 574 (https://doi.org/10.3390/coatings9090574)
28. M. P. Arrieta, M. D. Samper, M. Aldas, J. Lopez, *Materials (Basel)* **10** (2017) (https://doi.org/10.3390/ma10091008)
29. C. Diaz, H. Y. Pao, S. Kim, *J. App. Packag.Res.* **8** (2016) (doi: 10.14448/japr.08.0018)

30. S. Su, R. Kopitzky, S. Tolga, S. Kabasci, *Polymers (Basel)* **11** (2019) (doi: 10.3390/polym11071193. (10.3390/polym11071193)
31. Q. Ou-Yang, B. Guo, J. Xu, *ACS Omega* **3** (2018) 14309 (https://doi.org/10.1021/acsomega.8b02549)
32. M. Nofar, D. Sacligil, P. J. Carreau, M. R. Kamal, M. C. Heuzey, *Int. J. Biol. Macromol.* **125** (2019) 307 (https://doi.org/10.1016/j.ijbiomac.2018.12.002)
33. D. Maga, M. Hiebel, N. Thonemann, *Resour. Conserv. Recycl.* **149** (2019) 86 (https://doi.org/10.1016/j.resconrec.2019.05.018)
34. F. Gu, J. Guo, W. Zhang, P.A. Summers, P. Hall, *Sci. Total Environ.* **601**–**602** (2017) 1192 (https://doi.org/10.1016/j.scitotenv.2017.05.278)
35. M. Niaounakis, *Eur. Polym. J.* **114** (2019) 464 (https://doi.org/10.1016/j.eurpolymj.2019.02.027)
36. I. Wojnowska-Baryła, D. Kulikowska, K. Bernat, *Sustainability* **12** (2020) 2088 (https://doi.org/10.3390/su12052088)
37. A. Calmon, S. Guillaume, V. Bellon-Maurel, P. Feuilloley, F. Françoise Silvestre, *J. Environ. Polym. Degrad.* **7** (1999) 157 (https://doi.org/10.1023/A:1022849706383)
38. E. Rudnik, D. Briassoulis, *Ind. Crops Prod.* **33** (2011) 648 (https://doi.org/10.1016/j.indcrop.2010.12.031)
39. M. Karamanlioglu, G. D. Robson, *Polym. Degrad. Stab.* **98** (2013) 2063 (https://doi.org/10.1016/j.polymdegradstab.2013.07.004)
40. A. S. Al Hosni, J.K. Pittman, G. D. Robson, *Waste Manag.* **97** (2019) 105 (https://doi.org/10.1016/j.wasman.2019.07.042)
41. Y. Tokiwa, B. P. Calabia, *Appl. Microbiol. Biotechnol.* **72** (2006) 244 (https://doi.org/10.1007/s00253-006-0488-1)
42. B. G. Kale, R. Auras, S. P. Singh, *Packag. Technol. Sci.* **20** (2007) 49 (https://doi.org/10.1002/pts.742)
43. H. Tsuji, K. Suzuyoshi, *Polym. Degrad. Stab.* **75** (2002) 347 (https://doi.org/10.1016/S0141-3910(01)00240-3)
44. H. Tsuji, K. Suzuyoshi, *Polym. Degrad. Stab.* **75** (2002) 357 (https://doi.org/10.1016/S0141-3910(01)00239-7)
45. G.-Q. Chen, *Chem. Soc. Rev.* **38** (2009) 2434 (https://doi.org/10.1039/B812677C)
46. A. Steinbüchel, H. E. Valentin, *FEMS Microbiol. Lett.* **128** (1995) 219 (https://doi.org/10.1111/j.1574-6968.1995.tb07528.x)
47. A. Anjum, M. Zuber, K. M. Zia, A. Noreen, M. N. Anjum, S. Tabasum, *Int. J. Biol. Macromol.* **89** (2016) 161 (https://doi.org/10.1016/j.ijbiomac.2016.04.069)
48. C. S. K. Reddy, R. Ghai, Rashmi, V. C. Kalia, *Bioresour. Technol.* **87** (2003) 137 (https://doi.org/10.1016/S0960-8524(02)00212-2)
49. Y. Zhong, P. Godwin, Y. Jin, H. Xiao, *Adv. Ind. Eng. Polym. Res.* **3** (2020) 27 (https://doi.org/10.1016/j.aiepr.2019.11.002)
50. S. Y. Li, C. L. Dong, S. Y. Wang, H. M. Ye, G.-Q. Chen, *Appl. Microbiol. Biotechnol.* **90** (2011) 659 (https://doi.org/10.1007/s00253-010-3069-2)
51. A. Mukheem, M. Hossain, S. Shahabuddin, K. Muthoosamy, S. Manickam, K. Sudesh, R. Saidur, N. Sridewi, *Material* **11** (2018) 1673 (https://doi.org/10.3390/ma11091673)
52. I. Zembouai, M. Kaci, S. Bruzaud, A. Benhamida, Y.-M. Corre, Y. Grohens, *Polym. Test.* **32** (2013) 842 (https://doi.org/10.1016/j.polymertesting.2013.04.004)
53. Z. Li, J. Yang, X. J. Loh, *NPG Asia Mat.* **8** (2016) 265 (https://doi.org/10.1038/am.2016.48)

54. S. Godbole, S. Gote, M. Latkar, T. Chakrabarti, *Bioresour. Technol.* **86** (2003) 33 (https://doi.org/10.1016/S0960-8524(02)00110-4)
55. P. Mousavioun, W. O. S. Doherty, G. George, *Ind. Crops Prod.* **32** (2010) 656 (https://doi.org/10.1016/j.indcrop.2010.08.001)
56. K. Dietrich, M.-J. Dumont, L. F. Del Rio, V. Orsat, *Sustain. Prod. Consum.* **9** (2017) 58 (https://doi.org/10.1016/j.spc.2016.09.001)
57. G.-Q. Chen, X.-Y. Chen, F.-Q. Wu, J.-C. Chen, *Adv. Ind. Eng. Polym. Res.* **3** (2020) 1 (https://doi.org/10.1016/j.aiepr.2019.11.001)
58. M. Koller, L. Maršálek, M. M. de Sousa Dias, G. Braunegg, *New Biotechnol.* **37** (2017) 24-38 (https://doi.org/10.1016/j.nbt.2016.05.001)
59. Y. F. Tsang, V. Kumar, P. Samadar, Y. Yang, J. Lee, Y. S. Ok, H. Song, K.-H. Kim, E. E. Kwon, Y. J. Jeon, *Environ. Int.* **127** (2019) 625 (https://doi.org/10.1016/j.envint.2019.03.076)
60. T. U. Gerngross, D. P. Martin, *PNAS* **92** (1995) 6279 (https://doi.org/10.1073/pnas.92.14.6279)
61. A. M. Gumel, M. S. M. Annuar, Y. Chisti, *J. Polym. Environ.* **21** (2013) 580 (https://doi.org/10.1007/s10924-012-0527-1)
62. M. R. Kosseva, E. Rusbandi, *Int. J. Biol. Macromol.* **107** (2018) 762 (https://doi.org/10.1016/j.ijbiomac.2017.09.054)
63. D. H. Vu, D. Åkesson, M. J. Taherzadeh, J. A. Ferreira, *Bioresour. Technol.* **298** (2020) 122393 (https://doi.org/10.1016/j.biortech.2019.122393)
64. A. Soroudi, I. Jakubowicz, *Eur. Polym. J.* **49** (2013) 2839 (https://doi.org/10.1016/j.eurpolymj.2013.07.025)
65. M. Zaverl, M. Ö. Seydibeyoğlu, M. Misra, A. Mohanty, *J. Appl. Polym. Sci.* **125** (2012) E324-E331 (https://doi.org/10.1002/app.36840)
66. H. Ariffin, H. Nishida, M. A. Hassan, Y. Shirai, *Biotechnol. J.* (2010) 484 (https://doi.org/10.1002/biot.200900293)
67. S. M. Emadian, T. T. Onay, B. Demirel, *Waste Manage.* **59** (2017) 526 (https://doi.org/10.1016/j.wasman.2016.10.006)
68. V. Bátori, D. Åkesson, A. Zamani, M. J. Taherzadeh, I. S. Horváth, *Waste Manage.* **80** (2018) 406-413 (https://doi.org/10.1016/j.wasman.2018.09.040)
69. F. Ruggero, R. Gori, C. Lubello, *Waste Manage. Res.* **37** (2019) 959 (https://doi.org/10.1177/0734242X19854127)
70. D. I. Martínez-Tobón, M. Gul, A. L. Elias, D. Sauvageau, *Appl. Microbiol. Biotechnol.* **102** (2018) 8049 (https://doi.org/10.1007/s00253-018-9153-8)
71. A. K. Urbanek, A. M. Mirończuk, A. García-Martín, A. Saborido, I. de la Mata, M. Arroyo, *Biochim. Biophys. Acta, Proteins Proteomics* **1868** (2020) 140315 (https://doi.org/10.1016/j.bbapap.2019.140315)
72. E. Hablot, S. Dharmalingam, D. G. Hayes, L. C. Wadsworth, C. Blazy, R. Narayan, *J. Polym. Environ.* **22** (2014) 417 (https://doi.org/10.1007/s10924-014-0697-0)
73. A. Nakayama, N. Yamano, N. Kawasaki, *Polym. Degrad. Stab.* **166** (2019) 290 (https://doi.org/10.1016/j.polymdegradstab.2019.06.006)
74. V. Gopinath, S. Saravanan, A. R. Al-Maleki, M. Ramesh, J. Vadivelu, *Biomed. Pharmacother.* **107** (2018) 96 (https://doi.org/10.1016/j.biopha.2018.07.136)
75. R. Song, M. Murphy, C. Li, K. Ting, C. Soo, Z. Zheng, *Drug Des., Dev. Ther.* **12** (2018) 3117 (https://doi.org/10.2147/DDDT.S165440)
76. L. Averousa, L. Moroa, P. Doleb, C. Fringantc, *Polymer* **41** (2000) 4157 (https://doi.org/10.1016/S0032-3861(99)00636-9)

77. M. Labet, W. Thielemans, A. Dufresne, *Biomacromolecules* **8** (2007) 2916 (https://doi.org/10.1021/bm700468f)
78. A. J. Salgado, O. P. Coutinho, R. L. Reis, *Macromol. Biosci.* **4** (2004) 743 (https://doi.org/10.1002/mabi.200400026)
79. E. J. Bealer, S. Onissema-Karimu, A. Rivera-Galletti, M. Francis, J. Wilkowski, D. Salas-de la Cruz, X. Hu, *Polymers* **12** (2020) 464 (https://doi.org/10.3390/polym12020464)
80. R. Whistler, J. Daniel, *Starch*, John Wiley & Sons, Inc., Hoboken, NJ, 2005
81. O. O. Ige, L. E. Umoru, S. Aribo, *ISRN Mater. Sci.* **2012** (2012) 983062 (https://doi.org/10.5402/2012/983062)
82. R. de Bragança, P. Fowler, *Industrial markets for starch*, The Biocomposites Centre, University of Wales, Bangor, Gywnedd, 2004 (http://bc.bangor.ac.uk/_includes/docs/pdf/indsutrial%20markets%20for%20starch.pdf
83. I. Vroman, L. Tighzert, *Materials (Basel)* **2** (2009) 307 (https://doi.org/10.3390/ma2020307)
84. M. S. Peresin, Y. Habibi, J. O. Zoppe, J. J. Pawlak, O. J. Rojas, *Biomacromolecules* **11** (2010) 674 (https://doi.org/10.1021/bm901254n)
85. R. J. Moon, A. Martini, J. Nairn, J. Simonsen, J. Youngblood, *Chem. Soc. Rev.* **40** (2011) 3941 (https://doi.org/10.1039/C0CS00108B)
86. A. Majeed, R. A. Najar, W. Ul Rehman, S. Choudhary, S. Thakur, A. Singh, G. Sharma, P. Bhardwaj, in *Natural Polymers: Derivatives, Blends and Composites*, Vol. I, S. Ikram, S. Ahmed (Eds.), Nova Science Publishers, New York, 2016, pp. 23 (ISBN: 978-1-63485-831-1)
87. R. Mohammadinejad, A. Kumar, M. Ranjbar-Mohammadi, M. Ashrafizadeh, S. S. Han, G. Khang, Z. Roveimiab, *Polymers (Basel)* **12** (2020) 176 (https://doi.org/10.3390/polym12010176)
88. P. Chmielarz, *eXPRESS Polym. Lett.* **11** (2017) 140 (https://doi.org/10.3144/expresspolymlett.2017.15)
89. B. V. Mohite, S. V. Patil, *Biotechnol. Appl. Biochem.* **61** (2014) 101 (https://doi.org/10.1002/bab.1148)
90. P. A. Richmond, in *Biosynthesis and Biodegradation of Cellulose*, C. H. Haigler, P. J. Weimer (Eds.), Marcel Dekker, Inc., New York, 1999 (ISBN 0–8247–8387–5)
91. J. K. Park, J. Y. Jung, Y. H. Park, *Biotechnol. Lett.* **25** (2003) 2055 (https://doi.org/10.1023/B:BILE.0000007065.63682.18)
92. J. Y. Jung, J. K. Park, H. N. Chang, *Enzyme Microb. Technol.* **37** (2005) 347 (https://doi.org/10.1016/j.enzmictec.2005.02.019)
93. H. S. Barud, J. Gutierrez, W. R. Lustri, M. F. S. Peres, S. J. L. Ribeiro, S. Saska, A. Tercjak, *Bacterial Cellulose* (2016) 384 (https://doi.org/10.1002/9781119126218.ch21)
94. S. P. Lin, I. Loira Calvar, J. M. Catchmark, J. R. Liu, A. Demirci, K. C. Cheng, *Cellulose* **20** (2013) 2191 (https://doi.org/10.1007/s10570-013-9994-3)
95. N. Shah, M. Ul-Islam, W. A. Khattak, J. K. Park, *Carbohydr. Polym.* **98** (2013) 1585 (https://doi.org/10.1016/j.carbpol.2013.08.018)
96. H. S. Barud, C. Barrios, T. Regiani, R. F. C. Marques, M. Verelst, J. Dexpert-Ghys, Y. Messaddeq, S. J. L. Ribeiro, *Mater. Sci. Eng., C* **28** (2008) 515 (https://doi.org/10.1016/j.msec.2007.05.001)
97. A. M. Arévalo Gallegos, S. H. Carrera, R. Parra, T. Keshavarz, H. M. N. Iqbal, *Bioresour. Technol.* **11** (2016) 5641 (https://doi:10.15376/biores.11.2.Gallegos)
98. A. Banerjee, K. Chatterjee, G. Madras, *Mater. Sci. Technol.* **30** (2014) 567 (https://doi.org/10.1179/1743284713Y.0000000503)

99. D. Beaton, P. Pelletier, R. R. Goulet, *Front. Microbiol.* **10** (2019) 204 (https://doi.org/10.3389/fmicb.2019.00204)
100. W. Czaja, A. Krystynowicz, S. Bielecki, R. M. Brown, *Biomaterials* **27** (2006) 145 (https://doi.org/10.1016/j.biomaterials.2005.07.035)
101. Y. Z. Wan, H. Luo, F. He, H. Liang, Y. Huang, X. L. Li, *Compos. Sci. Technol.* **69** (2009) 1212 (https://doi.org/10.1016/j.compscitech.2009.02.024)
102. R. Jayasekara, I. Harding, I. Bowater, G. B. Y. Christie, G. T. Lonergan, *J. Polym. Environ.* **11** (2003) 49 (https://doi.org/10.1023/A:1024219821633)
103. R. Gattin, A. Copinet, C. Bertrand, Y. Couturier, *Int. Biodeterior. Biodegrad.* **50** (2002) 25 (https://doi.org/10.1016/S0964-8305(02)00039-2)
104. H.-T. Liao, C.-S. Wu, *Mater. Sci. Eng., A* **515** (2009) 207 (https://doi.org/10.1016/j.msea.2009.03.003)
105. G. Wypych, in *Handbook of Material Weathering (Fifth Edition)*, G. Wypych (Ed.), Elsevier, Oxford, 2013, pp. xi–xii (ISBN: 9781895198621)
106. D. R. Ruka, P. Sangwan, C. J. Garvey, G. P. Simon, K. M. Dean, *Environ. Sci. Technol.* **49** (2015) 9979 (https://doi.org/10.1021/es5044485)
107. S. Keshk, A. El-Kott, *Natural bacterial biodegradable medical polymers: Bacterial cellulose*, Elsevier, King Khalid University, 2017, p. 295 (https://doi.org/10.1016/B978-0-08-100372-5.00010-6)
108. I. Leppänen, M. Vikman, A. Harlin, H. Orelma, *J. Polym. Environ.* **28** (2020) 458 (https://doi.org/10.1007/s10924-019-01621-w)
109. S. Zhang, J. Yang, X. Liu, J. Chang, A. Cao, *Biomacromolecules* **4** (2003) 437 (https://doi.org/10.1021/bm0201183)
110. Y. Tokiwa, B. P. Calabia, C. U. Ugwu, S. Aiba, *Int. J. Mol. Sci.* **10** (2009) 3722 (https://doi.org/10.3390/ijms10093722)
111. J. Xu, B.-H. Guo, *Biotechnol. J.* **5** (2010) 1149 (https://doi.org/10.1002/biot.201000136)
112. J. Xu, B.-H. Guo, in *in Plastics from Bacteria: Natural Functions and Applications, Microbiology Monographs*, G. Guo-Qiang Chen (Ed.), Springer-Verlag, Berlin, 2010, pp. 347–388 (ISBN 978-3-642-03287-5)
113. N. Cheroennet, S. Pongpinyopap, T. Leejarkpai, U. Suwanmanee, *J. Cleaner Prod.* **167** (2016) 987 (https://doi.org/10.1016/j.jclepro.2016.11.152)
114. Y.-S. Tai, M. Xiong, P. Jambunathan, J. Wang, J. Wang, C. Stapleton, K. Zhang, *Nat. Chem. Biol.* **12** (2016) 247 (https://doi.org/10.1038/nchembio.2020)
115. K.-K. Cheng, X.-B. Zhao, J. Zeng, J.-A. Zhang, *Biofuels Bioprod. Biorefin.* **6** (2012) 302 (https://doi.org/10.1002/bbb.1327)
116. *P. S. P. Market Report: Bioplastics: technologies and global markets (market report)*
117. G. Ahrens, I. Roy, B. Pilic, P. Morganti, M. B. Coltelli, S. Danti, C. Lacoste, A. Gagliardini, R. Arias, *EU Commun.* (2017) (https://cordis.europa.eu/project/id/745839)
118. Y. Y. H. Maeda, K. Abe, F. Hasegawa, M. Machida, R. Ishioka, K. Gomi, T. Nakajima, *Appl. Microbiol. Biotechnol.* **67** (2005) 778 (https://doi.org/10.1007/s00253-004-1853-6)
119. *Bioplastics magazine, Bio-Based Polymers Have Potential in Biomedicine, Agricultural Markets* (2019) (https://www.bioplasticsmagazine.com/en/)
120. T. Fujimaki, *Polym. Degrad. Stab.* **59** (1998) 209 (https://doi.org/10.1016/S0141-3910(97)00220-6)
121. R. Ishioka, E. Kitakuni, Y. Ichikawa, *Biopolymers* **4** (2002) 275 (https://application.wiley-vch.de/books/biopoly/con_v04.html)

122. J. Xu, B.-H. Guo, in *Plastics from Bacteria: Natural Functions and Applications, Microbiology Monographs*, Springer-Verlag, Berlin, 2010, pp. 1–16 (ISBN 978-3-642-03287-5)
123. *The Draft of the Integrated Plastic Waste Management Plan (2017-2021).* Pollution Control Department, Bangkok, 2017
124. K. Changwichan, T. Silalertruksa, H. Gheewala, *Sustainability* **10** (2018) 952 (https://doi.org/10.3390/su10040952)
125. T. Haider, C. Vçlker, J. Kramm, K. Landfester, F. R. Wurm, *Angew. Chem. Int. Ed.* **58** (2019) 50 (https://doi.org/10.1002/anie.201805766)
126. K. Chavalitdamrong, https://challenges.openideo.com/challenge/next-gen-cup-challenge/ideas/new-gen-biopbs-coated-cup-recyclable-home-compostable-cup, accessed June 30, 2020
127. M. Velrajan, *Int. J. Innov. Res. Develop.* **3** (2014) 185 (http://internationaljournalcorner.com/index.php/ijird_ojs/article/view/135025)
128. M. Puchalski, G. Szparaga, T. Biela, A. Gutowska, S. Sztajnowski, I. Krucinska, *Polymers* **10** (2018) 251 (https://doi.org/10.3390/polym10030251)
129. D. Danso, J. Chow, W. R. Streit, *Appl. Environ. Microbiol.* **85** (2019) 01095 (https://doi:10.1128/AEM.01095-19)
130. I. Voevdina, A. Kržan, *Bio-based polymers*, Project Plastice report, 2013 (https://www.umsicht.fraunhofer.de/content/dam/umsicht/de/dokumente/ueber-uns/nationale-infostelle-nachhaltige-kunststoffe/bio-based-polymers.pdf)
131. C. M. Mendieta, M. E. Vallejos, F. E. Felissia, G. Chinga-Carrasco, M. C. Area, *J. Polym. Environ.* (2017) (https://doi.org/10.1007/s10924-019-01582-0)
132. J. Gotro, *Bio Polyethylene: Drop-in Replacement* (https://polymerinnovation-blog.com/bio-polyethylene-drop-in-replacement/, accessed May 15, 2020)
133. A. Lesiuk, S. Pasieczna-Patkowska, *Chemik* **67** (2013) 863 (in Polish)
134. S. Lambert, M. Wagner, *Chem. Soc. Rev.* **46** (2017) 6855 (https://doi.org/10.1039/C7CS00149E)
135. A. C. S. Bonhommea, A-M. Delortb, J. Lemairea, M. Sancelmeb, G. Scottc, *Polym. Degrad. Stab.* **81** (2003) 441 (https://doi.org/10.1016/S01413910(03)001290)
136. M. Mierzwa-Hersztek, K. Gondek, M. Kopeć, *J. Polym. Environ.* **27** (2019) 600 (https://doi.org/10.1007/s10924-019-01368-4)
137. AZoCleantech, *Recycling of High-Density Polyethylene (HDPE or PEHD)*, 2012, https://www.azocleantech.com/article.aspx?ArticleID=255, accessed May 15, 2020
138. ABA Australasian Bioplastics Association, https://bioplastics.org.au/bioplastics/break-down-process-explained/, accessed May 15, 2020
139. I. Kyrikou, D. Briassoulis, *J. Polym. Environ.* **15** (2007) 125 (https://doi.org/10.1007/s10924-007-0053-8)
140. S. Walker, R. Rothman, *J. Cleaner Prod.* **261** (2020) 121158 (https://doi.org/10.1016/j.jclepro.2020.121158)
141. A. Chamas, H. Moon, J. Zheng, Y. Qiu, T. Tabassum, J. H. Jang, M. Abu-Omar, S. L. Scott, S. Suh, *ACS Sustainable Chem. Eng.* **8** (2020) 3494 (https://doi.org/10.1021/acssuschemeng.9b06635)
142. T. Tiso, T. Narancic, R. Wei, E. Pollet, N. Beagan, K. Schröder, A. Honak, M. Jiang, S. T. Kenny, N. Wierckx, R. Perrin, L. Avérous, W. Zimmermann, K. O'Connor, L. M. Blank, *bioRxiv* (2020) (https://doi.org/10.1101/2020.03.16.993592)
143. L. A. Román-Ramírez, P. McKeown, C. Shah, J. Abraham, M. D. Jones, J. Wood, *Ind. Eng. Chem. Res.* **59** (2020) 11149 (https://doi.org/10.1021/acs.iecr.0c01122).

Journal of the Serbian Chemical Society
JSCS-info@shd.org.rs • www.shd.org.rs/JSCS
J. Serb. Chem. Soc. 85 (12) S550–S558 (2020) *Supplementary material*

SUPPLEMENTARY MATERIAL TO

Understanding bioplastic materials – Current state and trends

SANJA JEREMIC[1], JELENA MILOVANOVIC[1], MARIJA MOJICEVIC[2], SANJA SKARO BOGOJEVIC[1] and JASMINA NIKODINOVIC-RUNIC[1]*

[1]*Institute of Molecular Genetics and Genetic Engineering, Vojvode Stepe 444a, 11042 Belgrade 152, Serbia and* [2]*Athlone Institute of Technology, Dublin Road, Athlone, Co. Westmeath, Ireland*

J. Serb. Chem. Soc. 85 (12) (2020) 1507–1538

TABLE S-I. Global PLA producers

Brand name	Supplier	Material	Application	Description	Patent No
Ecovio®	BASF SE, Germany	film	versatile	Ecoflex®(fossil based) + PLA	
PLA-HI-GF10	Clariant, Switzerland	filament	3D printing	glass fiber reinforced PLA	
PLA 3D				NatureWorks Ingeo™ Biopolymer 3D850 with Clariant Hostanox® P-EPQ® and Hostavin® ARO 8	
	Danimer Scientific, US (formerly known as Meredian Holdings Group Inc. and MHG)			custom made copolymers with PLA	
RESOMER® (product range)	Evonik, Germany	pellets, filaments	medical devices	PLA/PCL, PLA/PEG, PLA composites	

* Corresponding author. E-mail: jasmina.nikodinovic@imgge.bg.ac.rs

Futerro PLA	Futerro, Belgium	pellets	raw material	Galactic and Total Petrochemicals join forces to create Futerro, a joint venture dedicated to the production of PLA	WO 2015/086613
Bio-Flex®	FKuR, Germany	granules	raw material	PLA containing copolyester and additives	
Recycled PLA	Loopla (Galactic), Belgium	granules	raw material		WO2010118954A1 WO2010118955A1
ECOLOJU®	Mitsubishi Chemical, Japan	film, sheet	versatile		
BIOCRYL RAPIDE™	Mitek Sports Medicine, US		medical implants	PLA/PLGA plus β-TCP	
Ingeo (product range)	NatureWorks, US	resin, fiber-grade resin, monofilament	raw material		US5247059A US5142023A
EarthFirst™	PACO Label, US	film	labels, packaging	Based on NatureWorks® PLA	
CornLeaf	Radici Group, Italy	fibres, nonwovens	versatile	Based on Ingeo PLA	
Sulzer PLA	Sulzer Ltd, Switzerland	pellets	raw material	Production technology was jointly developed with Purac	
EcoPlan	SK Chemicals, South Korea	film	packaging film, fiber for sanitary products		10501604
Styrex BioFoam	Synbra Technology BV, Netherlands	foam	technical products, packaging solutions		EP3053947A1
Luminy PLA (high heat, low heat, standard, PDLA)	Total Corbion, Netherlands	resin	raw material	Total Corbion PLA is a joint venture between Total (FR) and Corbion (NL). Corbion was previously called Purac.	

PLAneo® (different MW)	Thyssenkrupp AG, Germany	pellets	raw material

TABLE S-II. Global PHA producers

Brand name	PHA type	Supplier	Application	Production t/year
VersaMer™ PHA	PHOHHx, PHNHHp, PHNHHpHN:HUD:	PolyFerm Canada Inc.	Raw materials (pellets, latex)	
Ecoman		Shenzhen Ecomann Biotechnology Co., Ltd.	Bags, printer filaments	75000
PHBH™X131A PHBH™ X331N PHBH™ X151A	PHBV copolymers PHBHHx	Kaneka (Japan)	Food packaging materials, agricultural and civil engineering materials, marine materials, etc.	5000
Minerv -SB™ Minerv -SC™	PHA	Bio-On, (Italy)	Automotive, beverages, electronics, foodpack, fibers, pharma	10000
Natureplast		Natureplast (France)	Agricultural applications; consumer applications	
AirCarbonTM	PHA (unclear)	Newlight Technologies (USA)	Electronics, construction, apparel etc.	
Nodax™	(PHB-HH)	Danimer scientific (USA)	Detergent bottles, coffee containers, paper cups and plates, plastic bags, foam containers, baby wipes.	

Biocycle	PHBV	PHB Industrial, (Brazil)	Veterinary applications, agricultural, packaging	10000
Biomer	PHBV, PHBH, PHBO	Biomer Biotechnol. (Germany)		
Enmat	PHBV PHBV/PLA	TianAn Biopolymer, (China)		2000
Biogreen	PHB	Mitsubishi Gas Chemical Company, Inc.	Film, bags	
TephaFLEX	P4HB	Tepha (USA)	Medical materials	
Mirel , Mvera	P3HB	Metabolix, (USA) Or Yield10 Bioscience	Agricultural applications; caps; closures	50000
	Mcl-PHA	MHG Bio, (USA)		20
Hydal		Bochemie (Czech)		
SogreenTM	Etyl 3-HB P(3HB,4HB)	Tianijin GreenBio (China)		10000
Solon		RWDC Industries (Singapore)		4000
		Mango materials (USA)		
		Full Cycle Bioplastics (USA)		3000
		Bluepha Co. Ltd. (China)		

TABLE S-III. Patents related to PHA

Patent	Year	Patent No
Method for producing polyhydroxyalkanoic acid, and microbes	2020	US2020109423A1
Method for producing polyhydroxyalkanoates (pha) from organic waste	2019	US20190360008A1
Transformant that produces PHA copolymer containing 3HH unit, and method for producing PHA	2018	WO2018021046A1
Process for extraction of bioplastic and production of monomers from the bioplastic	2016	WO2016085396A1
Method for decomposing polyhydroxyalkanoic acid, and microorganism preparation	2015	WO2015122190A1
Pseudomonas mutant strain and application of *Pseudomonas* mutant strain to production of (R)-3-hydroxybutyrate	2015	CN104328062A
Method of producing polyhydroxyalkanoates (PHA) from oil substrate	2014	WO2014032633A1
Green process for producing polyhydroxyalkanoates and chemicals using a renewable feedstock	2012	WO2012149162
Process for producing microbial copolyesters from sucrose-containing feedstocks	2011	EP2780461A1
Copolyester degradation bacterial strain of beta-hydroxy-butanoic acid and beta-hydroxyl radical valeric acid, and breeding method	2008	CN101245365A

TABLE S-IV. Patents related to starch and cellulose

Patent	Year	Patent No
Starch		
Addition of biodegradability lending additives to plastic materials	2019	WO2018006061A1
Biodegradable polymer composition and method of producing the same	2019	WO2020037394A1
Process for preparing biological substrate-based degradable packaging material	2018	WO2020034958A1
Biodegradable plastic	2018	WO2019155398A1
Carbohyrate-based polymeric materials	2017	WO2018125897A1
Biodegradable polymer-based biocomposites with tailored properties	2016	WO2016138593A1
Process for producing starch from microalgae	2016	WO2017130106A1
Partial shell for packaging a food product	2016	WO2018041779A1
Coated particles and methods of making and using the same	2016	WO2017091463A1
Starch/thermoplastic polyurethane (TPU) composite material	2012	CN102585485B
Cellulose		
Method for manufacturing crystal nano-cellulose	2019	WO2019221535A1
Method of producing three dimensional autologous fat graft	2019	WO2020035734A1
Process for producing a nanocelullosic material comprising at least two stages of defibrillation	2018	WO2020014762A1
Device and method for producing nanocellulose	2018	WO2020015884A1
Nanostructured polymer-based compositions	2018	WO2018187782A1
Nanocellulose-reinforced corrugated medium	2017	WO2017192476A1
Cellulose derivative and use thereof	2016	WO2017061190A1
Method for manufacturing a cellulose product	2016	WO2017160218A1
Multi-phase bacterially-synthesized-nanocellulose biomaterials	2016	WO2016113400A1
Modified bacterial nanocellulose and its uses in chip cards and medicine	2016	WO2016174104A1
Methods of producing bacterial nanocellulose from cassava bagasse	2014	WO2016029432A1

TABLE S-V. Global PBS producers

Brand name	Supplier	Application	Description	Production t/year	Patent no.
FD92 (PM/PB)	Mitsubishi Chemical Performance Polymers (MCPP) Japan / PTT MCC Biochem	Barrier packaging	It is derived from natural resources such as sugarcane, cassava and corn. It is compostable at open-air landfill site in an ambient condition (30°C), without requiring a specialized composting facility.	3000	US 20180058010A1

FZ71 (PM/PB)		Coffee capsule cutlery	It is derived from natural resources such as sugarcane, cassava and corn. It is compostable at open-air landfill site in an ambient condition (30°C), without requiring a specialized composting facility.	3000	US 20180058010A1
FD72 (PM/PB)		Injection molding articles for general purpose	It is soft and flexible semi-crystalline polyester with excellent properties	3000	US 20140021574A1
FZ79AC		Paper coating	It is soft and flexible semi-crystalline polyester with excellent properties	3000	
FZ91 (PM/PB)		Coffee capsule cutlery	It is compostable at open-air landfill site in an ambient condition (30°C), without requiring a specialized composting facility.	3000	US 20180058010A1
FZ78TM		Synthetic fiber	It is derived from natural resources and It decomposes into biomass, carbon dioxide & water BioPBS FZ78TM - Natural Colored Resin (max thickness 74 microns)	3000	
Bionolle 3001 MD	SHOWA DENKO Japan	Trash bag, plant pot, filament, yarn, net, bottle, gloves, container, laminated paper, tray, comb, frame of fan and peg	Stable under ordinary conditions it becomes biodegradable in the presence of microorganism, e.g. compost, wet soil, fresh water, seawater and activated sludge.	5000	US20030015826A1

Bionolle 1903 MD	SHOWA DENKO Japan	It is an aliphatic polyester resin that has the versatility of common plastics. It becomes biodegradable in the presence of microorganism, e.g. compost, wet soil, fresh water, seawater and activated sludge.	5000	US20020094444A1
Bionolle 3020 MD		It is an aliphatic polyester resin that has the versatility of common plastics. It becomes biodegradable in the presence of microorganism, e.g. compost, wet soil, fresh water, seawater and activated sludge.	5000	US7265188B2
Bionolle 1001 MD		Stable under ordinary conditions it becomes biodegradable in the presence of microorganism, e.g. compost, wet soil, fresh water, seawater and activated sludge.	5000	WO2010151798A2
Bionolle 1020 MD		Stable under ordinary conditions it becomes biodegradable in the presence of microorganism, e.g. compost, wet soil, fresh water, seawater and activated sludge.	5000	WO2016105217A1

Eco-Solutions GP330-1	Minima Technology Co., Ltd. Taiwan	Injection process	Eco Solution GP300 is a PLA (polyactide) based alloy with PBS (Poly Butylene Succinate) and is certified as a biodegradable resin and meet ASTM D6400, EN13432		CN105152255A
Eco-Solutions GP330-S			Eco Solution GP300 is a PLA (polyactide) based alloy with PBS (Poly Butylene Succinate) and is certified as a biodegradable resin and meet ASTM D6400, EN13432		CN105152255A
Eco-Solutions GP335C			Eco Solution GP300 is a PLA (polyactide) based alloy with PBS (Poly Butylene Succinate) and is certified as a biodegradable resin and meet ASTM D6400, EN13432		CN105152255A
EnPol G4560	Ire Chemical Limited South Corea	Monofilament, multifilament	G4560 is biodegradable, aliphatic polyester based on the monomers, 1,4-butanediol and succinic acid.	3500	WO2016189228A1
Bio-Flex® FS 5630	FKuR Kunststo GmbH and Fraunhofer UMSICHT Germany	Flat sheet extrusion and injection process	Made of PLA/PBS blends	3000	N.A.

TABLE S-VI. Global Bio-PE producers

Brand name	Supplier	Application	Description	Production t/year
HDPE LDPE LLDPE	Braskem Brasil (producing 45 different materials)	Thermoplastics, bags, boxes	Exhibits high stiffness, low gels content, excellent appearance of films, good mechanical and optical properties.	200000
Terralene	FKuR Germany (producing 7 diff. mat.)	Buildings, constructions, termoplastics	Is polyethylene reinforced with 30% glass fiber, exhibits high stiffness.	20000
Cardia Biohybrid BL-F, H-F	Cardia Bioplastics Australia	Bottles, standard, bags, shopping, blow molding	Homogenous blend of thermoplastic starch (TPS) with polyethylene (PE). It is compatibilized to offer a high level of mechanical strength	
Yparex® RENEW 0H	The Compound Company Netherlands (3 diff. mat,)	Packaging, extrusion	Possesses good melt flow index, melting temperature and the level of functional groups	30000-60000
TRUCIRCLE™	SABIC Saudi Arabia	Packaging food	Is a 100% recyclable linear low density polyethylene (LLDPE).	
MCGB Duramaze™ CC HDPE	MCG BioComposites Netherlands	Pipes	Its typical size is 0.0156 inch. The product should be stored in a cool, dry, and sanitary area to achieve maximum stability.	
ParsaBio™ 6010	Parsa Polymer Sharif Iran	Injection molding, thermoplastics	Linear low density polyethylene (LLDPE) grade by Parsa Polymer Sharif.	18000
Solaplast 1312	Algix USA	Ellectronics, cellular phones, bottles	Is an ethylene vinyl acetate base resin (EVA) with food-grade aquatic biomass and an odor adsorbent.	27000
Nano4elec – BioPE EC12	Nano4 Greece	Building constructions, electrical markets, switches	Is an electrically conductive bio-based polyethylene (PE) grade.	

Journal of the Serbian Chemical Society
JSCS-info@shd.org.rs • www.shd.org.rs/JSCS
J. Serb. Chem. Soc. 85 (12) 1539–1551 (2020)
JSCS–5391
UDC 547.722.1'472.3+542.913:576+615.9:615.277
Original scientific paper

Synthesis and antiproliferative activity of simplified goniofufurone analogues

BOJANA SREĆO ZELENOVIĆ[1#], SANJA GRABEŽ[1], MIRJANA POPSAVIN[1#], VESNA KOJIĆ[2], JOVANA FRANCUZ[1#] and VELIMIR POPSAVIN[1,3*#]

[1]*Department of Chemistry, Biochemistry and Environmental Protection, Faculty of Sciences, University of Novi Sad, Trg Dositeja Obradovića 3, 21000 Novi Sad, Serbia,* [2]*Oncology Institute of Vojvodina, Put Dr. Goldmana 4, 21204 Sremska Kamenica, Serbia and* [3]*Serbian Academy of Sciences and Arts, Kneza Mihaila 35, 11000 Belgrade, Serbia*

(Received 30 July, accepted 10 September 2020)

Abstract: Several (+)-goniofufurone analogues with simplified structures were designed, synthesized and evaluated for their *in vitro* antitumour activity, against a panel of human tumour cell lines. Dephenylated compounds **2** and **3** demonstrated remarkable antitumour activities, in the cultures of K562 and Raji cells with IC_{50} values in the range of 3.0–9.3 nM. Each of goniofufurone analogues lacking the tetrahydrofuran ring (**4**, **5** and **6**) strongly inhibited the growth of at least one malignant cell line, with IC_{50} values in the range of 11-30 nM. Brief structure–activity relationship (SAR) analysis showed that the simplified goniofufurone analogues, designed by removing the phenyl group from C-7, or by opening the THF ring, could show stronger antiproliferative effects compared to control molecules. It is noticeable that analogues **2**–**8** are completely inactive with respect to the normal MRC-5 cell line. These findings, together with their potent antitumour activities, provide a suitable basis for the development of new and selective antitumour drugs.

Keywords: structure simplification based drug design; goniofufurone mimics; furanolactones; cytotoxicity; Wittig olefination; oxa-Michael ring-closure; SAR analysis.

INTRODUCTION

The development of practical and efficient routes for the synthesis of natural products and their analogues is of considerable interest for drug design and discovery.[1–3] However, the complex chemical structures of natural products often complicate the general synthesis procedure, SAR investigations and structural optimizations, or result in unfavourable ADMET (absorption, distribution, meta-

* Corresponding author. E-mail: velimir.popsavin@dh.uns.ac.rs
# Serbian Chemical Society member.
https://doi.org/10.2298/JSC200730056S

bolism, excretion, toxicity) properties.[4] Therefore, simplifying complex structures without the decrease of biological activity is an effective strategy for improving synthetic accessibility and accelerating the drug development process.[5]

The styryl lactones from the plants of *Goniothalamus* genus are an interesting class of naturally occurring compounds, many of which were found to exhibit impressive biological activities.[6–9] One of the most important among them is (+)-goniofufurone (**1**; Fig. 1), a naturally occurring styryl lactone that have attracted considerable attention since its isolation from the stem bark of *Goniothalamus giganteus* (Annonaceae).[10] Its structure was elucidated by spectroscopic methods, and the relative configurations determined by X-ray crystallography. The absolute configuration of **1** was established independently by Shing[11] and Jäger[12] from the syntheses of its opposite enantiomer, (−)-goniofufurone. Due to its unique structural features and promising antitumour activities,[6–9] the natural product **1**, along with a number of its analogues and derivatives have been the targets of many total syntheses.[13–15] We have also been involved in the synthesis of **1** and related compounds.[16] Our preliminary results on antiproliferative properties of analogues **2** and **3** showed that they exhibit moderate to potent citotoxicity,[17] which led us to prepare a number of analogues for a detailed SAR analysis. More potent analogues can be designed by manipulation of functional groups, by changing the stereochemistry or conformational constraints, and after closing or opening a ring in the natural lead.[3,5] This paper summarizes the application of the structural simplification of (+)-goniofufurone (**1**), in order to elucidate the role of the phenyl group and the tetrahydrofuran ring in antiproliferative activity.

1 R = Ph, R^1 = H
2 R = R^1 = H
7 R = Ph, R^1 = Bn
8 R = H, R^1 = Bn

3

4 R = Ph, R^1 = H
5 R = R^1 = H

6

Fig. 1. Chemical structures of (+)-goniofufurone (**1**) and the corresponding analogues (**2**–**8**).

EXPERIMENTAL

General procedures

Melting points were determined on Büchi 510 or on Hot Stage Microscope Nagema PHMK 05 apparatus and were not corrected. Optical rotations were measured on Autopol IV (Rudolph Research) automatic polarimeter. IR spectra were recorded by a FTIR Nexus 670 (Thermo-Nicolet) spectrophotometer. NMR spectra were recorded on a Bruker AC 250 E, or a Bruker Avance III 400 MHz instrument and chemical shifts are expressed in ppm downfield from tetramethylsilane. Low resolution mass spectra were recorded on Finnigan-MAT 8230 (CI) and VG AutoSpec (FAB) mass spectrometers. High-resolution mass spectra were taken on an LTQ OrbitrapXL (Thermo Fisher Scientific Inc., USA) mass spectrometer. TLC was

performed on DC Alufolien Kieselgel 60 F254 (E. Merck). Flash column chromatography was performed using Kieselgel 60 (0.040–0.063, E. Merck). All organic extracts were dried with anhydrous Na_2SO_4. Organic solutions were concentrated in a rotary evaporator under reduced pressure at a bath temperature below 35 °C. The purities of final products were established by high performance liquid chromatography–high resolution mass spectrometry (HPLC-HRMS), or by elemental microanalysis, and were found to be >95 % pure. The characterization data of synthesized compounds are given in the Supplementary material to this paper.

Synthetic procedures

3,6-Anhydro-5,7-di-O-*benzyl-2-deoxy-D*-ido-*heptono-1,4-lactone* ***(10)*** *and methyl (*E*)--5,7-di*-O-*benzyl-2,3-dideoxy-D*-xylo-*hept-2-enonate* ***(11)****.* Procedure A: $Ph_3P{=}CHCO_2Me$ (0.417 g, 1.2 mmol) was added to a solution of **9** (0.332 g, 1.0 mmol) in dry MeOH (10 mL) and the reaction mixture was stirred at room temperature for 24 h. An additional amount of reagent was then added (0.561 g, 1.68 mmol) and the reaction mixture was left at room temperature for another 24 h. The solution was evaporated and the residue purified by flash chromatography (Et_2O) in order to separate the product from Ph_3PO. Subsequent chromatographic purification on a column of flash silica (9:1 hexane/Et_2O) gave pure **10** (0.216 g, 61 %), as a semisolid. Recrystallization from MeOH afforded an analytical sample **10**, m.p.: 90 °C, $[\alpha]_D$ = +8.6° (*c* 1.2, $CHCl_3$), R_f = 0.62 (4:1 hexane/Et_2O). The subsequent elution of the column gave the (*E*)-olefin **11** (0.098 g, 25 %), as a colourless syrup, $[\alpha]_D$ = −188.9° (*c* 1.1, $CHCl_3$), R_f = 0.50 (4:1 Et_2O/hexane). Procedure B: $Ph_3P{=}CHCO_2Me$ (0.434 g, 1.3 mmol) was added to a solution of **9** (0.355 g, 1.08 mmol) in dry benzene (10 mL) and the reaction mixture was stirred under reflux for 24 h. After workup as described above, pure olefin **11** was obtained as the main product (0.274 g, 66 %), while the lactone **10** (0.091 g, 24 %) was isolated as a minor product under these reaction conditions. ^{1}H- and ^{13}C-NMR spectral data of both **10** and **11** were identical to those previously reported.[17,18]

3,6-Anhydro-5,7-di-O-*benzyl-2-deoxy-D*-ido-*heptono-1,4-lactone* ***(10)*** *and methyl 3,6--anhydro-5,7-di*-O-*benzyl-2-deoxy-D*-gulo-*heptonoate* ***(12)****.* A solution containing compound **11** (0.182 g, 0.48 mmol) and imidazole (0.034 g, 0.5 mmol) in dry benzene (18 mL) was stirred under reflux for 11 h. The mixture was poured in 10 % aq. NaCl (40 mL) and extracted with CH_2Cl_2 (3×20 mL). The combined extract was dried and evaporated and the residue purified on a column of flash silica (9:1 hexane/Et_2O). Pure lactone **10** (0.085 g, 51 %) was first isolated as a semisolid. Recrystallization from MeOH afforded an analytical sample **10**, m.p.: 90 °C, $[\alpha]_D$ = +8.6° (c 1.2 in $CHCl_3$), R_f = 0.62 (4:1 hexane/Et_2O). The spectral data of thus obtained sample were in full agreement with the data previously reported by us.[17,18] Tetrahydrofuran derivative **12** (0.015 g, 17 %) was next isolated as a colourless oil, $[\alpha]_D$ = = −18.7 (*c* 1.0, $CHCl_3$), R_f = 0.50 (4:1 Et_2O/hexane). ^{1}H- and ^{13}C-NMR spectral data were identical to those previously reported by us.[17,18]

Methyl 3,6-anhydro-5,7-di-O-*benzyl-2-deoxy-D*-gulo-*heptonoate* ***(12)*** *and methyl 5,7-di--*O-*benzyl-2,3-dideoxy-4-oxo-D*-threo-*heptonate* ***(13)****.* A solution of **11** (0.091 g, 0.24 mmol) in 0.1 M NaOMe in MeOH (0.5 mL, 0.05 mmol) was stirred at room temperature for 20 min. The mixture was poured into 10 % aq. NH_4Cl (10 mL) and extracted with EtOAc (3×5 mL). The combined organic solutions were evaporated and the residue purified on a column of flash silica (7:3 Et_2O/hexane). Pure **13** was first isolated as a bright yellow oil (0.029 g, 32 %), $[\alpha]_D$ = −69.9° (*c* 1.4, $CHCl_3$), R_f = 0.71 (4:1 Et_2O/hexane). Spectroscopic data (^{1}H-, ^{13}C-NMR and MS) are in complete agreement with the structure **13** (see Supplementary material). After further elution of the column, the pure product **12** (0.020 g, 22 %) was isolated in the form of

a colourless syrup, $[\alpha]_D = -18.7°$ (*c* 1.0, $CHCl_3$), $R_f = 0.50$ (4:1 Et_2O/hexane). ^1H- and ^{13}C--NMR spectral data of **12** were identical to those previously reported by us.[17,18]

3,6-Anhydro-2-deoxy-D-ido-*heptono-1,4-lactone (**2**).* A solution of **10** (0.484 g, 1.37 mmol) in EtOH (30 mL) was hydrogenated over 10 % Pd/C (0.308 g, 0.29 mmol) for 24 h at room temperature. The mixture was filtered through a Celite pad, the catalyst was washed with EtOH. The combined organic solutions were evaporated and the residue (0.225 g) was purified by flash chromatography (19:1 CH_2Cl_2/MeOH) to afford pure **2** (0.208 g, 87 %) as transparent needles, m.p.: 71–73 °C (EtOAc/MeOH), $[\alpha]_D = +26.8°$ (*c* 1.8, H_2O), lit.[19] m.p.: 72–74 °C, $[\alpha]_D = +28.4°$ (*c* 1.9, H_2O), $R_f = 0.72$ (9:1 CH_2Cl_2/MeOH). The spectroscopic data of compound **2** thus obtained were identical to those previously reported by us.[17]

2,3-O-*Isopropylidene-5*-O-*triphenylmethyl-D-lyxofuranose* (**20**). TrCl (0.884 g, 3.64 mmol) was added to a solution of compound **15**[21] (0.389 g, 2.05 mmol) in anhydrous pyridine (5 mL) and the reaction mixture was left at room temperature for 48 h. The solution was poured into 10 % aq HCl and extracted with CH_2Cl_2. The extract was washed with water, dried and evaporated. The residue (1.234 g) was purified by flash column chromatography (9:1 toluene/EtOAc) to give pure compound **20** (0.630 g, 71 %) which crystallizes from MeOH in the form of white needles, m.p.: 173 °C, $[\alpha]_D = -5.2 \rightarrow -7.8°$ (48 h, *c* 0.7, $CHCl_3$), anomeric ratio (from ^1H-NMR): $\alpha/\beta \approx 7:1$ (48 h), $R_f = 0.29$ (9:1 toluene/EtOAc).

Methyl 3,6-anhydro-2-deoxy-4,5-O-*isopropylidene-D*-talo- *(**18**) and D*-galacto-*heptanoate (**19**).* Procedure A: To a solution of **15**[21] (0.355 g, 1.87 mmol) in anhydrous CH_3CN (10 mL), was added $Ph_3P{=}CHCO_2Me$ (0.954 g, 2.86 mmol) and the reaction mixture was heated under reflux for 4 h. The solution was then evaporated and the Ph_3PO precipitated by the addition of Et_2O, while standing at 4 °C for 2 h. After filtration and evaporation, the residue was purified on a column of flash silica (3:2 EtOAc/hexane) to give a 1:1.4 mixture of **16** and **17** (0.397 g, 88 %) as determined by ^1H-NMR. The mixture was chromatographically homogeneous material, $R_f = 0.32$ (2:1 EtOAc/hexane). A solution of purified mixture of **16** and **17** (0.391 g, 1.61 mmol) in dry MeOH (20 mL), was added 0.1 M solution of NaOMe u MeOH (1.6 mL, 0.16 mmol) and the reaction mixture was heated under reflux for 48 h. After neutralization with acidic ion exchange resin, IRA-120 and filtration, the solution was evaporated. A mixture of **16** and **17** in the respective ratio of 2:1 (0.350 g, 90 %) was obtained. A 2:1 mixture of **16** and **17** (0.350 g, 1.44 mmol) was treated with TrCl (0.806 g, 3.32 mmol) in anhydrous pyridine (5 mL) at room temperature for 3 days. The mixture was then poured into 10 % aqueous HCl (pH ~ 1) and extracted with CH_2Cl_2. The extract was washed with water (to pH ~ 7), dried and evaporated. Flash column chromatography of the residue (toluene → 19:1 toluene/EtOAc), gave pure **18** (0.069 g, 10 %) and **19** (0.486 g, 69 %). Procedure B: $Ph_3P{=}CHCO_2Me$ (0.550 g, 1.65 mmol) was added to a solution of **20** (0.456 g, 1.06 mmol) in anhydrous CH_3CN (10 mL), and the resulting solution was refluxed for 24 h. A new portion of reagent (0.160 g, 0.48 mmol) was added and heating was continued for additional 24 h. The solution was evaporated, the Ph_3PO precipitated with Et_2O (4 °C), filtered of and the solution again evaporated. The residue was purified on a column of flash silica (toluene → 19:1 toluene/EtOAc), whereby pure product **19** (0.223 g, 43 %) was obtained as a colourless oil. Stereoisomer **18** (0.246 g, 48 %) was also isolated as a solid which crystallizes from MeOH, as white needles. Procedure C: 0.1 M solution of NaOMe in MeOH (0.5 mL, 0.05 mmol) was added to a solution of **18** (0.2464 g, 0.51 mmol) in dry MeOH (15 mL). The mixture was heated under reflux for 48 h, and then neutralized with acidic ion exchange resin IRA-120. The resin was separated by filtration and the filtrate was evaporated. Flash column chromatography of the residue (19:1 toluene/EtOAc) gave **19** (0.151 g, 61 %) as a colourless oil,

$[\alpha]_D$ = −26.3° (*c* 1.0, $CHCl_3$), R_f = 0.35 (19:1 toluene/EtOAc). A small amount of stereoisomer **18** (0.015 g, 6 %) was also isolated as a solid, which crystallizes from MeOH, in the form of white needles, m.p.: 138 °C, $[\alpha]_D$ = −21.7° (*c* 0.8, $CHCl_3$), R_f = 0.30 (19:1 toluene/ /EtOAc).

3,6-Anhydro-2-deoxy-D-galacto-*heptono-l,4-lactone* (**3**). A solution of compound **19** (0.741 g, 1.52 mmol) in a 2:1 mixture TFA/H_2O (9 mL) was stirred at room temperature for 18 h. The reaction mixture was evaporated and the traces of acid were removed by co-distillation with toluene. The residue was purified by flash column chromatography (EtOAc) to give pure product **3** (0.210 g, 80 %), which crystallized from $CHCl_3$ in the form of white needles, m.p.: 126–127 °C, $[\alpha]_D$ = −98.0° (*c* 0.9, MeOH), R_f = 0.20 (EtOAc).

*Methyl (*E*)-5,7-di*-O-*benzyl-2,3-dideoxy-D*-lyxo-*hept-2-enoate* (**22**). $Ph_3P{=}CHCO_2Me$ (0.370 g, 1.11 mmol) was added to a solution of **21**[22] (0.286 g, 0.87 mmol) in anhydrous benzene (7 mL) and the resulting mixture was stirred under reflux for 24 h. The solvent was then evaporated and the Ph_3P was removed by flash chromatography (Et_2O). Pure **22** (0.226 g, 68 %) was obtained after crystallization from a mixture toluene/hexane, in the form of colourless, transparent needles, m.p.: 95–96 °C, $[\alpha]_D$ = +14.0° (*c* 1.1, $CHCl_3$), R_f = 0.45 (4:1 Et_2O/ /hexane). The mother liquor was evaporated and purified by column chromatography on flash silica (7:3 Et_2O/hexane), whereby a small amount of pure lactone **10** (0.027 g, 9 %) was obtained.

2,3-Dideoxy-D-lyxo-*heptono-1,4-lactone* (**6**). A solution of **22** (0.087 g, 0.23 mmol) in EtOH (3.5 mL) was hydrogenated over 10 % Pd/C (0.054 g) for 24 h, at room temperature and normal pressure of hydrogen. The catalyst was separated by the filtration through a Celite pad, the filtrate was evaporated and the residue was treated with 2:1 TFA/H_2O (3 mL), at room temperature for 20 h. The reaction mixture was evaporated by co-distillation with toluene, and the residue was purified by flash chromatography (47:3 EtOAc/MeOH). Pure product **6** (0.020 g, 50 %) was obtained as a pale yellow syrup, $[\alpha]_D$ = −1.2° (*c* 0.4, $CHCl_3$), R_f = 0.21 (47:3 EtOAc/MeOH).

Compounds **4**, **5** and **8** have been prepared according to procedures previously reported by us.[18,20]

MTT assay. The colorimetric MTT assay was carried out using the reported procedure.[23]

Test cells. The cytotoxicity of the test compounds was assessed against seven human tumour cell lines: K562 (ATCC CCL 243, chronic myeloid leukaemia), HL-60 (ATCC CCL 240, promyelocytic leukaemia), Jurkat (ATCC CCL 1435, T cell leukaemia), Raji (ATCC CCL 86, Burkitt's lymphoma), HT-29 (ATCC HTB38, colorectal adenocarcinoma), MDA--MB 231 (ATCC HTB-26, ER^- brest adenocarcinoma), and HeLa cells (ATCC CCL2, human cervix adenocarcinoma). Cytotoxicity toward a single normal cell line, MRC-5 (ATCC CCL 171, foetal lung fibroblasts) was also evaluated.

RESULTS AND DISCUSSION

Chemistry

The synthesis of dephenylated goniofufurone analogues **2** and **8** is presented in Scheme 1. Although analogue **2** can be obtained in one step by cyclocondensation of D-xylose with Meldrum's acid,[24] we planned to prepare it *via* a protected furano-lactone **10** in order to explore a possible divergent route that would allow access to monobenzyl derivative **8**. The known[22] and readily available D-xylofuranose lactol derivative **9** was used as a convenient starting material for this part of the work.

Treatment of **9** with the stabilized ylide, $Ph_3P{=}CHCO_2Me$, in anhydrous methanol gave the expected furanolactone **10** (61 %), as a product of the initial (*Z*)-selective Wittig olefination[25] followed by γ-lactonization. A minor amount (25 %) of the corresponding (*E*)-enoate **11** (δ_H 6.16 ppm, $J_{2,3}$ = 15.6 Hz, H-2) was also obtained from this reaction. Both **10** and **11** had been prepared earlier in our laboratory, under the (*E*)-selective Wittig conditions ($Ph_3P{=}CHCO_2Me$, DMF, 70 °C)[25] but in a completely different product ratio (74 % of **11**, 12 % of **10**).[18]

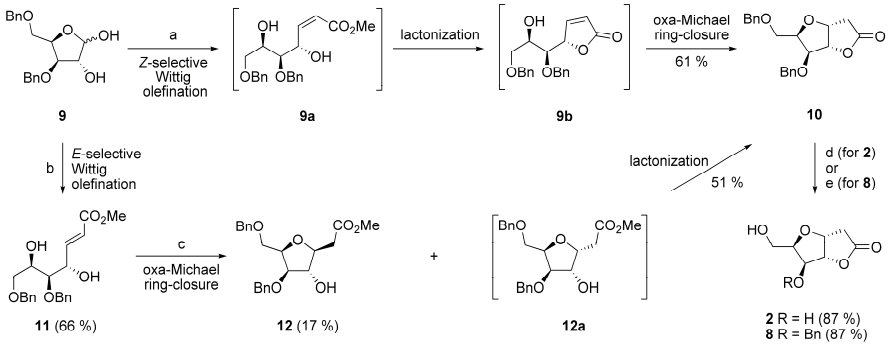

Scheme 1. Reagents and conditions: a) $Ph_3P{=}CHCO_2Me$, MeOH, rt, 48 h; b) $Ph_3P{=}CHCO_2Me$, C_6H_6, reflux, 24 h; c) imidazole, C_6H_6, reflux, 11 h; d) H_2, 10 % Pd/C, EtOH, rt, 24 h; e) H_2, 10 % Pd/C (0.1 equiv of Pd), abs. EtOH, rt, 105 min.

In this paper, we examined alternative conditions for the (*E*)-selective Wittig olefination ($Ph_3P{=}CHCO_2Me$, C_6H_6, under reflux), whereby the (*E*)-enoate **11** was obtained in 66 % yield. We supposed that **11** could be used to verify that conversion of **9** to **10** involves initial lactonization, followed by subsequent oxa-Michael cyclization. If the sequence included the oxa-Michael cyclization that precedes lactonization, we would find at least traces of the *β-C*-furanoside **12** in the reaction mixture, which from steric reasons cannot lactonize. In an alternative sequence, in which Michael's ring closure precedes lactonization, (*E*)-enoate **11** was treated with imidazole in hot benzene for 11 h. Under these reaction conditions, the lactone **10** was obtained in 51 % yield, along with a minor amount of the *β-C*-glycoside **12** (17 %) thus providing an indirect proof for the mechanism of conversion of **9** to **10**. By the catalytic reduction of **10** over 10 % Pd/C (0.1 M eq. of Pd), for 105 min at room temperature, the benzyl group was selectively removed from the primary position to give the required alcohol **8** in 87 % yield. When the catalytic hydrogenolysis of **10** was performed with twice the amount of catalyst (0.2 M eq. Pd), with an extension of the reaction time to 24 h, the known[17] analogue **2** (87 %) was obtained, with physical constants and spectral data in good agreement with the reported values.[17]

In an attempt to convert enone **11** to lactone **10** in an alternative manner, compound **11** was treated with NaOMe in MeOH at room temperature (Scheme

2). Quite unexpectedly, under these reaction conditions, γ-ketoester **13** was preferentially formed (32 %) as a result of enolization. The tetrahydrofuran derivative **12** was also isolated (22 %) as a product of the oxa-Michael cyclization process.

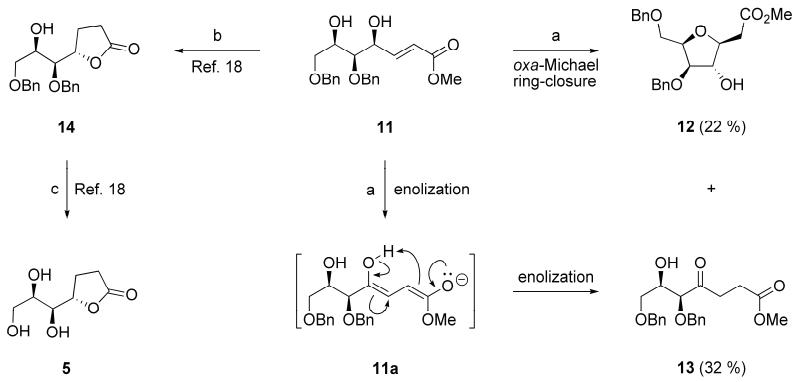

Scheme 2. Reagents and conditions: a) NaOMe, MeOH, rt, 20 min; b) H_2, PtO_2, AcOH, rt, 51 h; c) H_2, 5 % Pd/C, rt, 20 h.

Finally, compound **11** was converted to target **5** (in 44 % overall yield), using the known[18] two-step sequence shown on the left-hand side of Scheme 2. Since this synthetic sequence is described in in our earlier work,[18] it will not be further discussed here.

The synthesis of furofuranone **3** is shown in Scheme 3. The sequence started from D-lyxofuranose derivative **15**, which is readily available from D-lyxose in one step.[21] We have planned two independent routes to the key intermediate **19**.

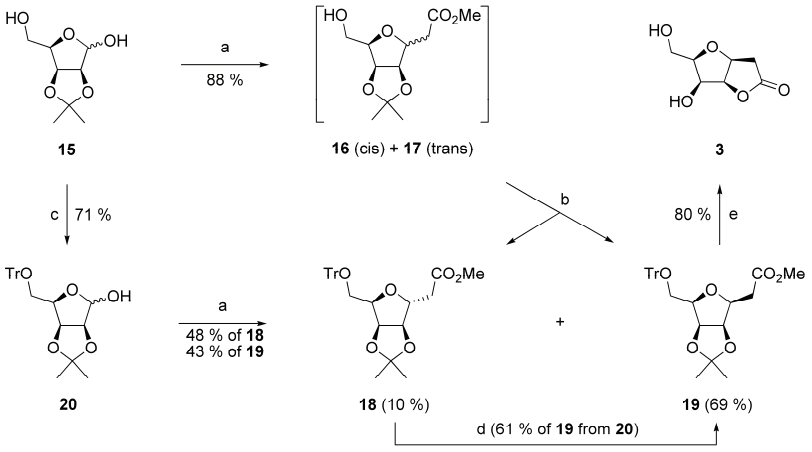

Scheme 3. Reagents and conditions: a) $Ph_3P{=}CHCO_2Me$, MeCN, reflux, 4 h for **15**, 48 h for **20**; b) *i*, NaOMe, MeOH, reflux, 48 h, *ii*, TrCl, Py, rt, 72 h; c) TrCl, Py, rt, 48 h; d) NaOMe, MeOH, reflux, 48 h; e) 2:1 TFA/H_2O, rt, 18 h.

The first one started with the reaction of **15** with $Ph_3P{=}CHCO_2Me$, in boiling MeCN, whereupon an inseparable mixture of the corresponding *α*- and *β*-*C*-furanoside (**16** + **17**) was obtained as a result of the initial Wittig olefination of **15**, followed by the subsequent oxa-Michael cyclization. This mixture further reacted with TrCl in dry pyridine to give stereoisomeric triphenylmethyl ethers **18** and **19** which were successfully separated by flash chromatography. The treatment of purified **18** with NaOMe in MeOH resulted in equilibration, *via* a ring-opening and ring-closure mechanism, similar to that observed in *α*- and *β*-*C*-ribofuranoside derivatives.[26] This procedure gave a 7:1 mixture of **19** and **18**, with the *β*-*C*--glycoside **19** as the major product. The overall yield of **19** according to this route was 55 % with respect to starting compound **15**.

The second synthetic route started with the selective protection of primary hydroxyl group of **15** using trityl chloride in pyridine (Scheme 3) to give the corresponding 5-*O*-trityl ether **20** in 71 % yield. Lactol **20** readily reacted with the stabilized ylide $Ph_3P{=}CHCO_2Me$, in dry acetonitrile, to give the approximately equal amounts of the expected *C*-glycosides **18** and **19**, which were readily separated by flash column chromatography. The isomerisation of *α*-*C*-glycoside **18** (NaOMe, MeOH, under reflux) provided an additional amount of *β*-isomer, so that the required stereoisomer **19** was obtained in a total yield of 64 % relative to starting compound **15**. The hydrolytic removal of the isopropylidene protective group in **19** with aqueous trifluoroacetic acid occurred with the related lactonization and de-*O*-tritylation, in order to give the target molecule **3** in 80 % yield.

The synthesis of *γ*-lactone **6**, an analogue of **3,** which lacks a tetrahydrofuran ring, is shown in Scheme 4. Partially protected D-lyxose derivative **21**, which is readily available from D-xylose in several synthetic steps,[22] served as a convenient starting compound for this part of the work. Reaction of **21** with $Ph_3P{=}CHCO_2Me$, in boiling benzene, gave two reaction products: the main one

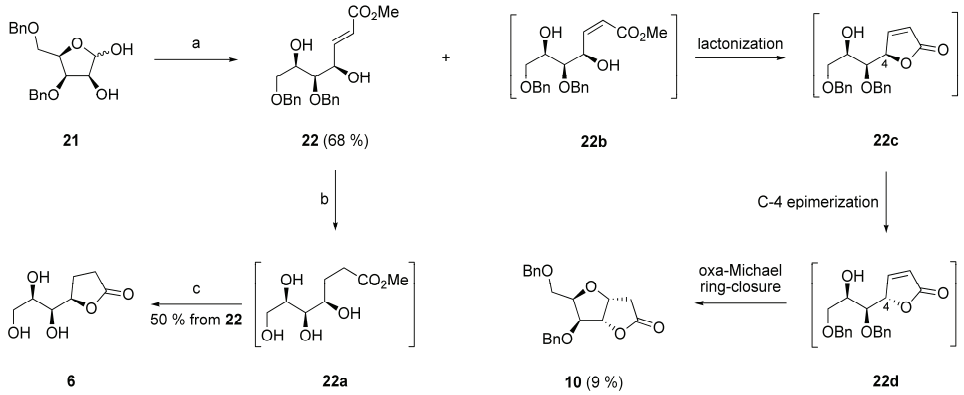

Scheme 4. Reagents and conditions: a) $Ph_3P{=}CHCO_2Me$, C_6H_6, reflux, 24 h; b) H_2, 10 % Pd/C, EtOH, rt, 24 h; c) 2:1 TFA/H_2O, rt, 20 h.

was the (*E*)-unsaturated ester **22**, which was formed as a consequence of the expected Wittig (*E*)-selective olefination process. A minor amount of furanolactone **10** was unexpectedly obtained in this reaction, presumably as a product of a three-step sequence, comprised of the initial γ-lactonization of the minor (*Z*)--olefin **22b**, followed by the successive C-4 epimerization, and the final oxa--Michael cyclization process. A catalytic reduction of **22** over 10 % Pd/C resulted in a simultaneous reduction of the double bond and the hydrogenolytic removal of the benzyl groups. Intermediate **22a** was not purified, but was in non-purified form further treated with aqueous TFA, whereby the target lactone **6** was obtained in 50 % overall yield from the last two steps.

In vitro *antiproliferative activity and SAR analysis*

The biological activities of synthesized compounds **2**–**8** were evaluated by an *in vitro* cytotoxicity test against a panel of seven human malignant cell lines, including human myelogenous leukaemia (K562), human promyelocytic leukaemia (HL-60), T cell leukaemia (Jurkat), Burkitt's lymphoma (Raji), colorectal adenocarcinoma (HT-29), ER^- breast adenocarcinoma (MDA-MB 231) and cervix carcinoma (HeLa). Cytotoxicity was also evaluated against one normal human cell line, MRC-5. The purpose of this test was to determine whether the synthesized compounds showed the selectivity against tumour cells. Cell growth inhibition was evaluated using the standard MTT assay[23] after the exposure of cells to the test compounds for 72 h*. (+)-Goniofufurone (**1**) and the commercial antitumour agent doxorubicin (DOX) were used as positive controls. The results are presented in Table I, which displays that the natural product **1** and the corresponding analogues show variable activities towards the tested cells ranging from nanomolar IC_{50} values to complete inactivity for individual cells. Such different activities indicate that the synthesized lactones do not act on the same molecular target. However, much more work is needed to confirm this assumption. This could be the subject of our future work.

It is to be noted that five analogues (compounds **2**–**4**, **7** and **8**) showed submicromolar cytotoxicities against K562 malignant cells, with IC_{50} values ranging from 0.003 to 0.54 μM. The remaining two analogues (compounds **5** and **6**) showed a strong cytotoxicity, with IC_{50} values in the micromolar range (4.21 and 3.54 μM, respectively). The most active compounds against these cells are the furanolactones **2** and **3**, which exhibited a powerful cytotoxicity (IC_{50} of 3.0 and 5.1 nM, respectively). Accordingly, compound **2** was over 130-fold more active than natural product **1** and over 80-fold more potent than the commercial antitumor agent DOX. Compound **3** showed slightly lower, but still noticeable cyto-

* Antiproliferative activities of analogues **2** and **3** against three malignant and one normal cell line were reported in the preliminary communication, but after 24-h of cells treatment (see reference[17]).

toxicity (80-fold higher potency than lead **1** and 49-fold higher activity than DOX). Also, analogue **2** showed a notable antiproliferative activity in the culture of HeLa cells (IC_{50} = 0.01 μM), showing over 800-fold higher activity than the natural lead **1** and 6.5-fold higher potency than DOX. Compound **3** however, exhibited a significant activity against Raji cells (IC_{50} = 9.3 nM) being over 1980-fold more active than the natural product **1**, and over 320-fold more potent than the commercial antitumor drug DOX. The demonstrated antitumour properties of lactones **2** and **3**, as well as their complete inactivity against the normal MRC-5 cells, make these analogues suitable leads for further development of new antitumour drugs.

TABLE I. *In vitro* cytotoxicity (+)-goniofufurone (**1**), DOX and analogues **2**–**8** after 72 h

Compound	IC_{50} / μM[a]							
	K562	HL-60	Jurkat	Raji	HT-29	MDA-MB 231	HeLa	MRC-5
1	0.41	>100	32.45	18.45	0.59	75.34	8.32	>100
2	0.003	5.56	3.73	>100	>100	75.31	0.01	>100
3	0.0051	>100	>100	0.0093	0.056	0.11	>100	>100
4	0.54[b]	0.09 [b]	2.23[b]	2.21[b]	>100	>100	2.34[b]	>100
5	4.21	0.02	>100	>100	94.35	0.011	>100	>100
6	3.54	>100	11.84	89.64	0.12	>100	4.10	>100
7	0.12	20.62	9.45	56.37	12.45	67.50	0.03	>100
8	0.065	0.09	1.02	11.39	>100	>100	5.92	>100
DOX	0.25	0.92	0.03	2.98	0.15	0.09	0.065	0.10

[a]IC_{50} is the concentration of compound required to inhibit the cell growth by 50 % compared to an untreated control. Values are means of three independent experiments. Coefficients of variation were less than 10 %; [b]taken from reference[27]

Analogue **3** proved to be the most potent antiproliferative agent in the HT-29 cell culture (IC_{50} = 0.056 μM). It showed over 10-fold stronger activity than the natural product **1** and almost 3-fold higher activity then DOX in the culture of these cells.

The most active compound in HeLa cell culture is analogue **2** (IC_{50} = 0.01 μM) being over 830- and 6.5-fold more active than the lead **1** and DOX, respectively.

The analogue **8** exhibited the strongest cytotoxicity in K562 and HL-60 cell cultures (IC_{50} of 0.065 and 0.09 μM, respectively). In the K562 cell culture, it showed almost 6 times the potency of the lead **1**, as well as 3.6 times the activity of DOX. In cell culture HL-60 (where the lead **1** is inactive), the analogue **8** showed 10 times stronger activity than DOX. The same activity towards these cells was shown by the analogue **4** (IC_{50} = 0.09 μM, 10-fold more potent than DOX).

All synthesized analogues (**2**–**8**) as well as the lead **1**, were completely inactive against normal MRC-5 cells. On the contrary, the commercial antitumour agent DOX exhibited a potent cytotoxicity against this cell line (IC_{50} = 0.10 μM). These

results do suggest that the natural product **1** and the analogues **2**–**8** are more selective anticancer agents than DOX, but such a conclusion should be supported by the additional *in vitro* experiments with a larger number of normal cell lines.

We performed a brief SAR analysis in order to identify structural features beneficial for potencies of analogues (such as the presence phenyl and/or tetrahydrofuran ring, and the influence of stereochemistry at the C-3 and/or C-4 positions).

As shown in Table I, the removal of phenyl ring from the C-7 position in **1** increase the activities of the resulting analogues **2**, **4** and **6**, against three to four cell lines. In a slightly smaller number of malignant cell lines the control compounds retained stronger potencies. (For a graphical presentation see, Fig. S-1a of the Supplementary material). The analogues designed by opening of the THF ring (**4**–**6**) showed essentially the same cytotoxic effects. Similar effects on the antiproliferative activity were observed when the stereochemistry was changed at C-3 and C-4. (Fig. S-1b and c of the Supplementary material). As it can be seen from Table I (and from Fig. S-1 of the Supplementary material), the results of the SAR analysis are relatively inconsistent. In order to draw more reliable conclusions, a larger number of analogues should be prepared, and the SAR analysis repeated. This will be the subject of our further work.

CONCLUSION

In conclusion, several novel (+)-goniofufurone analogues were designed and synthesized starting from D-xylose or D-lyxose. The synthesized molecules were evaluated for their *in vitro* antitumour activity against a panel of human malignant cell lines. The strongest potency, in the region of low, nanomolar IC_{50} values, was shown by the following compounds: dephenylated analogues **2** (IC_{50} = 3.0 nM, K562) and **3** (IC_{50} = 5.1 nM, K562 and 9.3 nM, Raji). In addition, each of the synthesized compounds showed submicromolar activity (IC_{50} 0.01–0.54 μM) against at least one tumour cell line under evaluation.

Preliminary SAR analysis showed that the dephenylated goniofufurone analogues (designed by removing the aromatic ring from C-7), as well as the analogues with open tetrahydrofuran ring (designed by disconnecting the C_3–O_6 bond), could show improved antiproliferative activity. Changing the stereochemistry at C-4 in the analogue **5** may increase cytotoxicity, while changing the configuration at both C-3 and C-4 in the bicyclic analogue **2** causes a decrease in cytotoxicity in most of the cells tested.

We believe that the potent antitumour activities of the synthesized analogues **2**–**8** toward the malignant cells, as well as their complete inactivity against normal MRC-5 cell line, make them suitable leads for further development of more potent and selective antitumour agents.

SUPPLEMENTARY MATERIAL

Additional data are available electronically at the pages of journal website: https://www.shd-pub.org.rs/index.php/JSCS/index, or from the corresponding author on request.

Acknowledgements. This work was supported by research grants from the Ministry of Education, Science and Technological Development of the Republic of Serbia (Contract No. 451-03-68/2020-14/200125). This work has also received funding from the Serbian Academy of Sciences and Arts under Strategic projects programme (Grant agreement No. 01-2019-F65), as well as by a research project from the same institution (Grant No. F-130).

И З В О Д

СИНТЕЗА И АНТИПРОЛИФЕРАТИВНА АКТИВНОСТ ПОЈЕДНОСТАВЉЕНИХ АНАЛОГА ГОНИОФУФУРОНА

БОЈАНА СРЕЋО ЗЕЛЕНОВИЋ[1], САЊА ГРАБЕЖ[1], МИРЈАНА ПОПСАВИН[1], ВЕСНА КОЈИЋ[2], ЈОВАНА ФРАНЦУЗ[1] и ВЕЛИМИР ПОПСАВИН[1,3]

[1]Департман за хемију, биохемију и заштиту животне средине, Природно–математички факултет, Трг Доситеја Обрадовића 3, 21000 Нови Сад, [2]Онколошки институт Војводине, Пут др Голдмана 4, 21204 Сремска Каменица и [3]Српска академија наука и уметности, Кнеза Михаила 35, 11000 Београд

Више нових аналога (+)-гониофуфурона је дизајнирано и синтетизовано полазећи из D-ксилозе, односно из D-ликсозе. Испитана је способност аналога да инхибирају раст одабраних хуманих туморских ћелијских линија. Најактивнији молекули, који показују ниску наномоларну цитотоксичност, су дефениловани аналози **2** (IC_{50} = 3,0 nM, K562) и **3** (IC_{50} = 5,1 nM, K562 и 9,3 nM, Raji). Коначно, свако од добијених једињења показало је суб-микромоларну активност (IC_{50} 0,01–0,54 μM) према најмање једној од седам испитиваних малигних ћелијских линија. Прелиминарном SAR анализом је утврђено да дефениловани аналози гониофуфурона (дизајнирани уклањањем ароматичног прстена са C-7), а такође и аналози са отвореним тетрахидрофуранским прстеном (синтетисани раскидањем C_3–C_6 везе) могу показати побољшану антипролиферативну активност. Такође, промена стереохемије на C-4 у молекулу 5 може повећати цитотоксичност аналога, док промена конфигурације на C-3 и C-4 у бицикличном аналогу 2 смањује активност према већини испитиваних ћелија. Снажна антитуморска активност испољена према малигним ћелијама и потпуна неактивност синтетизованих аналога **2**–**8** према нормалним ћелијама MRC-5, представљају погодну основу за даљи развој нових, потентнијих и селективнијих антитуморских агенаса.

(Примљено 30. јула, прихваћено 10. септембра 2020)

REFERENCES

1. D. J. Newman, G. M. Cragg, *J. Nat. Prod.* **79** (2016) 629 (https://doi.org/10.1021/acs.jnatprod.5b01055)
2. E. A. Crane, K. Gademann, *Angew. Chem.* **55** (2016) 3882 (https://doi.org/10.1002/anie.201505863)
3. Z. Xiao, S. L. Morris-Natschke, K.-H. Lee, *Med. Chem. Res.* **36** (2016) 32 (https://doi.org/10.1002/med.21377)
4. T. Rodrigues, D. Reker, P. Schneider, G. Schneider, *Nature Chem.* **8** (2016) 531 (https://doi.org/10.1038/nchem.2479)
5. S. Wang, G. Dong, C. Sheng, *Acta Pharm. Sinica, B* **9** (2019) 880 (https://doi.org/10.1016/j.apsb.2019.05.004)

6. C.-Y. Choo, N. Abdullah, M. Diederich, *Phytochem Rev*. **13** (2014) 835 (https://doi.org/10.1007/s11101-014-9372-2)
7. C. Wiart, *Evid. Based Complement. Altern. Med*. **4** (2007) 299 (https://doi:10.1093/ecam/nem009)
8. A. de Fatima, L. V. Modolo, L. S. Conegero, R. A. Pilli, C. V. Ferreira, L. K. Kohn, J. E. de Carvalho, *Curr. Med. Chem*. **13** (2006) 3371 (https://doi.org/10.2174/092986706779010298)
9. H. B. Mereyala, M. Joe, *Curr. Med. Chem. Anti-Cancer Ag*. **1** (2001) 293 (https://doi.org/10.2174/1568011013354606)
10. X. P. Fang, J. E. Anderson, C. J. Chang, P. E. Fanwick, J. L. McLaughlin, *J. Chem. Soc. Perkin.Trans. 1* (1990) 1655 (https://dx.doi.org/10.1039/P19900001655)
11. T. K. M. Shing, H. C. Tsui, Z. H. Zhou, *Tetrahedron* **48** (1992) 8659 (https://doi.org/10.1016/S0040-4020(01)89441-2)
12. T. Gracza, V. Jäger, *Synlett* **3** (1992) 191 (https://doi.org/10.1055/s-1992-21309)
13. M. Mondon, J.-P. Gesson, *Curr. Org. Synth.* **3** (2006) 41 (https://doi.org/10.2174/157017906775473966)
14. G. Zhao, B. Wu, X. Y. Wu, Y. Z. Zhang, *Mini-Rev. Org. Chem.* **2** (2005) 333 (https://doi.org/10.2174/157019305774322699)
15. Y. Zhang, X. Liu, F. Shui, F. Zhou, J. Cui, X. Chen, *Tetrahedron Lett*. **60** (2019) 1784, and cited references. https://doi.org/10.1016/j.tetlet.2019.06.001
16. J. Francuz, I. Kovačević, M. Popsavin, G. Benedeković, B. Srećo Zelenović, V. Kojić, D. Jakimov, L. Aleksić, G. Bogdanović, T. Srdić-Rajić, E. Lončar, M. V. Rodić, V. Divjaković, V. Popsavin, *Eur. J. Med. Chem*. **128** (2017) 13, and cited references (https://doi.org/10.1016/j.ejmech.2017.01.024)
17. V. Popsavin, S. Grabež, M. Popsavin, I. Krstić, V. Kojić, G. Bogdanović, V. Divjaković, *Tetrahedron Lett*. **45** (2004) 9409 (https://doi.org/10.1016/j.tetlet.2004.10.122)
18. V. Popsavin, S. Grabež, I. Krstić, M. Popsavin, D. Djoković, *J. Serb. Chem. Soc*. **68** (2003) 795
19. B. A. Dimitriev, A. Y. Chernyak, I. K. Kochetkov, *Zhur. Org. Khim*. **41** (1972) 2757
20. B. Srećo, G. Benedeković, M. Popsavin, P. Hadžić, V. Kojić, G. Bogdanović, V. Divjaković, V. Popsavin, *Tetrahedron* **67** (2011) 9358 (https://doi.org/10.1016/j.tet.2011.09.132)
21. J. Barbat, J. Gelas, D. Horton, *Carbohydr. Res.* **219** (1991) 115 (https://doi.org/10.1016/0008-6215(91)89046-I)
22. V. Popsavin, S. Grabež, B. Stojanović, M. Popsavin, V. Pejanović, D. Miljković, *Carbohydr. Res*. **321** (1999) 110 (https://doi.org/10.1016/S0008-6215(99)00164-0)
23. D. A. Scudiero, R. H. Shoemaker, K. D. Paull, A. Monks, S. Tierney, T. H. Nofziger, M. J. Currens, D. Seniff, M. R. Boyd, *Cancer. Res*. **48** (1988) 4827 (https://pdfs.semanticscholar.org/3299/2997d7d34c82c2ce34937b25c5a770dbd735.pdf)
24. F. Z. Mata, M. B. Martinez, J. A. G. Perez, *Carbohydr. Res*. **201** (1990) 223 (https://doi.org/10.1016/0008-6215(90)84238-P)
25. S. Valverde, M. Martin-Lomas, B. Herradon, S. Garcia-Ochoa, *Tetrahedron* **43** (1987) 1895 (https://doi.org/10.1016/S0040-4020(01)81502-7)
26. H. Ohrui, G. H. Jones, J. G. Moffatt, M. L. Maddox, A. T. Christensen, S. K. Byram, *J. Am. Chem. Soc*. **97** (1975) 4602 (https://doi.org/10.1021/ja00849a023)
27. V. Popsavin, B. Srećo, G. Benedeković, J. Francuz, M. Popsavin, V. Kojić, G. Bogdanović, *Eur. J. Med. Chem.* **45** (2010) 2876 (https://doi.org/10.1016/j.ejmech.2010.03.010).

Journal of the Serbian Chemical Society
JSCS-info@shd.org.rs • www.shd.org.rs/JSCS
J. Serb. Chem. Soc. *85* (12) S559–S565 (2020) *Supplementary material*

SUPPLEMENTARY MATERIAL TO

Synthesis and antiproliferative activity of simplified goniofufurone analogues

BOJANA SREĆO ZELENOVIĆ[1], SANJA GRABEŽ[1], MIRJANA POPSAVIN[1], VESNA KOJIĆ[2], JOVANA FRANCUZ[1] and VELIMIR POPSAVIN[1,3]*

[1]*Department of Chemistry, Biochemistry and Environmental Protection, Faculty of Sciences, University of Novi Sad, Trg Dositeja Obradovića 3, 21000 Novi Sad, Serbia,* [2]*Oncology Institute of Vojvodina, Put Dr. Goldmana 4, 21204 Sremska Kamenica, Serbia and* [3]*Serbian Academy of Sciences and Arts, Kneza Mihaila 35, 11000 Belgrade, Serbia*

J. Serb. Chem. Soc. *85* (12) (2020) 1539–1551

PHYSICAL AND SPECTRAL DATA OF SYNTHESIZED COMPOUNDS

*3,6-Anhydro-5,7-di-*O*-benzyl-2-deoxy-D-ido-heptono-1,4-lactone (**10**).*

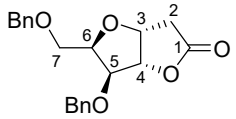

10

Colourless needles, m.p.: 90 °C (MeOH), $[\alpha]_D$ = +8.6° (*c* 1.2, $CHCl_3$), R_f = 0.62 (4:1 hexane/Et_2O). ^{1}H-NMR (250 MHz, $CDCl_3$): δ 2.71 (*m*, 2 H, $J_{2a,3}$ = 4.4, $J_{2b,3}$ = 2.9 Hz, H-2), 3.73 (*d*, 2 H, $J_{6,7}$ = 5.5 Hz, 2×H-7), 4.22 (*dd*, 1 H, $J_{4,5}$ = 0.6, $J_{5,6}$ = 4.1 Hz, H-5), 4.31 (*m*, 1 H, H-6), 4.59 and 4.64 (4×*d*, partially overlapped, 4 H, J_{gem} = 11.9 Hz, 2×CH_2Ph), 4.93 (*dd*, 1 H, $J_{3,4}$ = 4.8, $J_{4,5}$ = 0.6 Hz, H-4), 4.96 (*m*, 1 H, H-3), 7.26-7.42 ppm (*m*, 10 H, 2×Ph). ^{13}C-NMR (62.9 MHz, $CDCl_3$): δ 36.0 (C-2), 68.2 (C-7), 72.8 and 73.6 (2×*C*H_2Ph), 77.0 (C-3), 79.7 (C-6), 81.6 (C-5), 85.6 (C-4), 127.8, 127.9, 128.2, 128.5, 128.7, 137.3, 138.0 (2×Ph), 175.5 ppm (C-1). LRMS (CI): *m*/*z* 355 (M^++H), 263 (M^+−Bn). Anal.: Found: C, 70.89; H, 6.39. Calcd. for $C_{21}H_{22}O_5$: C, 71.17; H, 6.26.

* Corresponding author. E-mail: velimir.popsavin@dh.uns.ac.rs

*Methyl (*E*)-5,7-di-*O*-benzyl-2,3-dideoxy-D-xylo-hept-2-enonate (**11**).*

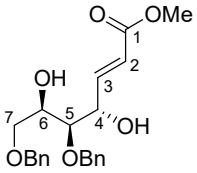

11

Colourless syrup, $[\alpha]_D$ = −188.9° (*c* 1.1, $CHCl_3$), R_f = 0.50 (4:1 Et_2O/ /hexane). IR (film): ν_{max} 3430 (OH), 1730 (C=O), 1670 (C=C), 1610 cm^{-1} (Ph). ^{1}H-NMR (250 MHz, $CDCl_3$): δ 2.81 and 3.22 (2×d, 1 H each, exchangeable with D_2O, J = 6.1 Hz, 2×OH), 3.52 (*dd*, 1 H, $J_{6,7a}$ = 5.6, $J_{7a,7b}$ = 9.7 Hz, H-7a), 3.60 (*dd*, 1 H, $J_{7a,7b}$ = 9.7, $J_{6,7b}$ = 5.7 Hz, H-7b), 3.62 (*t*, 1 H, $J_{4,5} = J_{5,6} =$ = 4.1 Hz, H-5), 3.76 (*s*, 3 H, OMe), 3.97 (*m*, 1 H, H-6), 4.50 (*m*, 1 H, $J_{3,4}$ = 4.3, $J_{2,4}$ = 2.0 Hz, H-4), 4.51 (*s*, 2 H, CH_2Ph), 4.61 (2×*d*, 2 H, J_{gem}=11.3 Hz, CH_2Ph), 6.16 (*dd*, 1 H, $J_{2,3}$ = 15.6 Hz, H-2), 7.03 (*dd*, 1 H, $J_{3,4}$ = 4.3, $J_{2,3}$ = 15.6 Hz, H-3), 7.25–7.42 ppm (*m*, 10 H, 2×Ph). ^{13}C-NMR (62.9 MHz, $CDCl_3$): δ 51.5 (OMe), 70.7 (C-4), 70.8 (C-6), 71.1 (C-7), 73.4 and 74.7 (2×CH_2Ph), 80.6 (C-5), 121.1 (C-2), 127.9, 128.1, 128.2, 128.4, 128.45, 137.3, 137.4 (2×Ph), 147.5 (C-3), 166.7 ppm (C-1). LRMS (FAB): *m/z* 409 (M^++Na), 387 (M^++H). Anal.: Found: C, 68.10; H, 6.83. Calcd. for $C_{22}H_{26}O_6$: C, 68.38; H, 6.78.

*Methyl 3,6-anhydro-5,7-di-*O*-benzyl-2-deoxy-D-gulo-heptonoate (**12**).*

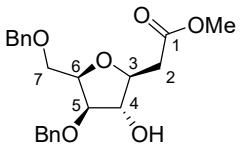

12

Colourless oil, $[\alpha]_D$ = −18.7° (*c* 1.0, $CHCl_3$), R_f = 0.50 (4:1 Et_2O/hexane). ^{1}H-NMR (250 MHz, $CDCl_3$): δ 2.68 (*dd*, 1 H, $J_{2a,3}$ = 9.6, $J_{2a,2b}$ = 17 Hz, H-2a), 2.97 (*dd*, 1 H, $J_{2b,3}$ = 5.0, $J_{2a,2b}$ = 17 Hz, H-2b), 3.12 (*bs*, 1 H, OH), 3.60–3.80 (*m*, 5 H, 2×H-7 and OMe), 3.93 (*m*, 1 H, H-3), 3.99 (*dd*, 1 H, $J_{4,5}$ = 2.3, $J_{5,6} =$ = 5.1 Hz, H-5), 4.08 (dd, 1 H, $J_{3,4}$ = 4.9, $J_{4,5}$ = 2.3 Hz, H-4), 4.23 (*m*, 1 H, H-6), 4.48–4.72 (4×*d*, 1 H each, J_{gem} = 12.0 Hz, 2×CH_2Ph), 7.24–7.39 ppm (*m*, 10 H, 2×Ph). ^{13}C-NMR (62.9 MHz, $CDCl_3$): δ 38.3 (C-2), 52.0 (OMe), 68.7 (C-7), 71.6 and 73.4 (2×CH_2Ph), 79.7 (C-6), 80.8 (C-3), 81.1 (C-4), 85.3 (C-5), 127.5, 127.6, 127.8, 128.3, 128.4, 137.9, 138.1 (Ph), 172.9 ppm (C-1).

*Methyl 5,7-di-*O*-benzyl-2,3-dideoxy-4-oxo-D-threo-heptonate (**13**).*

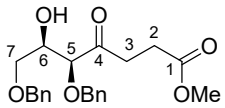

13

Bright yellow oil, $[\alpha]_D$ = −69.9° (*c* 1.4, $CHCl_3$), R_f = 0.71 (4:1 Et_2O/ /hexane). ^{1}H-NMR (250 MHz, $CDCl_3$): δ 2.59 (*t*, 2 H, *J* = 6.4 Hz, H-2a and H-2b), 2.84 (*bs*, 1 H, exchangeable with D_2O, OH), 2.87 and 2.88 (2×*t*, 1 H each, *J* = 6.4 Hz, H-3a and H-3b), 3.52 (*dd*, 1 H, $J_{7a,7b}$ = 9.5, $J_{6,7a}$ = 6.1 Hz, H-7a), 3.60 (*dd*, 1 H, $J_{6,7b}$ = 5.6 Hz, H-7b), 3.68 (*s*, 3 H, OMe), 4.04 (*d*, 1 H, $J_{5,6}$ = 3.3 Hz, H-5), 4.11 (*m*, 1 H, H-6), 4.42–4.55 (*m*, 3 H, 2×PhCH_2), 4.74 (*d*, 1 H, J_{gem} = = 11.5 Hz, PhCH_2), 7.25–7.42 ppm (*m*, 10 H, 2×*Ph*CH_2). ^{13}C-NMR ($CDCl_3$): δ 27.2 (C-2), 34.4 (C-3), 51.8 (OMe), 70.1 (C-7), 71.1 (C-6), 73.2 and 73.3 (2×PhCH_2), 83.9 (C-5), 127.6, 127.65, 128.0, 128.1, 128.2, 128.4, 136.9 and 137.6 (2×*Ph*CH_2), 173.3 (C-1), 210.4 ppm (C-4). LRMS (FAB): *m/z* 409 (M^++Na), 387 (M^++H).

*3,6-Anhydro-2-deoxy-D-ido-heptono-1,4-lactone (**2**).*

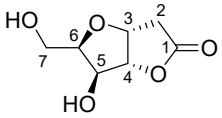

2

Transparent needles, m.p.: 71–73 °C (EtOAc/MeOH), $[\alpha]_D$ = +26.8° (*c* 1.8, H_2O), lit[1] m.p.: 72–74 °C, $[\alpha]_D$ = +28.4° (*c* 1.9, H_2O), R_f = 0.72 (9:1 CH_2Cl_2/MeOH). ^{1}H-NMR (250 MHz, acetone-d_6): δ 2.47 (*d*, 1 H, $J_{2a,2b}$ = 18.8 Hz, H-2a), 2.85 (*dd*, 1 H, $J_{2b,3}$ = 6.1, $J_{2a,2b}$ = 18.8 Hz, H-2b), 3.66 (*dd*, 1 H, $J_{7a,7b}$ = 11.6, $J_{6,7a}$ = 5.2 Hz, H-7a), 3.75 (*dd*, 1 H, $J_{6,7b}$ = 5.1, $J_{7a,7b}$ = 11.6 Hz, H-7b), 3.96 (*m*, 1 H, $J_{5,6}$ = 1.8 Hz, $J_{6,7a}$ = 5.2, $J_{6,7b}$ = 5.1 Hz, H-6), 4.25 and 5.01 (*bs*, 2 H, exchangeable with D_2O, 2×OH), 4.34 (*d*, 1 H, $J_{5,6}$ = 1.8 Hz, H-5), 4.88 (*d*, 1 H, $J_{3,4}$ = 4.4 Hz, H-4), 4.94 ppm (*dd*, 1 H, $J_{2b,3}$ = 6.1, $J_{3,4}$ = 4.4 Hz, H-3). ^{13}C-NMR (62.9 MHz, acetone-d_6): δ 36.2 (C-2), 60.0 (C-7), 73.9 (C-5), 77.2 (C-3), 81.9 (C-6), 88.9 (C-4), 177.7 ppm (C-1). LRMS (FAB): *m/z* 371 ($2M^+$+Na), 349 ($2M^+$+H), 197 (M^++Na), 175 (M^++H), 157 (M^+−OH).

Methyl 3,6-anhydro-2-deoxy-4,5-O-*isopropylidene-D-talo-heptanoate* (***18***).

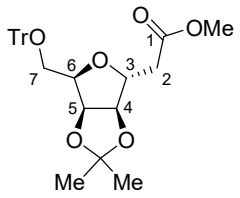

18

White needles, m.p.: 138 °C (MeOH), $[\alpha]_D$ = −21.7° (*c* 0.8, $CHCl_3$), R_f = = 0.30 (19:1 toluene/EtOAc). ^{1}H-NMR (250 MHz, $CDCl_3$): δ 1.31 and 1.35 (2×*s*, 3 H each, CMe_2), 2.47 (*dd*, 1 H, $J_{2a,2b}$ = 15.3, $J_{2a,3}$ = 7.9 Hz, H-2a), 2.57 (*dd*, 1 H, $J_{2a,2b}$ = 15.3, $J_{2b,3}$ = 7.4 Hz, H-2b), 3.37 (*dd*, 1 H, $J_{7a,7b}$ = 9.5, $J_{6.7a}$ = 6.3 Hz, H-7a), 3.45 (*dd*, 1 H, $J_{7a,7b}$ = 9.5, $J_{6,7b}$ = 5.7 Hz, H-7b), 3.73 (*s*, 3 H, OMe), 3.97 (*m*, 1 H, $J_{5,6}$ = 3.9 Hz, H-6), 4.47 (*td*, 1 H, $J_{3,4}$ = 1.1 Hz, H-3), 4.61 (*dd*, 1 H, $J_{3,4}$ = 1.1, $J_{4,5}$ = 6.1 Hz, H-4), 4.78 (*dd*, 1 H, $J_{4,5}$ = 6.1, $J_{5,6}$ = 3.9 Hz, H-5), 7.19–7.54 ppm (*m*, 15 H, 3×Ph). ^{13}C-NMR (62.9 MHz, $CDCl_3$): δ 25.3 and 26.2 (C*Me*$_2$), 36.3 (C-2), 51.9 (OMe), 61.7 (C-7), 79.3 (C-6), 80.3 (C-3), 81.0 (C-5), 84.8 (C-4), 86.8 (Ph$_3$*C*), 112.7 (*C*Me$_2$) 126.9, 127.7, 128.82, 144.0 (3×Ph), 170.8 ppm (C-1). LRMS (FAB): *m*/*z* 511 (M^++Na), 411 (M^+−Ph), 243 (Ph_3C^+). Anal.: Found: C, 73.48; H, 6.53. Calcd. for $C_{30}H_{32}O_6$: C, 73.75; H, 6.60.

Methyl 3,6-anhhydro-2-deoxy-4,5-O-*isopropylidene-D-galacto-heptanoate* (***19***).

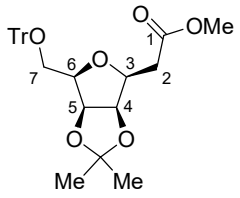

19

Colourless oil $[\alpha]_D$ = −26.3° (*c* 1.0, $CHCl_3$), R_f = 0.35 (19:1 toluene/EtOAc). ^{1}H-NMR (250 MHz, $CDCl_3$): δ 1.43 and 1.36 (2×*s*, 3 H each, CMe_2), 2.78 (*dd*, 1 H, $J_{2a,3}$ = 6.6, $J_{2a,2b}$ = 16.7 Hz, H-2a), 2.83 (*dd*, 1 H, $J_{2a,2b}$ = 16.7, $J_{2b,3}$ = = 7.0 Hz, H-2b), 3.42 (*dd*, 1 H, $J_{6,7a}$ = 6.4, $J_{7a,7b}$ = 9.5 Hz, H-7a), 3.49 (*dd*, 1 H, $J_{7a,7b}$ = 9.5, $J_{6,7b}$ = 6.0 Hz, H-7b), 3.70 (*td*, 1 H, $J_{5,6}$ = 2.9 Hz, H-6), 3.72 (*s*, 3 H, OMe), 3.94 (*td*, 1 H, $J_{3,4}$ = 2.9 Hz, H-3), 4.78 (*m*, 2 H, H-4 and H-5), 7.17–7.58 ppm (*m*, 15 H, 3×Ph). ^{13}C-NMR (62.5 MHz, $CDCl_3$): δ 25.2 and 25.8 (C*Me*$_2$), 33.4 (C-2), 51.7 (OMe), 61.3 (C-7), 77.4 (C-3), 80.6 (C-6), 81.0 and 81.1 (C-4 and C-5), 86.8 (Ph$_3$*C*), 112.2 (*C*Me$_2$), 126.8, 127.6, 128.8, 144.0 (3×Ph), 171.5 ppm (C-1).

*3,6-Anhydro-2-deoxy-D-galacto-heptono-1,4-lactone (**3**).*

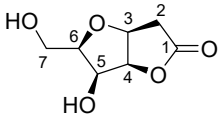

3

White crystals, m.p.: 126–127 °C ($CHCl_3$), $[\alpha]_D$ = −98.0° (*c* 0.9, MeOH), R_f = 0.20 (EtOAc). ^{1}H-NMR (250 MHz, acetone-d_6): δ 3.92 and 4.46 (*bs*, 2 H, exchangeable with D_2O, 2×OH), 2.50 (*dd*, 1 H, $J_{2a,2b}$ = 18.4, $J_{2a,3}$ = 2.6 Hz, H-2a), 2.80 (*dd*, 1 H, $J_{2a,2b}$ = 18.4, $J_{2b,3}$ = 7.3 Hz, H-2b), 3.63 (*dd*, 1 H, $J_{7a,7b}$ = = 11.6, $J_{6,7a}$ = 4.6 Hz, H-7a), 3.78 (*dd*, 1 H, $J_{7a,7b}$ = 11.6, $J_{7b,6}$ = 5.8 Hz, H-7b), 3.93 (*m*, 1 H, $J_{5,6}$ = 5.0 Hz, H-6), 4.45 (*t*, 1 H, $J_{4,5}$ = 5.0 Hz, H-5), 4.69 (*ddd*, 1 H, $J_{2a,3}$ = 2.6, $J_{2b,3}$ = 7.3, $J_{3,4}$ = 6.0 Hz, H-3), 5.03 ppm (*t*, 1 H, H-4). ^{13}C-NMR (62.9 MHz, acetone-d_6): δ 36.9 (C-2), 61.4 (C-7), 72.1 (C-5), 76.6 (C-3), 83.4 (C-6), 83.9 (C-4), 176.5 ppm (C-1). LRMS (FAB): *m*/*z* 371 ($2M^+$+Na), 349 ($2M^+$+H), 197 (M^++Na), 175 (M^++H). Anal.: Found: C, 48.56; H, 5.48. Calcd. for $C_7H_{10}O_5$: C, 48.28; H, 5.79.

*Methyl (*E*)-5,7-di-*O*-benzyl-2,3-dideoxy-D-lyxo-hept-2-enoate (**22**).*

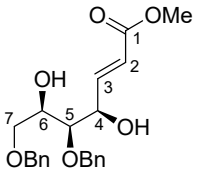

22

Colourless needles, m.p.: 95–96 °C (toluene/hexane), $[\alpha]_D$ = +14.0° (*c* 1.1, $CHCl_3$), R_f = 0.45 (4:1 Et_2O/hexane). IR ($CHCl_3$): ν_{max} 3368 (OH), 1724 (C=O), 1660 cm^{-1} (C=C). ^{1}H-NMR (250 MHz, $CDCl_3$): δ 2.85 and 3.60 (2×*bs*, 1 H each, 2×OH), 3.47 (*dd*, $J_{7a,7b}$ = 9.4, $J_{6,7a}$ = 5.8 Hz, H-7a), 3.51 (*dd*, 1 H, $J_{4,5}$ = = 7.0, $J_{5,6}$ = 2.4 Hz, H-5), 3.58 (*dd*, 1 H, $J_{7a,7b}$ = 9.4, $J_{6,7b}$ = 6.4 Hz, H-7b), 3.73 (*s*, 3 H, OMe), 4.01 (*td*, 1 H, H-6), 4.48–4.50 (4×*d*, 1 H each, J_{gem} = 11.4 and 11.7 Hz, 2×PhCH_2), 4.60 (*m*, 1 H, $J_{2,4}$ = 2.0, $J_{3,4}$ = 4.0 Hz, H-4), 6.20 (*dd*, 1 H, $J_{2,4}$ = 2.0, $J_{2,3}$ = 15.6 Hz, H-2), 7.00 (*dd*, 1 H, $J_{3,4}$ = 4.0, $J_{2,3}$ = 15.6 Hz, H-3), 7.24–7.38 ppm (*m*, 10 H, 2×Ph). ^{13}C-NMR (62.9 MHz, $CDCl_3$): δ 51.6 (OMe), 70.4 (C-6), 70.7 (C-4), 71.1 (C-7), 73.0 and 73.5 (2×PhCH_2), 78.9 (C-5), 121.4 (C-2), 127.9, 128.1, 128.2, 128.5, 128.53, 137.2, 137.5 (Ph), 147.0 (C-3), 166.7 ppm (C-1). LRMS (FAB): *m*/*z* 387 (M^++H), 409 (M^++Na). Anal.: Found: C, 68.10; H, 6.83. Calcd. for $C_{22}H_{26}O_6$: C, 68.38; H, 6.78.

*2,3-Dideoxy-D-lyxo-heptono-1,4-lactone (**6**).*

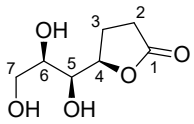

6

Pale yellow syrup, $[\alpha]_D$ = −1.2° (*c* 0.4, $CHCl_3$), R_f = 0.21 (47:3 EtOAc/ /MeOH). IR (KBr): ν_{max} 3377 (OH), 1755 cm^{-1} (C=O). ^{1}H-NMR (250 MHz, acetone-d_6): δ 2.28 (*m*, 2 H, $J_{2,3}$ = 8.3, $J_{3,4}$ = 7.3 Hz, 2×H-3), 2.48 (*t*, $J_{2,3}$ = 8.3 Hz, 2 H, H-2), 3.54–3.68 (*m*, 3 H, $J_{5,6}$ = 2.5 Hz, H-6 and 2×H-7), 3.74 (*dd*, 1 H, $J_{4,5}$ = 5.8, $J_{5,6}$ = 2.5 Hz, H-5), 4.61 ppm (*m*, 1 H, H-4). ^{13}C-NMR (62.9 MHz, acetone-d_6): δ 24.0 (C-3), 28.7 (C-2), 64.0 (C-7), 71.9 (C-6), 72.7 (C-5), 80.7 (C-4), 177.7 ppm (C-1). HRMS (ESI): *m*/*z* 177.0764 (M^++H). Calcd. for $C_7H_{13}O_5$: 177.0758.

*3,6-Anhydro-5-*O*-benzyl-2-deoxy-D-ido-heptono-1,4-lactone (**8**).*

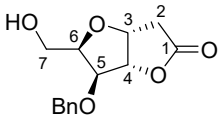

8

Colourless syrup, $[\alpha]_D$ = +4.3° (*c* 1.0, $CHCl_3$), R_f = 0.31 (Et_2O). IR ($CHCl_3$): ν_{max} 3467 (OH), 1789 cm^{-1} (C=O). ^{1}H-NMR (250 MHz, $CDCl_3$): δ 2.52 (*bs*, 1 H, OH), 2.58–2.78 (*m*, 2 H, 2×H-2), 3.76 (*dd*, 1 H, $J_{6,7a}$ = 4.3, $J_{7a,7b}$ = = 12.0 Hz, H-7a), 3.84 (*dd*, 1 H, $J_{6,7b}$ = 5.1, $J_{7a,7b}$ = 12.0 Hz, H-7b), 4.17 (*m*, 1 H, $J_{5,6}$ = 4.9 Hz, H-6), 4.25 (*d*, 1 H, $J_{5,6}$ = 4.9 Hz, H 5), 4.56 and 4.71 (2×*d*, J_{gem} = 11.9 Hz, CH_2Ph), 4.91–5.01 (*m*, 2 H, H-3 and H-4), 7.26–7.42 ppm (*m*, 5 H, Ph). ^{13}C-NMR (62.9 MHz, $CDCl_3$): δ 35.8 (C-2), 61.1 (C-7), 72.7 (*C*H_2Ph), 76.7 (C 3), 80.7 (C-6), 82.1 (C-5), 85.7 (C-4), 127.6, 128.2, 128.6, 136.7 (Ph), 175.2 ppm (C-1). HRMS (ESI): *m*/*z* 265.1066 (M^++H), Calcd. for $C_{14}H_{17}O_5$: 265.1070.

SAR ANALYSIS

The structure–activity relationships were accessed as follows: the IC_{50} values of two compounds were compared, and the Δlog IC_{50} was calculated (Δlog IC_{50} is the difference between the log IC_{50} values of an analogue and the corresponding control compound). Positive Δlog IC_{50} values show a decrease of antiproliferative activity, whereas negative values indicate an increase in the activity upon the structural modification being considered. The results are presented in Fig. S-1.

TABLE S-1. Cytotoxicity data for SAR analysis

Compound	IC_{50} / μM[a], 72 h						
	K562	HL-60	Jurkat	Raji	HT-29	MDA-MB 231	HeLa
1	0.41	201.32	32.45	18.45	0.59	75.34	8.32
2	0.003	5.56	3.73	115.78	564.31	75.31	0.01
3	0.0051	221.32	321.52	0.0093	0.056	0.11	312.46
4	0.54 [b]	0.09 [b]	2.23 [b]	2.21[b]	2001.21	5031.23	2.34 [b]
5	4.21	0.02	102.89	364.25	94.35	0.011	486.25
6	3.54	112.89	11.84	89.64	0.12	489.16	4.10
7	0.12	20.62	9.45	56.37	12.45	67.50	0.03
8	0.065	0.09	1.02	11.39	669.48	664.25	5.92

[a]IC_{50} is the concentration of compound required to inhibit the cell growth by 50 % compared to an untreated control. Values are means of three independent experiments. Coefficients of variation were less than 10 %; [b]taken from reference[2]

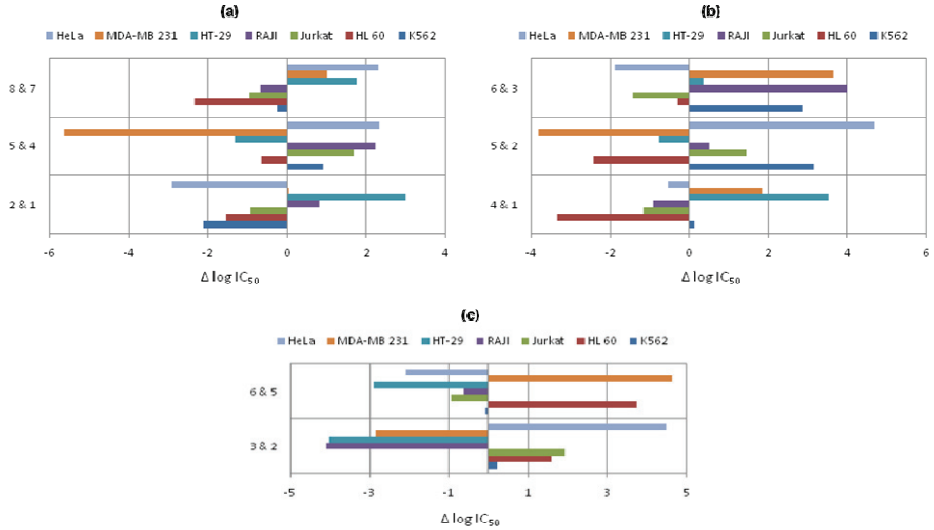

Fig. S-1. SAR analysis of goniofufurone (**1**) and analogues (**2**–**8**): (a) influence of the phenyl group; (b) influence of the tetrahydrofuran ring; (c) influence of stereochemistry at C-3 and/or C-4.

REFERENCES

1. B. A. Dimitriev, A. Y. Chernyak, I. K. Kochetkov, *Zhur. Org. Khim*. **41** (1972) 2757
2. V. Popsavin, B. Srećo, G. Benedeković, J. Francuz, M. Popsavin, V. Kojić, G. Bogdanović, *European Journal of Medicinal Chemistry*, **45** (2010) 2876 (https://doi.org/10.1016/j.ejmech.2010.03.010).

Journal of the Serbian Chemical Society
JSCS-info@shd.org.rs • www.shd.org.rs/JSCS
J. Serb. Chem. Soc. *85* (12) 1553–1563 (2020)
JSCS–5392
UDC 582.639+581.4:665.3:66.094.3:536.7:615.279
Original scientific paper

Stabilization of rose hip oil with pomegranate peel extract during accelerated storage

JELENA MUDRIĆ[1]*, ZORICA DRINIĆ[1], GORDANA ZDUNIĆ[1], MARINA TODOSIJEVIĆ[2], DUBRAVKA BIGOVIĆ[1], NEBOJŠA MENKOVIĆ[1] and KATARINA ŠAVIKIN[1]

[1]*Institute for Medicinal Plant Research "Dr. Josif Pančić", Tadeuša Košćuška 1, 11000 Belgrade, Serbia and* [2]*Faculty of Chemistry, University of Belgrade, Studentski trg 10–12, 11000 Belgrade, Serbia*

(Received 24 April, revised 8 October, accepted 9 October 2020)

Abstract: Rose hip seed oil is a rich source of polyunsaturated fatty acids, as well as tocopherols, carotenoids, sterols, phospholipids, and phenolic compounds. On the other hand, due to the high content of polyunsaturated fatty acids, this oil is prone to oxidation. The aim of this study was to investigate the influence of a natural antioxidant, *i.e.*, pomegranate peel extract, and its combination with butylated hydroxytoluene as a commonly used synthetic antioxidant, on the stability of rose hip oil. The stability of samples without and with different antioxidants was monitored through analysis of the fatty acid composition and measurement of the quality and stability parameters of the oil (peroxide value, *p*-anisidine value, thiobarbituric acid reactive substances inhibition, total phenolic content and antiradical activity) during a storage period of 12 days at 65 °C. Pomegranate peel extract (0.1 %) inhibited more effectively the second stage of oxidation than butylated hydroxytoluene (0.02 %), while the first stage of oxidation was better prevented by the synthetic antioxidant. Furthermore, the addition of pomegranate peel extract increased the total phenolic content of the rose hip oil as well as its antiradical activity. Thus, pomegranate peel extract could be used as a potent natural antioxidant for the stabilization of beneficial but unstable rose hip oil.

Keywords: *Rosa canina*; lipid oxidation; natural antioxidants; thermal stability; oxidative stability; *Punica granatum*.

INTRODUCTION

Rose hip is the pseudo-fructus or pseudocarp of rose plants, which belong to the *Rosa* genus of the *Rosaceae* family. *Rosa canina* is one of the most abundant rose species in Europe.[1] The content of seeds in the fruit is approximately 30–35

* Corresponding author. E-mail: jmudric@mocbilja.rs
https://doi.org/10.2298/JSC200424064M

%, while the remaining 65–70 % is pericarp.[2] The seeds were considered as a waste product by the food industry for a long time.[3] The quantity of oil in the rose hip seeds is between 5 and 18 % and it is known as a rich source of poly-unsaturated fatty acids (PUFA), as well as tocopherols, carotenoids, sterols, phospholipids and phenolic compounds.[1,4,5] It was reported previously that rose hip seed oil could be used for the treatment of eczema, skin ulcers, neurodermitis, cheilitis, skin scars, as well as for moisturizing and prevention of skin ageing.[6,7] Furthermore, it was noted that topical application of rose hip oil together with oral application of a poly-vitamin preparation of fat-soluble vitamins could exhibit a synergistic effect.[4] Diet supplemented with 15 % rose hip oil caused a hypolipidemic effect in rat plasma as a consequence of the high content of PUFA.[8] Therefore, rose hip oil could be beneficial in various products such as cosmetics, pharmaceutics, and nutraceuticals. However, oils with a high content of PUFA are prone to oxidation. Lipid oxidation is related to the occurrence of unpleasant odors, flavors, and discoloration. Furthermore, during the oxidation, toxic degradation products are formed.[9]

It was reported that nano-encapsulation was able to protect rose hip oil from oxidation under UVA and UVC light.[10] However, this procedure is considered as expensive and complex. Therefore, synthetic antioxidants, such as butylated hydroxyanisole (BHA), butylated hydroxytoluene (BHT) and *tert*-butylhydroquinone (TBHQ), are used usually to delay and prevent lipid oxidation. On the other hand, long-term intake of synthetic antioxidants is related to possible toxic effects and, as a result, the safety of synthetic antioxidants is controversial.[11] Consequently, there is growing interest to replace synthetic with natural antioxidants.[12] According to the literature, antioxidants from the phenolic family are the most active in the stabilization of oils among other natural ingredients.[12] Moreover, by incorporating polyphenol-rich extracts in the oils, a higher intake of such compounds in the diet is enabled, thus, additional health benefits could be expected.[13,14]

It is known that pomegranate (*Punica granatum* L.) peel extract is a valuable source of phenolics, such as ellagitannins, proanthocyanidins, flavonoids, and phenolic acids. Consequently, pomegranate peel extract has a strong antioxidative and anti-microbial activity.[15,16] Therefore, it was speculated that pomegranate peel extract could be used as a natural additive for food preservation. Previously, it was reported that pomegranate peel extract was a more potent antioxidant (at a concentration of 0.1 %) for the stabilization of sunflower oil than BHT (at a concentration of 0.02 %).[16] Furthermore, pomegranate peel extract (10 mg equiv. phenolics/100 g meat) prevented lipid oxidation in cooked chicken patties and it was shown that the efficiency of the extract was higher than vitamin C (50 mg/100 g meat) as well as BHT (10 mg/100 g meat).[17,18] On the other

hand, pomegranate peel is usually recognized as a by-product in the production of pomegranate juice.[19]

Apart from the established health benefits of rose hip seed oil and pomegranate seed extract, these valuable products are underestimated. The aim of this study was to investigate the influence of pomegranate peel extract, as a substituent of commonly used synthetic antioxidants (BHT), on the stability of rose hip oil, which is prone to oxidation due to high content of PUFA.

EXPERIMENTAL

Plant material, standards and reagents

Rose hip seeds were purchased from the Institute for Medicinal Plants Research "Dr. Josif Pančić" from Belgrade, Serbia. The pomegranates were collected during November 2018 at a natural locality in the Village Do, Bosnia and Herzegovina. The peel of the pomegranate was manually separated from the seeds, air-dried at room temperature for 4–6 days and ground using a laboratory mill. Subsequently, the peel was sieved and particles ranging between 0.75 and 2 mm were used for the extraction. The following chemicals and reagents were used: acetic acid, hydrochloric acid, ethanol (96 %) and distilled water (Zorka Pharma, Serbia), thiobarbituric acid and 3-chloroacetic acid (Sigma Chemicals Co.), sodium hydroxide and sodium thiosulfate (Alfapanon, Serbia), petroleum ether, 4-methoxyaniline and isooctane (Fisher Chemical, UK), chloroform and potassium iodide (Carlo Erba, Spain), and Folin–Ciocalteu phenol reagent (Sigma–Aldrich). All chemicals were of analytical grade.

Preparation of pomegranate peel extract

Pomegranate peels were extracted by an ultrasound-assisted method, using ethanol (59 vol. %), for 25 min, under a temperature of 80 °C, while solid to solvent ratio was 1:44. These conditions were considered as optimal for the extraction of valuable compounds from pomegranate peels according to Živković *et al.*[19] The dry extract was obtained using a vacuum evaporator at under 50 °C (Laboxact SEM842, KNF, UK), and then stored at 4 °C.

Samples preparation and storage conditions

Ground rose hip seeds were extracted with *n*-hexane for 8 hours using a Soxhlet apparatus. Then, the *n*-hexane was evaporated in a vacuum evaporator at under 50 °C (Laboxact SEM842, KNF, UK). In order to evaluate the influence of pomegranate peel extract on the stability of rose hip oil, the pomegranate peel extract (0.1 %) was added to the oil. Butylated hydroxytoluene (BHT) was used in the maximal allowed concentration (0.02 %) as a positive control. A combination of pomegranate peel extract (0.05 %) and BHT (0.05 %) was added to the oil in order to evaluate a possible synergistic interaction of these antioxidants. Therefore, samples including rose hip oil without antioxidant, with BHT, with pomegranate peel extract, and with the combination of pomegranate peel extract and BHT were placed in dark glass bottles (three different bottles for each sample) with cups made from high-density polyethylene and stored in a thermostat for 3, 6, 9 and 12 days at 65 °C, according to previously published data that one day under a temperature of 65 °C corresponds to the one-month storage at ambient temperature.[20]

Fatty acid composition

The fatty acid composition of the rose hip seed oil was determined according to the method described by Zdunić *et al.*, with slight modifications.[21] The analyses were performed on an Agilent 7890A GC equipped with 5975 C inert XLEI/CI MSD and FID detector con-

nected by capillary flow technology 2-way splitter with make-up. A DB-23 capillary column (60 m×0.25 mm×0.25 μm) was used. The temperature for the GC oven was from 50 °C (hold for 1 min), then raised to 175 °C at 25 °C min^{-1}, raised to 235 °C at 4 °C min^{-1} and hold for 5 min. Helium was used as the carrier gas at 54.814 psi (constant pressure mode). The sample was analyzed (5 μL of sample was dissolved in 1 mL dichloromethane) in the split mode with split ratio of 10/1. The injection volume was 1 μL. The detector temperature was 300 °C. MS data was acquired in EI mode, with a scan range 40–550 *m*/*z*. The source temperature was 230 °C and quadrupole temperature was 150 °C. The solvent delay was 3 min. Area percent reports, obtained from standard processing of the FID chromatograms, were used as the basis for quantification purposes. The identification of the constituents was performed by comparing their mass spectra listed in the NIST/Wiley spectra libraries, using different types of search (PBM/NIST) and available literature data. Prior to analysis, fatty acid methyl esters were prepared according to the International Association of Official Analytical Communities (AOAC) (Official Surplus Method 965.4).[22]

Peroxide value

The peroxide value was determined according to the method described in the European Pharmacopeia with a slight modification.[23] The sample (approximately 5 g) was dissolved in a mixture (30 mL) of glacial acetic acid and chloroform (3:2 volume ratio) and a saturated solution of potassium iodide was added and shaken for 1 min. Then, water (100 mL) was added and the mixture was titrated against sodium thiosulfate (0.01 mol L^{-1}) until the disappearance of the yellow color. Afterwards, starch solution (5 mL) was added and titration was continued until the color disappeared. A blank sample was analyzed under the same conditions. The peroxide value of each sample was determined in triplicate and expressed as milli-equivalent of active oxygen per 1 kg of oil (meq. O_2 per kg).

p-*Anisidine value*

The *p*-anisidine value was determined according to the procedure described in the European Pharmacopeia.[23] Firstly, the test solution (a) was prepared by dissolving the oil (approximately 0.5 g) in isooctane (25 mL). Then, test solution (b) was prepared by adding 1 mL of *p*-anisidine solution in glacial acetic acid (2.5 g L^{-1}) to 5 mL of test solution (a). The reference solution was a mixture of isooctane (5 mL) and *p*-anisidine solution in glacial acetic acid. The absorbance of test solution (a) – A_2 and test solution (b) – A_1 after standing for 10 min was measured at 350 nm, while isooctane was used as the compensation liquid in a case of test solution (a) and the reference solution in the case of test solution (b). The *p*-anisidine value was calculated according to Eq. (1), where *m* is the weight of the sample in grams:

$$p\text{-Anisidine value} = \frac{25(1.2A_1 - A_2)}{m} \quad (1)$$

Thiobarbituric acid reactive substances (TBARS) assay

Thiobarbituric acid reactive substances (TBARS) were determined according to the procedure reported by Drinić *et al.* with slight modifications.[24] 3-Chloroacetic acid (15 g) was added in hydrochloric acid (0.25 M, 100 mL) and then thiobarbituric acid (0.375 g) was added to obtain thiobarbituric acid solution. The oil sample (0.5 g) was added to the thiobarbituric acid solution (2.5 mL) and then the mixture was heated in a boiling water bath for 10 min, cooled, sonicated for 30 min and centrifuged at 3000 rpm for 10 min. The absorbance of the sample supernatant was measured at 532 nm.

Total phenolic content (TPC) and DPPH radical scavenging activity

Methanol extracts of oils were obtained by liquid/liquid extraction of the oil samples (1 g) by methanol (1 mL) three times. In these samples, total the phenolic content and antioxidant activity were measured. Total phenolic content (TPC) was measured according to the Folin–Ciocalteu (FC) method by a slightly modified procedure described by Waterman and Mole.[25] The results are expressed as milligrams of gallic acid equiv. per g of oil (mg GAE g^{-1}). The anti-radical activity of the extract was determined by the DPPH (2,2-diphenyl-1-picryl-hydrazyl) assay with slight modifications.[26] Mixtures of the methanol extract of the oil sample and methanol solutions of DPPH (1400 μL, 40 μg mL^{-1}) were incubated for 20 min in a dark at room temperature. The absorbance of the mixture was measured at 517 nm, while methanol was used instead of the methanol extract of oil as a control. The antiradical activity is expressed in percent of DPPH radical scavenging capacity.

Statistical analyses

All experiments were performed in triplicate and the results are expressed as mean values with the standard deviation. Differences among mean values of collected data were estimated by one-way-analysis of variance (ANOVA) followed by the *post hoc* Tukey's test with significant levels of 95 % ($P < 0.05$). The statistical analysis was performed using MS Office Excel, version 2010.

RESULTS AND DISCUSSIONS

Fatty acid composition

The fatty acid composition of rose hip oil was determined at the beginning of the experiment in fresh oil (day 0) and after accelerated aging (12 days at 65 °C) in the samples with and without antioxidants (Table I). The rose hip oil samples

TABLE I. Fatty acid composition (%) of rose hip seed oil during storage without or with antioxidants. The results in the table were presented as mean ± standard deviations ($n = 3$); the same letters in the same row are not significantly different according to the Tukey's test, $p < 0.05$; N.I. – non-identified; A – without antioxidant at day 0, B – without antioxidant after 12 days of storage, C – with BHT (0.02 %) after 12 days of storage, D – with pomegranate peel extract (0.1 %) after 12 days of storage, E – with pomegranate peel extract (0.05 %) and BHT (0.01 %) after 12 days of storage

Fatty acid	Conditions				
	A	B	C	D	E
Palmitic acid	4.24±0.22^{a}	4.30±0.41^{a}	4.37±0.44^{a}	5.77±0.47^{b}	4.31±0.28^{a}
Stearic acid	3.01±0.3^{a}	2.97±0.23^{a}	2.85±0.35^{a}	4.96±0.27^{b}	2.82±0.32^{a}
Oleic acid	17.06±1.2^{ab}	17.22±0.96^{ab}	16.78±1.57^{a}	20.62±1.80^{b}	16.77±1.17^{a}
N.I.	0.43±0.02^{ab}	0.46±0.06^{ab}	0.41±0.05^{a}	0.53±0.02^{b}	0.42±0.04^{a}
Linoleic acid	55.01±3.92^{a}	54.84±3.67^{a}	55.02±4.54^{a}	52.04±4.71^{a}	54.96±2.91^{a}
α-linolenic acid	18.21±1.52^{b}	18.04±0.93^{b}	18.67±1.73^{b}	13.56±0.74^{a}	18.68±1.16^{b}
Eicosanoic acid	1.28±0.18^{a}	1.32±0.10^{a}	1.21±0.11^{a}	1.62±0.13^{b}	1.27±0.23^{a}
cis-11-Eicosenoic acid	0.36±0.03^{b}	0.39±0.04^{b}	0.33±0.02^{a}	0.43±0.03^{b}	0.37±0.05^{b}
cis-11,14-Eicosadienoic acid	0.14±0.01^{a}	0.18±0.01^{b}	0.12±0.01^{a}	0.17±0.0^{a}	0.12±0.01^{a}
Behenic acid	0.26±0.02^{b}	0.28±0.02^{b}	0.24±0.02^{a}	0.31±0.02^{b}	0.28±0.02^{b}

with and without antioxidants were characterized by high content of unsaturated fatty acids (86.82–90.92 %), as well as PUFA (65.77–73.81 %). The oils with high contents of unsaturated fatty acids should be related to the potential health benefits, but also higher susceptibility to oxidation. The main fatty acid in all samples was linoleic acid (52.04–55.02 %), followed by oleic (16.77–20.62 %) and α-linolenic acid (13.56–18.68 %), palmitic (4.24–5.77 %), and stearic acids (2.82–4.96 %). It was reported in the majority of articles that the dominant components in rose hip seed oil are linoleic (35.94–55.70 %), *α*-linolenic (14.30––24.65 %) and oleic acid (13.17–22.82 %).[2,3,5,7,27,28] Variation in the rose hip seed oil composition was probably influenced by different factors, such as genetic, climatic, ecologic, soil conditions, as well as extraction type and conditions.[1,5]

After accelerated aging, the content of linoleic acid (52.04–55.02 %) was not statistically different from that at the beginning (55.01 %) of the experiment in all investigated samples. Statistically higher contents of palmitic and stearic acid were determined in the sample stabilized with pomegranate peel extract after accelerated aging, while the content of *α*-linolenic acid was statistically lower, than at the beginning of the experiment. In the samples with BHT and combination of BHT and pomegranate peel extract, as well as in the sample without antioxidant content of *α*-linolenic, oleic, stearic and palmitic acid was not statistically different from oil at the beginning of the experiment.

Peroxide value

The peroxide value is a widely used index for the estimation of oil oxidative stability. The concentration of peroxides and hydroperoxides formed in the oil during the initial stages of lipid oxidation can be evaluated using this method.[9,29] It is known that oils with higher stability are characterized by a lower peroxide value. According to the obtained results, the peroxide value in the fresh oil without antioxidants was 2.32 meq. O_2 kg^{-1}, which is similar to the previously reported results obtained by Grajzer *et al.* where the peroxide value of fresh cold-pressed rose hip oil (*R. canina*) ranged from 1.2 to 2.1 meq. O_2 kg^{-1}.[30] However, Jakovljević *et al.* recorded a significantly higher peroxide value for rose hip oil obtained by supercritical CO_2 extraction (4.70–29.69 mmol O_2 kg^{-1}), which could be explained by the different extraction parameters.[31] In the present samples, a constant increase of peroxide values was noticed during 12 days of storage at 65 °C with a maximal value of 74.67 meq. O_2 kg^{-1} in the sample without antioxidant (Fig. 1). Oil with pomegranate peel extract as an antioxidant was characterized with the lowest peroxide value among investigated oils until 9 days of storage at 65 °C. On the other hand, after 12 days at 65 °C, a sharp increase in the peroxide value was recorded in all samples, especially in the sample without antioxidant (74.67±4.72 meq. O_2 kg^{-1}) but also in the sample with pomegranate peel extract (72.13±4.56 meq. O_2 kg^{-1}). Lower peroxide

values after 12 days at 65 °C were noticed for the sample with BHT (43.73±2.76 meq. O_2 kg^{-1}) and in the sample stabilized with a combination of BHT and pomegranate peel extract (57.14±3.61 meq. O_2 kg^{-1}). The present results indicate that pomegranate peel extract could be used as a good antioxidant for the stabilization of rose hip oil, but further studies on the selection of optimal extract concentration are necessary.

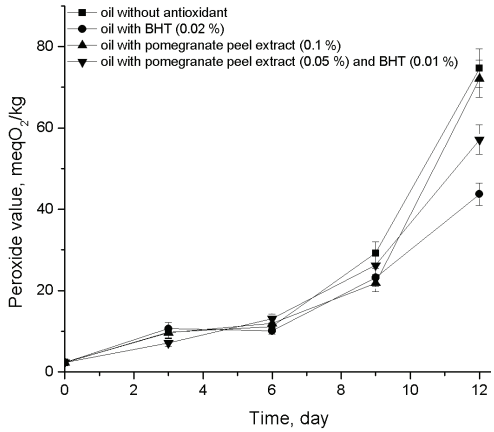

Fig. 1. Peroxide value of rose hip oil with or without antioxidant during accelerated storage.

p-*Anisidine value*

The *p*-anisidine value is a measure of secondary oxidation products (high molecular weight saturated and unsaturated carbonyl compounds) that arise from initially formed peroxides and hydroperoxides in oils and fats.[29,32] The present study showed a minor raise of the *p*-anisidine value in rose hip oil with or without antioxidants during the first 6 days of storage at 65 °C but thereafter, a period of rapid increase in the *p*-anisidine value was noticed (Fig. 2, Table S-I of the Supplementary material to this paper). Moreover, the rose hip oil was characterized by a rather high *p*-anisidine value (7.19) at the beginning of the experiment (day 0), probably due to high carotenoids content and strong color of rose hip oil.[32] On the other hand, such a result is in accordance with the results of Grajzer *et al.*, who reported that *p*-anisidine values of cold-pressed rose hip oils were 2.5 and 7.7, depending on the source.[30] Rose hip oil stabilized with pomegranate peel extract was characterized by the lowest *p*-anisidine value among the investigated samples after 9 and 12 days of storage, 32.91 and 55.89, respectively), indicating significantly better antioxidative activity of pomegranate peel extract than BHT (40.84 and 62.43, respectively) and the combination of BHT and pomegranate peel extract (43.20 and 70.18, respectively).

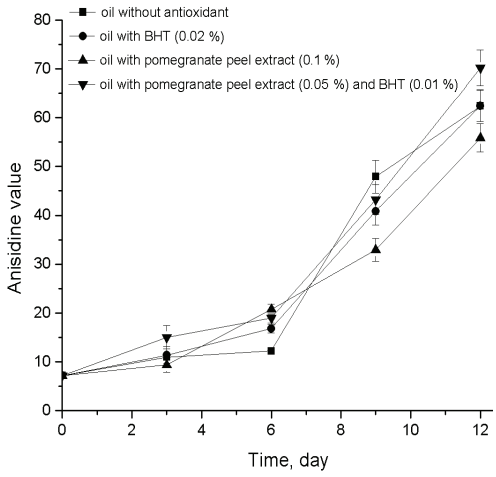

Fig. 2. Anisidine value of rose hip oil with or without antioxidant during accelerated storage.

TBARS *value*

For the estimation of rose hip oil oxidation, the TBARS test was also used. Generally, this test was developed for the determination of malondialdehyde (MDA), a compound with the potential mutagenic activity that is formed during secondary oxidation of unsaturated fatty acids.[33] Results of the inhibition of TBARS formation in rose hip oils with or without antioxidants during 12 days of storage at 65 °C are presented in Fig. 3 and Table S-II of the Supplementary material. During the first 9 days of storage, there was no significant difference between the samples and in all of them, a decrease in TBARS inhibition was evident. After 12 days of storage, inhibition of TBARS in rose hip oil stabilized with pomegranate peel extract was significantly different from that that in samples stabilized with BHT or a combination of BHT and pomegranate peel extract. Pomegranate peel extract has inhibited TBARS formation in rose hip oil more effectively than the other investigated antioxidants.

Total phenolic content and antioxidant activity

The total phenolic content (TPC) of fresh rose hip oil was 0.13 mg GAE g^{-1}, which was lower than in the research of Turan *et al*. who reported 0.37 mg GAE g^{-1} in rose hip oil extracted by petroleum ether,[5] but higher than in the case of Grajzer *et al.* who reported TPC values of 783.5 and 570.7 μg kg^{-1} in cold-pressed rose hip, depending on the sample.[30] After 12 days of storage at 65 °C, the TPC was significantly higher in oil with pomegranate peel extract (0.22 mg GAE g^{-1}) than in the sample without antioxidant (0.07 mg GAE g^{-1}), the sample with BHT (0.07 mg GAE g^{-1}) and the sample with a combination of pomegranate peel extract and BHT (0.11 mg GAE g^{-1}, Table S-II). The antiradical activity of fresh rose hip oil was 16.54 %, expressed as % of DPPH radical scavenging activity. After 12 days of storage at 65 °C, the antiradical activities of rose hip oil without

antioxidant (15.11 %), with BHT (13.52 %) and with a combination of BHT and pomegranate peel extract (14.80 %) were lower than in fresh oil. On the other hand, the antiradical activity of rose hip oil with pomegranate peel extract was significantly higher (29.42 %) than in the other samples after 12 days of storage, as well as in fresh rose hip oil. This result is in accordance with the total phenolic content of the investigated samples. Therefore, rose hip oil stabilized with pomegranate peel extract was fortified with polyphenols, and thus better antiradical activity was achieved, which could be related to higher stability and beneficial health effects.

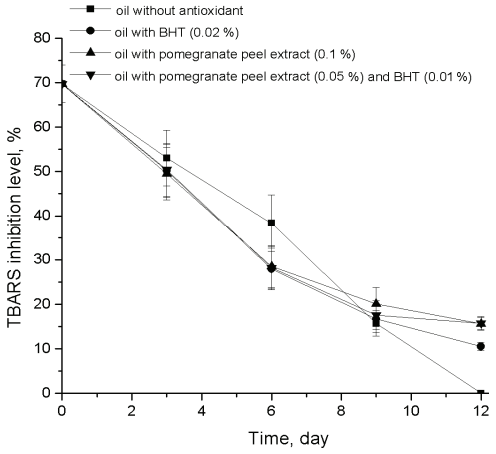

Fig. 3. Inhibition of the level of thiobarbituric acid reactive substances (TBARS) in rose hip oil with or without antioxidant during accelerated storage.

CONCLUSIONS

The results of the resent study indicate that, although rose hip oil is difficult to stabilize due to the high content of PUFA, pomegranate peel extract could be used as an antioxidant for the stabilization of rose hip oil instead of synthetic antioxidant (BHT). Pomegranate peel extract in a concentration of 0.1 % was more effective in inhibition of the second stage of oxidation than BHT at its legal limit (0.02 %), while the first stage of oxidation was prevented better by BHT. Moreover, the addition of polyphenol rich pomegranate peel extract increased the total phenolic content of the rose hip oil as well as its antiradical activity. Therefore, pomegranate peel extract could be used as a potent natural antioxidant for stabilization of beneficial rose hip oil. Further research is needed to find the optimal concentration of pomegranate peel extract that could inhibit oxidation to a higher extent, especially in the first stage of oxidation.

SUPPLEMENTARY MATERIAL

Additional data are available electronically at the pages of journal website: https://www.shd-pub.org.rs/index.php/JSCS/index, or from the corresponding author on request.

Acknowledgment. This work was supported by the Ministry of Education, Science and Technological Development of the Republic of Serbia (451-03-68/2020-14/200003).

ИЗВОД

СТАБИЛИЗАЦИЈА УЉА СЕМЕНА ШИПУРКА ЕКСТРАКТОМ КОРЕ НАРА ПОД УСЛОВИМА УБРЗАНОГ СТАРЕЊА

ЈЕЛЕНА МУДРИЋ[1], ЗОРИЦА ДРИНИЋ[1], ГОРДАНА ЗДУНИЋ[1], МАРИНА ТОДОСИЈЕВИЋ[2], ДУБРАВКА БИГОВИЋ[1], НЕБОЈША МЕНКОВИЋ[1] и КАТАРИНА ШАВИКИН[1]

[1]*Институт за проучавање лековитог биља „Др Јосиф Панчић“, Тадеуша Кошћушка 1, Београд и* [2]*Хемијски факултет, Универзитет у Београду, Студентски трг 10–12, 11000 Београд*

Уље семена шипурка богато је полинезасићеним масним киселинама, али и супстанцама као што су токофероли, каротеноиди, стероли, фосфолипиди и полифеноли. Услед високог садржаја полинезасићених масних киселина ово уље лако подлеже оксидацији. Стога, циљ овог рада је био упоредити стабилност уља семена шипурка уз додатак природног антиоксиданса – екстракта коре плода нара, као и комбинације природног и синтетског антиоксиданса тј. екстракта коре плода нара и бутил-хидрокси-толуена са често коришћеним синтетским антиоксидансом, бутил-хидрокси-толуеном. Стабилност узорка са или без додатка антиоксиданса праћена је испитивањем садржаја масних киселина и мерењем параметара квалитета и стабилности уља (пероксидног броја, анизидинског броја, инхибиције продуката липидне пероксидације, укупног садржаја полифенола, антиоксидативне активности) у току чувања од 12 дана на 65 °C. Екстракт плода коре нара у концентрацији од 0,1 % је показао већу ефикасност у инхибицији секундарне оксидације у односу на бутил-хидрокси-толуен који је у концентрацији од 0,02 % био ефикаснији у заштити уља од примарне оксидације. Додатак екстракта коре плода нара утицао је на повећање садржаја полифенола у уљу семена шипурка, као и на побољшање стабилности и повећање антирадикалске активности. На основу добијених резултата може се закључити да је екстракт коре плода нара потентан антиоксиданс који може бити коришћен за стабилизацију корисног, али нестабилног уља семена шипурка.

(Примљено 24. априла, ревидирано 8. октобра, прихваћено 9. октобра 2020)

REFERENCES

1. I. Mármol, C. Sánchez-de-Diego, N. Jiménez-Moreno, C. Ancín-Azpilicueta, M. J. Rodríguez-Yoldi, *Int. J. Mol. Sci* **18** (2017) 1137 (https://doi.org/10.3390/ijms18061137)
2. F. Çelik, F. Balta, S. Ercişli, A. Kazankaya, I. Javidipour, *J. Food Agric. Environ*. **8** (2010) 482
3. K. Szentmihályi, P. Vinkler, B. Lakatos, V. Illés, M. Then, *Bioresour. Technol.* **82** (2002) 195 (https://doi.org/10.1016/S0960-8524(01)00161-4)
4. M. Kiralan, G. Yildirim, *Springer Chem*. **43** (2019) 803 (https://doi.org/10.1007/978-3-030-12473-1_43)
5. S. Turan, R. Solak, M. Kiralan, M. F. Ramadan, *Grasas Aceites* **69** (2018) 248 (https://doi.org/10.3989/gya.1114172)
6. P. Valerón-Almazán, A. J. Gómez-Duaso, N. Santana-Molina, M. A. García-Bello, G. Carretero, *JCDSA* **5** (2015) 161. (https://doi.org/10.4236/jcdsa.2015.52019)
7. M. Dąbrowska, E. Maciejczyk, D. Kalemba, *Eur. J. Lipid Sci. Technol.* **121** (2019) 1 (https://doi.org/10.1002/ejlt.201800440)
8. I. Gonzalez, M. Escobar, P. Olivera, *Rev. Esp. Fisiol.* **53** (1997) 199 (https://doi.org/10.1002/ejlt.201800440)

9. A. A. Mohdaly, I. Smetanska, M. F. Ramadan, M. A. Sarhan, A. Mahmoud, *Ind. Crops Prod.* **34** (2011) 959. (https://doi.org/10.1016/j.indcrop.2011.02.018)
10. R. V. Contri, I. C. Kulkamp-Guerreiro, S. J. da Silva, L. A. Frank, A. R. Pohlmann, S. S. Guterres, *AAPS PharmSciTech* **17** (2016) 863
11. M. Taghvaei, S. M. Jafari, *J. Food Sci. Technol.* **52** (2015) 1272 (https://doi.org/10.1007/s13197-013-1080-1)
12. F. Shahidi, P. Ambigaipalan, *J. Funct. Foods* **18** (2015) 820 (https://doi.org/10.1016/j.jff.2015.06.018)
13. F. Shahidi, *Food Nahrung* **44** (2000) 158 (https://doi.org/10.1002/1521-3803(20000501)44:3<158::AID-FOOD158>3.0.CO;2-L)
14. S. Akhtar, T. Ismail, D. Fraternale, P. Sestili, *Food Chem.* **174** (2015) 417 (https://doi.org/10.1016/j.foodchem.2014.11.035)
15. I. Živković, K. Šavikin, G. Zdunić, J. Živković, D. Bigović, N. Menković, D. Radin, *Nat. Med. Mat.* **38** (2018) 31 (http://dx.doi.org/10.5937/leksir1838031Z)
16. S. Iqbal, S. Haleem, M. Akhtar, M. Zia-ul-Haq, J. Akbar, *Food Res. Int.* **41** (2008) 194 (https://doi.org/10.1016/j.foodres.2007.11.005)
17. B. M. Naveena, A. R. Sen, R. P. Kingsly, D. B. Singh, N. Kondaiah, *Int. J. Food Sci. Technol.* 43 (2008) 1807 (https://doi.org/10.1111/j.1365-2621.2007.01708.x)
18. B. M. Naveena, A. R. Sen, S. Vaithiyanathan, Y. Babji, N. Kondaiah, *Meat Sci.* **80** (2008) 1304 (https://doi.org/10.1016/j.meatsci.2008.06.005)
19. J. Živković, K. Šavikin, T. Janković, N. Ćujić, N. Menković, *Sep. Purif. Technol.* **194** (2018) 40 (https://doi.org/10.1016/j.seppur.2017.11.032)
20. Y. M. Chong, S. K. Chang, W. C. M. Sia, H. S. Yim, *Food Biosci.* **12** (2015) 18 (https://doi.org/10.1016/j.fbio.2015.07.002)
21. G. Zdunić, D. Gođevac, K. Šavikin, D. Krivokuća, M. Mihailović, Z. Pržić, N. Marković, *Chem. Biodivers.* **16** (2019) e1900053 (https://doi.org/10.1002/cbdv.201900053)
22. *AOAC method, Official Surplus Method 965.4, Fatty Acids in Oils and Fats, Preparation of Methyl Esters*, Final Action 1984, Surplus, 1965
23. *Pharacopoeia European*, 8th ed., Council of Europe, Strasbourg, 2014
24. Z. Drinić, J. Mudrić, G. Zdunić, D. Bigović, K. Šavikin, *Nat. Med. Mat.* **39** (2019) 40 (http://dx.doi.org/10.5937/leksir1939040D)
25. P. G. Waterman, S. Mole, *Analysis of phenolic plant metabolites*, Blackwell Scientific, Oxford, 1994 (ISBN 0632029692)
26. M. S. Blois, *Nature* **181** (1958), 1199
27. R. Nowak, *Acta Soc. Bot. Pol.* **74** (2005) 229
28. H. Ilyasoğlu, *Int. J. Food Prop.* **17** (2014) 1591 (https://doi.org/10.1080/10942912.2013.777075)
29. E. N. Frankel, *Lipid oxidation*, Woodhead Publishing, Cambridge, 2005 (ISBN 9780953194988)
30. M. Grajzer, A. Prescha, K. Korzonek, A. Wojakowska, M. Dziadas, A. Kulma, H. Grajet, *Food Chem.* **188** (2015) 459 (https://doi.org/10.1016/j.foodchem.2015.05.034)
31. M. Jakovljević, T. Moslavac, M. Bilić, M. Aladić, K. Bakula, S. Jokić, *Croat. J. Food Sci. Technol.* **10** (2018) 197 (https://doi.org/10.17508/CJFST.2018.10.2.08)
32. A. Ismail, G. Bannenberg, H. B. Rice, E. Schutt, D. MacKay, *Lipid Technol.* **28** (2016) 55 (https://doi.org/10.1002/lite.201600013)
33. A. Papastergiadis, E. Mubiru, H. Van Langenhove, B. Meulenaer, *Agric. Food. Chem.* **60** (2012) 9589 (https://doi.org/10.1021/jf302451c).

Journal of the Serbian Chemical Society
JSCS-info@shd.org.rs • www.shd.org.rs/JSCS
J. Serb. Chem. Soc. 85 (12) S566–S567 (2020) *Supplementary material*

SUPPLEMENTARY MATERIAL TO

Stabilization of rose hip oil with pomegranate peel extract during accelerated storage

JELENA MUDRIĆ[1]*, ZORICA DRINIĆ[1], GORDANA ZDUNIĆ[1], MARINA TODOSIJEVIĆ[2], DUBRAVKA BIGOVIĆ[1], NEBOJŠA MENKOVIĆ[1] and KATARINA ŠAVIKIN[1]

[1]Institute for Medicinal Plant Research "Dr. Josif Pančić", Tadeuša Košćuška 1, 11000 Belgrade, Serbia and [2]Faculty of Chemistry, University of Belgrade, Studentski trg 10–12, 11000 Belgrade, Serbia

J. Serb. Chem. Soc. 85 (12) (2020) 1553–1563

TABLE S-I. Peroxide value (*I*p), *p*-anisidine value (*A*) and inhibition of TBARS of different rose hip seed oil samples during a storage period of 12 days at 65°C. The results in the table are presented as mean ± *SD* (n = 3); the same letters in the same row are not significantly different according to the Tukey's test, $p < 0.05$

Parameter	Day	Oil without antioxidant	Oil with BHT (0.02%)	Oil with pomegranate peel extract (0.1%)	Oil with pomegranate peel extract (0.05%) and BHT (0.01%)
I_p / meqO_2 kg^{-1}	3	9.80±1.39^{a}	10.65±1.51^{a}	9.69±1.37^{a}	7.18±1.02^{a}
	6	11.13±0.92^{ab}	10.11±0.83^{b}	11.89±0.98^{ab}	13.12±1.08*a*
	9	29.20±2.83^{a}	23.20±2.25^{ab}	21.85±2.11^{b}	26.22±2.54^{ab}
	12	74.67±4.72^{a}	43.73±2.76^{c}	72.13±4.56^{a}	57.14±3.61 b
A	3	10.96±1.73^{ab}	11.37±1.79^{ab}	9.34±1.47^{b}	15.03±2.37^{a}
	6	12.21±0.64^{c}	16.80±0.88^{b}	20.75±1.08^{a}	18.95±0.99^{ab}
	9	47.92±3.36^{a}	40.84±2.86^{a}	32.91±2.31^{b}	43.20±3.03^{a}
	12	62.40±3.24^{ab}	62.43±3.25^{ab}	55.89±2.91^{b}	70.18±3.65^{a}
TBARS inhibition, %	3	53.05±6.28^{a}	50.20±5.94^{a}	49.53±5.86^{a}	50.42±5.96^{a}
	6	38.36±6.43^{a}	27.89±4.68^{a}	28.50±4.78^{a}	28.20±4.73^{a}
	9	15.68±2.86^{a}	16.71±3.05^{a}	20.13±3.67^{a}	17.59±3.21^{a}
	12	0.00±0.00^{c}	10.51±0.96^{b}	15.61±1.43^{a}	15.76±1.45^{a}

Means followed by different letters are significantly different according to the *post hoc* Tukey's test (P<0.05)

* Corresponding author. E-mail: jmudric@mocbilja.rs

TABLE S–II. Total phenolic content (*TPC*) and antioxidative activity (*DPPH RSA*) of different rose hip seed oil samples during a storage period of 12 days at 65°C. The results in the table are presented as mean ± *SD* (n = 3); the same letters in the same row are not significantly different according to the Tukey's test, $p < 0.05$

Parameter	Oil without antioxidant	Oil with BHT (0.02 %)	Oil with pomegranate peel extract (0.1 %)	Oil with pomegranate peel extract (0.05 %) and BHT (0.01 %)
DPPH RSA, %	15.11±1.71^{b}	13.52±1.53^{b}	29.42±3.33^{a}	14.80±1.67^{b}
TPC, mg GAE g^{-1}	0.07±0.00^{c}	0.07±0.00^{c}	0.22±0.01^{a}	0.11±0.01^{b}

Means followed by different letters are significantly different according to the *post hoc* Tukey's test (p<0.05)

Journal of the Serbian Chemical Society
JSCS-info@shd.org.rs • www.shd.org.rs/JSCS
J. Serb. Chem. Soc. *85* (12) 1565–1575 (2020)
JSCS–5393
UDC 635.71+544.022:665.52/.54–024
Short communication

SHORT COMMUNICATION

Composition of essential oils and headspace constituents of *Artemisia annua* L. and *A. scoparia* Waldst. et Kit.

JOVANA D. ICKOVSKI, KATARINA D. STEPIĆ and GORDANA S. STOJANOVIĆ#*

Department of Chemistry, Faculty of Science and Mathematics, University of Niš, Višegradska 33, 18000 Niš, Serbia

(Received 27 July, revised 22 September, accepted 26 September 2020)

Abstract: Headspace volatiles (HS) and hydrodistilled essential oils (EO) of fresh aerial parts of *Artemisia annua* L. and *A. scoparia* Waldst. et Kit., were analyzed by GC–MS/FID. Artemisia ketone was found to be the most abundant component among the EO volatiles (55.8 %), as well as among HS (52.1 %) of *A. annua*. Additionally, in both *A. annua* samples, EO and HS, *α*-pinene (12.7 and 24.2 %, respectively) was found in high percentage. On the other hand, it has been determined that the dominant components of *A. scoparia* EO and HS were different; in the essential oil capillene (63.8 %) was found as the main constituent, while *β*-pinene (26.1 %), (*Z*)-*β*-ocimene (23.8 %) and limonene (10.7 %) were the major components among the HS. This is the first report on the composition of HS volatiles of the *A. annua* and *A. scoparia* obtained by direct static headspace.

Keywords: gas chromatography–mass spectrometry; artemisia ketone; capillene; pinene.

INTRODUCTION

Static headspace is an analytical technique for the easy and effective extraction of multifarious types of compounds, from various types of samples.[1–3] Even though headspace GC is extensively used a limited number of papers is focused on the analysis of headspace volatiles obtained directly from the plant material under static conditions.[4–11] More papers are related to HS-SPME analysis some of which refer to *A. scoparia*[12] and *A. annua.*[13–17]

Static headspace analysis of plants is a very fast and inexpensive method. Also, no special sample preparation is required, it could be performed even without a solvent and the conditions of analysis are not vigorous, so degradation of the components of the sample is minimized and the loss of the most volatile com-

* Corresponding author. E-mail: gocast@pmf.ni.ac.rs
# Serbian Chemical Society member.
https://doi.org/10.2298/JSC200727061I

ponents is greatly reduced. Additionally, the plant material amount that is used for the analysis is only a few grams (or less), so it is useful in cases when not enough plant material could be provided.

If those fact are considered, it is unclear why there is so little data on this type of direct headspace analysis of volatile organic components. All of the above-mentioned is exactly the main reason why we have decided to supplement the existing data on headspace volatiles and compare the chemical composition of the essential oils (EO) and the headspace samples (HS) of two representatives of the genus *Artemisia*. For the purpose of this research, we selected species that were not previously investigated from the point of view of the direct static headspace gas chromatography–mass spectrometry (GC–MS) technique: *Artemisia annua* L. (sweet wormwood) and *Artemisia scoparia* Waldst. et Kit. (virgate wormwood, capillary wormwood, redstem wormwood). The selected species are significant in terms of the biological activity of their essential oils and volatile components, as it has been shown for both to have, among other potentials, a high fumigant and repellent activity.[18–20]

EXPERIMENTAL

Plant material. The aerial parts (flowers, leaves and stems) of *Artemisia annua* L. and *Artemisia scoparia* Waldst. et Kit. were collected in Niška Banja, near Niš, southeast Serbia, in September 2018 in the full-blooming stage. Both species were harvested from the same site. The voucher specimens were deposited in the Herbarium Moesiacum Niš (HMN), Department of Biology and Ecology, Faculty of Science and Mathematics, University of Niš, under the acquisition number No. 13813 for *A. annua* and acquisition number No. 13815 for *A. scoparia*.

Sample preparation for HS and EO isolation. 550 g of fresh plant material (each species separately) was ground in a mixer. Further, for the distillation of the essential oil 500 g of this mass was taken. 1500 mg of the rest of the plant material was taken and divided into three parts and used for three separate headspace analysis.

Essential oil isolation. Fresh plant biomass samples (500 g each) were hydrodistilled in Clevenger-type glass apparatus for 2.5 h. The essential oil samples were dried over anhydrous magnesium sulfate and analyzed by GC and GC–MS. The essential oil yields (%) (g of the essential oil/g biomass) were calculated on a fresh weight basis. For *A. annua* the oil yield was determined to be 0.9 % and for *A. scoparia* 0.3 %. For the GC–MS/FID analysis both essential oil solutions in hexane (1:100) were put in three vials each.

GC–MS/FID analysis and identification. The samples (three repetitions) were analyzed by a 7890/7000B GC/MS/MS triple quadrupole system in MS1 scan mode (Agilent Technologies, USA) equipped with a Combi PAL sampler and Headspace for G6501B/G6509B. The fused silica capillary column HP-5 MS (5 % phenylmethylsiloxane, 30 m×0.25 mm, film thickness 0.25 μm) was used. The injector and interface operated at 230 and 300°C, respectively. Temperature program: from 45 to 290 °C at a heating rate of 4 °C/min. The carrier gas was He with a flow of 1.0 mL/min. For the essential oil solution injection volume was 1 μL and split ratio was adjusted at 40:1. For the HS volatiles 500 mg of milled plant material was put into 20 mL HS vial and then soaked with 2 mL of distilled water. The sample was heated at 80 °C for 20 min with the following mixing program: shaking for 5 s, pause for 2 s. The aliquot of vapor generated from the samples (500 μL) was drawn out from the vial using a

gas-tight syringe (90 °C) and injected directly in the chromatographic column via a transfer line (75 °C). The split ratio was set to 10:1. Post run: back flash for 1.89 min, at 280 °C, with helium pressure of 50 psi. MS conditions were as follows: ionization voltage of 70 eV, acquisition mass range 40–440 Da, scan time 0.32 s. The GC analysis was carried out under the same experimental conditions using the same column as described for the GC–MS. The percentage composition was computed from the GC peak areas without any corrections and was given as mean ± standard deviation.

Identification of volatile compounds. Components were identified by comparison of their mass spectra with those of Wiley 6, Adams (2007) and NIST 11 libraries, applied on Agilent Mass Hunter Workstation (B.06.00) and AMDIS (2.1, DTRA/NIST, 2011) software and confirmed by comparing of calculated retention indexes (relative to C_8–C_{40} *n*-alkanes) with the literary values of the retention indices.

RESULTS AND DISCUSSION

The GC and GC–MS analysis resulted in the identification of 64 components in the *A. annua* EO, representing 98.6 % of the essential oil and 40 components in the *A. annua* HS, representing 99.2 % of the HS sample (Table I). All of the HS components were ingredients of EO, except *n*-hexanol and propyl isobutyrate. The more volatile components such as *α*-pinene and 1,8-cineole were present in a higher percentage in HS (24.2 and 6.6 %, respectively), than in EO (12.7 and 2.7 %, respectively). The dominant component artemisia ketone (55.8 % in the oil and 52.1 % in the HS) was represented approximately equally in the EO and HS. The most dominant class of compounds in EO and HS of *A. annua* were oxygenated monoterpenes (78.4 and 67.5 %, respectively). Additionally, the ratio of oxygenated monoterpenes to hydrocarbon monoterpenes in the essential oil of *A. annua* was approximately 5, while the ratio of oxygenated monoterpenes to hydrocarbon monoterpenes in the headspace samples was approximately 2.5. None of the sesquiterpenes was present in HS sample of *A. annua*.

The number of identified components of the *A. scoparia* essential oil and HS (36 in EO, representing 99.1 % of the essential oil and 28 in HS, representing 99.4 % of the HS sample) was less than in *A. annua* EO and HS. Hexanal, (2*E*)--hexenal, (3*Z*)-hexenol and *n*-hexanol (which are known as green leaf volatiles GLV, the components which are released when the plant is under attack/stress and by which a plant communicate with other plants and insects in its surroundings) were identified only in HS of *A. scoparia*. The most dominant components of *A. scoparia* EO were phenyldiacetylenes: capillene (63.8 %) and 2,4-pentadiynyl-benzene (10.0 %), while in the HS monoterpenes: *β*-pinene (26.1 %) and (*Z*)-*β*-ocimene (23.8 %) were the most abundant. The difference in the composition of *A. scoparia* essential oil and HS volatiles is a presumably consequence of their volatility. Namely, capillene boiling point is 140.00 to 143.00 °C at 10.00 mm Hg* while the boiling point of *β*-pinene is 163.00 to 166.00 °C at 760.00 mm Hg.

* 760 mm Hg = 101.325 Pa

TABLE I. Chemical composition of the essential oil and headspace volatiles of *A. annua* and *A. scoparia* (the results of this study are presented in parallel with the obtained literature data); * – identified by NIST Chemistry WebBook Retention indices; tr: traces (<0.1 %); –: not detected. Components represented by more than 5 % at least in one of the samples are given in bold

Compound	*RL*	*RI*[a]	Content[b], %								Class
			A. annua				*A. scoparia*				
			EO	EO[13]	HS	HS[13]	EO	EO[12]	HS	HS[12]	
Methyl 2-methyl-butyrate	783	783*	t		0.2±0.1		–		–		CD
Hexanal	801	801	t		t		–		0.1±0.0		O
Ethyl 2-methylbu-tyrate	845	846*	0.2±0.1		2.1±0.3		–		–		CD
Ethyl isovalerate	849	849	t		0.2±0.1		–		–		CD
(2*E*)-Hexenal	851	846	–		–	3.05	–		t		O
(3*Z*)-Hexenol	849	850	–		–		–		t		O
Propyl isobutylrate	853	853	–		0.1±0.0		–		–		CD
n-Hexanol	866	863	–		t		–		t		O
Santolina triene	905	906	0.1±0.0		0.2±0.1		–		–		M
Tricyclene	920	921	t		t		–		–		M
α-Thujene	925	924	t		t		–		–		M
α-Pinene	932	932	12.7±0.8	4.79	24.2±0.9	12.03	0.9±0.2	0.8	6.8±1.0	4.6	M
Propyl 2-methyl-butyrate	943	944*	0.2±0.1		0.6±0.2		–		–		CD
Camphene	947	946	0.3±0.1	2.74	0.7±0.2	4.90	t		t		M
Thuja-2,4(10)-diene	952	953	t		t		–		–		M
Sabinene	972	969	0.3±0.1		0.6±0.2		0.1±0.0	0.2	1.3±0.2	1.4	M
β-Pinene	975	974	1.1±0.3	1.25	1.8±0.3	2.74	3.5±0.4	3.3	26.1±1.3	20.8	M
Myrcene	988	988	0.1±0.0		0.1±0.0		0.9±0.2	1.0	8.0±0.5	12.8	M
Yomogi alcohol	997	999	0.9±0.2		0.8±0.3		–		–		MO
α-Terpinene	1015	1014	t		0.2±0.1		t		0.2±0.0		M
o-Cymene	1023	1022	t		0.1±0.0		0.5±0.1		3.4±0.3		M
Limonene	1027	1024	0.1±0.0		t	0.99	1.7±0.2	1.3	10.7±0.5	11.0	M
1,8-Cineole	1030	1026	2.7±0.2	4.38	6.6±0.5	6.76	0.1±0.0	0.2	0.5±0.2	0.9	MO
Santolina alcohol	1034	1034	0.2±0.1		0.1±0.0		–		–		MO
(*Z*)-*β*-Ocimene	1035	1032	t		–		4.3±0.3	1.0	23.8±0.8	16.4	M
(*E*)-*β*-Ocimene	1046	1044	–		–		0.3±0.1		0.6±0.2	0.4	M
γ-Terpinene	1057	1054	0.2±0.0		0.1±0.0		4.0±0.3	0.2	7.0±0.4	3.8	M
Artemisia ketone	1060	1056	55.8±1.5	8.79	52.1±1.3	11.24	0.3±0.1		–		MO
cis-Sabinene hydrate	1067	1065	0.5±0.2		0.4±0.2		–		–		MO
Artemisia alcohol	1082	1080	3.1±0.4	2.61	2.0±0.3	3.34	t		–		MO
Terpinolene	1087	1086	t		t		–		–		M
α-Pinene oxide	1089	1099	t		–		–		–		MO
trans-Sabinene hydrate	1097	1098	0.1±0.0		–		–		–		MO
n-Nonanal	1102	1100	–		–		t		–		O

TABLE I. Continued

Compound	*RL*	*RI*[a]	Content[b], %								Class
			A. annua				*A. scoparia*				
			EO	EO[13]	HS	HS[13]	EO	EO[12]	HS	HS[12]	
2-Methylbutyl-2-methylbutyrate	1003	1100	t		t		–		–		CD
3-Methyl-3-butenyl isovalerate	1111	1112	0.2±0.0		0.2±0.1		–		–		CD
trans-Pinene hydrate	1121	1119	t		–		–		–		MO
α-Campholenal	1125	1122	0.5±0.2		0.2±0.1		–		–		MO
allo-Ocimene	1127	1128	–		–		t		t		M
cis-*p*-Mentha-2,8-dien-1-ol	1134	1133	t		–		–		–		MO
trans-Pinocarveol	1139	1135	6.4±0.5		2.1±0.4		t		–		MO
Camphor	1145	1141	0.3±0.1	16.30	0.2±0.0	11.37	–		–		MO
Sabina ketone	1156	1154	0.2±0.1		–		–		–		MO
Pinocarvone	1163	1160	5.6±0.4	1.73	2.6±0.4	1.23	t		–		MO
Borneol	1166	1165	0.4±0.2	1.77	t	1.21	–		–		MO
Lavandulol	1166	1165	–		–		0.4±0.1		0.1±0.0		MO
Terpinen-4-ol	1177	1174	0.3±0.1	1.34	0.1±0.0		t		–		MO
α-Terpineol	1190	1186	t		t		t		–		MO
Myrtenal	1198	1195	0.8±0.2		0.2±0.0		–		–		MO
trans-Carveol	1218	1215	0.1±0.0		–		–		–		MO
(3*Z*)-Hexenyl 2-methylbutyrate	1230	1229	t		0.1±0.0		t		t		CD
(3*Z*)-Hexenyl 3-methylbutyrate	1234	1232	–		–		t		t		CD
Hexyl-2-methyl-butyrate	1234	1233	t		t		–		–		CD
Hexyl 3-methyl-butyrate	1240	1241	–		t		–		–		CD
Carvone	1244	1239	t		–		–		–		MO
2,4-pentadi- ynyl-Benzene	1294	1298	–		–		10.0±0.6		7.7±0.4		P
cis-Pinocarvyl acetate	1307	1311	0.1±0.0		–		–		–		MO
(3*Z*)-Hexenyl tiglate	1323	1319	–		–		0.2±0.1		t		CD
Eugenol	1357	1356	t		–	1.94	2.0±0.2	0.1	0.3±0.1		PP
α-Copaene	1378	1374	0.3±0.1		–		–		–		S
Benzyl isovalerate	1386	1385	0.1±0.0		–		–		–		CD
α-Isocomene	1390	1387	–		–		t		–		S
β-Cubebene	1392	1387	t		–		–		–		S
β-Elemene	1393	1389	t		–		–		–		S
(*E*)-Caryophyllene	1423	1417	0.8±0.2	3.82	–	0.65	2.2±0.3	9.6	0.3±0.1	16.4	S
(*E*)-*β*-Farnesene	1455	1454	t	2.32	–	2.67	–		–		S
α-Humulene	1457	1452	t		–		0.2±0.1	0.7	t	0.4	S
γ-Curcumene	1480	1481	–		–		0.3±0.2	0.3	t	0.3	S

TABLE I. Continued

Compound	*RL*	*RI*[a]	Content[b], %								Class
			A. annua				*A. scoparia*				
			EO	EO[13]	HS	HS[13]	EO	EO[12]	HS	HS[12]	
Germacrene D	1485	1484	1.1±0.3	7.14	–	0.7	0.3±0.1	0.5	–	0.4	S
β-Selinene	1490	1489	0.1±0.0	10.41	–		–		–		S
Capillene	1498	1493	–		–		63.8±1.6	53.1	2.2±0.2	3.2	P
Bicyclogermacrene	1500	1500	0.4±0.1		–		–	4.2	t	4.9	S
δ-Cadinene	1525	1522	t		–		t		–		S
Spathulenol	1576	1577	t		–		0.9±0.2	6.5	–		SO
Viridiflorol	1585	1592	0.1±0.0		–		–		–		SO
Caryophyllene oxide	1588	1582	0.2±0.0	1.65	–		0.5±0.2	2.6	–		SO
allo-Aromadendrene epoxide	1630	1639	0.2±0.1		–		–		–		SO
Selina-3,11-di-en--6-*α*-ol	1635	1642	0.2±0.1		–		–		–		SO
β-Eudesmol	1656	1649	–		–		1.4±0.3		–		SO
Amorpha-4,9-di-en-2-ol	1691	1700	0.2±0.1		–		–		–		SO
Number of components			**64**		**40**		**36**		**28**		
Class of compounds											
Monoterpenes			**93.6**		**95.7**		**17.2**		**88.6**		
Hydrocarbons (M)			15.2		28.2		16.3		88.0		
Oxygenated (MO)			78.4		67.5		0.9		0.6		
Sesquiterpenes			**4.1**		**–**		**5.8**		**0.4**		
Hydrocarbons (S)			3.1		–		3.0		0.4		
Oxygenated (SO)			1.0		–		2.8		–		
Carbonic acid derivatives (CD)			0.8		3.4		0.3		t		
Phenyldiacetylenes (P)			**–**		**–**		**73.8**		**9.9**		
Phenylpropenes (PP)			t		–		2.0		0.3		
Other (O)			0.1		0.1		t		0.2		
Total identified			**98.6**		**99.2**		**99.1**		**99.4**		

[a]Compounds are listed in order of elution from a HP-5 MS column; *RL*: literature retention indices; *RI*: experimental retention indices relative to C_8–C_{40} *n*-alkanes; [b]the percentage composition of the individual components is given as the mean ± standard deviation, and for the classes of compounds as the mean

The situation with *A. annua* EO and HS is different. The main component, artemisia ketone, is the same in both, EO and HS. This is because its boiling point (181.00 °C at 760.00 mm Hg) is low enough to evaporate even under HS analysis conditions. In general, more volatile components were present to a greater extent in HS samples of *A. scoparia* than in essential oil, just like in the

case of *A. annua*. The predominant class of compounds in HS were hydrocarbon monoterpenes (88.0 %), while oxygenated monoterpenes were present in percentage less than one in both samples of *A. scoparia*. Also, hydrocarbon sesquiterpenes were determined only in traces, while none of the oxygenated sesquiterpenes were found.

In the case of *A. annua* both methods applied yielded volatiles with a very similar composition in monoterpene fraction. Likewise, this was the case for the *A. scoparia*, for which the two analyses showed minor qualitative variations in monoterpenes. Quantitative differences of the volatiles in HS sample and essential oil in *A. annua* were noticeable, but not overly expressed (*e.g.*, the percentage of artemisia ketone in both samples was almost equal; the percentage of *α*-pinene in the HS sample was less than 2 times higher than that in the essential oil). On the contrary, the differences in the quantity of the components present in both, the EO and the HS sample of *A. scoparia* were significant (*e.g.*, the percentage of capillene in the EO sample was 29 times higher than that in the HS sample; the percentage of myrcene in the HS sample was almost 9 times higher than that in the EO sample).

The chemical composition of the EO obtained from both plants was the subject of several scientific papers, but we have concentrated here only on those papers that deal with these plants in the same developmental phase as ours and whose essential oil was obtained from fresh aboveground parts of the plant. Apart from same developmental phase, the volatile chemical composition has been very diverse depending on a large number of factors, such as geographic locations, weather conditions, soil type, and others.

Composition of the essential oil of *A. annua* at the blooming stage determined by Rana *et al.* [21] showed that camphor was represented with 28.6 %, 1,8-cineole with 12.9 % and limonene with 4.5 %. The *A. annua* essential oil obtained from species growing wild in Bulgaria was analyzed by Tzenkova *et al.*[22] and the results showed the presence of *α*-caryophillene (24.73 %), *α*-cubebene (13.53 %), *α*-copaene (7.42 %), *α*-selinene (8.21 %) and artemisia ketone (8.45 %). The chemical composition of the essential oils with 85 compounds from *A. annua* from Hungary was determined by Héthelyi *et al.*[23] The main components of the essential oil obtained from fresh flowering shoots were artemisia ketone (33-75 %) and artemisia alcohol (15-56 %). Artemisia ketone (52.9 %), 1,8-cineole (8.4 %) and camphor (6.0 %) were the major constituents of the essential oil from Northern India, obtained by Jain *et al.*[24] The principal components of the Indian *A. annua* essential oil determined by Rao *et al.* [25] were 1,8-cineole (11.1 %), camphor (36.6 %), *β*-caryophyllene (5.7 %) and germacrene D (5.9 %). 1,8-cineole (15.1 %) was prominent component followed by *α*-terpineole (14 %), *p*-cymene (12.9 %), carvone (12 %), *γ*-elemene (6.2 %) and *Z*-*α*-bisabolene (5.4 %) according to Mukhtar *et al*.[26]

The major components of the essential oil from Iran determined by Rasooli *et al.* [27] were artemisia ketone (24.2 %), *α*-pinene (12.1 %), 1,8-cineole (9.8 %), camphor (8.4 %), *α*-selinene (7.5 %) and borneol (6.0 %). Nekoei *et al.* [13] also examined samples from Iran and compared the composition of the EO and the volatiles obtained by headspace-solid phase microextraction (HS-SPME) from the fresh aerial parts of *A. annua* L. Compounds represented by more than 10 % in at least one sample were camphor (EO 16.30 %; HS-SPME 11.37 %), *β*-selinene (EO 10.41 %), *α*-pinene (HS-SPME 12.03 %) and artemisia ketone (HS--SPME 11.24 %). Compared to the sample examined here, a similarity in the qualitative composition could be noticed, which could not be said for the quantitative composition for both, EO and HS volatiles. The difference in content is especially pronounced for artemisia ketone, camphor, germacrene D and *β*-selinene (Table I).

The major constituents of the essential oil from mature leaves of Indian *A. scoparia* detected by Singh *et al.*[29] were *p*-cymene (27.06 %), acenaphthalene (24.4 %), *β*-myrcene (20.89 %) and (+)-limonene (12.63 %).[28] The essential oil analyzed by Singh *et al.*[29] was rich in *β*-myrcene (29.27 %), followed by (+)-limonene (13.3 %), (*Z*)-*β*-ocimene (13.37 %) and *γ*-terpinene (9.51 %). The most abundant volatile constituents from another Indian *A. scoparia* essential oil were *γ*-terpinene (21.8 %), eugenol (20.4 %), eugenyl valerate (5.5 %), limonene (5.0 %) and *p*-cymene (4.6 %) according to Ali *et al*.[30] The major components of the essential oil from Iranian plant analyzed by Morteza-Semnani and Akbarzadeh[31] were camphor (37.9 %), 1,8-cineole (27.8 %) and borneol (21.1 %). Acenaphthene (36.86 %) was the major component of *A. scoparia* from India, while *p*--cymene (20.5 %) was the major monoterpene constituent, followed by *β*-myrcene (13.95 %) and (+)-limonene (12.53 %) according to Kaur *et al*.[32] The essential oil of *A. scoparia* from Korea was rich in 1,8-cineole (21.5 %), camphor (11.0 %) and *β*-caryophyllene (6.8 %) as the major compounds according to Cha *et al*.[33] Contrary to the above references, the composition of *A. scoparia* EO and HS-SPME volatiles from Turkey examined by Demirci *et al.*[12] was very similar to the composition of *A. scoparia* EO and HS examined through our work, except for 2,4-pentadiynyl-benzene. In the sample analyzed here, the content of 2,4-pentadiynyl-benzene was 10.0 % in EO and 7.7 % in HS volatiles, while in the sample from Turkey it was not detected at all. In the volatile components obtained by direct HS and HS-SPME, the higher percentage (16.4 %) of (*E*)-caryophyllene could be noticed in HS-SPME volatiles, compared to those directly obtained HS components (0.3 %).

CONCLUSION

This is the first report on the chemical volatile composition of the samples of *A. annua* and *A. scoparia* obtained by direct static headspace. After extensive

research and comparative analysis of the essential oil and HS samples, the following could be concluded:

– Artemisia ketone was found to be the most abundant component in EO and HS sample of *A. annua*, while *α*-pinene was found to be the second most abundant.

– On the contrary, the dominant components in *A. scoparia* samples were different by two methods; in EO capillene was the main constituent, while in HS sample it was *β*-pinene probably due to their volatility.

– For *A. annua* and *A. scoparia*, both applied methods yielded volatiles with a very similar composition in monoterpene fraction.

– Quantitative differences of the volatiles in HS and EO samples of *A. annua* and *A. scoparia* were noticeable, wherein these differences are more pronounced in *A. scoparia.*

– Comparing the composition of volatile components obtained by direct HS and HS-SPME, for both examined species, a similarity in the qualitative composition could be noticed, which could not be said for the quantitative composition.

– Direct headspace is an easy and fast method that could be used for analyzing the monoterpene fraction of the samples and it is less demanding than HS-SPME which includes adsorption and desorption from a suitable adsorbent. However, both of these methods could not replace an essential oil analysis, which gives a much more complete picture of the plant's volatile profile.

Acknowledgment. Financial support of the Ministry of Education, Science and Technological Development of Serbia (Project No. 451-03-68/2020-14/200124) is gratefully acknowledged.

ИЗВОД

САСТАВ ЕТАРСКОГ УЉА И "HEADSPACE" САСТОЈЦИ *Artemisia annua* L. И *A. scoparia* Waldst. et Kit

ЈОВАНА Д. ИЦКОВСКИ, КАТАРИНА Д. СТЕПИЋ и ГОРДАНА С. СТОЈАНОВИЋ

Департман за хемију, Природно–математички факултет, Универзитет у Нишу, Вишеградска 33, 18000 Ниш

"Headspace" испарљива једињења и састојци хидродестилованих етарских уља свежих надземних делова *Artemisia annua* L. и *Artemisia scoparia* Waldst. et Kit., анализирани су GC–MS/FID методом. Артемизија-кетон (55,8 %) је најзаступљенији састојак етарског уља, као и испарљивих "headspace" једињења (52,1 %) узорка *A. annua*. Поред тога, у оба узорка *A. annua*, у етарском уљу и "headspace" узорку, *α*-пинен (12,7 и 24,2 %, редом) нађен је у високом проценту. С друге стране, утврђено је да су доминантне компоненте *A. scoparia* у етарском уљу и "headspace" узорку биле различите; у етарском уљу је као главна компонента одређен капилен са 63,8 %, док су *β*-пинен (26,1 %), (*Z*)-*β*-оцимен (23,8 %) и лимонен (10,7 %) главне компоненте у "headspace" узорку. Ово су први резултати о саставу испарљивих компонената *A. annua* и *A. scoparia* добијени директним статичким "headspace" техником.

(Примљено 27. јула, ревидирано 22. септембра, прихваћено 26. септембра 2020)

REFERENCES

1. N. H. Snow, G.C. Slack, *TRAC - Trends Anal. Chem.* **21** (2002) 608 (https://doi.org/10.1016/S0165-9936(02)00802-6)
2. B. Kolb, L.S. Ettre, *Static Headspace Gas Chromatography: Theory and Practice*, Wiley–VCH, New York, 1997, ISBN: 0-471-19238-4
3. B. V. Ioffe, A. G. Vitenberg, *Head-Space Analysis and Related Methods in Gas Chromatography* (translated by I. A. Mamantov), Wiley, New York, 1984, ISBN: 978-0-471-06507-4
4. G. Stojanović, O. Jovanović, G. Petrović, V. Mitić, V. Jovanović, *Nat. Vol. Essent. Oils* **1** (2014) 60 (https://dergipark.org.tr/tr/pub/nveo/issue/19770/211762)
5. J. Rzepa, L. Wojtal, D. Staszek, G. Grygierczyk, K. Labe, M. Hajnos, T. Kowalska, M. Waksmundzka-Hajnos, *J. Chromatogr. Sci.* **47** (2009) 575 (https://doi.org/10.1093/chromsci/47.7.575)
6. G. M. Petrovic, J. G. Stamenkovic, O. P. Jovanovic, G. S. Stojanovic, *Nat. Prod. Commun.***14** (2019) (https://doi.org/10.1177/1934578X19850691)
7. G. M. Petrovic, J. G. Stamenkovic, G. S. Stojanovic, V. D. Mitic, B. K. Zlatkovic, *Nat. Prod. Commun.* **12** (2017) 1513 (https://doi.org/10.1177/1934578X1701200932)
8. I. R. Kostevski, G. M. Petrovic, G. S. Stojanovic, J. G. Stamenkovic, B. K. Zlatkovic, *Nat. Prod. Commun.* **11** (2016) 543 (https://doi.org/10.1177/1934578X1601100431)
9. S. C. Jovanovic, O. P. Jovanovic, G. M. Petrovic, G. S. Stojanovic, *Nat. Prod. Commun.* **10** (2015) 661 (https://doi.org/10.1177/1934578X1501000434)
10. O. P. Jovanovic, B. K. Zlatkovic, S. C. Jovanovic, G. M. Petrovic, G. S. Stojanovic, *J. Essent. Oil Res.* **27** (2015) 182 (https://doi.org/10.1080/10412905.2015.1014119)
11. O. P. Jovanović, G. S. Stojanović, *Facta Univ. Ser. Phys Chem. Tech.* **12** (2014) 41 (DOI:10.2298/FUPCT1401041J)
12. B. Demirci, F. Demirci, K. H. C. Başer, *Flavour Fragr. J.* **20** (2005) 395 (https://doi.org/10.1002/ffj.1426)
13. M. Nekoei, M. Mohammadhosseini, H. Akhlaghi, *J. Essent. Oil-Bear. Plants* **15** (2012) 926 (https://doi.org/10.1080/0972060X.2012.10662595)
14. A. R. Jassbi, R. Miri, Ian T. Baldwin, *Chem. Nat. Compd.* **49 (**2014) 1148 (https://doi.org/10.1007/s10600-014-0846-7)
15. E. M. Lopes, F. Guimarães-Dias, T. S. S. Gama, A. L. Macedo, A. L. Valverde, M. C. Moraes, A. C. A. Aguiar-Dias, H. R. Bizzo, M. Alves-Ferreira, E. S. Tavares, A. F. Macedo, *Plant Cell Rep.* **39** (2020) 101 (https://doi.org/10.1007/s00299-019-02476-0)
16. S. Reale, P. Fasciani, L. Pace, F. Angelis, G. Marcozzi, *Rapid Commun. Mass Spectrom.* **25 (**2011) 2511 (https://doi.org/10.1002/rcm.5155)
17. H.Sun, F. Zhang, S. Chen, Z. Guan, J. Jiang, W. Fang, F. Chen, *Biochem. Sys. Ecol.* **60** (2015) 225 (https://doi.org/10.1016/j.bse.2015.04.023)
18. D. Goel, R. Goel, V. Singh, M. Ali, G. Mallavarapu, K. Sushil, *J. Nat. Med.* **61** (2007) 458 (https://doi.org/10.1007/s11418-007-0175-2)
19. N. Zhang, L. Tang, W. Hu, K. Wang, Y. Zhou, H. Li, C. Huang, J. Chun, Z. Zhang, *J. Insect Sci.* **14** (2014) 241 (https://www.ncbi.nlm.nih.gov/pmc/articles/PMC5634023/)
20. M. Negahban, S. Moharramipour, F. Sefidkon, *J. Asia-Pac. Entomol.* **9** (2006) 381 (https://doi.org/10.1016/S1226-8615(08)60318-0)
21. V. S. Rana, K. Abirami, M. A. Blázquez, S. Maiti, *J. Spices Aromat. Crops* **22** (2013) 181 (https://updatepublishing.com/journal/index.php/josac/article/view/5031)
22. R. Tzenkova, Z. Kamenarska, A. Draganov, A. Atanassov, *Biotechnol. Biotechnol. Equip.* **24** (2010) 1833 (https://doi.org/10.2478/V10133-010-0030-6)

23. E. B. Héthelyi, I. B. Cseko, M. Grósz, G. Márk, J. J. Palinkás, *J. Essent. Oil Res.* **7** (1995) 45 (https://doi.org/10.1080/10412905.1995.9698460)
24. N. Jain, S. K. Srivastava, K. K. Aggarwal, S. Kumar, K. V. Syamasundar, *J. Essent. Oil Res.* **14** (2002) 305 (https://doi.org/10.1080/10412905.2002.9699863)
25. B. R. Rao, K. V. Syamasundar, R. P. Patel, *J. Essent. Oil Res.* **26** (2014) 486 (https://doi.org/10.1080/10412905.2014.949881)
26. H. M. Mukhtar, S. H. Ansari, M. Ali, S. R. Mir, M. Z. Abdin, P. Singh, *J. Essent. Oil Bear. Plants* **10** (2007) 168 (https://doi.org/10.1080/0972060X.2007.10643537)
27. I. Rasooli, M. B. Rezaee, M. L. Moosavi, K. Jaimand, *J. Essent. Oil Res.* **15** (2003) 59 (https://doi.org/10.1080/10412905.2003.9712268)
28. H. P. Singh, S. Kaur, S. Mittal, D. R. Batish, R. K. Kohli, *Food Chem. Toxicol.* **48** (2010) 1040 (https://doi.org/10.1016/j.fct.2010.01.017)
29. H. P. Singh, S. Kaur, S. Mittal, D. R. Batish, R. K. Kohli, *J. Chem. Ecol.* **35** (2009) 154 (https://link.springer.com/article/10.1007/s10886-009-9595-7)
30. M. Ali, A. Chaudhari, A. Velasco-Negueruela, M. J. Pérez-Alonso, *J. Essent. Oil Res.* **12** (2000) 64 (https://doi.org/10.1080/10412905.2000.9712043)
31. K. Morteza-Semnani, M. Akbarzadeh, *J. Essent. Oil Res.* **17** (2005) 321 (https://doi.org/10.1080/10412905.2005.9698918)
32. S. Kaur, H. P. Singh, S. Mittal, D. R. Batish, R. K. Kohli, *Ind. Crops Prod.* **32** (2010) 54 (https://doi.org/10.1016/j.indcrop.2010.03.007)
33. J. D. Cha, M. R. Jeong, S. I. Jeong, S. E. Moon, J. Y. Kim, B. S. Kil, Y. H. Song, *Planta Med*. **71** (2005) 186 (https://www.thieme-connect.de/products/ejournals/abstract/10.1055/s-2005-837790).

Journal of the Serbian Chemical Society
JSCS-info@shd.org.rs • www.shd.org.rs/JSCS
J. Serb. Chem. Soc. 85 (12) 1577–1590 (2020)
JSCS–5394
UDC 546.268.5+546.742:532.14:
537.622.4:519.677
Original scientific paper

Assessment of density functional approximations for calculation of exchange coupling constants in thiocyanato and cyanato double bridged binuclear Ni(II) complexes

MATIJA ZLATAR[1#], FILIP VLAHOVIĆ[2], DRAGANA MITIĆ[2#], MARIO ZLATOVIĆ[3#] and MAJA GRUDEN[3#*]

[1]*University of Belgrade – Institute of Chemistry, Technology and Metallurgy, Njegoševa 12, 11000 Belgrade, Serbia,* [2]*Innovation center of the Faculty of Chemistry, University of Belgrade, Studentski trg 12–16, 11000 Belgrade, Serbia and* [3]*University of Belgrade – Faculty of Chemistry, Studentski trg 12–16, 11000 Belgrade, Serbia*

(Received 6 November, accepted 12 November 2020)

Abstract: In the present work, we examine the magnetic properties of 8 "end-to-end" thiocyanato, and 3 "end-to-end" cyanato double bridged Ni(II) binuclear complexes. Thiocyanato complexes are weakly ferromagnetic. Cyanato bridged complexes exhibit weak antiferromagnetic coupling. Therefore, it is a challenge for computational chemistry to calculate the exchange coupling constant in these systems accurately. 17 different density functional approximations with different flavours are used to find the method of choice to study magnetic properties in binuclear Ni(II) complexes within the broken-symmetry approach. It is found that M06-2X and PWPB95 performed the best compared to the experimental values for the entire set of examined complexes. Furthermore, the magneto-structural correlation rationalizes the results.

Keywords: BS-DFT; ferromagnetic coupling; antiferromagnetic coupling; magneto-structural correlations; double-hybrid functionals.

INTRODUCTION

Due to important and versatile applications in industry, medicine, and technology, various bi- and poly-nuclear transition metal (TM) based magnetic materials have been investigated.[1–5] These kinds of complexes are characterized by two or more paramagnetic metal centers, often bridged through one or more small ligands. The partially filled *d*-orbitals of TM centers lead to ferromagnetic (FM) or antiferromagnetic (AF) exchange coupling.[6,7] Various symmetrical[8,9] and unsymmetrical[10,11] polydentate ligands are responsible for promoting the

* Corresponding author. E-mail: gmaja@chem.bg.ac.rs
# Serbian Chemical Society member.
https://doi.org/10.2298/JSC201106071Z

formation of polynuclear core. However, bridging units have a more critical influence on the electronic structure. The thiocyanato (SCN^-) and cyanato (OCN^-) ions are ambidentate ligands that can coordinate *via* nitrogen or chalcogen (sulfur or oxygen) as monodentate or bridging ligands.[12] As bridging ligands, like their well-examined azide (N_3^-) ion analog, they predominantly coordinate in "end-on" (μ-1,1) and "end-to-end" (μ-1,3) fashion (Fig. 1).[13,14] This additionally enriches the structural versatility of these molecules. The bridging mode strongly influences the magnetic interactions between TM ions and the magnetic characteristics of a molecule.

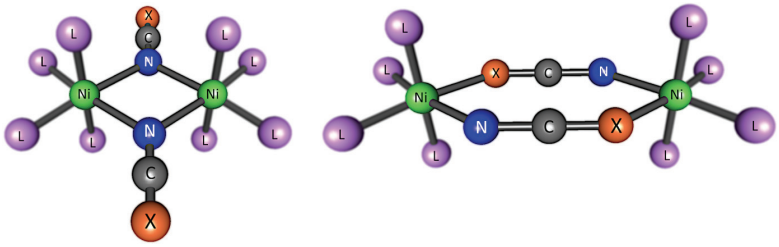

Fig. 1. Possible double bridging modes of cyanato and thiocyanto ions in binuclear nickel(II) complexes; "end-on" on the left and "end-to-end" mode on the right; X= O or S; L – spectator ligands.

In contrast to thiocyanato-bridged polynuclear complexes of some other metals (like, for example, Cu(II)[15–20]), the number of Ni(II) complexes is considerably smaller, whereby only a few binuclear cyanato-bridged complexes have been synthesized and characterized. "End-to-end" thiocyanato double bridged complexes are weakly FM,[7,14,21] while "end-to-end" cyanato double bridged complexes exhibit weak AF coupling.[22,23]

Although much has been explained and learned in the field of electronic structure, a clear understanding of magnetization phenomena remains a challenge. From a quantum chemical point of view, the accurate description of this fundamental characteristic requires precise modeling of magnetic energy levels associated with the magnetic interaction between two open-shell centers. Although density functional theory (DFT)[24,25] has evolved into a method that can be used to describe and even predict various molecular properties, due to its single-determinantal nature, the determination of exchange coupling (constants) may seem out of reach. Exchange coupling constant (J) is a measure of the energy differences between the electronic states with different spin multiplicity.[26] If the state of the highest spin multiplicity is the ground state, the coupling is FM (positive J value). If the low-spin state is the ground state, AF coupling occurs (negative J value). Since only the FM states can be described with a single determinant and hence directly computed, in all other cases, broken-symmetry DFT (BS-DFT)[27–30] approach is commonly utilized.

In the present work, we examine the magnetic properties of 8 “end-to-end” thiocyanato (Fig. 2) and 3 “end-to-end” cyanato (Fig. 3) double bridged Ni(II) binuclear complexes by calculating the *J* constants within the framework of BS--DFT. DFT is, in principle, the exact theory, however, in practical computational work requires approximations (density functional approximations – DFAs) on its path to solutions. The choice of the DFA strongly influences the accuracy of calculations. It was usually found that for magnetic systems, hybrid DFAs and range-separated hybrid DFAs provide much better agreement with experimental data than semi-local DFAs.[31–35] However, this does not need to be true always. For example, in the case of double “end-on” azido bridged binuclear Ni(II) complexes, it was found that hybrid DFAs did not improve the results compared to general gradient approximations (GGA).[36] In that study, it was shown[36] that only double-hybrid functionals[37,38] (MP2 correlation energy added to the hybrid or meta-hybrid energy) give acceptable accuracy. Even more importantly, only double-hybrids predicted the sign of *J* correctly in all complexes.[36] It is noteworthy to mention that double-hybrids do not always give better results than the hybrid functionals.[35,39] This implies that the choice of DFAs for the calculation of magnetic coupling is firmly system dependent. Here we address the question of DFAs’ influence on the overall DFT accuracy for calculation of *J* constant in double bridged “end-to-end” thiocyanato and cyanato Ni(II) binuclear complexes. These systems are challenging because the weak FM or AF coupling is observed (*J* value ranges from –4.8 to +6.3 cm^{-1}). 17 different DFAs, with different flavors, are used: GGAs, meta-GGAs, hybrid functionals, meta-hybrid functionals, long-range corrected and double-hybrid functionals. Furthermore, the magneto-structural correlations in these systems will be examined.

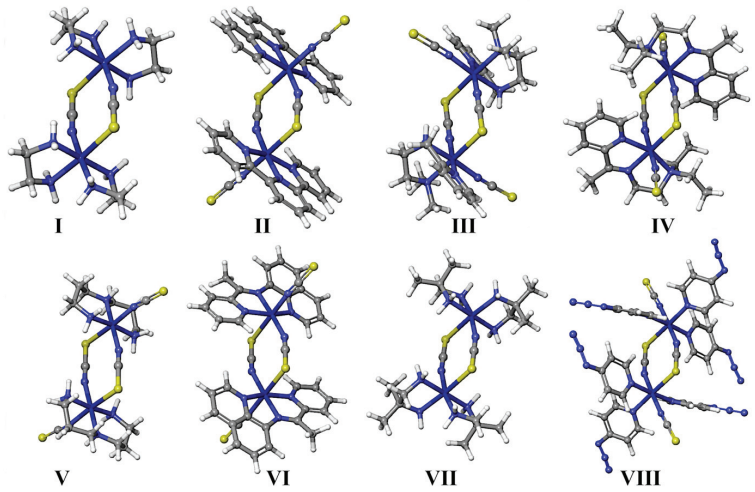

Fig. 2. “End-to-end” thiocyanato double bridged Ni(II) binuclear complexes.

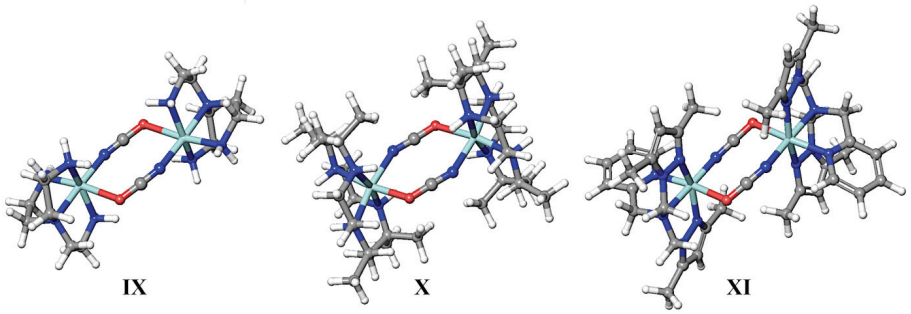

Fig. 3. “End-to-end” cyanato double bridged Ni(II) binuclear complexes.

METHODOLOGY

All DFT calculations have been performed with the ORCA program package (version 4.1.2)[40,41] with ZORA-def2-TZVP(-f)[42,43] basis set for all atoms. Zero-order-regular-approximation (ZORA)[44] has been used to account for scalar-relativistic effects. For GGA and meta--GGA functionals, RI approximation in the Split-RI-J variant was used. The scalar relativistically recontracted SARC/J[43,45,46] auxiliary basis sets have been used to fit the Coulomb integrals in the resolution of the identity (RI) approximation.[47] The chain-of-spheres approximation to the exact exchange (COSX)[48] was employed for hybrid, meta-hybrid, long-range corrected, and double hybrid DFAs. The RI approach was used in the MP2 part of the calculation for double-hybrid functionals, combined with def2-TZVP/C[49] correlation fitting basis sets.

Choice of DFAs

The choice of DFAs used in this work include: i) GGA functionals in the form of BP86,[50–52] BLYP,[50,53–55] OLYP[53–56] and OPBE[56,57] ii) meta-GGA in the form of M06-L[58,59] and TPSS[60,61] iii) hybrid functionals B3LYP,[62] B3LYP*[63] and BHandHLYP iv) meta-hybrid TPSSh,[60,61] M06[58,59] and M06-2X[58,59] v) double-hybrid B2PLYP[37] and PWPB95[64] vi) long-range corrected[65] LC-BLYP,[66] cam-B3LYP,[67] and wB97X.[68] DFAs used have different amount of the exact exchange: 0 % (GGAs and meta-GGAs), 10 % (TPSSh), 15 % (B3LYP*), 20 % (B3LYP), 27 % (M06), 50 % (BHandHLYP and PWPB95), 53 % (B2PLYP), 54 % (M06-2X). LC-BLYP has 0 % exact exchange in the short-range, while 100% in the long-range; cam-B3LYP has 19 % in the short-range and 65 % in the long-range; wB97X has 16 % in the short-range and 100 % in the long-range. B2PYLP is the standard double-hybrid functional with the perturbative treatment of correlation on top of the DF energy. PWPB95 is double-hybrid, which accounts for the correlation of opposite-spin electron pairs solely.

Binuclear Ni(II) complexes

Binuclear Ni(II) complexes analyzed in this work are: $[\{Ni(en)_2\}_2(\mu_{1,3}\text{-}NCS)_2]^{2+}$ (en = = ethylenediamine) **I**, $[\{Ni(terpy)(NCS)\}_2(\mu_{1,3}\text{-}NCS)_2]$ (terpy = 2,2';6',2"-terpyridine) **II**, $[\{NiL^1\text{-}(NCS)\}_2(\mu_{1,3}\text{-}NCS)_2]$ (L^1 = *N*,*N*-dimethyl-*N*′-(pyrid-2-ylmethyl)-ethylenediamine) **III**, $[\{NiL^2\text{-}(NCS)\}_2(\mu_{1,3}\text{-}NCS)_2]$ (L^2 = *N*,*N*-diethyl-*N*′-(1-pyridin-2-yl-ethylidene)-ethylenediamine) **IV**, $[\{NiL^3(NCS)\}_2(\mu_{1,3}\text{-}NCS)_2]$ (L^3 = *bis*(3-aminopropyl)amine) **V**, $[\{NiL^4(NCS)\}_2(\mu_{1,3}\text{-}NCS)_2]$ (L^4 = 1-(pyridin-2-yl)-N-(quinolin-8-yl)ethan-1-imine) **VI**, $[\{NiL_2^5\}_2(\mu_{1,3}NCS)_2]^{2+}$ (L^5 = 1,2-diamino-2-methylpropane) **VII**, $[\{Ni(4\text{-azpy})_6\}_2(\mu_{1,3}\text{-}NCS)_2]$ (4-azpy = 4-azidopyridine) **VIII**, $[\{Ni(tren)\}_2(\mu_{1,3}\text{-}OCN)_2]^{2+}$ (tren =tris(2-aminoethyl)amine) **IX**, $[\{Ni(Me_6[14]aneN_4)\}_2(\mu\text{-}OCN)_2]^{2+}$ ($Me_6[14]aneN_4$ = DL-5,5,7,12,12,14-hexamethyl-

-1,4,8,11-tetraazacyclotetradecane) **X**, $[\{NiL^6\}_2(\mu_{1,3}\text{-}OCN)_2]^{2+}$ (L^6 = *N,N-bis*(3,5-dimethyl-pyrazol-1-ylmethyl)aminomethylpyridine). Complexes **I**–**VIII** are bridged with two "end-to-end" thiocyanato ligands and complexes **IX-XI** with two "end-to-end" cyanato ligands. Each Ni(II) center is hexacoordinated in distorted octahedral environment with two bridging ligands, one bonded *via* nitrogen donor atom and other *via* chalcogen (sulfur or oxygen donor atoms). Remaining coordination places around Ni(II) centers are occupied by two bidentate ligands (**I**, **VII**), one tridentate ligand and monodentate NCS^- (coordination *via* N atom; **II**–**V**), one tetradentate ligand (**VI**, **IX**–**XI**), or six monodentate ligands (**VIII**). Therefore, the first coordination sphere around each Ni(II) is NiN_5X (X = S/O). All the calculations were performed on the complexes from the experimental X-ray structures: **I** (CCDC 1219660),[69] **II** (CCDC 1261119),[21] **III** (CCDC 263465),[70] **IV** (CCDC 772821),[14] **V** (CCDC 180314),[71] **VI** (CCDC 1918388),[7] **VII** (CCDC 1206993),[72] **VIII** (CCDC 1010020),[73] **IX** (CCDC 1275667),[22] **X** (CCDC 1245877),[74] **XI** (CCDC 782334).[75] Solvent molecules (complex **III**) and counter-ions (complexes **I**, **VII**, **IX**–**XI**) were removed, missing hydrogen atoms were added to complex **I**. Positions of hydrogen atoms were optimized in all structures, assuming the high-spin state, using BP86 functional with Grimme's third-generation dispersion energy correction[76] and Becke-Johnson damping,[77] *i.e.*, BP86-D3. In the X-ray structure of **V**, both the binuclear and central part of tetranuclear units are considered. Terminal Ni(II) units of tetranuclear structure in **V** are removed because they are connected with a single NCS bridge to the central part (coordination to the central part *via* S atom, *i.e.*, *trans*-NiN_4S_2 coordination sphere).[71]

Exchange coupling

The exchange coupling constant J of the Heisenberg–Dirac–van Vleck spin-Hamiltonian ($H = -2JS_1S_2$) was calculated with BS-DFT formalism[27-30] according to the Yamaguchi:[40,78] $J=(E_{HS} - E_{BS})/(\langle S^2\rangle_{HS} - \langle S^2\rangle_{BS})$. $\langle S^2\rangle_{HS}$ and $\langle S^2\rangle_{BS}$ are the spin expectation values of the high-spin and broken-symmetry states, respectively. E_{HS} and E_{BS} are corresponding energies. When the Hamiltonian is in the form $H = -JS_1S_2$ (complexes **IV**, **X**, **XI**), the reported J values from the literature are divided by two to compare calculated and experimental values. In the case of **V**, the average of the two computed J values is compared with the experiment because only one J is reported for double-bridged pathways.[71]

RESULTS AND DISCUSSION

Results for calculation of J constants in complexes **I**–**XI** with GGAs and meta-GGAs are presented in Table I. On the same complexes, results of calculations with three hybrid and three meta-hybrid DFAs are summarized in Table II. Finally, Table III shows the results obtained with double-hybrid and long-range corrected DFAs. In Table II, DFT only values of double-hybrids are given as well. In all tables, mean error (*ME*), mean absolute error (*MAE*), minimal absolute error (Min *AE*), and maximal absolute error (Max *AE*) with respect to the experimental values are given. The results indicate the accuracy of a given functional for the investigated set of complexes. Generally speaking, GGAs do not perform well, as indicated by the largest MAE (more than 10 cm^{-1}). Meta-GGAs do not improve the results comparing to GGAs. In some cases, there is an overestimation of FM coupling (**II**, **III**, **VI**, **VII**), while in other cases AF coupling is more pronounced. This is different than in double "end-on" azido bridged binuclear Ni(II) complexes where all GGAs largely overestimated FM coupling.[36] BP86,

TABLE I. Exchange coupling constants(J / cm^{-1}), calculated with selected GGAs and meta-GGAs for 8 "end-to-end" thiocyanato (Fig. 2, **I**–**VIII**) and 3 "end-to-end" cyanato (Fig. 3, **IX**–**XI**) double bridged Ni(II) binuclear complexes and comparison with experimentally determined values. Mean error (*ME*), mean absolute error (*MAE*), minimal absolute error (Min *AE*) and maximal absolute error (Max *AE*)

Complex	Exp.	GGA					
		BP86	BLYP	OLYP	OPBE	M06-L	TPSS
I	4.50[69]	0.38	1.77	8.41	11.07	6.48	2.04
II	4.90[21]	19.49	18.6	25.59	27.15	16.33	16.37
III	3.90[70]	7.49	6.46	13.98	16.48	9.68	6.54
IV	0.34[14]	–12.12	–13.33	–4.12	–2.01	0.29	–8.39
V	2.73[71]	–5.38	–6.61	0.65	3.25	2.11	–3.80
VI	4.71[7]	17.96	17.43	23.14	22.65	13.31	14.11
VII	6.33[72]	28.48	27.35	45.24	46.17	21.98	21.30
VIII	1.56[73]	–1.98	–3.07	5.60	7.58	4.62	–1.19
IX	–4.41[23]	–12.46	–12.93	–9.15	–7.88	–4.73	–10.30
X	–4.80[74]	–31.55	–32.05	–28.89	–15.41	–15.98	–25.86
XI	–3.10[75]	–21.65	–22.42	–17.71	–15.41	–9.58	–17.86
ME		–2.54	–3.22	4.19	7.00	2.53	–2.15
MAE		12.29	12.32	13.28	12.23	5.93	9.16
Min *AE*		3.54	2.56	2.085	0.52	0.05	2.46
Max *AE*		26.75	27.25	38.94	39.87	15.68	21.06

BLYP, and TPSS, predict the wrong sign of J constant in cases **IV**, **V** and **VIII**. OLYP and OPBE revealed the opposite sign only in the case of **IV**. This complex is also problematic for B3LYP* and TPSSh (Table II). M06-L is the only DFA from these functionals that qualitatively gives correct results (Table I). As expected, hybrid functionals performed much better giving MAE in the range 2.2-3.8 cm^{-1}. DFAs with a higher percentage of the exact exchange (50% in BHandHLYP and 54 % in M06-2X) give somewhat better results. Meta-hybrid M06-2X has the lowest *MAE* (1.4 cm^{-1}) among chosen "standard DFAs" (Tables I and II) and Max *AE* of 3.6 cm^{-1}. Long-range corrected functionals do not perform better than standard hybrid functionals for herein studied complexes (Table III). Double-hybrid DFAs give good agreement with experimental values. PWPB95, double-hybrid with only opposite-spin correlation, is the best of all 17 selected functionals with MAE of 1.1 cm^{-1} and Max *AE* = 2.8 cm^{-1}. DFT only values of double-hybrids (without perturbational corrections) are similar to the results obtained with BHandHLYP and M06-2X. Considering the high computational cost of double-hybrids, the use of M06-2X is recommended for double-bridged NCS/NCO binuclear Ni(II) complexes.

Magneto-structural correlations

Herein analyzed thiocyanato "end-to-end" double-bridged binuclear Ni(II) complexes show weak FM coupling (J value from 0.3 to 6.3 cm^{-1}), while rare cya-

TABLE II. Exchange coupling constants (J / cm^{-1}), calculated with selected hybrid and meta--hybrid DFAs for 8 "end-to-end" thiocyanato (Fig. 2, **I**–**VIII**) and 3 "end-to-end" cyanato (Fig. 3, **IX**–**XI**) double bridged Ni(II) binuclear complexes and comparison with experimentally determined values. Mean error (*ME*), mean absolute error (*MAE*), minimal absolute error (Min *AE*), and maximal absolute error (Max *AE*)

Complex	Exp.	DFA					
		B3LYP	B3LYP*	BHandHLYP	TPSSh	M06	M06-2X
I	4.50[69]	4.37	3.79	4.06	6.4	6.95	3.25
II	4.90[21]	11	12.7	7.37	10.99	13.8	5.97
III	3.90[70]	5.97	7.15	5.59	7.09	8.21	3.93
IV	0.34[14]	1.6	–0.42	3.49	–2.53	1.43	1.83
V	2.73[71]	1.54	2.13	3.22	0.115	2.39	1.345
VI	4.71[7]	8.83	8.89	5.71	8.63	11.63	4.88
VII	6.33[72]	13.00	15.94	12.01	15.89	17.41	9.74
VIII	1.56[73]	1.11	1.00	3.60	3.86	4.47	2.32
IX	–4.41[23]	–4.06	–4.02	–0.26	–3.57	–1.54	–0.77
X	–4.80[74]	–9.78	–12.58	–2.9	–14.32	–8.65	–3.51
XI	–3.10[75]	–6.69	–8.75	–1.79	–7.69	–5.19	–2.19
ME		0.93	0.84	2.13	0.75	3.12	0.92
MAE		2.81	3.76	2.21	4.31	4.26	1.40
Min *AE*		0.13	0.38	0.44	0.83	0.34	0.03
Max *AE*		6.7	9.64	5.71	9.59	11.11	3.63

TABLE III. Exchange coupling constants (J / cm^{-1}), calculated with selected double-hybrid and long-range corrected DFAs for 8 "end-to-end" thiocyanato (Fig. 2, **I**–**VIII**) and 3 "end-to--end" cyanato (Fig. 3, **IX**–**XI**) double bridged Ni(II) binuclear complexes and comparison with experimentally determined values. Mean error (*ME*), mean absolute error (*MAE*), minimal absolute error (Min *AE*), and maximal absolute error (Max *AE*) in cm^{-1}. DFT only values for double-hybrids is given

Complex	Exp.	DFA						
		B2PLYP (DFT)	B2LYP	PWPB95 (DFT)	PWPB95	LC-BLYP	Cam-B3LYP	wB97X
I	4.50[69]	4.49	4.75	3.7	2.92	5.25	4.63	4.88
II	4.90[21]	7.62	8.10	6.36	6.43	13.18	9.64	9.29
III	3.90[70]	5.86	5.89	4.45	4.23	6.07	6.4	5.98
IV	0.34[14]	3.72	1.81	2.34	0.73	0.46	3.16	3.78
V	2.73[71]	3.16	3.03	1.7	0.93	1.08	1.82	2.49
VI	4.71[7]	6.12	6.96	4.63	5.16	9.30	8.44	8.03
VII	6.33[72]	12.33	6.14	10.17	4.57	15.20	13.73	12.23
VIII	1.56[73]	4.28	4.17	2.92	2.29	4.57	3.69	4.78
IX	–4.41[23]	–0.09	–0.33	–0.74	–1.55	–4.22	–2.14	–0.45
X	–4.80[74]	–2.91	–4.85	–3.23	–5.36	–10.53	–6.86	–5.24
XI	–3.10[75]	–0.32	–2.87	–1.89	–3.29	–6.03	–4.73	–4.8
ME		2.51	1.47	1.25	0.04	1.61	1.92	2.21
MAE		2.51	1.51	1.60	1.10	3.48	2.76	2.65
Min *AE*		0.01	0.05	0.07	0.19	0.12	0.13	0.24
Max *AE*		6.03	4.07	3.87	2.85	8.9	7.43	5.93

nato ones show weak AF coupling (from –3.1 to –4.8 cm^{-1}). All complexes have similar coordination around Ni(II) centers and similar Ni–Ni distances (thiocyanato in the range 5.5–5.7 Å, and cyanato in the range 5.1–5.5 Å). The correlation between the magnetic properties of these complexes with their geometries reveals the importance of symmetry of the bridging unit.[7,23,74,79] The more symmetric the bridge is, the more AF coupling is pronounced. The measure of symmetry/ /asymmetry of a bridge, δ, is defined as a difference between Ni–X (X = O/S) and Ni–N bond lengths.[7] In Fig. 4, where experimental J values are plotted *vs*. δ (from corresponding X-ray structures), linear dependence is observed (R^2 = 0.89). The AF coupled cyanate bridged complexes have smaller δ (0.1–0.3 Å) than FM coupled thiocyanato bridged complexes. The same trend is observed with DFT calculated J coupling, Fig. 5 (R^2 = 0.96 and R^2 = 0.87 for M06-2X and PWPB95, respectively). The symmetry of the double pseudohalide bridges is known to be important for other binuclear complexes as well.[80]

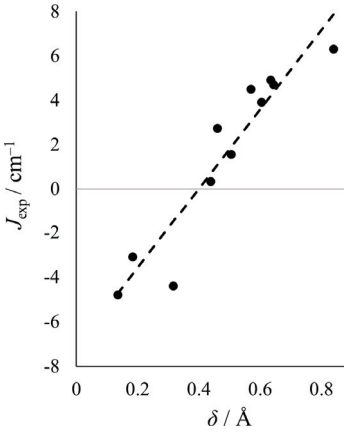

Fig. 4. Relationship between experimental exchange coupling constant J_{exp} and symmetry of the bridge δ (from corresponding X-ray structures).

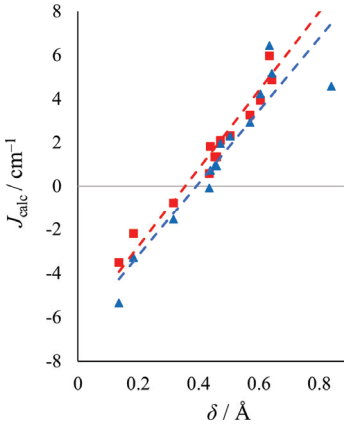

Fig. 5. Relationship between calculated exchange coupling constant J_{calc} and symmetry of the bridge δ (from corresponding X-ray structures); J_{calc} by M06-2X – squares and PWPB95 – triangles.

Interestingly, there exists a linear relationship between the error of GGAs (J_{calc}–J_{exp}) and δ (R^2 = 0.88 and R^2 = 0.92 for BP86 and OPBE, respectively). In Fig. 6 relationship between J_{calc}–J_{exp} and δ for BP86, OPBE, and PWPB95 are shown.

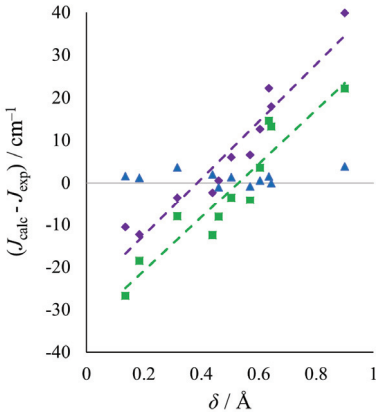

Fig. 6. Relationship between J_{calc}–J_{exp} and δ (from corresponding X-ray structures) – J_{calc} by BP86 (squares), OPBE (diamonds) and PWPB95 (triangles).

When δ is small, GGAs tend to overestimate AF coupling. This is in line with the known tendency of GGAs to stabilize the low-spin states.[81] OPBE, which is suitable for spin-state energetics of mononuclear complexes[81] corrects this behavior, albeit not sufficiently. As δ is increasing, AF coupling becomes less critical, as discussed above (Fig. 4). When δ is larger, FM coupling, dominated by the high-spin state's spin-delocalization, becomes more important. In these cases, GGAs enlarge FM coupling because of its nature to overestimate electron spin delocalization.[82] On the other hand, DFAs with exact exchange tend to stabilize the high-spin state and to localize the spin density.[81,83] Therefore, hybrid and meta-hybrid DFAs showed better performance (Table II). Double hybrids improve the results because MP2 correlation corrects the over-stabilization of the high-spin states, and there is no correlation between the J_{calc}–J_{exp} and δ (ME for PWPB95 is 0.04 cm^{-1}).

CONCLUSION

In this study, the performance of 17 DFAs with different flavors for the calculation of the magnetic coupling in 11 binuclear Ni(II) complexes have been presented. These results are compared to experimentally determined J values. Furthermore, the magneto-structural correlation between the J constant and symmetry of the bridging unit has been examined. This study shows that M06-2X and PWPB95 are the methods of choice for studying magnetic coupling in binuclear Ni(II) complexes, which can be used for predictive analyses. It is noteworthy that these results are somewhat different from double "end-on" azido bridged binuclear Ni(II) complexes,[36] where M06-2X gave the wrong sign of J in one

case, showing the importance of bridging ligands. Magneto-structural correlation delved deeper into the origin of various DFAs' behavior and gave a rational explanation of their tendencies.

Although most polynuclear complexes are obtained accidentally, this study will guide the smart choice of polydentate and bridging ligands. This can open a door for rational tuning of the electronic structure, magnetic interactions, and thus all general properties of a binuclear complex.

Acknowledgements. This work was financially supported by the Ministry of Education, Science and Technological Development of the Republic of Serbia (Grants 451-03--68/2020-14/200026, 451-03-68/2020-14/200288 and 451-03-68/2020-14/200168).

И З В О Д

ИСПИТИВАЊЕ АПРОКСИМАТИВНИХ ФУНКЦИОНАЛА ГУСТИНЕ ЗА ИЗРАЧУНАВАЊЕ КОНСТАНТИ КУПЛОВАЊА У ДВОСТРУКО ПРЕМОШЋЕНИМ ТИОЦИЈАНАТО И ЦИЈАНАТО БИНУКЛЕАРНИМ Ni(II) КОМПЛЕКСИМА

МАТИЈА ЗЛАТАР[1], ФИЛИП ВЛАХОВИЋ[2], ДРАГАНА МИТИЋ[2], МАРИО ЗЛАТОВИЋ[3] и МАЈА ГРУДЕН[3]

[1]Универзитет у Београду – Институт за хемију, технологију и металургију, Институт од националног значаја за Републику Србију, Његошева 12, 11000 Београд, [2]Иновациони центар Хемијског факултета, Студентски трг 12–16, 11000 Београд и [3]Универзитет у Београду – Хемијски факултет, Студентски трг 12–16, 11000 Београд

Проучавана су магнетна својства 8 „*end-to-end*“ тиоцијанато, и 3 „*end-to-end*“ цијанато двоструко премошћених Ni(II) бинуклеарних комплекса. Тиоцијанато премошћени комплекси су слабо феромагнетни. Комплекси премошћени цијанато лигандима показују слабо антиферомагнетно куповање. Због тога је прецизно израчунавање константи купловања у овим системима изазов за рачунарску хемију. Константе купловања у овим системима су израчунате *Broken-Symmetry* приступом у оквиру теорије функционала густине. Седамнаест апроксимативних функционала густине су коришћени како би се пронашао најпоузданији ниво теорије за проучавање магнетних својстава бинуклеарних Ni(II) комплекса. Утврђено је да су M06-2X и PWPB95 показали најбоље слагање са експерименталним вредностима за цео скуп испитиваних комплекса. Напослетку, резултати су рационализовани магнетно-структурном корелацијом.

(Примљено 6. новембра, прихваћено 12. новембра 2020)

REFERENCES

1. G. Li, D. Zhu, X. Wang, Z. Su, M. R. Bryce, *Chem. Soc. Rev.* **49** (2020) 765 (https://doi.org/10.1039/c8cs00660a)
2. D. M. Zink, M. Bächle, T. Baumann, M. Nieger, M. Kühn, C. Wang, W. Klopper, U. Monkowius, T. Hofbeck, H. Yersin, S. Bräse, *Inorg. Chem.* **52** (2013) 2292 (https://doi.org/10.1021/ic300979c)
3. J. He, M. Zeng, H. Cheng, Z. Chen, F. Liang, *Zeitschrift Anorg. Allg. Chem.* **639** (2013) 1834 (https://doi.org/10.1002/zaac.201300153)
4. N. Xiong, G. Zhang, X. Sun, R. Zeng, *Chinese J. Chem.* **38** (2020) 185 (https://doi.org/10.1002/cjoc.201900371)
5. M. Jarenmark, H. Carlsson, E. Nordlander, *Comptes Rendus Chim.* **10** (2007) 433 (https://doi.org/10.1016/j.crci.2007.02.015)

6. D. Venegas-Yazigi, D. Aravena, E. Spodine, E. Ruiz, S. Alvarez, *Coord. Chem. Rev.* **254** (2010) 2086 (https://doi.org/10.1016/j.ccr.2010.04.003)
7. P. Ghorai, P. Brandão, S. Benmansour, C. J. G. García, A. Saha, *Polyhedron* **188** (2020) 114708 (https://doi.org/10.1016/j.poly.2020.114708)
8. A. L. Gavrilova, C. J. Qin, R. D. Sommer, A. L. Rheingold, B. Bosnich, *J. Am. Chem. Soc.* **124** (2002) 1714 (https://doi.org/10.1021/ja012386z)
9. C. Incarvito, A. L. Rheingold, C. J. Qin, A. L. Gavrilova, B. Bosnich, *Inorg. Chem.* **40** (2001) 1386 (https://doi.org/10.1021/ic0012773)
10. K. Shanmuga Bharathi, S. Sreedaran, A. Kalilur Rahiman, V. Narayanan, *Spectrochim. Acta, A* **105** (2013) 245 (https://doi.org/10.1016/j.saa.2012.12.031)
11. D. Ghosh, S. Mukhopadhyay, S. Samanta, K.-Y. Choi, A. Endo, M. Chaudhury, *Inorg. Chem.* **42** (2003) 7189 (https://doi.org/10.1021/ic034314)
12. J. Burmeister, *Coord. Chem. Rev.* **105** (1990) 77 (https://doi.org/10.1016/0010-8545(90)80019-P)
13. T. S. Mahapatra, S. Chaudhury, S. Dasgupta, V. Bertolasi, D. Ray, *New J. Chem.* **40** (2016) 2268 (https://doi.org/10.1039/c5nj02410b)
14. P. Bhowmik, S. Chattopadhyay, M. G. B. Drew, C. Diaz, A. Ghosh, *Polyhedron* **29** (2010) 2637 (https://doi.org/10.1016/j.poly.2010.06.014)
15. T. Mallah, M. L. Boillot, O. Kahn, J. Gouteron, S. Jeannin, Y. Jeannin, *Inorg. Chem.* **25** (1986) 3058 (https://doi.org/10.1021/ic00237a027)
16. O. Kahn, T. Mallah, J. Gouteron, S. Jeannin, Y. Jeannin, *J. Chem. Soc. Dalt. Trans.* (1989) 1117 (https://doi.org/10.1039/DT9890001117)
17. J. Carranza, J. Sletten, F. Lloret, M. Julve, *J. Mol. Struct.* **890** (2008) 31 (https://doi.org/10.1016/j.molstruc.2007.11.034)
18. A. E. Mauro, S. I. Klein, J. S. Saldaña, C. A. De Simone, J. Zukerman-Schpector, E. E. Castellano, *Polyhedron* **9** (1990) 2937 (https://doi.org/10.1016/S0277-5387(00)84204-7)
19. S. Youngme, J. Phatchimkun, U. Suksangpanya, C. Pakawatchai, G. A. Van Albada, J. Reedijk, *Inorg. Chem. Commun.* **8** (2005) 882 (https://doi.org/10.1016/j.inoche.2005.06.024)
20. C. Diaz, J. Ribas, M. Salah El Fallah, X. Solans, M. Font-Bardía, *Inorg. Chim. Acta* **312** (2001) 1 (https://doi.org/10.1016/S0020-1693(00)00281-4)
21. T. Rojo, R. Cortés, L. Lezama, M. I. Arriortua, K. Urtiaga, G. Villeneuve, *J. Chem. Soc. Dalt. Trans.* (1991) 1779 (https://doi.org/10.1039/DT9910001779)
22. D. M. Duggan, D. N. Hendrickson, *Inorg. Chem.* **13** (1974) 2056 (https://doi.org/10.1021/ic50139a003)
23. D. M. Duggan, D. N. Hendrickson, *Inorg. Chem.* **13** (1974) 2929 (https://doi.org/10.1021/ic50142a031)
24. W. Koch, M. C. Holthausen, *A Chemist's Guide to Density Functional Theory*, Wiley-VCH Verlag GmbH, Weinheim, 2001 (https://doi.org/10.1002/3527600043)
25. R. G. Parr, *Density Functional Theory of Atoms and Molecules*, in *Horizons Quantum Chem.*, Springer, Amsterdam, 1980, pp. 5–15 (https://doi.org/10.1007/978-94-009-9027-2_2)
26. O. Kahn, *Molecular magnetism*, VCH-Verlag, Weinheim, 1993 (ISBN 3-527-89566-3)
27. L. Noodleman, *J. Chem. Phys.* **74** (1981) 5737 (https://doi.org/10.1063/1.440939)
28. L. Noodleman, E. R. Davidson, *Chem. Phys.* **109** (1986) 131 (https://doi.org/10.1016/0301-0104(86)80192-6)
29. F. Neese, *Coord. Chem. Rev.* **253** (2009) 526 (https://doi.org/10.1016/j.ccr.2008.05.014)

30. A. Bencini, F. Totti, *J. Chem. Theory Comput.* **5** (2009) 144 (https://doi.org/10.1021/ct800361x)
31. G. David, N. Guihéry, N. Ferré, *J. Chem. Theory Comput.* **13** (2017) 6253 (https://doi.org/10.1021/acs.jctc.7b00976)
32. S. Ninova, V. Lanzilotto, L. Malavolti, L. Rigamonti, B. Cortigiani, M. Mannini, F. Totti, R. Sessoli, *J. Mater. Chem., C* **2** (2014) 9599 (https://doi.org/10.1039/c4tc01647e)
33. J. E. Peralta, J. I. Melo, *J. Chem. Theory Comput.* **6** (2010) 1894 (https://doi.org/10.1021/ct100104v)
34. J. J. Phillips, J. E. Peralta, *J. Chem. Phys.* **138** (2013) 174115 (https://doi.org/10.1063/1.4802776)
35. N. A. G. Bandeira, B. Le Guennic, *J. Phys. Chem., A* **116** (2012) 3465 (https://doi.org/10.1021/jp300618v)
36. T. Keškić, Z. Jagličić, A. Pevec, B. Čobeljić, D. Radanović, M. Gruden, I. Turel, K. Anđelković, I. Brčeski, M. Zlatar, *Polyhedron* **191** (2020) 114802 (https://doi.org/10.1016/j.poly.2020.114802)
37. S. Grimme, *J. Chem. Phys.* **124** (2006) 034108 (https://doi.org/10.1063/1.2148954)
38. L. Goerigk, S. Grimme, *Wiley Interdiscip. Rev. Comput. Mol. Sci.* **4** (2014) 576 (https://doi.org/10.1002/wcms.1193)
39. D. A. Pantazis, *Inorganics* **7** (2019) 57 (https://doi.org/10.3390/inorganics7050057)
40. F. Neese, *Wiley Interdiscip. Rev. Comput. Mol. Sci.* **2** (2012) 73 (https://doi.org/10.1002/wcms.81)
41. F. Neese, *Wiley Interdiscip. Rev. Comput. Mol. Sci.* **8** (2018) e1327 (https://doi.org/10.1002/wcms.1327)
42. F. Weigend, R. Ahlrichs, *Phys. Chem. Chem. Phys.* **7** (2005) 3297 (https://doi.org/10.1039/b508541a)
43. D. A. Pantazis, X.-Y. Chen, C. R. Landis, F. Neese, *J. Chem. Theory Comput.* **4** (2008) 908 (https://doi.org/10.1021/ct800047t)
44. C. van Wüllen, *J. Chem. Phys.* **109** (1998) 392 (https://doi.org/10.1063/1.476576)
45. D. A. Pantazis, F. Neese, *J. Chem. Theory Comput.* **5** (2009) 2229 (https://doi.org/10.1021/ct900090f)
46. F. Weigend, *Phys. Chem. Chem. Phys.* **8** (2006) 1057 (https://doi.org/10.1039/b515623h)
47. F. Neese, *J. Chem. Phys.* **115** (2001) 11080 (https://doi.org/10.1063/1.1419058)
48. F. Neese, F. Wennmohs, A. Hansen, U. Becker, *Chem. Phys.* **356** (2009) 98 (https://doi.org/10.1016/j.chemphys.2008.10.036)
49. A. Hellweg, C. Hättig, S. Höfener, W. Klopper, *Theor. Chem. Acc.* **117** (2007) 587 (https://doi.org/10.1007/s00214-007-0250-5)
50. A. D. Becke, *Phys. Rev., A* **38** (1988) 3098 (https://doi.org/10.1103/PhysRevA.38.3098)
51. J. P. Perdew, *Phys. Rev., B* **33** (1986) 8822 (https://doi.org/10.1103/PhysRevB.33.8822)
52. J. P. Perdew, *Phys. Rev., B* **34** (1986) 7406 (https://doi.org/10.1103/PhysRevB.34.7406)
53. C. Lee, W. Yang, R. G. Parr, *Phys. Rev., B* **37** (1988) 785 (https://doi.org/10.1103/PhysRevB.37.785)
54. B. G. Johnson, P. M. W. Gill, J. A. Pople, *J. Chem. Phys.* **98** (1993) 5612 (https://doi.org/10.1063/1.464906)
55. T. V. Russo, R. L. Martin, P. J. Hay, *J. Chem. Phys.* **101** (1994) 7729 (https://doi.org/10.1063/1.468265)
56. N. C. Handy, A. J. Cohen, *Mol. Phys.* **99** (2001) 403 (https://doi.org/10.1080/00268970010018431)

57. M. Swart, A. W. Ehlers, K. Lammertsma, *Mol. Phys.* **102** (2004) 2467 (https://doi.org/10.1080/00268970420002750 17)
58. Y. Zhao, D. G. Truhlar, *Theor. Chem. Acc.* **120** (2008) 215 (https://doi.org/10.1007/s00214-007-0310-x)
59. Y. Zhao, D. G. Truhlar, *J. Chem. Phys.* **125** (2006) 194101 (https://doi.org/10.1063/1.2370993)
60. V. N. Staroverov, G. E. Scuseria, J. Tao, J. P. Perdew, *J. Chem. Phys.* **119** (2003) 12129 (https://doi.org/10.1063/1.1626543)
61. J. Tao, J. Perdew, V. Staroverov, G. Scuseria, *Phys. Rev. Lett.* **91** (2003) 146401 (https://doi.org/10.1103/PhysRevLett.91.146401)
62. A. D. Becke, *J. Chem. Phys.* **98** (1993) 5648 (https://doi.org/10.1063/1.464913)
63. M. Reiher, O. Salomon, B. Artur Hess, *Theor. Chem. Accounts Theory, Comput. Model. (Theor. Chim. Acta)* **107** (2001) 48 (https://doi.org/10.1007/s00214-001-0300-3)
64. L. Goerigk, S. Grimme, *J. Chem. Theory Comput.* **7** (2010) 291 (https://doi.org/10.1021/ct100466k)
65. H. Iikura, T. Tsuneda, T. Yanai, K. Hirao, *J. Chem. Phys.* **115** (2001) 3540 (https://doi.org/10.1063/1.1383587)
66. Y. Tawada, T. Tsuneda, S. Yanagisawa, T. Yanai, K. Hirao, *J. Chem. Phys.* **120** (2004) 8425 (https://doi.org/10.1063/1.1688752)
67. T. Yanai, D. P. Tew, N. C. Handy, *Chem. Phys. Lett.* **393** (2004) 51 (https://doi.org/10.1016/j.cplett.2004.06.011)
68. J. Da Chai, M. Head-Gordon, *J. Chem. Phys.* **128** (2008) 084106 (https://doi.org/10.1063/1.2834918)
69. A. E. Shvelashvili, M. A. Porai-Koshits, A. S. Antsyshkina, *J. Struct. Chem.* **10** (1969) 552 (https://doi.org/10.1007/BF00743627)
70. H. D. Bian, W. Gu, Q. Yu, S. P. Yan, D. Z. Liao, Z. H. Jiang, P. Cheng, *Polyhedron* **24** (2005) 2002 (https://doi.org/10.1016/j.poly.2005.06.011)
71. T. Kumar Maji, G. Mostafa, J. M. Clemente-Juan, J. Ribas, F. Lloret, K. Okamoto, N. R. Chaudhuri, *Eur. J. Inorg. Chem.* **2003** (2003) 1005 (https://doi.org/10.1002/ejic.200390123)
72. M. Monfort, J. Ribas, X. Solans, *Inorg. Chem.* **33** (1994) 4271 (https://doi.org/10.1021/ic00097a013)
73. F. A. Mautner, M. Scherzer, C. Berger, R. C. Fischer, R. Vicente, S. S. Massoud, *Polyhedron* **85** (2015) 20 (https://doi.org/10.1016/j.poly.2014.08.031)
74. A. Escuer, R. Vicente, M. S. El Fallah, X. Solans, M. Font-Bardía, *J. Chem. Soc., Dalton Trans.* (1996) 1013 (https://doi.org/10.1039/DT9960001013)
75. Z. Mahendrasinh, S. Ankita, S. B. Kumar, A. Escuer, E. Suresh, *Inorg. Chim. Acta* **375** (2011) 333 (https://doi.org/10.1016/j.ica.2011.05.027)
76. S. Grimme, J. Antony, S. Ehrlich, H. Krieg, *J. Chem. Phys.* **132** (2010) 154104 (https://doi.org/10.1063/1.3382344)
77. S. Grimme, S. Ehrlich, L. Goerigk, *J. Comput. Chem.* **32** (2011) 1456 (https://doi.org/10.1002/jcc.21759)
78. T. Soda, Y. Kitagawa, T. Onishi, Y. Takano, Y. Shigeta, H. Nagao, Y. Yoshioka, K. Yamaguchi, *Chem. Phys. Lett.* **319** (2000) 223 (https://doi.org/10.1016/S0009-2614(00)00166-4)
79. A. P. Ginsberg, R. L. Martin, R. W. Brookes, R. C. Sherwood, A. P. Ginsberg, R. L. Martin, R. W. Brookes, R. C. Sherwood, *Inorg. Chem.* **11** (1972) 2884 (https://doi.org/10.1021/ic50118a006)

80. C. Adhikary, S. Koner, *Coord. Chem. Rev.* **254** (2010) 2933 (https://doi.org/10.1016/j.ccr.2010.06.001)
81. M. Swart, M. Gruden, *Acc. Chem. Res.* **49** (2016) 2690 (https://doi.org/10.1021/acs.accounts.6b00271)
82. Y. Zhang, W. Yang, *J. Chem. Phys.* **109** (1998) 2604 (https://doi.org/10.1063/1.476859)
83. M. Parthey, M. Kaupp, *Chem. Soc. Rev.* **43** (2014) 5067 (https://doi.org/10.1039/C3CS60481K).

Journal of the Serbian Chemical Society
JSCS-info@shd.org.rs • www.shd.org.rs/JSCS
J. Serb. Chem. Soc. *85* (12) 1591–1603 (2020)
JSCS–5395
UDC 546.561'131+547.261+546.223.1:
66.095.21:542.9–77
Original scientific paper

Reaction of a 3-aryilidene-2-thiohydantoin derivative with polymeric *trans*-$[CuCl_2(DMSO)_2]_n$ complex: unexpected isomerization to dinuclear *cis*-$[\{CuCl(DMSO)_2\}(\mu\text{-}Cl)]_2$

PETAR B. STANIĆ[1], MARKO V. RODIĆ[2], TANJA V. SOLDATOVIĆ[3], ALEKSANDAR B. PAVIĆ[4], NATAŠA S. RADAKOVIĆ[4], BILJANA M. ŠMIT[5]* and MARIJA D. ŽIVKOVIĆ[6]**

[1]*University of Kragujevac, Faculty of Science, Department of Chemistry, Radoja Domanovića 12, 34000 Kragujevac, Serbia,* [2]*University of Novi Sad, Faculty of Sciences, Trg Dositeja Obradovića 3, 21000 Novi Sad, Serbia,* [3]*State University of Novi Pazar, Department of Chemical–Technological Sciences, Vuka Karadžića bb, 36300 Novi Pazar, Serbia,* [4]*University of Belgrade, Institute of Molecular Genetics and Genetic Engineering, Vojvode Stepe 444a, 11000 Belgrade, Serbia,* [5]*University of Kragujevac, Institute for Information Technologies, Department of Science, Jovana Cvijića bb, 34000 Kragujevac, Serbia and* [6]*University of Kragujevac, Faculty of Medical Sciences, Department of Pharmacy, Svetozara Markovića 69, 34000 Kragujevac, Serbia*

(Received 17 September, accepted 20 September 2020)

Abstract: The 3-arylidene-2-thiohydantoin derivative, 3-[(2-hydroxybenzylidene)amino]-2-thioxoimidazolidin-4-one, was synthesized in a two-step condensation reaction of 2-hydroxybenzaldehyde, thiosemicarbazide and ethyl chloroacetate. The ligand was structurally characterized by NMR and IR spectroscopy, as well as by elemental analysis. In the reaction of the well-known polymeric *trans*-$[CuCl_2(DMSO)_2]_n$ complex with the polydentate thiohydantoin type ligand, instead of the corresponding copper thiohydantoin complex, unexpectedly, the dinuclear *cis*-$[\{CuCl(DMSO)_2\}(\mu\text{-}Cl)]_2$ complex (**1**) was formed predominantly as the final stable product. The structure of the complex **1** was confirmed by single crystal X-ray diffraction analysis. The *cis*-complex is obtained through assisted isomerization of the *trans*-form, in which the thiohydantoin derivative has a crucial role.

Keywords: Cu(II) complex; spectroscopic characterization; single crystal X-ray analysis; antimicrobial activity.

INTRODUCTION

Thiohydantoins are important class of heterocyclic compounds. Many of them exhibit diverse biological activities, such as anticonvulsant, antitumor, anti-

* Corresponding authors. E-mail: (*)biljana.smit@uni.kg.ac.rs; (**)mzivkovic@kg.ac.rs
https://doi.org/10.2298/JSC200917060S

viral, antifungal, herbicidal, *etc.*[1] 2-Thiohydantoin units are attractive ligands because they can coordinate to metal ions via nitrogen and/or sulfur donor atoms.[2,3] Moreover, 2-thiohydantoins which posses different endo- and exocyclic electron-donating atoms, could act as effective polydentate ligands towards metal ions. Coordination of these compounds with transition metal ions sometimes enhances their antiviral and antitumor activity.[4]

Dimethyl sulfoxide (DMSO) is widely used as a monodentate ligand in various types of metal complexes.[5,6] Bonding of DMSO with metal ions can occur through the oxygen or through the sulphur atom. Which atom will be the donor atom can be determined through the rule of the "hardness" or "softness" of the metal centre. According to this, hard metal centres preferably bind through oxygen, and soft metal centres bind through sulphur donor atoms. X-ray crystallographic analysis of sulfoxide complexes showed that most of metal ions form O-bounded complexes with DMSO ligands, probably due to the high polarization of the S–O bond. Complexes with S-bound sulfoxides are preferred ones for the metal ions in the 8–10 groups of the periodic table of elements. On the other hand, different oxidation states of the same metal can bind through S or O, as well as S- and O-bound sulfoxides within the same complex.[7]

Applications of these metal complexes with DMSO and other sulfoxides could be described through their catalytic role, biological activity and very often as precursors in reactions of synthesis of some other coordination compounds.[8–10]

DMSO molecules in copper(II) complexes with the general formula $[CuX_2(DMSO)_2]$ (DMSO ligands in *trans* position), as well as in dicationic complex with four DMSO ligands, $[Cu(DMSO)_4](ClO_4)_2$, are coordinated mostly through the oxygen atom.[11–13] Nevertheless, the coordination of DMSO through the sulfur atom, showing quite long Cu–S bound distances, has been reported in some polymeric copper(II) complexes.[14,15] The polymeric *trans*-$[CuCl_2(DMSO)_2]_n$ complex was synthesized and spectroscopically and structurally characterized,[11,16] but the corresponding *cis*-form of the $[CuCl_2(DMSO)_2]$ complex has not been reported for a long time. Recently, formation of the dinuclear copper(II) complex, *cis*-$[\{CuCl(DMSO)_2\}(\mu\text{-}Cl)]_2$, has been reported as a consequence of decomposition of a tetranuclear $[Cu_4Cl_8(DMSO)_8(hmta)]$ complex (hmta is hexamethylenetetramine).[17]

Keeping in mind the coordination potential of 2-thiohydantoins and the significance of copper DMSO complexes, our attempt was to obtain the corresponding copper DMSO thiohydantoin complex. In this study, we report the synthesis and the spectroscopic characterization of 2-thiohydantoin type ligand, 3-[(2-hydroxybenzylidene)amino]-2-thioxoimidazolidin-4-one, and its reaction with *trans*-$[CuCl_2(DMSO)_2]_n$ complex, in which an isomerization occurs instead of coordination.

EXPERIMENTAL

Materials and methods. All chemicals and reagents are commercially available (purchased from either Sigma–Aldrich or Acros) and were used as received without further purification. Solvents were purified by distillation prior use. Anhydrous methanol was prepared by standard drying procedure. The starting complex, *trans*-$[Cu(DMSO)_2Cl_2]_n$, was prepared according to a literature procedure.[16] The purity and identity of the synthesized compounds were checked by elemental analysis and standard spectroscopic methods. IR spectra were recorded as KBr pellets on a Perkin–Elmer FT-IR spectrometer model Spectrum One over the range 4000–450 cm^{-1}. ^1H- and ^{13}C-NMR spectra were recorded on a Varian Gemini 2000 NMR spectrometer (^1H at 200 MHz, ^{13}C at 50 MHz) in DMSO-d_6 as solvent, using TMS as the internal standard. Elemental analysis was performed on an elemental Vario ELIII CHNSO analyzer in the Microanalytical Laboratory, Faculty of Chemistry, University of Belgrade. Diffraction data were collected by using ω-scan mode on an Oxford Diffraction Gemini S diffractometer, equipped with a sealed tube Mo$K\alpha$ X-ray source, and Sapphire CCD detector. Instrument control and data reduction were performed with the CrysAlisPRO.[18] Intensities were correct for the absorption effects by the multi-scan method.[19] The crystal structure was solved with the SHELXT[20] and refined with the SHELXL.[21] All non-hydrogen atoms were refined anisotropically. The methyl group hydrogen atoms were introduced in idealized positions and refined by employing the riding model which allowed refinement of the torsion angle. Their U_{iso} are approximated from U_{eq} of their parent atoms. The ShelXle software[22] was used as a graphical user interface for refinement procedures. The crystal structure model was validated by using Platon[23] and Mercury.[24]

Synthesis and characterization of 3-[(2-hydroxybenzylidene)amino]-2-thioxo-imidazolidin-4-one

The preparation of 3-[(2-hydroxybenzylidene)amino]-2-thioxoimidazolidin-4-one was done according to a previously reported protocol.[7] Salicylaldehyde (0.01 mol) and thiosemicarbazide (0.01 mol) were heated under reflux in 30 ml of methanol for 3 h and then cooled. The solid formed was filtered off, dried, and purified by re-crystallization with methanol, giving the corresponding thiosemicarbazone. A mixture of the thiosemicarbazone (0.01 mol), ethyl chloroacetate (0.01 mol) and anhydrous sodium acetate (0.03 mol) was heated under reflux in 50 ml of methanol for 6 h. The mixture was cooled and poured into cold water. The resulting solid was filtered off, washed with hot water, dried, and purified by re-crystallization with hot methanol. The structure was confirmed by elemental analysis, IR and NMR spectroscopy (Figs. S-1–S-3 of the Supplementary material to this paper).

Synthesis of cis-*[{CuCl(DMSO)$_2$}(μ-Cl)]$_2$ (**1**)*

0.76 mmol of thiohydantoin was dissolved in 10 ml of methanol under reflux. 0.76 mmol of the *trans*-$[CuCl_2(DMSO)_2]_n$ complex in 10 ml of methanol was slowly added dropwise. The mixture was heated under reflux overnight. The mixture was cooled at 0 °C and the solid was removed *in vacuo*. The off-white solid was washed with hot water. The filtrate was evaporated and the remaining solid was dissolved in a mixture of acetonitrile and chloroform (3:5). The solution was left to crystallize and two days later, big, rounded, green crystals were formed. Combustion analysis for $C_8H_{24}O_4S_4Cu_2Cl_4$: Calcd. C, 16.53, H, 4.16, S, 22.06; found C, 16.70, H, 4.35, S, 21.93. Crystallographic and refinement details are listed in Table S-I (Supplementary material).

Antimicrobial activity determination

Antimicrobial activity of the tested compounds was investigated on a panel of human pathogenic bacteria (ESKAPE panel: *Enterococcus faecium* ATCC 6037, *Staphylococcus aureus* ATCC43300, *Klebsiella pneumoniae* ATCC BAA2146, *Acinetobacter baumannii* ATCC 19606, *Pseudomonas aeruginosa* PAO1 and *Enterobacter cloacae* ATCC 13047) and fungi of *Candida* genus (*Candida albicans* SC5314, *Candida glabrata* ATCC 2001, *Candida parapsilosis* ATCC 22019 and *Candida krusei* ATCC 62528), all obtained from the National Collection of Type Cultures (NCTC) and the American Type Culture Collection (ATCC).

The minimum inhibitory concentrations (*MIC*s) against the tested bacteria and fungi were determined in accordance with the standard broth microdilution assay by CLSI (Clinical and Laboratory Standards Institute). Methods for Dilution Antimicrobial Susceptibility Tests for Bacteria That Grow Aerobically; Approved Standard – Tenth Edition M07-A10. CLSI)[25] and EUCAST (European Committee on Antimicrobial Susceptibility Testing, EUCAST antifungal *MIC* method for yeasts, v. 7.3.1),[26] respectively.

Bacteria and fungi were cultured in Luria-Bertani broth (Biolife Italiana s.r.l., Milano, Italy) and in RPMI 1640 medium with 2 % glucose and diluted in the respective media to give inocula with the final concentration of 5×10^5 and 10^5 CFU/ml, respectively. Stock solution of the tested compounds were made in DMSO and applied in a dose range from 1 to 250 μM. After 24-h incubation at 37 °C, the *MIC* values were determined measuring absorbance at 600 nm (OD600), using a Tecan Infinite 200 Pro multiplate reader (Tecan Group Ltd., Männedorf, Switzerland). The negative control (media only) and positive control (only microorganisms in liquid broth) on the same plate were used as references to determine the growth inhibition of bacteria. Samples with inhibition values above 90 % were classified as active agents.

RESULTS AND DISCUSSION

*Synthesis and characterization of 3-[(2-hydroxybenzylidene)amino]-2-thioxoimidazolidin-4-one and complex (**1**)*

As a starting ligand for the reaction with the *trans*-$[CuCl_2(DMSO)_2]_n$ complex, a derivative of 3-arylidene-2-thiohydantoin, 3-[(2-hydroxybenzylidene)-amino]-2-thioxoimidazolidin-4-one, was used. The thiohydantoin type ligand was prepared by the previously published two step procedure (Scheme 1).[4] In the first step 2-hydroxybenaldehyde reacted with thiosemicarbazide. The obtained 2-hydroxybenaldehydethiosemicarbazone in an intramolecular cyclocondenzation reaction with ethyl chloroacetate yielded 3-[(2-hydroxybenzylidene)amino]--2-thioxoimidazolidin-4-one. Identity and purity of the synthesized compound are confirmed by elemental analysis and IR and NMR spectroscopy.

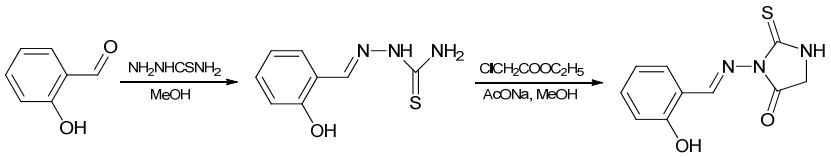

Scheme 1. Synthesis of 3-[(2-hydroxybenzylidene)amino]-2-thioxoimidazolidin-4-one.

As shown in Scheme 1, the synthesized 3-arylidene-2-tiohydantoin derivative has four potential donor atoms in its thiohydantoin nucleus: the oxygen atom of the carbonyl group, the sulphur atom of thiocarbonyl group and the two amide nitrogen atoms, as well as the exocyclic imine nitrogen atom and the oxygen atom of the phenol hydroxyl group. All these different electron-donating atoms make 3-[(2-hydroxybenzylidene)amino]-2-thioxoimidazolidin-4-one an interesting chelating ligand towards metal ions. Some complexes with transition metal ions are already prepared, such as Ag(I),[27] Hg(II),[28] Co(II),[29,30] Ni(II)[29,30] and Cu(II).[29–31]

The mononuclear *trans*-$[CuCl_2(DMSO)_2]_n$ complex was prepared according to the procedure reported by Selbin *et al.*, dissolving anhydrous copper(II) chloride in an ethanol solution of DMSO.[16] Equimolar amounts of the *trans*-$[CuCl_2(DMSO)_2]_n$ complex and 3-[(2-hydroxybenzylidene)amino]-2-thioxoimidazolidin-4-one ligand were mixed in methanol. But, in the reaction of *trans*-$[CuCl_2(DMSO)_2]_n$ complex with the polydentate 3-[(2hydroxybenzylidene)-amino]-2-thioxoimidazolidin-4-one ligand, coordination did not occur at all and the dinuclear copper(II) complex, *cis*-$[\{CuCl(DMSO)_2\}(\mu\text{-}Cl)]_2$ (**1**), was formed predominantly as the final stable product (Scheme 2). The starting thiohydantoin-type ligand is mostly recovered after the reaction.

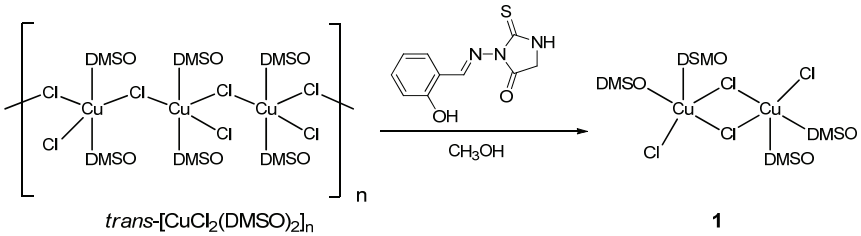

Scheme 2. Synthesis of complex **1.**

*Crystal structure description of **1***

The molecular structure of complex **1** is depicted in Fig. 1, and selected structural parameters are listed in Table I. Structural parameters of **1** are in excellent agreement (*rmsd* of all atoms is 0.0283 Å) with those published by Vakulka and Goreshnik.[17] For the sake of more rigorous comparison, the chemical coordinates of the molecular structures (excluding hydrogen atoms), expressed as independent distances, d_i, and corresponding standard uncertainties, $\sigma(d_i)$, are calculated for both structures. Although the number of non-hydrogen atoms, N, is 24, there are only 30 independent distances ($(3N - 6)/2$), since the point group of the molecule is C_i. Differences Δp_i between pairs of independent distances in the two structures, $d(1)_i$ and $d(2)_i$, are examined in a half-normal probability plot (Fig. 2).[32] The values $\delta m_i = \Delta p_i/\sigma(\Delta p_i)$ are calculated by Eq. (1) for all indepen-

dent distances, arranged as ordered statistics, and plotted *versus* the expected values (α_i) for half-normal probability deviates. The corresponding plot is then analyzed by linear regression:

$$\delta m_i = |d(1)_i - d(2)_i| / [\sigma^2(d(1)_i) - \sigma^2(d(2)_i)]^{1/2} \quad (1)$$

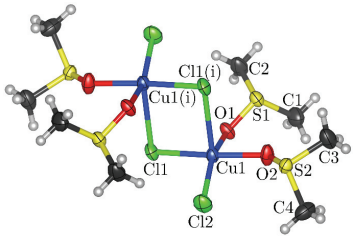

Fig. 1. Molecular structure of complex **1,** with atom labelling scheme. Symmetry code (i) $-x + 1, -y + 1, -z + 1$.

TABLE I. Structural parameters of complex **1**; symmetry code (i) $-x + 1, -y + 1, -z + 1$

Bond	Length, Å	Bonds	Angle, °
Cu1–O1	2.0082(16)	O1–Cu1–O2	83.57(7)
Cu1–O2	1.9662(18)	O1–Cu1–Cl1	88.70(5)
Cu1–Cl1	2.2631(7)	O2–Cu1–Cl2	92.71(5)
Cu1–Cl2	2.2484(7)	Cl1–Cu1–Cl2	94.40(3)
Cu1–Cl1^i	2.7164(8)	O1–Cu1–Cl1^i	91.62(6)
S1–O1	1.5322(17)	O2–Cu1–Cl1^i	91.71(7)
S2–O2	1.5300(18)	Cl1–Cu1–Cl1^i	88.44(2)
S1–C1	1.769(3)	Cl2–Cu1–Cl1^i	112.26(3)
S1–C2	1.767(3)	O1–Cu1–Cl2	155.96(6)
S2–C3	1.777(3)	O2–Cu1–Cl1	172.26(5)
S2–C4	1.765(3)	Cu1–Cl1–Cu1^i	91.56(2)

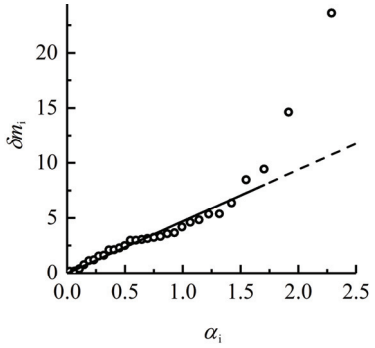

Fig. 2. Half normal probability plot of experimental deviates between two structural determination of complex **1**. The equation of the linear regression line is $\delta m_i = 4.7(2)\alpha_i - 0.01(17)$. Pearson correlation coefficient $R = 0.976$.

Results reveal that, apart from two outliers, the experimental deviates are normally distributed, indicating no significant geometrical differences between structures. The intercept (−0.01(17)), and the slope (4.7(2)) of the linear regression line, calculated after zero-weighting two outlier values, indicate the absence of systematic errors, and underestimation of the standard uncertainties of the

experimental interatomic distances by factor 4.7, respectively. It must be taken into consideration that two structures are determined at significantly different temperatures (295 K for our structure, and 150 K for structure by Vakulka and Goreshnik[17]), which affects the scale of standard uncertainties.

The crystal structure of **1** is composed of centrosymmetric dinuclear molecules, with Cu···Cu separation of 3.5827(7) Å. Cu(II) atoms are five-coordinated, by two DMSO molecules, and three chloride ions. Cu–ligand bond lengths lay in the wide range, from 1.9662(18) to 2.7164(8) Å, due to different nature of ligating atoms and the coordination polyhedron peculiarities. Coordination environment of Cu(II) atom is deformed, and can be best described as square pyramidal, so that basal plane consists of O1, O2, Cl1, Cl2, and the apical position is occupied by $Cl1^i$ (symmetry code (i) $-x + 1, -y + 1, -z + 1$). Three chloride ions constitute bonds with Cu(II) of different lengths. As expected, the shortest is the one incorporating non-bridging basal chloride ion (Cu1-Cl2 = 2.2484(7) Å); intermediate is the one incorporating bridging basal chloride ion (Cu1–Cl1 = = 2.2631(7) Å); the longest one incorporates apical chloride ion (Cl1–Cu1 = = 2.7164(8) Å).

The degree of coordination polyhedron deformation is assessed by several criteria. The simplest, Addison trigonality index,[33] which has value of 0 for a square pyramid with equal *trans*-basal angles (SPY-5), and 1 for a perfect trigonal bipyramid (TBPY-5), amounts 0.27 for complex **1**. More complex analysis by the Holmes method[34] yields slightly different degree of distortion, as percentage along Berry pseudorotation coordinate $C_{4v} \rightarrow C_{2v} \rightarrow D_{3h}$ is 39.7 (the chosen reference SPY-5 has *trans*-basal angles of 150°). Finally, when deformations were analyzed by continuous shape measures, according to which the coordination polyhedron is closer to SPY-5 (CShM = 2.175 if the *trans*-basal angles of the reference shape are 150°, and CShM = 3.005 if the *trans*-basal angles of the reference shape are 174°) then to TBPY-5 (CShM = 3.496). These CShM values point to substantial deformations from the reference shapes, and calculation of Berry pseudorotation coordinate is not reliable, as the distance of polyhedron at hand from minimal distortion path from SPY-5 to TBPY-5 is too severe. To exclude the effect of Cu–ligand bond lengths differences, and make the results comparable to Holmes method, calculation of continuous shape measures was also performed with equalized Cu–ligand bond lengths. The result shows that the polyhedron traversed 43.1 % along minimal distortion path from SPY-5 (with *trans*-basal angles of 174°) to TBPY-5, which is in good agreement with the value obtained by the Holmes method.

Molecular packing in the crystal structure of complex **1** is depicted in Fig. 3. Hirshfeld surface analysis of this complex reveals dominant intermolecular contacts. The H···H contacts are the most abundant (48 %), followed by Cl···H (31 %), and O···H (10 %), which is depicted through fingerprint plots in Fig. 4.

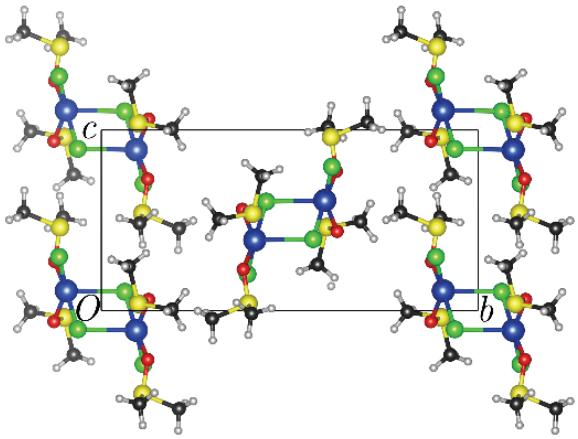

Fig. 3. Molecular packing in the crystal structure of complex **1** viewed along crystallographic *a*-axis.

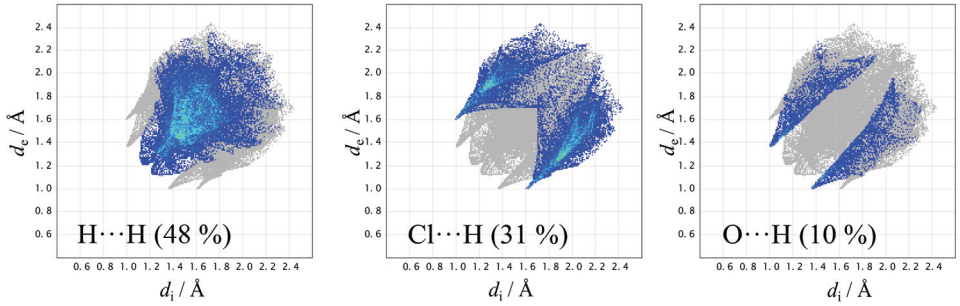

Fig. 4. Fingerprint plots of complex **1**.

The calculation of enrichment ratios, reveals that Cl···H and O···H intermolecular contacts are enriched ($E_{ClH} = 1.33$, $E_{OH} = 1.37$), S···H and H···H are slightly depleted ($E_{SH} = 0.84$, $E_{HH} = 0.91$.), while Cl···S, Cl···Cl, Cl···O, and O···O significantly or totally avoided ($E_{ClS} = 0.52$, $E_{ClCl} = 0$, $E_{ClO} = 0$, $E_{OO} = 0$) in the crystal structure of complex **1**. The Cl···H and O···H intermolecular contacts involve C3 and C4 methyl groups hydrogen atoms, as well as apical $Cl1^{i}$, and O1 atoms. Hirshfeld surface breakdown into element-specific contacts, and corresponding enrichment ratios are summarized in Table II.

Complex isomerization and stability study

Until now, only one procedure for the synthesis of complex **1** was reported, based on a specific preparation *via* decomposition of a tetranuclear $[Cu_4Cl_8(DMSO)_8(hmta)]$ complex. It should be noted that the *cis*-configuration of DMSO molecules in complex **1** was directly transferred from $[Cu_4Cl_8(DMSO)_8(hmta)]$, while the *trans*-$[CuCl_2(DMSO)_2]_n$ isomer was always

formed as the final stable product. The crystals of the template complex left under the parent solution slowly (after about one week) decomposed, while complex **1** appeared consequently. Crystals of **1** were also found to slowly decompose (after 1-2 weeks), resulting in formation of the *trans*-$[CuCl_2(DMSO)_2]_n$ complex only.[47]

TABLE II. Hirshfeld surface breakdown into element-specific contacts, and corresponding enrichment ratios for the crystal structure of complex **1**

Atom	Observed contact, %					
	Cu	Cl	S	O	C	H
Cu	0	0	0	0	0	1.4
Cl	0	0	0.4	0	0	18.0
S	0	0.4	1.5	0	0	3.5
O	0	0	0	0	0	5.3
C	0	0	0	0	0	0
H	1.3	12.5	2.5	4.8	0	48.4
	Enrichment ratio					
	Cu	Cl	S	O	C	H
Cu	–	–	–	–	–	–
Cl	–	0.00	–	–	–	–
S	–	0.52	–	–	–	–
O	–	0.00	–	0.00	–	–
C	–	–	–	–	–	–
H	–	1.33	0.84	1.37	–	0.91

In our reaction, under the given experimental conditions, complex **1** was the final stable product, as it did not decompose to the *trans*-isomer, like it was previously reported. This is supported by the fact that the initial filtrate of the reaction mixture was left to crystallize for 4-5 weeks. As crystals were not formed after the given period, the filtrate was evaporated and the *cis*-isomer was obtained through recrystallization.

The isomerization of *trans*-$[CuCl_2(DMSO)_2]_n$ to its *cis*-form occurred under the influence of the 2-thiohydantoin derivative. To confirm this, a simple control experiment was done. The reaction was repeated under the same experimental conditions, but without the 2-thiohydantoin derivative. Since in this case, the *cis*--isomer was not obtained, it is concluded that 3-[(2-hydroxybenzylidene)amino]--2-thioxoimidazolidin-4-one has a crucial role in the isomerization. Based on the results reported so far, we assume that some sort of unstable intermediate complex was formed, in which the DMSO ligands, due to their size and steric hindrance, occupy *cis*-position in respects to each other. Upon cleavage of the 2-thiohydantoin derivative, DMSO ligands retain the *cis*-configuration during the formation of dinuclear complex.

*Antimicrobial activity of **1***. The results of antimicrobial susceptibility assay showed that none of the tested compounds had antibacterial activity towards the ESKAPE pathogens and the tested *Candida* species, except of a moderate activity against *Candida krusei*. Among them, complex **1** showed better antifungal activity than *trans*-$[CuCl_2(DMSO)_2]_n$ complex on *C. krusei* ATCC 62528, showing the *MIC* value of 125 and 250 μM, respectively. Although *Candida albicans* remains the most common fungal isolate obtained from the blood of the patients with invasive fungal infection, the epidemiological studies conducted in last 20 years have demonstrated a trend toward an increased prevalence of infections with non-albicans *Candida* spp., such as *C. glabrata* and *C. krusei*.[35] Moreover, *C. krusei* was evidenced as the leading cause of candidemia in some hematologic malignancies, especially in the patients with neutropenia caused by chemotherapy.[35] Taken together, these data indicate that the tested complexes may be regarded for further derivatization, aimed to improve their anticandidal activity.

Our further investigation will be directed to the resolving of the mechanism of this reaction and the role of the presence of the starting thiohydantoin type ligand in the isomerization of *trans*-complex to *cis*-form by theoretical methods.

CONCLUSION

A 3-arylidene-2-thiohydantoin derivative, 3-[(2-hydroxybenzylidene)-amino]-2-thioxoimidazolidin-4-one, was synthesized and fully characterized. In the reaction of the thiohydantoin with the polymeric *trans*-$[CuCl_2(DMSO)_2]_n$ complex, instead of the corresponding copper-thiohydantoin complex, the dinuclear *cis*-$[\{CuCl(DMSO)_2\}(\mu\text{-}Cl)]_2$ (**1**) was obtained. The structure of the complex was fully characterized by X-ray crystallography and a deeper insight into the structure and molecular packing was achieved. The complex **1** showed moderate antimicrobial activity against *Candida krusei*. Decomposition of the *cis*-complex to the more stable *trans*-form was not observed and the *cis*-isomer was found to be the final stable product. A clear role of the thiohydantoin derivative in the isomerization of the complex is implied, since no isomerization occurred in the absence of the thiohydantoin.

SUPPLEMENTARY MATERIAL

Additional data are available electronically at the pages of journal website: https://www.shd-pub.org.rs/index.php/JSCS/index, or from the corresponding author on request. Crystallographic data associated with this publication are deposited with the Cambridge Crystallographic Data Centre under the CCDC Number 2023294. They can be obtained free of charge via https://www.ccdc.cam.ac.uk/structures/.

Acknowledgment. This work was supported by the Ministry of Education, Science and Technological Development of the Republic of Serbia (Contract Numbers: 451-03-68/2020-14/200378, 451-03-68/2020-14/200125 and 451-03-68/2020-14/200122).

ИЗВОД

РЕАКЦИЈА ДЕРИВАТА 3-АРИЛИДЕН-2-ТИОХИДАНТОИНА СА ПОЛИМЕРНИМ *trans*-[$CuCl_2(DMSO)_2]_n$ КОМПЛЕКСОМ: НЕОЧЕКИВАНА ИЗОМЕРИЗАЦИЈА У ДИНУКЛЕАРНИ *cis*-[{$CuCl(DMSO)_2$}(μ-Cl)]$_2$

ПЕТАР Б. СТАНИЋ[1], МАРКО В. РОДИЋ[2], ТАЊА В. СОЛДАТОВИЋ[3], АЛЕКСАНДАР Б. ПАВИЋ[4], НАТАША С. РАДАКОВИЋ[4], БИЉАНА М. ШМИТ[5] и МАРИЈА Д. ЖИВКОВИЋ[6]

[1]Универзитет у Крагујевцу, Природно–математички факултет, Институт за хемију, Радоја Домановића 12, 34000 Крагујевац, [2]Универзитет у Новом Саду, Природно–математички факултет, Трг Доситеја Обрадовића 3, 21000 Нови Сад, [3]Државни Универзитет у Новом Пазару, Департман за хемијско–технолошке науке, Вука Караџића бб, 36300 Нови Пазар, [4]Универзитет у Београду, Институт за молекуларну генетику и генетичко инжењерство, Војводе Степе 444а, 11000 Београд, [5]Универзитет у Крагујевцу, Институт за информационе технологије, Сектор за природно–математичке науке, Јована Цвијића бб, 34000 Крагујевац и [6]Универзитет у Крагујевцу, Факултет медицинских наука, Департман за фармацију, Светозара Марковића 69, 34000 Крагујевац

3-Арилиден-2-тиохидантоински дериват, 3-[(2-хидроксибензилиден)амино]-2-тиоксоимидазолидин-4-он, је синтетисан у двостепеној кондензационој реакцији 2-хидроксибензалдехида, тиосемикарбазида и етил-хлорацетата. Лиганд је структурно окарактерисан NMR и IR спектроскопијом, као и елементалном анализом. У реакцији добро познатог полимерног *trans*-[$CuCl_2(DMSO)_2]_n$ комплекса са овим полидентатним лигандом тиохидантоинског типа, уместо одговарајућег тиохидантоинског комплекса бакра(II), неочекивано је настао динуклеарни *cis*-[{$CuCl(DMSO)_2$}(μ-Cl)]$_2$ комплекс (**1**) као главни, коначни, стабилни производ. Молекулска структура комплекса **1** је одређена рендгенском структурном анализом. *cis*-Комплекс је добијен потпомогнутом изомеризацијом *trans*-облика, у којој тиохидантоински дериват има пресудну улогу.

(Примљено 17. септембра, прихваћено 20. септембра 2020)

REFERENCES

1. L. Konnert, F. Lamaty, J. Martinez, E. Colacino, *Chem. Rev.* **117** (2017) 13757 (https://doi.org/10.1021/acs.chemrev.7b00067)
2. M. M. Chowdhry, A. Burrows, D. M. Mingos, A. J. White, D. J. Williams, *J. Chem. Soc. Chem. Commun.* (1995) 1521 (https://doi.org/10.1039/C39950001521)
3. M. Arca, F. Demartin, F. Davillanova, A. Garau, F. Isaia, V. Lippolis, G. Verani, *Inorg. Chem.* **37** (1998) 4164 (https://doi.org/10.1021/ic9803681)
4. B. Šmit, R. Z. Pavlović, A. Radosavljević-Mihailović, A. Došen, M. G. Ćurčić, D. S. Šeklić, M. N. Živanović, *J. Serb. Chem. Soc*. **78** (2013) 217 (https://doi.org/10.2298/JSC120725154S)
5. M. Calligaris, O. Carugo, *Coord. Chem. Rev*. **153** (1996) 83 (https://doi.org/10.1016/0010-8545(95)01193-5)
6. G. Sipos, E. E. Drinkel, R. Dorta, *Chem. Soc. Rev.* **44** (2015) 3834 (https://doi.org/10.1039/C4CS00524D)
7. A. R. Davies, F. W. B. Einstein, N. P. Farrell, B. R. James, R. S. McMillan, *Inorg. Chem.* **17** (1978) 1965 (https://doi.org/10.1021/ic50185a054)
8. M. Brindell, E. Kuliś, S. K. C. Elmroth, K. Urbańska, G. Stochel. *J. Med. Chem*. **48** (2005) 7298 (https://doi.org/10.1021/jm0502992)
9. Y. M. Y. Haddad, H. B. Henbest, J. Husbands, T. R. B. Mitchell, J. Trocha-Grimshaw, *J. Chem. Soc., Perkin Trans. 1* (1974) 596 (https://doi.org/10.1039/P19740000596)
10. J. M. O'Connor, K. D. Bunker, A. L. Rheingold, L. Zakharov, *J. Am. Chem. Soc*. **127** (2005) 4180 (https://doi.org/10.1021/ja050160g)

11. R. D. Willett, K. Chang, *Inorg. Chim. Acta* **4** (1970) 447 (https://doi.org/10.1016/S0020-1693(00)93324-3)
12. R. D. Willett, F. H. Jardine, S. A. Roberts, *Inorg. Chim. Acta* **25** (1977) 97 (https://doi.org/10.1016/S0020-1693(00)95696-2)
13. A. J. Blake, R. S. Grimditch, S. Parsons, M. Schröder, *Acta Crystallogr., C* **52** (1996) 514 (https://doi.org/10.1107/S0108270195013795)
14. P. Chandrasekaran, J. T. Mague, M. S. Balakrishna, *Inorg. Chem*. **45** (2006) 6678 (https://doi.org/10.1021/ic060464j)
15. S. Mishra, E. Jeanneau, G. Ledoux, S. Daniele, *Inorg. Chem*. **53** (2014) 11721 (https://doi.org/10.1021/ic501963y)
16. J. Selbin, W. E. Bull, L. H. Holmes Jr. *J. Inorg. Nucl. Chem*. **16** (1961) 219 (https://doi.org/10.1016/0022-1902(61)80493-4)
17. A. Vakulka, E. Goreshnik, *J. Coord. Chem*. **70** (2017) 556 (https://doi.org/10.1080/00958972.2016.1261288)
18. Rigaku Oxford Diffraction, *CrysAlis*^{Pro} *Software system*, Rigaku Corporation, Wroclaw, Poland, 2019
19. R. H. Blessing, *Acta Crystallogr., A* **51** (1995) 33 (https://doi.org/10.1107/S0108767394005726)
20. G. M. Sheldrick, *Acta Crystallogr., A* **71** (2015) 3 (https://doi.org/10.1107/S2053273314026370)
21. G. M. Sheldrick, *Acta Crystallogr., C* **71** (2015) 3 (https://doi.org/10.1107/S2053229614024218)
22. C. B. Hübschle, G. M. Sheldrick, B. Dittrich, *J. Appl. Crystallogr.* **44** (2011) 1281 (https://doi.org/10.1107/S0021889811043202)
23. A. L. Spek, *Acta Crystallogr., D* **65** (2009) 148 (https://doi.org/10.1107/S090744490804362X)
24. C. F. Macrae, I. Sovago, S. J. Cottrell, P. T. A. Galek, P. McCabe, E. Pidcock, M. Platings, G. P. Shields, J. S. Stevens, M. Towler, P. A. Wood, *J. Appl. Crystallogr*. **53** (2020) 226 (https://doi.org/10.1107/S1600576719014092)
25. *CLSI.2008. Reference Method for Broth Dilution Antifungal Susceptibility Testing of Yeasts* - 3rd ed., CLSI document M27-A3, Clinical and Laboratory Standards Institute, Wayne, PA
26. *CLSI.2012. Methods for Dilution Antimicrobial Susceptibility Tests for Bacteria That Grow Aerobically*; Approved Standard - 9th ed., M07-A9, Clinical and Laboratory Standards Institute, Wayne, PA
27. A. A. Fedorchuk, Yu. I. Slyvka, V. Kinzhybalo, T. Lis, M. G. Mys'kiv, *Inorg. Chim. Acta* **484** (2019) 79 (https://doi.org/10.1016/j.ica.2018.09.029)
28. J. S. Casas, N. Playa, A. Sanchez, J. Sordo, J. M. Varela, E. M. Vazquez-Lopez, *Polyhedron* **18** (1998) 187 (https://doi.org/10.1016/S0277-5387(98)00283-6)
29. S. K. Kandil, G. B. El-Hefnawy, E. A. Baker, *Thermochim. Acta* **414** (2004) 105 (https://doi.org/10.1016/S0277-5387(98)00283-6)
30. F. A. Nour El Dien, M. A. Abdelaziz, M. A. Zayed, *Thermochim. Acta* **162** (1990) 399 (https://doi.org/10.1016/0040-6031(90)80360-B)
31. K. Tishchenko, E. K. Beloglazkina, M. Proskurnin, V. Malinnikov, D. Guk, M. Muratova, O. Krasnovskaya, A. Udina, D. Skvortsov, R. R. Shafikov, Y. Ivanenkov, V. Aladinskiy, I. Sorokin, O. Gromov, A. G. Majouga, N. V. Zyk, *J. Inorg. Biochem*. **175** (2017) 190 (https://doi.org/10.1016/j.jinorgbio.2017.07.015)

32. S. C. Abrahams, E. T. Keve, *Acta Crystallogr., A* **27** (1971) 157 (https://dx.doi.org/10.1107/S0567739471000305)
33. A. W. Addison, T. N. Rao, J. Reedijk, J. van Rijn, G. C. Verschoor, *J. Chem. Soc., Dalt. Trans.* (1984) 1349 (https://dx.doi.org/10.1039/DT9840001349)
34. R. R. Holmes, in *Progress in Inorganic Chememistry Vol. 32*, S. J. Lippard (Ed.), John Wiley & Sons, Ltd., New York, 1984, pp. 119–235 (https://dx.doi.org/10.1002/9780470166338.ch2)
35. R. Hachem, H. Hanna, D. Kontoyiannis, Y. Jiang, I. Raad, *Cancer* **112** (2008) 2493 (https://doi.org/10.1002/cncr.23466).

Journal of the Serbian Chemical Society
JSCS-info@shd.org.rs • www.shd.org.rs/JSCS
J. Serb. Chem. Soc. 85 (12) S568–S571 (2020) *Supplementary material*

SUPPLEMENTARY MATERIAL TO

Reaction of a 3-aryilidene-2-thiohydantoin derivative with polymeric *trans*-$[CuCl_2(DMSO)_2]_n$ complex: unexpected isomerization to dinuclear *cis*-$[\{CuCl(DMSO)_2\}(\mu\text{-}Cl)]_2$

PETAR B. STANIĆ[1], MARKO V. RODIĆ[2], TANJA V. SOLDATOVIĆ[3], ALEKSANDAR B. PAVIĆ[4], NATAŠA S. RADAKOVIĆ[4], BILJANA M. ŠMIT[5]* and MARIJA D. ŽIVKOVIĆ[6]**

[1]University of Kragujevac, Faculty of Science, Department of Chemistry, Radoja Domanovića 12, 34000 Kragujevac, Serbia, [2]University of Novi Sad, Faculty of Sciences, Trg Dositeja Obradovića 3, 21000 Novi Sad, Serbia, [3]State University of Novi Pazar, Department of Chemical–Technological Sciences, Vuka Karadžića bb, 36300 Novi Pazar, Serbia, [4]University of Belgrade, Institute of Molecular Genetics and Genetic Engineering, Vojvode Stepe 444a, 11000 Belgrade, Serbia, [5]University of Kragujevac, Institute for Information Technologies, Department of Science, Jovana Cvijića bb, 34000 Kragujevac, Serbia and [6]University of Kragujevac, Faculty of Medical Sciences, Department of Pharmacy, Svetozara Markovića 69, 34000 Kragujevac, Serbia

J. Serb. Chem. Soc. 85 (12) (2020) 1591–1603

TABLE S-I. Crystallographic and refinement details of *cis*-$[(DMSO)_2ClCu(\mu\text{-}Cl)_2CuCl(DMSO)_2]$

Crystal data	
Chemical formula	$C_4H_{12}Cl_2CuO_2S_2$
M_r	290.70
Crystal system	Monoclinic
Space group	$P2_1/c$
Temperature, K	295
a / Å	8.1773 (3)
b / Å	16.6064 (8)
c / Å	8.4323 (3)
β / °	109.356 (4)
V / Å^3	1080.35 (8)
Z	4
Radiation type	Mo $K\alpha$
μ / mm^{-1})	2.86
Crystal size, mm	0.58 × 0.47 × 0.38
Data collection	
Diffractometer	Gemini S (Oxford Diffraction)
Absorption correction	Multi-scan

* Corresponding authors. E-mail: (*)biljana.smit@uni.kg.ac.rs; (**)mzivkovic@kg.ac.rs

Crystal data	
T_{min}, T_{max}	0.822, 1.000
No. of measured reflections	6720
No. of independent reflections	2209
No. of observed [$I > 2\sigma(I)$] reflections	2000
R_{int}	0.018
$(\sin \theta/\lambda)_{max}$ / Å^{-1}	0.626

Refinement	
$R[F^2 > 2\sigma(F^2)]$	0.027
$wR(F^2)$	0.058
S	1.17
No. of reflections	2209
No. of parameters	104
H-atom treatment	Constrained
$\Delta\rho_{max}$, $\Delta\rho_{min}$ / e Å^{-3}	0.25, −0.40

3-[(2-hydroxybenzylidene)amino]-2-thioxo-imidazolidin-4-one. Yield: 2.103 g (89 %). IR (KBr): 3441*m*, 3318*m*, 3031*w*, 2958*m*, 2776*m*, 1718*s*, 1640*s*, 1623*s*, 1568*w*, 1492*w*, 1469*w*, 1334*m*, 1317*m*, 1266*m*, 1254*m*, 1204*m*, 1149*w*, 890*w*, 838*w*, 757*m*, 735*m*, 710*m*, 637*w*, cm^{-1}. ^{1}H-NMR (200 MHz, DMSO-d_6, δ / ppm): 12.10 (*bs*, NH, exchangeable with D_2O), 10.88 (*s*, OH, exchangeable with D_2O), 8.64 (*s*, 1H, H-7), 7.58 (*dd*, 1H, J = 8.0 and 1.9 Hz, H-6), 7.32 (*dt*, 1H, J = 7.8 and 1.8 Hz, H-1), 6.95 (*m*, 2H, H-4, H-5), 3.97 (*s*, 2H, CH_2-8). ^{13}C-NMR (50 MHz, DMSO-d_6, δ / ppm): 173.77, 164.44, 158.01, 157.76, 132.17, 130.62, 119.54, 118.50, 116.38, 33.46. Combustion analysis for $C_{10}H_9N_3O_2S$: Cald. C 51.05, H 3.86, N 17.86; found C 51.10, H 3.89, N 17.88.

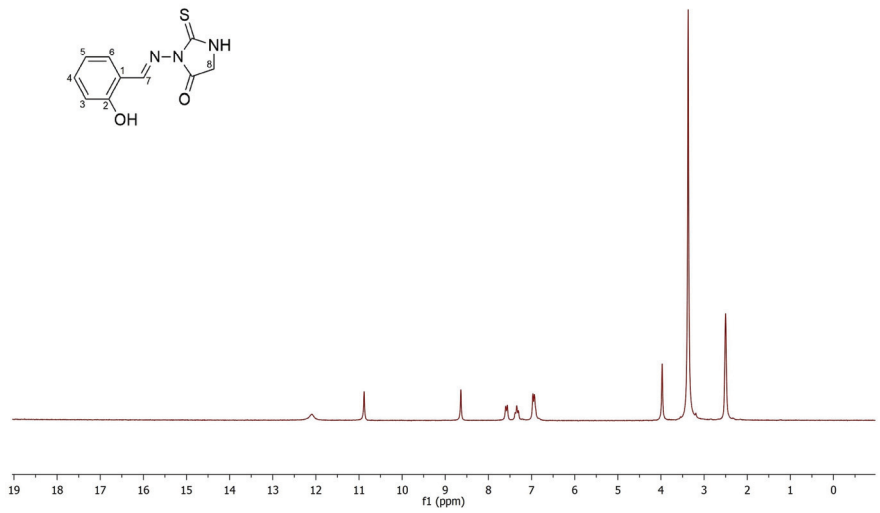

Fig. S-1. ^{1}H-NMR spectra of 3-[(2-hydroxybenzylidene)amino]-2-thioxoimidazolidin-4-one.

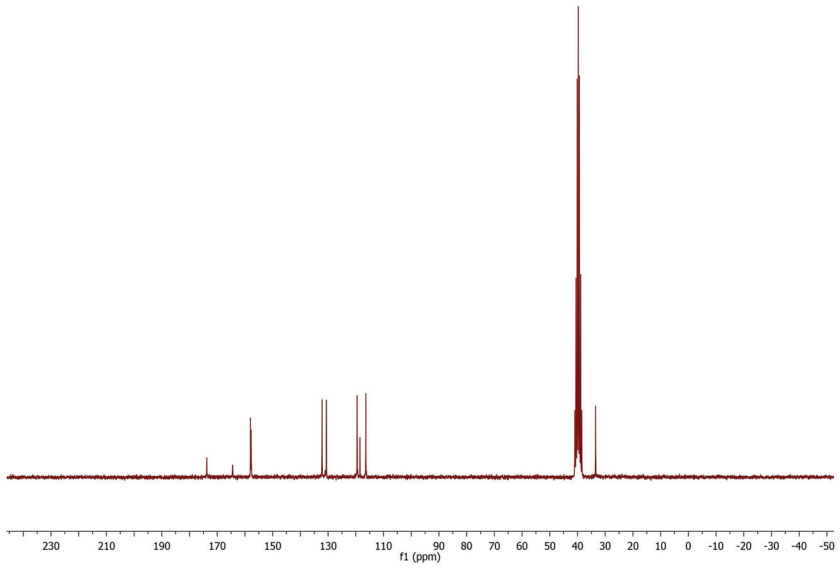

Fig. S-2. ^{13}C-NMR spectra of 3-[(2-hydroxybenzylidene)amino]-2-thioxoimidazolidin-4-one.

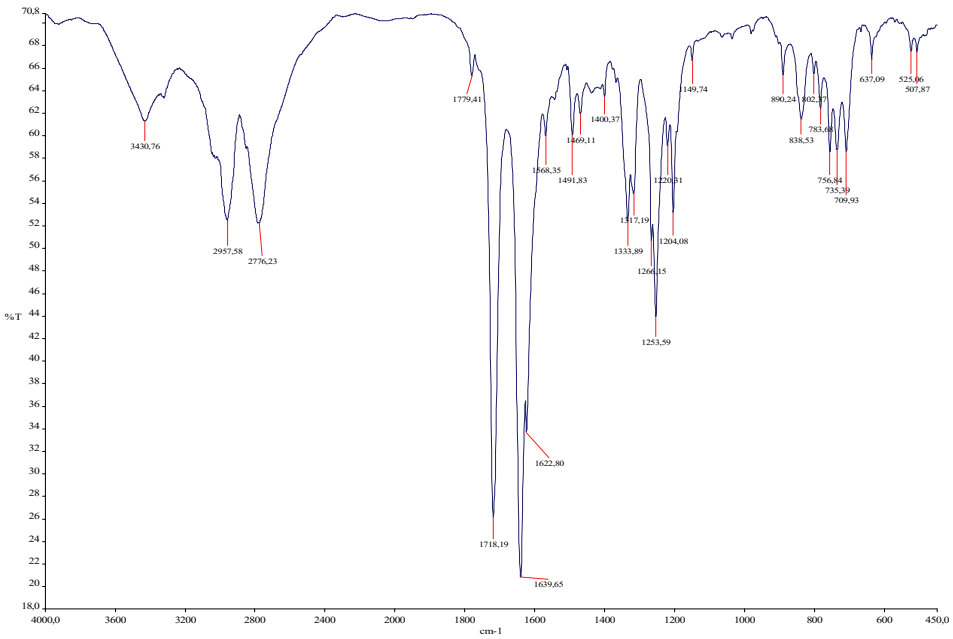

Fig. S-3. IR spectra of 3-[(2-hydroxybenzylidene)amino]-2-thioxoimidazolidin-4-one.

Journal of the Serbian Chemical Society
JSCS-info@shd.org.rs • www.shd.org.rs/JSCS
J. Serb. Chem. Soc. 85 (12) 1605–1619 (2020) UDC 624:666.946–913:564.3:535–34:537.872
JSCS–5396 *Original scientific paper*

Improvement and modification of the energy-dispersive X-ray fluorescence method for the determination of metal elements in cement leachates – A chemometric approach

NEVENKA N. MIJATOVIĆ[1]*, ANJA M. TERZIĆ[1], LATO L. PEZO[2], LJILJANA R. MILIČIĆ[1] and DRAGANA Z. ŽIVOJINOVIĆ[3]

[1]*Institute for Testing of Materials IMS, Vojvode Mišića Bul. 43, 11000 Belgrade, Serbia,* [2]*Institute of General and Physical Chemistry, University of Belgrade, Studentski trg 12–16, 11000 Belgrade, Serbia and* [3]*Faculty of Technology and Metallurgy, University of Belgrade, Karnegijeva 4, 11000 Belgrade, Serbia*

(Received 1 May, revised 24 August, accepted 27 October 2020)

Abstract: A modification of an analytical procedure for the energy-dispersive X-ray fluorescence (EDXRF) quantification of ten chemical elements (As, Ba, Cd, Co, Cr, Cu, Mo, Ni, Pb and Zn) in the leachates obtained from cement binders was developed. Twenty-nine testing samples were used in the experiment. All samples were based on Portland cement. Fly ash of different origin, zeolite and bentonite were employed as mineral additives in the cement binders. Distilled water was used as the leachate. Validation of the modified EDXRF procedure was conducted in terms of limits of detection and quantification, working range, linearity, selectivity, precision, trueness, and robustness. Traceability of the procedure was established using certified reference materials. Uncertainty of measurement was confirmed *via* an "in-house" laboratory validation approach. The expanded uncertainties for the ten analysed elements were obtained for the entire working range of the EDXRF method. Robustness of the modified EDXRF procedure was assessed by means of a chemometric in-house approach. The results obtained by the modified X-ray fluorescence method were additionally correlated to those acquired by inductively coupled plasma optical emission spectrometry to confirm that EDXRF could be used as an effective and reliable alternative method for analysis of cement leachates.

Keywords: in-house validation; mineral additives; cluster analysis; ICP-OES; EDXRF, building materials.

INTRODUCTION

Waste depots on which fly ash is being disposed are constantly producing significant amounts of waste water as a result of precipitation or contact with external water resources.[1] Fly ash leachates are characterized by high concentrations

* Corresponding author. E-mail: nevenka.mijatovic@institutims.rs
https://doi.org/10.2298/JSC200501067M

of toxic elements and high salinity.[2] The employment of fly ash as a componential material in the construction industry is a successful means for the removal of potential pollutants from the natural environment.[3–5] Addition of sorbent clays, such as zeolite and bentonite, in the mix-design of a construction material enables the immobilization of the toxic elements.[4]

Identification and quantification of the chemical elements contained in leachates can be acquired by various instrumental techniques: atomic absorption spectrometry (AAS),[6] optical emission inductively coupled plasma spectrometry (ICP-OES),[7] inductively coupled plasma-mass spectrometry (ICP-MS)[8] and X-ray fluorescence spectrometry (XRF).[9] The energy dispersive X-ray fluorescence (EDXRF) method is extensively being used in environmental protection[10] and construction materials studies.[11–13] However, the application of EDXRF for simultaneous multi elemental analysis of liquid samples and leachates is sparsely investigated. For instance, S. Zhoua *et al.*[14] successfully identified heavy metals in polluted water using a portable XRF. The authors indicated that at least two factors limit the application of this instrument for *in-situ* analysis of water samples, *i.e.*, high detection limits and water damage to the instrument. Marguí *et al.*[15] proved that XRF instrument can be used for precise quantitative chemical analysis of leachates obtained from waste material rich in heavy metals. Pearsona *et al.*[16] obtained highly comparable results from XRF analyses conducted on solid and liquid samples, thus proving the reliability of this non-destructive method.

The preparation of the XRF testing samples is rapid since a digestion procedure is not required, which makes XRF analysis low-cost and free of harmful chemicals.[17] However, water-based samples (leachate, waste water, *etc.*) require a specific optimization procedure for their preparation and analysis.[18] There is no standard method for EDXRF analysis of cement leachates. In addition, a fully validated EDXRF analytical methodology has not yet been established for the determination of toxic elements in leachates or wastewater. Therefore, the validation of multi elemental EDXRF analysis (As, Ba, Cd, Co, Cr, Cu, Mo, Ni, Pb and Zn) of cement leachates was conducted in this study. Cement-based binders with mineral additives (fly ash, zeolite and bentonite) were used in the experiments. Validation included the statistical evaluation of data from the linear calibration range for each analysed element, as well as the limits of detection and quantification. Precision and trueness were evaluated at different concentration levels. Robustness was evaluated by application of multivariate statistics. The amount of sample used for the preparation for plastic container and the different thickness of polyester film were employed as the main process parameters for the determination of the robustness of the EDXRF technique for liquid samples. Traceability and measurement uncertainty were determined by an "in-house" validation approach. The results obtained by modified X-ray fluorescence

method were additionally correlated to those acquired by inductively coupled plasma optical emission spectrometry.

EXPERIMENTAL

Preparation and characterization of the cement binders

The chemical composition of the componential materials (Portland cement CEM I 42.5R, Zeolite "Vranjska banja", Bentonite "Šipovo", Fly ash "Kolubara", fly ash "Kostolac", fly ash "TENT A" and fly ash "TENT B") used for preparation of the cement binders is given in Table I. Chemical analyses were performed by EDXRF method.[19]

TABLE I. Chemical composition of the raw materials used in the mix-design of the cement binders; *LoI* – loss of ignition

Parameter	Cement	Zeolite	Bentonite	Kolubara fly ash	Kostolac fly ash	TENT A fly ash	TENT B fly ash
c_{SiO_2} / %	20.6±1.4	63.7±1.8	48.1±1.7	58.3±1.6	55.3±1.7	57.5±1.7	59.7±1.6
$c_{Al_2O_3}$ / %	5.6±0.7	13.4±0.6	11.6±0.7	18.9±0.5	17.4±0.5	17.7±0.5	21.0±0.5
$c_{Fe_2O_3}$ / %	2.6±0.4	1.4±0.3	3.1±0.4	6.8±0.5	10.3±0.4	10.5±0.4	6.0±0.5
c_{K_2O} / %	0.8±0.1	1.6±0.3	0.7±0.1	1.2±0.2	0.6±0.1	0.6±0.1	5.8±0.1
c_{Na_2O} / %	0.20±0.02	1.2±0.1	2.9±0.2	0.5±0.03	0.4±0.03	0.40±0.03	0.40±0.03
c_{CaO} / %	61.6±1.3	3.5±0.8	3.5±0.8	8.7±0.9	7.9±0.9	7.0±0.8	5.8±0.7
c_{MgO} / %	2.4±0.4	1.2±0.3	2.4±0.4	2.3±0.4	2.3±0.4	2.0±0.4	2.2±0.4
c_{SO_3} / %	3.6±0.9	0.3±0.02	1.1±0.2	1.3±0.2	0.9±0.05	1.1±0.2	0.50±0.02
$c_{P_2O_5}$ / mg kg^{-1}	1000±190	500±80	800±100	300±50	300±50	200±40	200±40
c_{As} / mg kg^{-1}	<0.03	<0.03	<0.03	182±50	10±2	11±2	17±3
c_{Ba} / mg kg^{-1}	<0.03	<0.03	<0.03	86±20	49±10	52±10	62±10
c_{Cd} / mg kg^{-1}	<0.03	<0.03	<0.03	0.20±0.01	0.20±0.01	0.10±0.01	0.20±0.01
c_{Co} / mg kg^{-1}	<0.01	<0.01	<0.01	15±3	5±1	8±1	7±1
c_{Cr} / mg kg^{-1}	<0.01	<0.01	<0.01	135±40	105±25	98±25	170±50
c_{Cu} / mg kg^{-1}	<0.01	<0.01	<0.01	36±4	54±5	53±5	30±4
c_{Mo} / mg kg^{-1}	<0.05	<0.05	<0.05	10±1	5±0.5	5±0.5	3±0.3
c_{Ni} / mg kg^{-1}	<0.01	<0.01	<0.01	51±5	24±2	22±2	32±3
c_{Pb} / mg kg^{-1}	<0.01	<0.01	<0.01	25±4	14±3	16±3	18±3
c_{Zn} / mg kg^{-1}	46±4	<0.01	<0.01	57±5	50±5	53±5	27±3
LoI / %	1.4±0.3	13.7±0.7	19.6±0.8	1.8±0.3	4.5±0.7	2.9±0.4	2.9±0.4

Twenty-nine samples of cement binders based on Portland cement were prepared for the experiment. Mineral additives (fly ash, zeolite and bentonite) were employed in the mix-design in different ratios. The mix-design of the cement binders is provided in Fig. 1. The experimental mixtures were prepared according to the standard procedure provided in SRPS EN 196-1:2017: Methods of testing cement – Part 1: Determination of strength. After 28 days of solidification, the samples were crushed and subsequently ground in a laboratory mill.

Leaching test

The leaching test was conducted according to SRPS EN 12457-4:2008.[20] The leachability of heavy metals for each sample was investigated on the mixtures of the testing samples and deionised water using a 1:10 liquid to solid ratio. The mixtures were prepared in a laboratory mixer manufactured by the Institute IMS, Centre for Laboratory equipment (volume 15 L and a mixing speed 10 rpm) at room temperature (20±2 °C) during 24 h,

according to the above-mentioned EN standard.[20] Afterwards, the leachate was filtered over a membrane filter (0.45 μm). The concentrations of metal elements in the leachates obtained from 29 samples were determined using EDXRF and ICP-OES analyses.

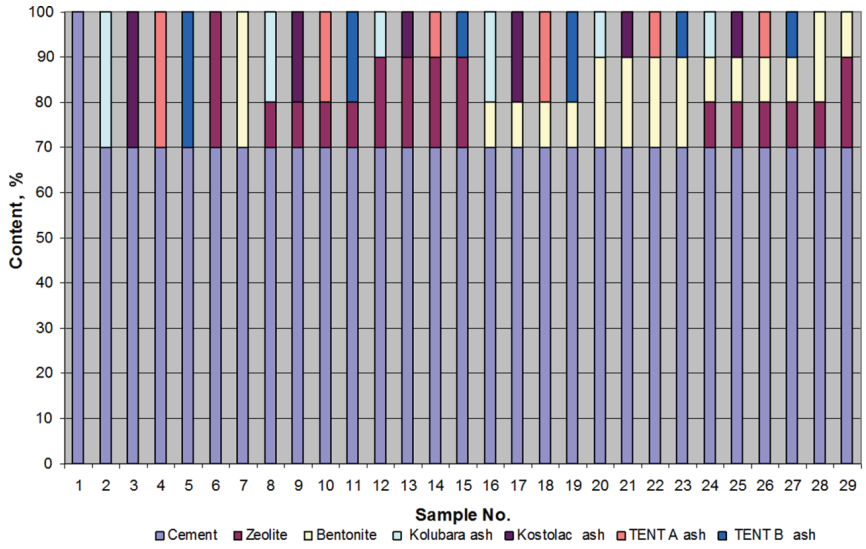

Fig 1. The mix-design of the cement binders.

Instrumentation and measurement conditions

The EDXRF analysis was performed using a Spectro Xepos system equipped with a 50 W and 60 V X-ray tube with a binary Co/Pd alloy thick target anode. The excitation mode of the X-ray tube was combined polarized/direct excitation. The characteristic radiation emitted by the elements present in the sample was detected by a silicon drift detector with Peltier cooler system. Spectro XRF Analyzer Pro, Xepos C Software was used. Liquid samples analysis was conducted in a helium atmosphere.

The multi element standard solution was diluted at different concentrations to obtain calibration standards. Stock solutions were prepared by a single dilution or series of dilutions in order to acquire a working concentration set in the range from 0.10 to 100.00 mg dm^{-3} for each element for the EDXRF technique. Liquid samples were packed in plastic containers. The diameter of the plastic container was 32 mm (24 mm inner diameter) with enough volume to cover the surface of the plastic container and give a depth of 10 mm (5 g for distilled water). The upper orifice of the container was covered with the polyester film (4.0 μm thickness) and with the help of two rings of the same material a taut wrinke free sample support window was created.

An ICP-OES (Spectro Genesis, Germany) analyser equipped with a plasma generator (27.12 MHz; 1.700 KW power) was used. The argon consumption was 16 L min^{-1}. The holographic grating had 2400 point mm^{-1}. The plasma with a wavelength range of 175–775 nm was positioned radially. High purity argon (99.9999 %) was used for the plasma initiation, as a carrier gas, and for cooling of the quartz system. Smart Analyzer Vision software was used.

Commercially available 1000 mg L^{-1} multi element standard solution in nitric acid (ICP multi element standard solution IV in 10 % nitric acid, Merck) containing Ag, Al, B, Ba, Bi,

Ca, Cd, Co, Cr, Cu, Fe, Ga, In, K, Li, Mg, Mn, Ni, Pb, Sr, Tl and Zn was used for the calibration of the ICP analysis. The calibration was performed for ten elements (As, Ba, Cd, Co, Cr, Cu, Mo, Ni, Pb and Zn). The wastewater sample for the proficiency test (test code 586) and reference material (test code 500) were provided by ERA. Ultra-pure deionized water, 0.5 μS cm^{-1}, obtained from a deionizer (Heming, Serbia) was used for dilution. Additional preparations of calibration standards, reference materials, and cement leachates were not necessary for the ICP-OES analysis.

Chemometric analysis

The applied experimental design corresponded to a 5×3 Latin square design with two factors (sample amount and different thickness of polyester film). All determinations were made in three repetitions and all data were averaged, expressed as mean ± standard deviation (*SD*). Analysis of variance (ANOVA) was used to analyse the variations of the element contents in cement leachates. Pattern recognition techniques (cluster analysis – CA) was applied to the experimental data (used as descriptors) to characterize and differentiate among the observed samples. The data were processed statistically using the software package Statistica 12 (StatSoft Inc., Tulsa, OK, USA, 2012).

RESULTS AND DISCUSSION

A full validation of the modified EDXRF method for liquid samples included the characterization of calibration curves, linearity, selectivity, limit of detection (*LOD*), limit of quantification (*LOQ*), precision (repeatability and reproducibility), trueness and robustness. Traceability and uncertainty of the method were also determined. Limits of detection were determined as:

$$LOD = 3.3\frac{\sigma}{S} \tag{1}$$

Limits of quantification were determined as:

$$LOQ = 10\frac{\sigma}{S} \tag{2}$$

where: σ – standard deviation of blank; S – slope of regression line.

The equations for *LOD* and *LOQ* were used according to the International Union of Pure and Applied Chemistry (IUPAC) Procedures.[21] The *LOD*s and *LOQ*s for the modified XRF method were determined for each metal element present in the cement leachates, *i.e.*, As, Ba, Cd, Co, Cr, Cu, Mo, Ni, Pb and Zn. In order to experimentally confirm the *LOQ*, six standard solutions with concentrations close to the *LOQ* were prepared and analysed. The calibration parameters were determined using Merck multi-element standard stock solutions in the concentration range from 0.10 to 100.00 mg dm^{-3}. The concentration reference value in CRM for all elements was 100 mg dm^{-3}. The calibration curves for all chemical elements were constructed using seven nominal points (working standards 0.10, 1.00, 5.00, 10.00, 20.00, 50.00 and 100.00 mg dm^{-3}) with addition of a nominal blank. Calculations for mean concentration values for the calibration curve points were obtained as replicates of two series of triplicate measurements.

Calibration parameters for all analytes were employed in ANOVA (MS Excel) analysis for producing the calibration and residual. The emission wavelengths, *Y*-intercepts, slopes, coefficients of determination, *LOD* and *LOQ*, working range and selectivity of calibration curve for metal elements are given in Table II.

TABLE II. Parameters of calibration curves of 10 chemical elements found in cement leachates

Element	Emission lines series / *E* / keV	*Y*-intercept, mg dm^{-3}	Slope	R^2	*LOD* mg dm^{-3}	*LOQ* mg dm^{-3}	Working range mg dm^{-3}	Ratio c_{Cal}/c_{CRM}
As	K-α / 10.542	0.048	0.999	0.999	0.028	0.092	0.092–110	1.07
Ba	K-α / 32.188	0.045	0.999	0.999	0.024	0.079	0.079–103	1.08
Cd	K-α / 23.170	0.054	0.998	0.999	0.044	0.102	0.102–108	1.01
Co	K-α / 6.929	0.064	1.001	0.999	0.068	0.224	0.224–105	1.05
Cr	K-α / 5.414	0.048	0.999	1.000	0.024	0.079	0.079–115	1.28
Cu	K-α / 8.046	0.080	0.999	0.999	0.087	0.287	0.287–110	1.03
Mo	K-α / 17.476	0.046	1.000	0.999	0.031	0.102	0.102–105	1.07
Ni	K-α / 7.477	0.076	0.999	0.999	0.084	0.277	0.277–105	1.08
Pb	L-α / 10.550	0.039	0.999	0.999	0.022	0.073	0.073–108	0.98
Zn	K-α / 8.637	0.065	1.000	0.999	0.068	0.224	0.224–110	0.96

The selectivity (c_{Cal}/c_{CRM}) was determined as the ratio of the obtained concentration of the observed element (in mg kg^{-1}) and its concentration in the certified reference material (CRM). If this ratio is close to 1.00, the selectivity for elements identified and quantified by developed the EDXRF method indicates that it can successfully assess the analyte in the presence of components that are expected to occur in the solution (Matrix effect).

Emission lines K-α type were used for all investigated elements. Only for lead, was the L-α emission line used. The calculated *Y*-intercepts for ten elements spanned from 0.039 mg dm^{-3} for lead to 0.080 mg dm^{-3} for copper. The steepest slope was obtained for cadmium (0.998), while cobalt (1.001) had the most even slope of the calibration curve. The obtained linearity was good for all investigated elements. Coefficients of determination (R^2) were in satisfactory interval from 0.999 (As, Ba, Cd, Co, Cu, Mo, Ni, Pb and Zn) to 1.000 (Cr). The values obtained for *LOD* varied between 0.022 (Pb) and 0.087 mg dm^{-3} (Cu), while the *LOQ* was between 0.073 (Pb) and 0.287 mg dm^{-3} (Cu). The calculated values of *LOD* and *LOQ* are in conformity with the waste acceptance criteria for leachates obtained from inorganic wastes.[22] The highest concentration limits obtained for the working ranges for the investigated elements were from 103 (Ba) to 115 mg dm^{-3} (Cr). The highest obtained selectivity value was for chromium (1.28). Zinc showed the lowest selectivity value (0.96). The high values of selectivity indicated that the matrix of the calibration standard corresponded adequately to the matrix of the tested cement leachates.

Traceability was determined using the results of the analyses of certified reference materials (CRM).[23] The precision was evaluated using the conditions that are normally employed for the determination of repeatability and reproducibility. Namely, the precision (which is expressed as repeatability and reproducibility) and trueness of the developed EDXRF method were evaluated through analysis of the certified reference materials for wastewater (ERA 500 and ERA 586). In addition, recovery tests for four levels of concentration (standard solutions of 0.05, 2.5, 30 and 80 mg dm^{-3}) were performed. Trueness was expressed as the recovery percent (R). The mean recovery for each analyte was calculated according to the formula reported in Guidelines for the In-House Validation of Methods of Analysis, IUPAC.[24] The calculations of the above-mentioned parameters included 10 independent measurements of CRM during 2 h for repeatability and 20 independent measurements (two operators per 10 measurements) of CRM over two consecutive days. All measurements were performed in triplicate for different concentrations levels of the same working range. The obtained results for precision, trueness, and expanded uncertainty for 10 elements detected in the liquid samples for different concentration levels (low, medium, high) of the working range (0.05–80.0 mg dm^{-3}) are given in Table III. "In-house" validation approach was used for the assessment of measurement uncertainties:[25]

$$u_c = \sqrt{u(R_w)^2 + \left(u(\text{Bias})\right)^2} \tag{3}$$

where: u_c is the combined standard uncertainty; $u(R_w)$ is the uncertainty of the estimated within-laboratory reproducibility; u(Bias) is the uncertainty of the estimation of the laboratory and the method bias;

$$u\left(\text{Bias}\right) = \sqrt{RSM_{\text{Bias}}{}^2 + u\left(\text{Cref}\right)^2} \tag{4}$$

where: u(Bias) is the contribution to the uncertainty from the bias; RMS_{Bias} is the root mean square of the individual bias values; u(Cref) is the standard uncertainty component for the certified or assigned value, *i.e.*, mean value of the individual uncertainties.

The CRM-s for the estimation the u(Bias) were analysed in at least 10 different analytical series (two operators on two consecutive days) in triplicate:

$$U(x) = k\, u(\text{x}) \tag{5}$$

where: $k = 2$ is the coverage factor corresponding to a 95 % confidence level.[25]

This approach is quick, easy and straightforward because it uses data from the in-house validation process. Therefore, this approach was adopted for the uncertainty budget estimation of the concentration of 10 elements in leachates of cement binders for different concentration levels of the working range (0.05–80.0 mg dm^{-3}).

TABLE III. Precision, trueness and expanded uncertainty for elements found in cement leachates

CRMs and standard solutions	ERA 500cal	ERA	Level 1 0.05 mg dm^{-3}	Level 2 2.5 mg dm^{-3}	Level 3 30 mg dm^{-3}	Level 4 80 mg dm^{-3}
				As		
Repeatability[a] *RSD*, %	1.8	1.7	1.2	1.7	1.1	1.6
Reproducibility[a] *RSD*, %	2.5	2.3	2.1	2.4	2.2	2.4
Trueness[a] Recovery, %	95.3	99.1	98.1	98.0	98.8	99.1
Expanded uncertainty, %	11.0	10.2	13.9	13.7	11.6	9.9
				Ba		
Repeatability[a] *RSD*, %	1.2	1.1	1.0	1.1	1.2	1.3
Reproducibility[a] *RSD*, %	1.8	1.7	1.9	1.7	1.9	1.9
Trueness[a] Recovery, %	99.2	100.3	98.8	98.9	102.2	103.2
Expanded uncertainty, %	10.1	11.9	12.1	10.3	10.5	11.3
				Cd		
Repeatability[a] *RSD*, %	1.8	1.5	1.4	1.6	1.7	1.6
Reproducibility[a] *RSD*, %	1.9	2.1	1.9	1.7	2.1	1.9
Trueness[a] Recovery, %	101.3	100.5	97.7	98.3	99.8	97.9
Expanded uncertainty, %	11.4	14.9	13.1	14.0	11.1	12.0
				Co		
Repeatability[a] *RSD*, %	1.3	1.5	1.7	0.8	0.7	0.7
Reproducibility[a] *RSD*, %	2.1	2.0	2.5	1.9	1.9	1.8
Trueness[a] Recovery, %	98.8	98.3	98.5	98.7	99.3	98.5
Expanded uncertainty, %	12.2	12.9	14.8	13.0	9.5	12.0
				Cr		
Repeatability[a] *RSD*, %	0.8	1.6	1.0	1.2	1.8	1.3
Reproducibility[a] *RSD*, %	1.6	2.3	1.7	1.4	2.0	1.8
Trueness[a] Recovery, %	101.3	100.5	100.3	100.1	98.8	98.9
Expanded uncertainty, %	11.5	11.0	15.2	14.0	9.1	11.8
				Cu		
Repeatability[a] *RSD*, %	2.5	2.4	2.8	3.1	2.8	3.4
Reproducibility[a] *RSD*, %	2.8	2.7	3.6	4.2	3.6	4.5
Trueness[a] Recovery, %	98.8	97.8	99.8	96.5	97.9	98.8
Expanded uncertainty, %	15.8	17.3	15.2	14.3	13.5	12.6
				Mo		
Repeatability[a] *RSD*, %	2.7	2.8	2.9	2.1	2.8	2.3
Reproducibility[a] *RSD*, %	2.9	3.2	3.7	4.0	3.1	4.1
Trueness[a] Recovery, %	97.8	98.9	95.8	96.6	98.8	97.8
Expanded uncertainty, %	16.3	17.4	15.1	14.1	13.3	12.9
				Ni		
Repeatability[a] *RSD*, %	0.9	1.7	1.8	1.9	1.9	1.8
Reproducibility[a] *RSD*, %	1.8	2.3	1.9	1.6	2.8	2.8
Trueness[a] Recovery, %	100.1	97.5	98.0	100.5	99.7	95.8
Expanded uncertainty, %	15.5	13.9	14.8	13.3	12.6	11.3

TABLE III. Continued

CRMs and standard solutions	ERA 500cal	ERA	Level 1 0.05 mg dm^{-3}	Level 2 2.5 mg dm^{-3}	Level 3 30 mg dm^{-3}	Level 4 80 mg dm^{-3}
				Pb		
Repeatability[a] *RSD*, %	1.1	1.9	1.8	1.9	2.2	2.3
Reproducibility[a] *RSD*, %	2.6	2.4	2.7	2.4	2.8	3.8
Trueness[a] Recovery, %	99.3	98.5	98.7	97.3	95.8	100.5
Expanded uncertainty, %	11.6	11.1	18.2	13.3	12.6	16.3
				Zn		
Repeatability[a] *RSD*, %	0.8	0.7	1.0	0.8	0.7	1.1
Reproducibility[a] *RSD*, %	1.5	1.3	1.2	1.3	1.3	1.6
Trueness[a] Recovery, %	98.3	100.1	99.5	98.8	100.1	97.7
Expanded uncertainty, %	9.2	10.3	19.1	18.0	15.2	12.4

[a]In triplicate

The obtained results for repeatability varied from 0.4 % for cobalt in the standard solution (80 mg dm^{-3}) to 3.4 % for copper in the standard solution (80 mg dm^{-3}). The values of *RSD* for reproducibility were from 1.2 % for zinc in the standard solution (0.05 mg dm^{-3}) to 4.5 % for copper in the standard solution (80 mg dm^{-3}). The investigated analytical method could be considered precise because the obtained precision parameters were below 10 %.[26] The recoveries varied from 95.3 % for As in CRM ERA 500 to 103.2 % for Ba in the standard solution (80 mg dm^{-3}). The expanded uncertainties of the measurements, expressed as the percentage of the concentration of an analyte, were between 9.1 % for chromium in the standard solution (30 mg dm^{-3}) and 19.1 % for zinc in the standard solution (0.05 mg dm^{-3}). When the uncertainty is not defined in a regulation, an additional criterion for tolerance level (20–30 %) could be considered in order to acknowledge the variability of the uncertainty estimation process.[27] High values of the measurement uncertainty for low concentration of an element could be explained by its low concentration in the analysed test solutions.

Chemometric analysis of the data obtained by modified EDXRF method

The robustness of the EDXRF method and the correlation between the obtained results and the experimental conditions were evaluated through the variation of two parameters: the amount of liquid sample and the thickness of the used polyester film. Samples were prepared with the following amounts of testing liquid (reference material ERA 500): 2.0, 3.0, 4.0, 5.0 and 6.0 g. The containers for liquid samples were covered with a polyester film of different thickness: 3.6, 4.0 and 5.0 μm. Fifteen tests on a XRF instrument were performed in order to monitor the influence of each input parameter on the final result. The results obtained from cups with 5.0 g of liquid sample and 4.0 μm thick polyester films (*i.e.*, calibration conditions) were adopted as optimal based on the manufactures instruction. The concentrations of metal elements in cement leachates

(modified XRF method) as an implication of the mass sample and film thickness are given in Table IV. Each value is the mean of three replicates. The standard deviation values are given in parentheses. The means in the same columns with different superscript letters are statistically different (at the level of statistical significance $p < 0.05$).

TABLE IV. The experimentally obtained metal element concentrations (mg dm^{-3}) using the XRF method on cement leachates depending on the mass of the sample and the film thickness

Sample amount, g	Polyester thickness, μm	Element									
		As	Ba	Cd	Co	Cr	Cu	Mo	Ni	Pb	Zn
2.0	3.6	482.3	1232.7	67.7	621.3	392.0	313.7	42.3	814.7	546.0	960.7
		(3.5)^{a}	(2.5)^{a}	(2.5)^{ab}	(1.5)^{a}	(3.5)^{a}	(11.8)^{a}	(2.5)^{a}	(12.7)^{a}	(3.6)^{a}	(3.1)^{a}
2.0	4.0	492.3	1296.0	73.3	618.3	397.3	317.0	45.0	823.3	545.0	956.0
		(2.5)^{a}	(5.3)^{b}	(3.1)^{b}	(3.5)^{a}	(0.6)^{ab}	(12.0)^{a}	(2.6)^{ab}	(2.1)^{a}	(2.6)^{a}	(5.3)^{a}
2.0	5.0	491.7	1253.3	66.3	620.3	394.0	319.7	41.3	822.0	551.7	957.0
		(4.5)^{a}	(7.6)^{a}	(3.1)^{a}	(0.6)^{a}	(1.0)^{a}	(1.5)^{a}	(1.5)^{a}	(2.6)^{a}	(1.5)^{a}	(3.0)^{a}
3.0	3.6	504.7	1476.7	98.0	659.0	402.7	428.3	54.0	854.0	569.3	1000.3
		(2.5)^{b}	(15.3)^{c}	(2.0)^{c}	(1.0)^{b}	(2.5)^{bc}	(4.7)^{b}	(1.0)^{c}	(3.6)^{b}	(7.0)^{b}	(1.5)^{b}
3.0	4.0	516.7	1504.3	96.7	662.3	403.3	424.0	52.7	851.7	568.7	1004.7
		(3.1)^{c}	(4.0)^{cd}	(1.5)^{c}	(2.5)^{bc}	(2.1)^{c}	(3.6)^{b}	(1.2)^{bc}	(3.2)^{b}	(1.5)^{b}	(0.6)^{bc}
3.0	5.0	517.3	1528.3	99.0	666.7	403.7	431.7	53.3	852.3	587.7	1009.7
		(5.0)^{c}	(20.2)^{d}	(3.6)^{c}	(1.5)^{c}	(1.5)^{c}	(1.5)^{b}	(2.5)^{c}	(2.1)^{b}	(7.1)^{c}	(0.6)^{c}
4.0	3.6	583.3	1620.0	114.7	713.3	593.3	526.3	109.0	1219.7	751.7	1158.0
		(3.5)^{d}	(17.4)^{e}	(3.5)^{d}	(1.5)^{de}	(3.1)^{d}	(5.5)^{c}	(3.6)^{d}	(1.5)^{cd}	(1.5)^{d}	(2.0)^{d}
4.0	4.0	591.7	1648.0	112.3	711.0	598.3	528.7	115.0	1204.0	751.7	1158.3
		(1.5)^{de}	(11.3)^{e}	(2.5)^{d}	(1.0)^{d}	(1.5)^{def}	(5.0)^{c}	(1.0)^{de}	(2.6)^{cd}	(2.1)^{d}	(0.6)^{d}
4.0	5.0	595.0	1653.3	118.0	716.3	595.0	529.3	115.3	1210.3	757.0	1161.7
		(1.0)^{e}	(25.2)^{e}	(1.0)^{de}	(1.5)^{ef}	(1.7)^{de}	(1.2)^{c}	(2.5)^{de}	(2.5)^{c}	(3.6)^{d}	(1.5)^{d}
5.0	3.6	587.0	1633.3	124.7	717.3	598.3	523.7	120.3	1215.3	751.7	1160.3
		(2.6)^{de}	(7.6)^{e}	(1.5)^{f}	(1.5)^{efg}	(1.5)^{def}	(3.5)^{c}	(2.5)^{ef}	(1.5)^{cd}	(2.1)^{d}	(1.5)^{d}
5.0	4.0	585.7	1657.7	124.7	721.3	598.0	534.7	124.7	1223.0	757.0	1160.3
		(2.3)^{de}	(6.8)^{e}	(1.2)^{f}	(1.5)^{g}	(1.7)^{def}	(5.0)^{c}	(1.5)^{f}	(9.8)^{d}	(2.6)^{d}	(1.5)^{d}
5.0	5.0	591.0	1637.7	122.3	721.0	599.0	531.0	124.0	1215.7	757.3	1157.3
		(2.6)^{de}	(17.5)^{e}	(1.2)^{ef}	(1.0)^{fg}	(1.0)^{def}	(1.0)^{c}	(1.0)^{f}	(1.5)^{cd}	(4.9)^{d}	(1.2)^{d}
6.0	3.6	590.3	1643.0	122.0	718.0	596.3	525.7	118.3	1222.3	752.0	1155.0
		(6.5)^{de}	(9.5)^{e}	(1.0)^{ef}	(1.0)^{efg}	(1.2)^{def}	(2.5)^{c}	(6.5)^{ef}	(3.1)^{d}	(1.0)^{d}	(5.0)^{d}
6.0	4.0	591.0	1659.3	122.0	718.3	601.0	529.0	117.3	1218.3	754.0	1158.0
		(4.6)^{de}	(16.7)^{e}	(1.0)^{ef}	(0.6)^{fg}	(1.0)^{ef}	(1.7)^{c}	(1.5)^{ef}	(8.6)^{cd}	(1.0)^{d}	(2.0)^{d}
6.0	5.0	593.7	1630.0	122.7	719.0	599.3	527.0	121.3	1210.7	751.7	1156.3
		(1.5)^{de}	(3.5)^{e}	(1.5)^{ef}	(1.0)^{fg}	(2.1)^{f}	(3.6)^{c}	(2.5)^{ef}	(2.1)^{cd}	(1.5)^{d}	(3.8)^{d}

As could be seen from Table IV, there was highly significant differences (level $p < 0.05$) between samples obtained using different sample amounts and polyester thicknesses. Grouping of the samples was presented by cluster analysis (CA) and the results are illustrated in Fig. 2. The dendrogram was obtained by

grouping variables using the Complete linkage method - City-block (Manhatten) distances.

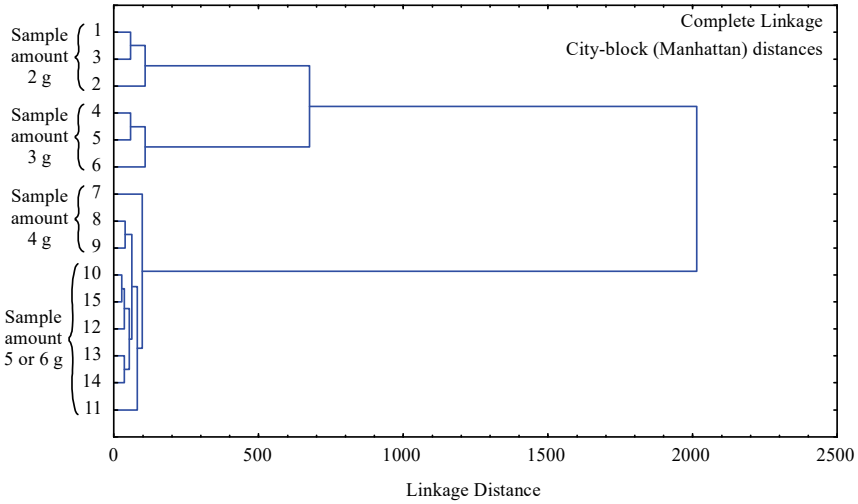

Fig. 2. Dendrogram for robustness of EDXRF data for liquid samples.

Four groups of samples were formed (4 clusters). The first group contained 2 g samples, the second group contained 3 g samples, and the third group contained samples prepared with 4 g samples, while the fourth cluster contained samples with 5 and 6 g samples. The shortest distance, *i.e.*, the strongest correlation was achieved between the first and the second group.

ANOVA exhibits the significant effect of independent variables as well as the interactions of these variables (Table V). This analysis revealed that the linear terms of sample amount (SA) in the second order polynomial (SOP) model were found statistically significant at $p < 0.01$ level, for each metal element calculations. The quadratic terms of the sample amount in the SOP models were statistically significant for Ba, Cd, Co, Cu and Zn calculation, statistically significant at $p < 0.01$ level, while the influence of the quadratic terms of sample amount in the SOP models for As, Mo and Pb calculation was statistically significant at the $p < 0.05$ level.

All SOP models had an insignificant lack of fit tests, which means that all the models represented the data satisfactorily.

Comparison of EDXRF and ICP-OES results by the linear regression method

Results obtained by the EDXRF and ICP-OES methods applied on cement leachates were compared and correlated *via* linear regression analysis. Linear regression parameters for the concentrations of metal elements in the analyzed leachates are presented in Table VI.

Table V. ANOVA table of the yield evaluation (sum of squares) for each element content in the leachates samples (df - degrees of freedom, PT- polyester thickness); SA – sample amount, g; PT – polyester thickness (μm); significant at level: $+p < 0.01$, $*p < 0.05$, $**p < 0.10$; error terms statistically insignificant

	SA	SA^2	*PT*	PT^2	*SA* × *PT*	Error	r^2
df	1	1	1	1	1	9	
As	22828.5^+	3080.0*	168.1	40.5	9.9	2758.96	0.907
Ba	236038.9^+	81664.4^+	940.9	2187.6	502.2	6125.4	0.982
Cd	5116.6^+	1023.5^+	0.2	0.3	0.6	51.288	0.992
Co	18807.7^+	3777.8^+	20.5	0.4	0.2	455.55	0.981
Cr	106476.4^+	9103.2**	6.9	21.1	0.3	23834.6	0.833
Cu	79441.6^+	22773.4^+	44.1	11.7	5.2	1495.0	0.986
Mo	14483.5^+	1329.8*	12.8	6.9	10.0	2009.62	0.889
Ni	390389.8^+	37640.2**	22.5	0.2	63.7	78372.2	0.849
Pb	100809.2^+	12058.8*	120.2	2.3	47.1	17996.0	0.866
Zn	88579.5^+	13849.1^+	5.9	0.1	1.6	11044.8	0.905

TABLE VI. Linear regression parameters for the results of EDXRF and ICP-OES analyses; correlations significant at level: $p < 0.01$; slope and intercept values statistically significant at the $p < 0.01$ level

Oxide/element	Determination coefficient	Slope	*SD*	Intercept	*SD*
As	0.9994	1.00357	0.01000	–0.01432	0.00014
Ba	0.9995	1.00045	0.00838	–0.02958	0.00029
Cd	0.9996	0.99894	0.00914	0.019277	0.00019
Co	0.9998	1.00102	0.00771	–0.03803	0.00038
Cr	0.9995	1.00701	0.00999	0.00226	0.00002
Cu	0.9994	1.00016	0.00826	0.00989	0.00010
Mo	0.9971	1.00042	0.00902	–0.00665	0.00007
Ni	0.9982	0.99527	0.00833	1.00101	0.01000
Pb	0.9989	0.99939	0.00769	0.00035	0.00000
Zn	0.96998	0.99889	0.00910	0.01008	0.00010

The obtained determination coefficients for the analysed chemical elements were within the confidence interval at a level of 95 %. The determination coefficients were in the range from 0.96998 (Zn) to 0.9998 (Co).

The determination coefficients (≈1.0) indicated that there were no significant differences between the outputs of the applied analyses methods. The statistical parameters of the intercepts and the slopes for the ten studied elements showed that the intercepts were in the range from –0.03803 (Co) and 1.00101 (Ni). The slopes (0.99527 for Ni–1.00701 for Cr) were not significantly different from 1. The regression parameters verified a good correlation between EDXRF and ICP--OES results, which means that both of techniques are adequate for the determination of metal elements in leachate of cement-based binders.

Regarding the analytical performances, the proposed and validated EDXRF method features a straightforward quantification method in which periodic recal-

ibration is not required. On the other hand, the ICP-OES method shows superior detection capabilities for low concentrations of elements. The cost of analyses, reagents and personnel expenses undoubtedly support the application of both ICP-OES and EDXRF techniques for liquid samples. However, on-site analyses support the EDXRF method.

CONCLUSIONS

A modified EDXRF analytical procedure for multi elemental determination of As, Ba, Cd, Co, Cr, Cu, Mo, Ni, Pb and Zn in leachates of cement binders with additions of fly ash, zeolite and bentonite was successfully developed. The modified analytical technique proved to be a reliable tool for the analysis of a wide variety of building materials based on cement. The former statement could be substantiated with faster unattended analysis of samples within a wide range of concentrations and matrices, different states of matter are applicable and simultaneous multi-trace detection is feasible. The obtained values for the detection limits were within the range from 0.022 (Pb) to 0.080 $mg \cdot dm^{-3}$ (Cu). Measurement uncertainty for the developed method ranged from 9.1 for Cr to 19.1 % for Zn. The robustness of the EDXRF technique for liquid samples was successfully evaluated in altered testing conditions (sample amount and variable film thickness). It was highlighted that different thickness of film did not significantly influence the final results unlike the amount of the liquid sample that induced significant variations in the outputs of EDXRF analysis. The precision of EDXRF method for liquid samples was confirmed by the high values obtained for coefficients of determination (≈1) in comparison with the ICP-OES results. This means that the modified EDXRF calibrations could be used with high precision in the analysis of the leachate of cement-based materials with mineral additives and that this validated EDXRF method could be a good and reliable alternative for the commonly used laboratory technique: ICP-OES.

Acknowledgment. This investigation was financially supported by the Ministry of Education, Science and Technological Development of the Republic of Serbia (Contract No.: 451-03-68/2020-14/200012).

ИЗВОД

УНАПРЕЂЕЊЕ И МОДИФИКАЦИЈА ЕНЕРГЕТСКИ ДИСПЕРЗИВНЕ РЕНДГЕНСКЕ ФЛУОРЕСЦЕНЦИЈЕ ЗА ОДРЕЂИВАЊЕ МЕТАЛА У ЕЛУАТУ ЦЕМЕНТНИХ ВЕЗИВА – ХЕМОМЕТРИЈСКИ ПРИСТУП

НЕВЕНКА Н. МИЈАТОВИЋ[1], АЊА М.ТЕРЗИЋ[1], ЛАТО Л. ПЕЗО[2], ЉИЉАНА Р. МИЛИЧИЋ[1] и ДРАГАНА З. ЖИВОЈИНОВИЋ[3]

Институт за испитивање материјала, Институт ИМС, Булевар војводе Мишића 43, 11000 Београд, [2]Институт за општу и физичку хемију, Универзитет у Београду, Студентски трг 12–16, 11000 Београд и [3]Технолошко–металуршки факултет, Универзитет у Београду, Карнегијева 4, 11000 Београд

У овом раду извршена је модификација аналитичке методе енергетски дисперзивне рендгенске флуоресценције (EDXRF) за квантификацију десет хемијскихелемената (As,

Ba, Cd, Co, Cr, Cu, Mo, Ni, Pb, Zn) у елуатима цемента. У експерименту је коришћено 29 узорка за тестирање. Сви узорци су на бази Портланд цемента. Као минерални додаци у цементним везивима коришћени су: летећи пепео различитог порекла, зеолит и бентонит. Дестилована вода је коришћена као медијум излуживање метала. Валидација модификованог поступка EDXRF извршена је у смислу границе детекције и квантификације, радног распона, линеарности, селективности, прецизности, истинитости и робусности. След поступка утврђен је коришћењем сертификованих референтних материјала. Несигурност мерења потврђена је „интерним“ лабораторијским приступом валидације. Проширене несигурности за десет анализираних елемената добијене су за цео радни опсег EDXRF методе. Робусност модификованог EDXRF поступка процењена је хемометријским интерним приступом. Резултати добијени модификованом методом рендгенске флуоресценције додатно су корелисани са онима добијеним методом оптичке емисионе спектрометрије са индуктивно спрегнутом плазмом (ICP-OES) применом регресионе анализе како би се утврдило да се EDXRF може користити као алтернативна метода за анализу елуата цемента.

(Примљено 1. маја, ревидирано 24. августа, прихваћено 27. октобра 2020)

REFERENCES

1. F. Jiao, L. Zhang, Z. Dong, T. Namioka, N. Yamada, *Fuel Process. Tech.* **152** (2016) 108 (https://doi.org/10.1016/j.fuproc.2016.06.013)
2. L. Zeyuan, Y. Yang, L. Ming, Z. Jia, S. Fucheng, H. Xin, Z. Jizhi, Q. Guangren, *Waste Manage.* **84** (2019) 329 (https://doi.org/10.1016/j.wasman.2018.11.049)
3. M. P. Mubiayi, M. E. Makhatha, E. T. Akinlabi, *Mater. Today* **5** (2018) 17802 (https://doi.org/10.1016/j.matpr.2018.06.105)
4. A. Terzić, L. Pezo, N. Mijatović, J. Stojanović, M. Kragović, Lj. Miličić, Lj. Andrić, *Con. Build. Mat.* **180** (2018) 199 (https://doi.org/10.1016/j.conbuildmat.2018.06.007)
5. N. Mijatović, A. Terzić, L. Pezo, Lj. Miličić, A. Milosavljević, D. Živojinović, *Sci. Sin.* **51** (2019) 429 (https://doi.org/10.2298/SOS1904429M)
6. A. Król, K. Mizerna, M. Bożym„*J. Hazard. Mater.* **384** (2020) 121502 (https://doi.org/10.1016/j.jhazmat.2019.121502)
7. M. Mahedia, B. Cetinb, A. Dayioglu, *Waste Manage.* **95** (2019) 334 (https://doi.org/10.1016/j.wasman.2019.06.018)
8. J. Haberl, R. Koralewska, S. Schlumberger, M. Schuster, *Waste Manage.* **75** (2018) 361 (https://doi.org/10.1016/j.wasman.2018.02.015)
9. L. Borgesea, R. Dalipia, A. Riboldia, F. Biloa, A. Zaccoa, S. Federicia, M. Bettinellic, E. Bontempia, L. Depero, *Talanta* **181** (2018) 165 (https://doi.org/10.1016/j.talanta.2017.12.087)
10. A. Chandrasekarana, R. Ravisankar, *Appl. Radiat. Isot*. **147** (2019) 76 (https://doi.org/10.1016/j.apradiso.2019.01.009)
11. M. Tiwari, S.K. Sahu, R.C. Bhangare, P.Y. Ajmal, G.G. Pandit, *Appl. Radiat. Isot*. **90** (2014) 53 (https://doi.org/10.1016/j.apradiso.2014.03.002)
12. Y. Fiamegos, M. Beatriz, *Spectrochim. acta, B* **150** (2018) 59 (https://doi.org/10.1016/j.sab.2018.10.009)
13. C. García-Florentinoa, M. Magureguib, H. Morillasa, I. Marcaidaa, J. Madariaga, *Microchem. J.* **133** (2017) 104 (https://doi.org/10.1016/j.microc.2017.03.020)
14. S. Zhoua, Z. Yuanb, Q. Chenga, Z. Zhanga, J. Yang, *Environ. Pollut.* **243** (2018) 1325 (https://doi.org/10.1016/j.envpol.2018.09.087)

15. E. Marguí, R. Van Grieken, C. Fontas, M. Hidalgo, I. Queralt, *Appl. Spectrosc. Rev.* **45** (2010) 179 (https://doi.org/10.1080/05704920903584198)
16. D. Pearsona, S. Chakrabortyb, B. Dudaa, B. Lic, D. Weindorfa, S. Debd, E. Brevike, D. Rayf, *J. Hydrol.* **544** (2017) 172 (https://doi.org/10.1016/j.jhydrol.2016.11.018)
17. A. Turner, A. Taylo, *Talanta* **190** (2018) 498 (https://doi.org/10.1016/j.talanta.2018.08.024)
18. P. Szajerskia, A. Bogobowicza, H. Bemb, A. Gasiorowskia, *J. Clean. Prod.* **222** (2019) 90 (https://doi.org/10.1016/j.jclepro.2019.03.010)
19. N. Mijatović, A. Terzić, L. Pezo, Lj. Miličić, D. Živojinović, *Spectrochim. acta, B* **162** (2019) 105729 (https://doi.org/10.1016/j.sab.2019.105729)
20. *SRPS EN 12457-4: Characterization of waste - Leaching - Compliance test for leaching of granular waste materials and sludges - Part 4: One stage batch test at a liquid to solid ratio of 10 l/kg for materials with particle size below 10 mm (without or with size reduction)*, 2008
21. *IUPAC, Nomenclature, symbols, units and their usage in spectrochemical analysis-III. Analytical flame spectroscopy and associated non-flame procedures*, *Spectrochim. Acta, B* **33** (1978) 247 (https://doi.org/10.1016/0584-8547(78)80045-7)
22. *Low Level Waste Repository Ltd.* (https://assets.publishing.service.gov.uk/government/uploads/system/uploads/attachment_data/file/690840/WasteAcceptanceCriteriaSupercompactableWSC-WAC-SUP.pdf), accessed 23. 04. 2020
23. V. Barwicka, S. Wood, *J. Anal. At. Spectrom*. **25** (2010) 785 (https://doi.org/10.1039/B919885G)
24. M. Thompson, S. Ellison, R. Wood, *Pure Appl. Chem.* **74** (2002) 835 (http://doi.org/10.1351/pac200274050835)
25. *Nordtest* (http://www.citac.cc/Bertil Magnusson - NORDTEST Guide on uncertainty - 2003.pdf), accessed 22. 04. 2020
26. D. Schiavo, L.C. Trevizan, E.R.P. Filho, J.A. Nóbrega, *Spectrochim. Acta, B* **64** (2009) 544 (https://doi.org/10.1016/j.sab.2009.05.009)
27. *Bureau international des poids et mesures* (https://www.bipm.org/en/publications/guides/gum.html), accessed 20. 04. 2020.

Journal of the Serbian Chemical Society
JSCS-info@shd.org.rs • www.shd.org.rs/JSCS
J. Serb. Chem. Soc. 85 (12) 1621–1627 (2020)
JSCS–5397
UDC 677.1+66.09:544.354.3:544.638
Original scientific paper

Electrokinetic properties of chemically modified jute fabrics

ALEKSANDRA M. IVANOVSKA[1#]* and MIRJANA M. KOSTIĆ[2#]

[1]*University of Belgrade, Innovation Center of the Faculty of Technology and Metallurgy, Karnegijeva 4, Belgrade 11000, Serbia and* [2]*University of Belgrade, Faculty of Technology and Metallurgy, Karnegijeva 4, Belgrade 11000, Serbia*

(Received 13 October, revised 2 November, accepted 3 November 2020)

Abstract: In this work, the electrokinetic properties of alkali and oxidatively modified jute fabrics were studied. In contrast to the control fabric, chemically modified jute fabrics had a small positive zeta potential in the basic pH range, which could be attributed to the presence of sodium cations (originating from the undertaken chemical modifications) on their surfaces. At lower pH values, the samples modified under milder alkali and oxidative conditions had about 2.2–3.5 times lower zeta potential since the protonation process led to the formation of a higher positive charge in the electrochemical double layer, causing higher adsorption of Cl^- (originating from the electrolyte). On the other hand, more intensive chemical modifications increased the zeta potential at lower pH values due to the increased amount of carboxyl groups and the ability of the fibres for water retention and hence swelling. The isoelectric point of the fabrics, having lower zeta potentials than that of the control fabric, was shifted towards higher pH values, indicating to a lower contribution of surface acidic groups of the fabrics. In the case of extensive oxidation conditions (60 and 90 min), the isoelectric point was shifted toward lower pH values because of lignin removal and the mentioned higher availability of newly formed carboxyl groups.

Keywords: zeta potential; isoelectric point; hemicelluloses; lignin.

INTRODUCTION

In the past, jute fibres were considered as a source of raw material for the packaging industry but nowadays, they have emerged as a versatile raw material for diverse applications, such as household textiles, floor coverings, biobased composites, *etc.* To meet the worldwide demand for jute fibres, their production, processing and quality should be improved.

* Corresponding author. E-mail: aivanovska@tmf.bg.ac.rs
# Serbian Chemical Society member.
https://doi.org/10.2298/JSC201013069I

Jute fibres are recognized by their complex structure and very heterogeneous chemical composition comprising of cellulose, hemicelluloses, lignin and other minor components. The main steps for the purification of jute fibres (*i.e.*, removal of non-cellulosic components) include the simplest, most direct, economical and efficient alkali and oxidative modifications. During these modifications, the selective removal of hemicelluloses and lignin in parallel with cellulose lateral swelling contributed to the liberation of elementary fibres, resulting in increased availability of surface functional groups.[1] The dissociation ability of these groups affects the distribution of the surface charge, as well as the thickness and distribution of the electrochemical double layer, altogether resulting in changed zeta potential and isoelectric point.[2] Accordingly, it could be stated that the alkali and oxidative modifications of raw jute fabric change its electrokinetic properties and alter its interaction with the components of the liquid phase. An extensive understanding of the electrokinetic properties of jute fabrics is still required to optimize the chemical modification processes, which might increase the utilization of such modified fabrics.

EXPERIMENTAL

Material

A raw jute fabric (in further text: control fabric or sample C) purchased from a commercial supplier was chemically modified with sodium hydroxide or sodium chlorite, as given in Fig. 1.

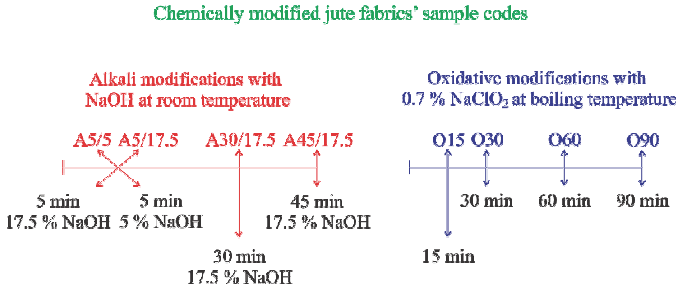

Fig. 1. Conditions for the chemical modifications of jute fabrics and the designation of the samples.

Characterization of the materials

Chemical composition of the jute fabrics. The chemical composition of the jute fabrics was determined according to a modified procedure described in the literature.[3]

Determination of the electrokinetic properties of the jute fabrics. The jute fabrics' electrokinetic properties, *i.e.*, the zeta potential (ζ) as a function of pH, were determined by a streaming potential method using a SurPASS electrokinetic analyzer (Anton Paar GmbH, Austria), according to the procedure described by Lazić *et al.*[4] Before the measurements, the samples were pre-swelled in distilled water to avoid the influence of fibre swelling on the zeta potential. Since the isoelectric point (IEP, the pH value where the value of ζ is 0) of jute fab-

rics is in the low pH region (*i.e.*, pH < 3), it was extrapolated from the experimental curve. Two measurements were performed for each sample, whereby the standard deviation was below 5 %.

RESULTS AND DISCUSSION

Chemical modification of jute fabric

The modification conditions shown in Fig. 1 were selected to obtain jute fabrics with different chemical compositions and to study their influence on the electrokinetic properties of the resulting fabrics.

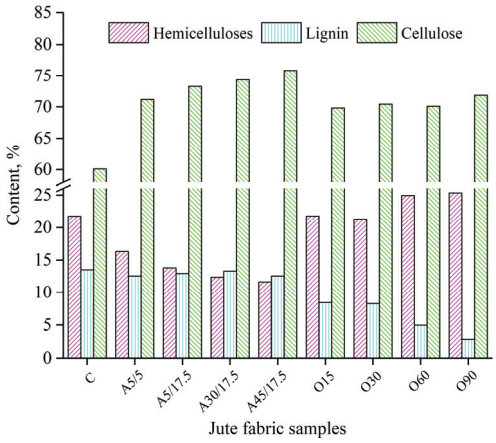

Fig. 2. Chemical composition of the jute fabrics.

By increasing the modification intensity (duration and/or concentration of the chemical agent), jute fabrics with gradually decreasing hemicellulose or lignin contents as well as increased cellulose content were obtained, Fig. 2. Namely, the alkali modifications decreased the hemicellulose content by 25–47 %, compared to the control jute fabric. Moreover, depending on the duration of the oxidative modification (15–90 min), jute fabrics with 38–79 % lower lignin content were obtained. A detailed discussion regarding the influence of the chemical modification conditions on the chemical composition and structure of jute fabrics is given in the literature.[3,5]

Electrokinetic properties of chemically modified jute fabrics

The chemical modifications of the fabrics not only lead to changes in their chemical composition, structure, sorption, mechanical and electro-physical properties,[3,5] but also change their electrokinetic properties, *i.e.*, surface charge of the fabrics. In this investigation, the measurement of the zeta potential was chosen to give valuable insight into the surface charge of the fabrics. In order to monitor the changes occurring on the surface of the fabrics (*i.e.*, the presence, availability and nature of surface groups) caused by chemical modifications, the zeta potential is measured over a wide pH range, Fig. 3. Furthermore, the pH

value where the smallest zeta potential was detected ($pH_{\zeta,min}$), the minimum value of zeta potential (ζ_{min}) and the isoelectric point (IEP) determined by extrapolation are given in Table I.

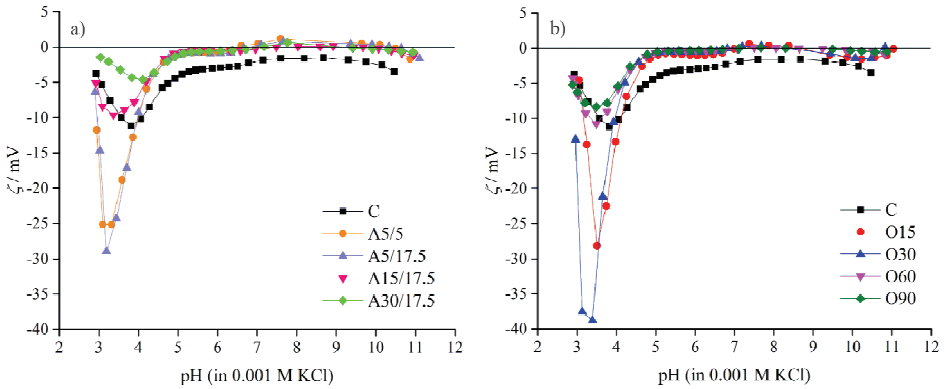

Fig. 3. Zeta potential (ζ) as a function of pH for control (C), alkali (a) and oxidatively modified jute fabrics (b).

TABLE I. pH Value where the smallest zeta potential was detected ($pH_{\zeta,min}$), zeta potential minimum value (ζ_{min}) and isoelectric point (IEP)

Sample code	$pH_{\zeta,min}$	ζ_{min} / mV	IEP
C	3.82	-11.17	2.52
A5/5	3.32	-25.16	2.84
A5/17.5	3.19	-28.93	2.83
A15/17.5	3.37	-9.60	2.44
A30/17.5	4.11	-4.61	2.67
O15	3.51	-28.11	2.98
O30	3.39	-38.79	2.74
O60	3.49	-10.76	2.46
O90	3.49	-8.34	2.24

The control jute fabric as other cellulosic materials has a negative zeta potential in the basic pH range (pH > 7, $\zeta_{plateau}$) due to the presence of anionic functional groups (*i.e.*, hydroxyl and carboxyl) on its surface,[6] Fig. 3. According to Hubbe *et al.*,[7] these groups are prone to dissociation in the high pH range. In contrast, the chemically modified jute fabrics have a small positive zeta potential value in the mentioned region ($\zeta_{plateau}$), which is probably caused by the presence of "strongly" adsorbed sodium cations (originating from the chemical modifications with NaOH or $NaClO_2$) on their surfaces.[8]

The applied chemical modifications increase the active surfaces of fabrics and the availability of their surface groups, which is characterized by a sudden change in the zeta potential of the fabrics at lower pH values (Fig. 3) and the $pH_{\zeta,min}$ values are shifted towards lower pH values (excluding sample A30/17.5,

Table I), which may be a consequence of the protonation of acetyl or ether linkages in cellulose or lignin residues.[9] Most remarkable decreases in the ζ_{min} values (by 2.2–3.5 times) at lower pH values and in shifts in the $pH_{\zeta,min}$ values toward lower pH values were noticed for the samples from which up to 36.6 % of the hemicelluloses (samples A5/5 and A5/17.5) and up to 38.8 % of the lignin (samples O15 and O30) had been removed, Figs. 2 and 3 and Table I. For these samples, protonation contributed to the formation of a higher positive charge in the electrochemical double layer, causing higher adsorption of Cl^- (originating from electrolyte), and therefore, resulting in a significant decrease in ζ_{min} values at lower pH values.[9] Change of the experimental curve shape in parallel with the decrease in ζ_{min} value and simultaneously increased $\zeta_{plateau}$ were also reported for alkali modified jute[8] and sisal[9] fibres, as well as oxidized cotton[2] and flax[4] fibres.

On the other hand, the removal of more than 36.6 % of the hemicelluloses (samples A15/17.5 and A30/17.5) and more than 38.8 % of the lignin (samples O60 and O90) increase the ζ_{min} value by 4–59 % compared to that of the control sample. The alkali and oxidative chemical modifications increase the amount of carboxyl groups and the fibre ability for water retention and hence swelling,[5] which together increase the ζ_{min} value of the fabrics. The results are in accordance with the data reported for mercerized cotton in which the ζ_{min} value increased due to the considerable increase in the available surface of the fibres caused by the intensive interfibrillar and intrafibrillar swelling of the fibres. It should be mention that in the case of sample A30/17.5 (the most intensive alkali modification conditions), the $pH_{\zeta,min}$ was shifted toward higher values ($pH_{\zeta,min}$ 4.11) compared to that of control fabric ($pH_{\zeta,min}$ 3.82), indicating that the protonation process became more difficult.

The IEP, as an indicator for the nature of functional groups and surface charge of fabrics, was determined by extrapolation, Table I. The IEP shifted towards higher pH values for fabrics with a lower ζ_{min} value than that of the control fabric (samples A5/5, A5/17.5, O15 and O30) as well as for sample A30/17.5, indicating to a lower contribution of the surface acidic groups of the fabrics. In the case of intensive oxidation conditions, the IEP was shifted towards lower pH values (from pH 2.52 for the control fabric to 2.46 and 2.24 for fabrics O60 and O90, respectively), which could be ascribed to selective lignin removal, *i.e.*, the formation of dicarboxylic groups and conversion of aldehyde to carboxyl groups during oxidations followed by the simultaneous increase in their availability.[5] The IEP at pH 2.46 and 2.44 extrapolated for the samples O60 and A15/17.5, respectively, indicate that these samples had very similar surface chemistry, while the lower $\zeta_{min}/\zeta_{plateau}$ value of fabric A15/17.5 reflects its higher swelling ability.

CONCLUSIONS

In this investigation, the effects of alkali and oxidative chemical modifications on the electrokinetic properties of jute fabrics were studied. The control fabric had a negative zeta potential in the basic pH range due to the presence of anionic functional groups on its surface, while the chemically modified fabrics has a small positive zeta potential in that region caused by the presence of sodium cations on their surfaces. The samples modified under milder conditions (5 % NaOH for 5 min, 17.5 % NaOH for 5 min and 0.7 % $NaClO_2$ for 15 and 30 min) had 2.2–3.5 times lower zeta potential at lower pH values; their isoelectric points were shifted toward higher pH values indicating a lower contribution of the surface acidic groups of the fabrics. In contrast, intensive oxidation conditions (0.7 % $NaClO_2$ for 60 and 90 min) increased the availability of newly formed carboxyl groups, which contributed to increased zeta potential at lower pH values and shifted the isoelectric point towards lower pH values.

Acknowledgments. This work was supported by the Ministry of Education, Science and Technological Development of the Republic of Serbia (Contract No. 451-03-68/2020-14/ /200135). The authors thank Matea Korica (Innovation Center of the Faculty of Technology and Metallurgy, University of Belgrade) for performing the zeta potential measurements.

И З В О Д

ЕЛЕКТРОКИНЕТИЧКА СВОЈСТВА ХЕМИЈСКИ МОДИФИКОВАНЕ ТКАНИНЕ ОД ЈУТЕ

АЛЕКСАНДРА М. ИВАНОВСКА[1] и МИРЈАНА М. КОСТИЋ[2]

[1]Универзитет у Београду, Иновациони центар Технолошко–металуршког факултета, Карнегијева 4, 11000 Београд Универзитет у Београду и [2]Универзитет у Београду, Технолошко–металуршки факултет, Карнегијева 4, 11000 Београд

У овом раду испитивана су електрокинетичка својства алкално модификоване и оксидисане тканине од јуте. Супротно сировој тканини, хемијски модификоване ткanине имају малу позитивну вредност зета потенцијала у базном подручју pH вредности, што може бити проузроковано присуством натријумових јона (који потичу из поменуте хемијске модификације) на површини тканине. При нижим pH вредностима, тканине модификоване при блажим алкалним и оскидативним условима имају око 2,2–3,5 пута мањи зета потенцијал што се може објаснити чињеницом да процес протонизације доводи до формирања већег позитивног наелектрисања у електрохемијском двојном слоју, што може да изазове повећану адсорпцију Cl^- (који потичу из електролита). С друге стране, интензивнији услови хемијског модификовања доводе до повећања зета потенцијала при нижим pH вредностима као резултат повећаног садржаја карбоксилних група и повећане способности влакана за задржавање воде, а самим тим и бубрење. Померање изоелектричне тачке ка вишим pH вредностима је запажено код тканина код којих је запажен мањи зета потенцијал у поређењу са сировом тканином, што указује на то да је допринос киселих група на површини тканина нижи. Код интензивнијих услова оксидације (у току 60 и 90 min), уочено је померање изоелектричне тачке ка нижој pH вредности због селективног уклањања лигнина, али и формирања нових карбоксилних група уз истовремено повећање њихове доступности.

(Примљено 13. октобра, ревидирано 2. новембра, прихваћено 3. новембра 2020)

REFERENCES

1. K. S. Kleinschek, V. Ribitsch, *Colloids Surfaces, A* **140** (1998) 127 (https://doi.org/10.1016/S0927-7757(97)00301-4)
2. A. Tarbuk, K. Grgić, E. Toshikj, D. Domović, D. Dimitrovski, V. Dimova, I. Jordanov, *Cellulose* **27** (2020) 3107 (https://doi.org/10.1007/s10570-020-03028-6)
3. A. Ivanovska, D. Cerovic, S. Maletic, I. Jankovic Castvan, K. Asanovic, M. Kostic, *Cellulose* **26** (2019) 5133 (https://doi.org/10.1007/s10570-019-02421-0)
4. B. D. Lazić, B. M. Pejić, A. D. Kramar, M. M. Vukčević, K. R. Mihajlovski, R. D. Rusmirović, M. M. Kostić, *Cellulose* **25** (2018) 697 (https://doi.org/10.1007/s10570-017-1575-4)
5. A. Ivanovska, K. Asanovic, M. Jankoska, K. Mihajlovski, L. Pavun, M. Kostic, *Cellulose* **27** (2020) 8485 (https://doi.org/10.1007/s10570-020-03360-x)
6. K. S. Kleinschek, S. Strand, V. Ribitsch, *Polym. Eng. Sci.* **39** (1999) 1412 (https://doi.org/10.1002/pen.11532)
7. M. A. Hubbe, S. H. Hasan, J. J. Ducoste, *BioResources* **6** (2001) 2161
8. A. Bismarck, J. Springer, A. K. Mohanty, G. Hinrichsen, M. A. Khan, *Colloid Polym. Sci.* **278** (2000) 229 (https://doi.org/10.1007/s003960050036)
9. A. Bismarck, A. K. Mohanty, I. Aranberri-Askargorta, S. Czapla, M. Misra, G. Hinrichsen, J. Springer, *Green Chem.* **3** (2001) 100 (https://doi.org/10.1039/B100365H).

Journal of the Serbian Chemical Society
JSCS-info@shd.org.rs • www.shd.org.rs/JSCS
J. Serb. Chem. Soc. *85* (12) 1629–1642 (2020)
JSCS–5398
UDC 577.742–035.57+66.067.38:608.2
Original scientific paper

Enhancement of ultrafiltration of milk proteins by application of twisted tapes: A sensitivity analysis using a response surface methodology

SVETLANA S. POPOVIĆ[1]*, MIRELA D. ILIČIĆ[1#] and IGOR L. GÁSPÁR[2]

[1]*Faculty of Technology Novi Sad, University of Novi Sad, Boulevard cara Lazara 1, Novi Sad, Serbia and* [2]*Szent István University, Faculty of Food Science, Food Engineering Department, H-1118. Budapest, Menesi st. 4, Hungary*

(Received 5 July, revised 29 October, accepted 18 November 2020)

Abstract: This paper presents intensification of the ultrafiltration of milk proteins by application of twisted tapes as turbulence promoters to minimize membrane fouling. The aim was to examine the influence of operating conditions and twisted tape dimensions on the alleviation of flux and the consumption of specific energy. A twisted tape was inserted in the ultrafiltration membrane (50 nm pore size) to alleviate turbulence and minimize fouling. The response surface methodology was used for the sensitivity analysis of the effects of operating conditions on the responses. The analysis showed that the linear effect of the aspect ratio of the twisted tape has a dominant significant effect on flux improvement. The linear effect of cross-flow rate has a positive dominant effect on the specific energy consumption. The linear effect of concentration and the mutual effect of aspect ratio and transmembrane pressure are statistically significant for both responses. By properly adjusting the operating conditions, a high flux improvement of 300 % could be reached with a specific energy consumption below 1.0 kW h m^{-3} using a twisted tape of an aspect ratio of 1.0 and imposing low transmembrane pressure.

Keywords: turbulence promoter; fouling minimization; membrane filtration; response surface methodology; sensitivity analysis.

INTRODUCTION

Ultrafiltration is commonly employed in the dairy industry for concentrating and fractionating proteins.[1] Even though the separation characteristics of ultrafiltration are excellent, the fouling of a membrane poses a problem in terms of process efficiency. The fouling by proteins is severe and difficult to mitigate and thus, the frequent cleaning of membranes is required causing membrane deterior-

* Corresponding author. E-mail: svetlana.popovic@uns.ac.rs
# Serbian Chemical Society member.
https://doi.org/10.2298/JSC2000705073P

ation and consequently their frequent replacement. The fouling occurs because of accumulation and adsorption of the proteins on the membrane surface and/or in the pores of the membrane.[2,3] The permeation flux declines during the filtration process resulting in lower process efficiency due to the appearance of both, concentration polarization and fouling. Concentration polarization and surface fouling can be controlled by applying hydrodynamic methods.

Among others, the simplest hydrodynamic method of fouling minimization is an acceleration of fluid, *i.e.*, an increase in the cross-flow velocity of the fluid. In this way, the turbulence in the fluid is increased and fouling particles are taken away from the membrane surface by the turbulent fluid flow. The hydrodynamic technique proved highly efficient is the insertion of motionless turbulence promoters in the membrane module. Besides the acceleration, the main impact of turbulence promoters is the formation of secondary flows additionally contributing to the disruption of the boundary layer and an improvement of mass transport. The effect of the geometry of the turbulence promoter on the flow field in the membrane channel and fouling minimization have been widely presented.[4–6] Turbulence promoters of diverse geometries were studied in the microfiltration of various mixtures, such as yeast,[7,8] skimmed milk,[4,6] bentonite,[9] *etc*. where excellent flux improvements were gained. Furthermore, they have been studied in several ultrafiltration processes, such as the ultrafiltration of oily wastewaters,[10,11] milk,[12] dispersion with colloidal SiO_2[13] and natural organic matter.[14] The ultrafiltration of milk was enhanced by a cork-screw thread turbulence promoter, which causes a high pressure drop along the membrane and operation under high transmembrane pressure,[12] which is energetically inefficient.

Generally, the drawback of the application of a turbulence promoter is an increase in pressure loss across the membrane module. However, it depends on geometrical characteristics and dimensions that influence the flux improvement greatly. Thus, it is necessary to find a compromise between flux improvement and the energy consumed per the cubic meter of the produced permeate. Other operating conditions cannot be disregarded and their influence has to be analysed as well.

Response surface methodology (RSM) is a simple and widely used tool for detecting and quantifying influences of the chosen independent variables (factors) on the dependent variables (responses) and for process optimization. The RSM approach is multivariate so the responses of the system are analysed by varying the multiple independent variables simultaneously. For analysis, the experimental measurement has to be organized using an appropriate design of experiments (DOE). The factorial design of the experiments allows wider and more differentiated information on the system and greatly usable conclusions.[15] There are various designs of experiments used for the planning of experiments. The RSM has been successfully used in studies on the membrane processes, to

examine the influence of the operating conditions and thereby to find the optimal process solutions.[7,11]

In previous studies, the focus was on the application of various geometries of turbulence promoters in the microfiltration of partially skimmed milk to prove the concept and to analyse the fluid dynamics in the membrane with a promoter.[5,6] Given that membrane fouling is considerably affected by the characteristics of filtered feed, case studies are needed to detect the influences of all possible factors.

This study was designed to identify the significance of particular operating conditions for intensification of the ultrafiltration of milk proteins. Twisted tapes as low-pressure loss turbulence promoters were for the first time used for fouling mitigation, thereby enhancement of the ultrafiltration of milk proteins. The sensitivity of the flux improvement and specific energy consumption to the dimension of twisted tape (aspect ratio), cross-flow rate, transmembrane pressure and the concentration of proteins were examined.

EXPERIMENTAL

Materials and methods

Ultrafiltration of reconstituted skimmed milk was performed using the microfiltration/ /ultrafiltration set-up described in details elsewhere.[6] The transmembrane pressure (*TMP*) was measured by digital pressure gauges (0–10 bar accuracy ±1 %, Cerebar M, Endress+Hauser, Germany) and the flow rate was measured using a rotameter. All experiments were realised at 50±0.5 °C. Ultrafiltration was operated completely recycling both streams, permeate and retentate, maintaining the concentration of the feed at a constant value. Each experiment took 90 min to assure the achievement of a steady-state flux. The permeate was gathered in a beaker placed on a digital balance. The mass of permeate with time was measured while the data were transferred to a PC unit and used for the calculation of the flux.

A single-channel ceramic membrane with a zirconium filtering layer on an α-alumina support was used for the ultrafiltration. The dimensions of the membrane were as follows: an average pore size of 50 nm, length of 250 mm and *OD*/*ID* 10 mm/6.8 mm (GEA, Germany). The active filtering area of a membrane was 46.2 cm^2.

Custom-made stainless-steel twisted tapes (Inox Bravarija, Bački Petrovac, Serbia) were used as turbulence promoters. An illustration of a membrane module with a twisted tape and the streamlines of fluid flow is shown in Fig. 1. The characteristics of the twisted tapes are given in Table I. For comparing various geometries and dimensions of turbulence promoters, the aspect ratio (*AR*) has usually been used. The *AR* is the ratio of the pitch length (L_e), to its diameter (D_{TP}).

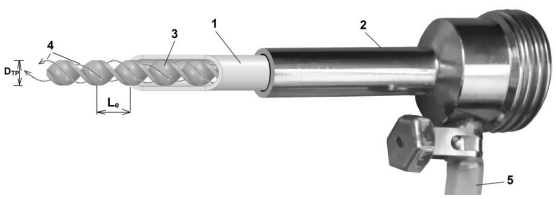

Fig. 1. An illustration of the membrane module with a twisted tape: 1 – membrane module, 2 – housing, 3 – twisted tape, 4 – streamlines in the retentate flow field and 5 – permeate.

TABLE I. Characteristics of the twisted tapes

Annotation	D_{TP} / mm	L_{TP} / mm	δ_{TP} / mm	L_e / mm	N_{twists}	*AR*
TT1.0	6.5	241	1.2	6.5	37	1.0
TT2.5	6.5	238	1.2	16.2	15	2.5
TT4.0	6.5	250	1.2	26	9.6	4.0

Reconstituted skimmed milk was used as the feed. The composition of the skimmed milk powder (Subotica Dairy Industry, Serbia) according to the manufacturer was as follows in mass %: proteins 33.55, fat 1.1, lactose 52.7, ash 7.8 and moisture 4.85. A batch of seven kilograms of milk was prepared a day before the filtration experiment by mixing the skimmed milk, anti-microbial agent (NaN_3 0.2 g L^{-1}), and deionised water. Firstly, a given mass of the skimmed milk was reconstituted to obtain 1 kg of the concentrated emulsion by stirring on a magnetic stirrer at 500 rpm for 10 min. Then it was mixed with the rest amount of water using an overhead stirrer at 1000 rpm for 15 min. The reconstituted milk was stored overnight in a refrigerator at 2–4 °C. Before the experiment, the reconstituted milk was heated to 50 °C. The pH of the feed was measured before and after each filtration experiment and it was stable at a value of 6.8±0.1. After each ultrafiltration experiment, the set-up unit was thoroughly cleaned and rinsed. The acid-based cleaning-in-place procedure was performed according to the membrane manufacturer recommendation. The membrane was considered as clean if 95 % of the new membrane water flux was restored.

Calculations

Response surface methodology (RSM) is a statistical method that allows a multifactorial analysis of data.[16] Using this approach, it is possible to identify the order of the effects of factors on the responses, and whether there are mutual effects of the factors. The experimental data are usually fitted with a second-order polynomial equation. The effects of the factors on the responses are analysed by subjecting the coefficients in the model equation to significance testing using an analysis of variance method (ANOVA). The level of confidence was set at 95 % (two-sided) and the probability expressed as a *p*-value at the significance level of 0.05. Box–Behnken experimental design (BBD) with four factors on three levels, –1, 0 and 1, was chosen (Table II). The concentration of milk proteins (*c*), cross-flow rate (*CFR*), transmembrane pressure (*TMP*) and aspect ratio (*AR*) of the twisted tape (TT) were chosen as the factors. The flux improvement, *FI,* and specific energy consumption, *E*, were chosen as responses. The flux improvement is the most important from the productivity perspective for membrane processes. The specific energy consumption is important from an economic point of view. The BB runs and the obtained responses are presented in Table S-I of the Supplementary material to this paper. The same experimental plan was used to obtain fluxes without twisted tape to calculate the flux improvement, %:

$$FI = 100\frac{J_{TT} - J_{NTP}}{J_{TT}} \quad (1)$$

where J_{TT} is the steady-state flux with a twisted tape, L m^{-2} h^{-1}, and J_{NTP} is the steady-state flux without the twisted tape, L m^{-2} h^{-1}.

For fitting experimental data, a second-order polynomial model equation was employed:

$$Y = b_0 + \sum_{i=1}^{k} b_i X_i + \sum_{i=1}^{k} b_{ii} X_i^2 + \sum_{1 \le i \le j}^{k} b_{ij} X_i X_j \quad (2)$$

where Y is the process response, X_i are the independent variables and b polynomial coefficients: b_0 the intercept, b_i the linear, b_{ii} the quadratic and b_{ij} the mutual effect of the independent variables.

TABLE II. Levels of factors and characteristics of the Box–Behnken design

No.	Factors	Low (–1)	Centre (0)	High (1)	Box–Behnken design	
1	c / %	2.0	2.5	3.0	Total runs	27
2	*CFR*, L min^{-1}	1.0	2.0	3.0	Centre points	3
3	*AR*	1.0	2.5	4.0	–	–
4	*TMP*, kPa	50	100	150	–	–

The specific energy consumption in kW h m^{-3} is suitable for comparing the energy consumption in the empty module and the module with an inserted twisted tape and can be calculated from[4]:

$$E=\frac{CFR\,\Delta P}{V_\mathrm{p}} \tag{3}$$

where *CFR* is the cross-flow rate, m^3 s^{-1}, ΔP is the pressure loss, Pa, and V_p is the volumetric flow of a permeate, m^3 s^{-1}.

Software Statistica 13 was used for the calculations. The least square method was chosen as the calculation method that should enable residual error near zero. The results of the ANOVA method were used for the sensitivity analysis of the responses to the variables.

RESULTS AND DISCUSSION

The time dependency of flux obtained during ultrafiltration with and without twisted tapes had the shape typically indicating the occurrence of concentration polarization with stable steady-state fluxes after an initial period of fouling (Fig. S-1 of the Supplementary material). The internal fouling of pores is more pronounced in ultrafiltration than in microfiltration of milk and thus, it has an influence on the decrease in the flux particularly when high TMPs are imposed. Yet, in this study, besides concentration polarization, the internal fouling was controlled due to the improved hydrodynamics by using a twisted tape. Therefore, the obtained steady-state fluxes are considerably higher than in conventional operation. Since the effects of cross-flow rate and twisted tapes on hydrodynamics are similar, statistical analysis has to be performed to confirm which variable is more effective.

The second-order polynomial equation in RSM was used for modelling the experimental data a presented in Table S-I of the Supplementary material. The equations obtained for the flux improvement and specific energy consumption are given in the Supplementary material (Eqs. (S-1) and (S-2), respectively). To validate the hypothesis that H_0: $b_i = b_{ii} = b_{ij} \cdots b_k = 0$, H_1: $b_i \neq 0$, the ANOVA test of the analysis of variance was performed. The model is proved to fit the experimental data when the regression coefficient is significant, and a lack of fit is non-significant within the confidence interval.

The results of the analysis of variance (ANOVA) and the lack-of-fit test for the flux improvement and specific energy consumption are given in Tables III and IV, respectively. The lack-of-fit test for both responses confirms that the null hypotheses could be rejected as the *p*-values are 0.74 and 0.81 (>0.05) for the flux improvement and specific energy consumption, respectively. The proposed model fits the experimental data very well over the entire experimental range. For the flux improvement, the coefficient of determination (R^2) and the adjusted coefficient of determination (R^2_{adj}) are 0.969 and 0.940, respectively. This means that less than 6 % of the variation in the flux improvement could not be explained by the model. For the specific energy consumption, the coefficient of determination (R^2) and the adjusted coefficient of determination (R^2_{adj}) are 0.996 and 0.992, respectively. Further, given that the *F*-value is 13.46 and 243.1 ($>F_{crit(\alpha/2,14,12)}$ = = 2.51), for the flux improvement and specific energy consumption, respectively, with *p*-value < 0.00001 confirms the consistency and robustness of both models.

TABLE III. Results of ANOVA analysis for flux improvement

Factor	Sum of squares	Degrees of freedom	Mean square	*F*-Ratio	*p*-Value
Model	59760.83	12	4268.63	13.46	0.0000[a]
c	3605.33	1	3605.33	11.36	0.0055[a]
c^2	31.15	1	31.15	0.098	0.7594
CFR	40.33	1	40.33	0.127	0.7276
CFR^2	1526.26	1	1526.26	4.811	0.0487[a]
AR	50052.08	1	50052.08	157.8	0.0000[a]
AR^2	28.01	1	28.01	0.088	0.7714
TMP	690.08	1	690.08	2.175	0.1659
TMP^2	158.90	1	158.90	0.500	0.4926
c×*CFR*	210.25	1	210.25	0.663	0.4314
c×*AR*	2.25	1	2.25	0.007	0.9343
c×*TMP*	961.00	1	961.00	3.029	0.1073
CFR×*AR*	30.25	1	30.25	0.095	0.7628
CFR×*TMP*	9.00	1	9.00	0.028	0.8690
AR×*TMP*	1892.25	1	1892.25	5.965	0.0310[a]
Error	3806.58	12	317.22	–	–
Total SS	63567.41	26	–	–	–
Lack-of-fit	2905.92	10	290.59	0.645	0.7407
Pure error	900.7	2	450.35	–	–

[a]Significant if *p*-value < 0.05

The response surfaces of flux improvement are shown in Fig. 2 for pairs of the aspect ratio of TT (*AR*) with the each of operating conditions: *CFR* (a), the concentration of proteins (b) and *TMP* (c). The effects of *AR* and *CFR* on the flux are shown in Fig. 2a for a concentration of proteins of 2.5 mass % and a TMP of 100 kPa (central point). It could be observed that flux improvement increases with decreasing *AR*. In the dependency of flux improvement on cross-flow rate, a

small maximum could be observed. It could be noticed that the flux improvement slightly increases with increasing cross-flow rate and then slightly decreases with further increasing in *CFR*. The fluxes are significantly higher when twisted tapes were used compared to the conventional operation. However, under higher *CFR*s, operation without promoters delivers higher fluxes and thus, the flux improvement as a relative value decreases slightly.

TABLE IV. Results of ANOVA analysis for specific energy consumption

Factor	Sum of squares	Degrees of freedom	Mean square	*F*-Ratio	*p*-Value
Model	7.02	12	0.50	243.1	0.0000[a]
c	0.16	1	0.16	79.1	0.0000[a]
c^2	0.003	1	0.003	1.53	0.2398
CFR	6.53	1	6.53	3165.4	0.0000[a]
CFR^2	0.12	1	0.12	59.5	0.0000[a]
AR	0.08	1	0.08	39.17	0.0000[a]
AR^2	0.047	1	0.05	22.93	0.0004[a]
TMP	0.012	1	0.012	6.1	0.0297[a]
TMP^2	0.000	1	0.000	0.000	0.9834
c×*CFR*	0.039	1	0.04	18.9	0.0009[a]
c×*AR*	0.005	1	0.006	2.8	0.1224
c×*TMP*	0.000	1	0.000	0.004	0.9484
CFR×*AR*	0.008	1	0.008	3.924	0.0709
CFR×*TMP*	0.002	1	0.002	1.211	0.2927
AR×*TMP*	0.016	1	0.016	7.569	0.0310[a]
Error	0.025	12	0.002	–	–
Total SS	7.05	26	–	–	–
Lack-of-fit	0.018	10	0.0018	0.51	0.8104
Pure error	0.007	2	0.0035	–	–

[a]Significant if *p*-value < 0.05

The effects of the *AR* and concentration of proteins on the flux improvement are shown in Fig. 2b for a *CFR* of 2.0 L min^{-1} and a *TMP* of 100 kPa (central point). The flux improvement increases with increasing the concentration of proteins for all the tested aspect ratios. Since the fouling is severe when the concentration of proteins is high, operation without promoters is very ineffective and so the flux improvement as a relative value increases with increasing concentration of proteins.

The effects of *AR* and *TMP* on the flux improvement are shown in Fig. 2c for a concentration of proteins of 2.5 mass % and a *CFR* of 2.0 L min^{-1} (central point). The influence of *TMP* decreases with decreasing aspect ratio. The flux improvement increases with an increase in *TMP* for the twisted tape of the aspect ratio 4.0. Yet, the influence of *TMP* can be neglected for the twisted tape of aspect ratio 1.0. Generally, the flux should increase with increasing *TMP* as the driving force but that could cause a build-up of fouling matters in the pores.

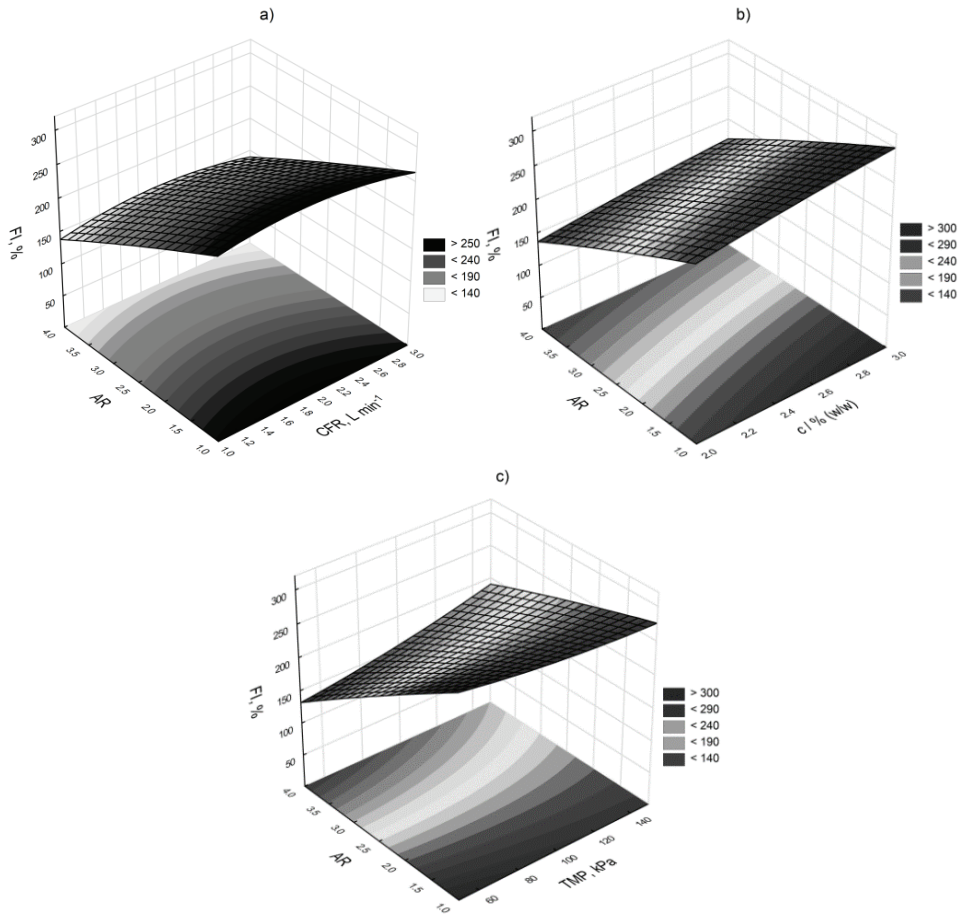

Fig. 2. Response surfaces for the flux improvement for pairs of the aspect ratio of TT with each of operating conditions: a) cross-flow rate, b) the concentration of proteins and c) *TMP*.

However, this also depends on imposed CFR. As the cross-flow velocity is higher for the twisted tape of *AR* 1.0 and both concentration polarization and in-pore fouling are minimized, the influence of *TMP* is shifted to higher values, beyond 150 kPa. The insertion of a twisted tape in the membrane module causes an acceleration of the fluid and changes in the flow field such as the, alternation of streamlines from straight to helical.[6,17] The acceleration of the fluid causes an increase in shear stress. An increase in the shear stress alleviates the detachment of the fouling matter from the membrane surface and its removal back to the bulk of the feed. In this way, the fouling boundary layer is disrupted and fouling is controlled by shear stress at the membrane surface. In microfiltration, fouling is predominantly controlled by shear stress but the *TMP* has no significant influence.[6]

The efficiency of a twisted tape is proven by the remarkably high flux improvements obtained under low *TMP*s. For instance, the flux improvement can reach 300 % for a concentration of proteins of 3 % under a *CFR* of 2.0 L min^{-1}, a *TMP* of 100 kPa and the smallest *AR* of 1.0 (Fig. 2b). However, it should be noted that for other concentrations of proteins, there is a combination of *CFR*, *TMP* and *AR* that can deliver very high flux improvements even beyond 300 %. Still, the flux improvement as the response has to be analysed alongside the specific energy consumption in decision making concerning the operating conditions that should be imposed.

The significance of effects for flux improvement was determined by analysing the ANOVA results presented in Table III. All factors with a *p*-value below 0.05 are statistically significant. Here, for flux improvement, the linear effects of concentration and *AR*, the squared effect of *CFR* and the mutual effect of *AR* and *TMP* are significant. The sensitivity of the response to the significant factors can be explained from a Pareto chart of the standardized effects presented in Fig. S-2 of the Supplementary material. The absolute values of the standardized effects are presented in descending order from the largest to the smallest one. Flux improvement is most sensitive to a linear variation in *AR* and the concentration, followed by the mutual effect of *AR* and *TMP*, and the quadratic effect of the *CFR*. The standardized effect of *AR* has a negative value –12.56 because the flux improvement decreases with increasing *AR*. The standardized effect of concentration is less influential than that of *AR* and has a positive value of 3.37, meaning that the flux improvement increases with increasing concentration of proteins. This confirms that the application of twisted tapes is more effective when the concentration of proteins is high. The standardized mutual effect of *AR* and *TMP* has a positive value of 2.44. Although the value is small, it shows that a simultaneous change in *TMP* and *AR* affects the flux improvement. In addition, the standardized quadratic effect of *CFR* is positive because the flux improvement increases with increasing *CFR*. However, its value of 2.19 indicates the low sensitivity of flux improvement. Based on the absolute values of standardized effects, the flux improvement is the most sensitive to the AR of turbulence promoter.

The response surfaces of specific energy consumption for the pairs of the *AR* of TT with each of the operating conditions are shown in Fig. 3, *CFR* (a), the concentration of proteins (b) and *TMP* (c). Fig. 3a shows the effects of *AR* and *CFR* on the specific energy consumption for a concentration of proteins of 2.5 mass % and a *TMP* of 100 kPa (central point). The specific energy consumption increases sharply with increasing cross-flow rate for all aspect ratios. A minor influence of *AR* on increasing specific energy consumption could be observed under higher *CFR* values.

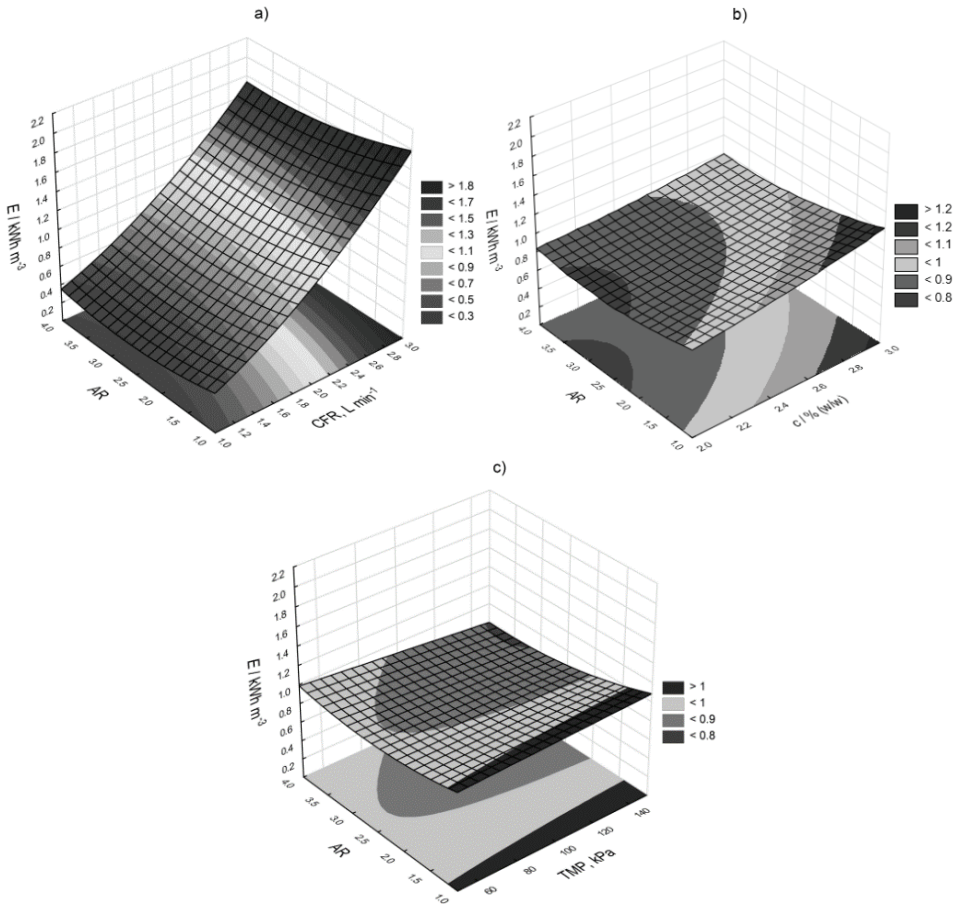

Fig. 3. Response surfaces for the specific energy consumption for pairs of the aspect ratio of TT with the operating conditions: a) cross-flow rate, b) the concentration of proteins and c) *TMP*.

The effects of *AR* and concentration of proteins on the specific energy consumption are shown in Fig. 3b for a *CFR* of 2.0 L min^{-1} and a *TMP* of 100 kPa (central point). The specific energy consumption increases slightly with increasing concentration of proteins for all tested *AR*s. This is because with a higher concentration of proteins, the membrane is more fouled and consequently the flux is lower.

The effects of *AR* and *TMP* on the specific energy consumption are shown in Fig. 3c for a concentration of proteins of 2.5 mass % and a *CFR* 2.0 L min^{-1} (central point). A significant influence of *TMP* on the specific energy consumption could not be observed. Only a slight decrease in the specific energy con-

sumption could be noticed with increasing *TMP* when the *AR* of twisted tape was 4.0. This is due to low pressure loss in the case of this aspect ratio.

The significance of effects for the specific energy consumption was determined by analysing the ANOVA results presented in Table IV. For the specific energy consumption, the linear effects of concentration, cross-flow rate, aspect ratio and *TMP*, squared effects of cross-flow rate and aspect ratio, and the mutual effects of concentration and cross-flow rate, and aspect ratio and *TMP* are significant. The sensitivity of the response to the significant effects could be analysed from the Pareto chart of the standardized effects presented in Fig. S-3 of the Supplementary material. The specific energy consumption is the most sensitive to the linear variation in *CFR* and concentration, followed by the quadratic variation in *CFR*, the linear and the quadratic variation in *AR*, and the mutual variation in *AR* and *TMP*. The linear effect of *CFR* has a positive value of 56.26, indicating that the specific energy consumption increases the most with increasing *CFR*. The standardized effect of concentration is less influential and has a positive value of 8.89, meaning that it is significantly less influential. The linear and the quadratic effect of *AR* are negative with values of –7.71 and –6.26, respectively, showing that the energy consumption decreases with increasing *AR*. The standardized effect of the mutual effect of concentration and *CFR* is positive (4.35), meaning that a simultaneous change in both factors increases the specific energy consumption. Given that twisted tapes cause pressure loss in a membrane module, it could be suggested the aspect ratio as the most significant effect for specific energy consumption. However, this analysis shows that the specific energy consumption is extremely more sensitive to the linear effect of *CFR* than to that of *AR*.

The consumption of specific energy can be low (below 1.0 kWh m^{-3}) in the enhanced ultrafiltration of proteins if the operating conditions are chosen appropriately. This applies especially to the choice of *CFR* as one of the most influential effects.

The analysis showed that energy consumption is not significantly sensitive to *AR* despite the pressure loss caused by the twisted tape. On the other hand, the flux improvement is highly sensitive to *AR*. Furthermore, the twisted tape of the smallest aspect ratio of 1.0 is proven to be the most efficient and suitable for the application. However, the efficiency of the process also depends on the concentration of proteins. In practice, concentrations above 3 mass % of proteins are expected and higher energy consumption should be expected due to operation under higher *CFR*. For conventional operation without a promoter, the specific energy consumption can reach 10 kWh m^{-3}. In the dairy industry, long membrane modules are used, typically 1.2 m, with a big pressure loss. Generally, the energy consumption is high due to the pressure loss, larger than in a short membrane with a promoter, and due to high *TMP*s applied in the ultrafiltration of

milk. Operation under high *TMP*s can be unbeneficial because the high *TMP*s worsen in-pore fouling. In the present study, however, it was shown that operation under low *TMP*s is possible despite the pressure loss caused by the twisted tape. Moreover, it was proved that the pressure loss and energy consumption dominantly depend on the imposed cross-flow rate. In commercial ultrafiltration of milk, high cross-flow velocities (4–10 m s^{-1}) and *TMP*s (300–700 kPa) are imposed to obtain fluxes ranging up to 50 L m^{-2} h^{-1},[18] and thus energy consumption is very high. Here, it should be noted that the fluxes could be slightly higher depending on the milk content and pre-treatment. When milk is skimmed and thermally treated, the milk proteins become partially denatured and they are more prone to fouling of the membrane. An increase in certain operating conditions, such as the concentration of proteins and transmembrane pressure, can exacerbate fouling in the ultrafiltration making it more challenging to mitigate. However, this is not the case with fouling in microfiltration. In previous studies on the microfiltration of partially skimmed milk, very high flux improvements were achieved with twisted tapes ranging from 400 to 600 %.[6] Flux improvements in the ultrafiltration are lower due to the different mechanisms of fouling compared to microfiltration. This is especially the case with the ultrafiltration of skimmed milk with the high content of proteins where in-pore fouling can be predominant under certain operating conditions, such as higher *TMP*s and lower cross-flow rates.

However, this study provides enhanced ultrafiltration of skimmed milk with operating fluxes above 70 L m^{-2} h^{-1} and low specific energy consumption below 1.0 kW h m^{-3}. Moreover, the overall energy consumption is lower due to *TMP* as low as 50 kPa. Generally, this study confirms the feasibility and sustainability of the application of twisted tapes as low-pressure turbulence promoters for the enhancement of ultrafiltration of milk proteins.

CONCLUSIONS

A sensitivity analysis of enhanced ultrafiltration of milk proteins has been presented in this study. For the enhancement of ultrafiltration, twisted tapes as low-pressure loss turbulence promoters were used. The effects of the operating conditions and twisted tape dimensions on flux improvement and specific energy consumption were analysed by application of response surface methodology. The fluxes are remarkably alleviated using twisted tapes due to minimisation of both concentration polarization and in-pore fouling of the membrane. The results of the goodness of fit justified the application of a second-order polynomial model for predicting both the flux improvement and the specific energy consumption. The analysis of variance (ANOVA) test showed that the aspect ratio has a dominant linear effect on flux improvement while the cross-flow rate has a dominant positive linear effect on the specific energy consumption. The linear effect of

concentration and the mutual effect of aspect ratio and *TMP* are significant for both responses. By proper adjustment of the operating conditions, a high flux improvement of 300 % could be attained with specific energy consumption below 1.0 kW h m^{-3} using a twisted tape with an aspect ratio of 1.0 and imposing a low transmembrane pressure.

SUPPLEMENTARY MATERIAL

Additional data are available electronically at the pages of journal website: https://www.shd-pub.org.rs/index.php/JSCS/index, or from the corresponding author on request.

Acknowledgement. This research was financed by The Ministry of Education, Science and Technological Development of the Republic of Serbia, Grant No. 451-03--68/2020-14/ 20013.

ИЗВОД

УНАПРЕЂЕЊЕ УЛТРАФИЛТРАЦИЈЕ ПРОТЕИНА МЛЕКА ПРИМЕНОМ УВИЈЕНИХ ТРАКА: ИСПИТИВАЊЕ ОСЕТЉИВОСТИ ПРИМЕНОМ МЕТОДЕ ОДЗИВНЕ ПОВРШИНЕ

СВЕТЛАНА С. ПОПОВИЋ[1], МИРЕЛА Д. ИЛИЧИЋ[1] и IGOR L. GÁSPÁR[2]

[1]*Технолошки факултет Нови Сад, Универзитет у Новом Саду, Булевар цара Лазара 1, Нови Сад и* [2]*Szent István University, Faculty of Food Science, Food Engineering Department, H-1118. Budapest, Menesi st. 4, Hungary*

У овом раду је презентована анализа утицаја радних услова на ултрафилтрацију протеина млека унапређену применом увијених трака као промотора турбуленције како би се смањило прљање, побољшао флукс и смањила потрошња енергије. Циљ рада је да се испита осетљивост унапређеног процеса на промене радних услова и димензије увијене траке. Увијена трака је уметнута у ултрафилтрациону мембрану (величина пора 50 nm) како би се повећала турбуленција и смањило прљање. Метода одзивне површине примењена је за моделовање и анализу утицаја радних услова и карактеристичне димензије увијене траке. Анализа је показала да карактеристична дименизија увијене траке има доминантан линеаран утицај на повећање флукса. Проток напојне смеше има доминантан линеаран утицај на специфичну потрошњу енергије. Линеаран утицај концентрације и заједнички утицај карактеристичне димензије и трансмембранског притиска су значајни за оба одзива. Погодним подешавањем радних услова, постиже се релативно велико повећање флукса од 300 % при специфичној потрошњи енергије мањој од 1,0 kW h m^{-3} применом увијене траке карактеристичне димензије 1,0 при ниском трансмембранском притиску.

(Примљено 5. јула, ревидирано 29. октобра, прихваћено 18. новембра 2020)

REFERENCES

1. Y. Pouliot, *Int. Dairy J.* **18** (2008) 735 (https://dx.doi.org/10.1016/j.idairyj.2008.03.005)
2. B. Antoine, Q. U. Peng, B. Patrice, G. Geneviève, *Langmuir* **30** (2013) 1 (https://dx.doi.org/https://doi.org/10.1021/la402865p)
3. G. Brans, C. G. P. H. Schroën, R. G. M. Van Der Sman, R. M. Boom, *J. Memb. Sci.* **243** (2004) 263 (https://dx.doi.org/10.1016/j.memsci.2004.06.029)
4. D. M. Krstić, M. N. Tekić, M. Đ. Carić, S. D. Milanović, *J. Memb. Sci.* **208** (2002) 303 (https://dx.doi.org/10.1016/S0376-7388(02)00308-3)

5. S. Popović, D. Jovičević, M. Muhadinović, S. Milanović, M. N. Tekić, *J. Memb. Sci.* **425**–**426** (2013) 113 (https://dx.doi.org/10.1016/j.memsci.2012.09.032)
6. S. Popović, M. Tekić, *J. Memb. Sci.* **384** (2011) 97 (https://dx.doi.org/10.1016/j.memsci.2011.09.016)
7. A. Jokić, Z. Zavargo, Z. Šereš, M. Tekić, *J. Memb. Sci.* **350** (2010) 269 (https://dx.doi.org/10.1016/j.memsci.2009.12.037)
8. B. B. Gupta, J. A. Howell, D. Wu, R. W. Field, *J. Memb. Sci.* **102** (1995) 31 (https://dx.doi.org/10.1016/0376-7388(94)00241-P)
9. N. Hilal, O. O. Ogunbiyi, N. J. Miles, *Sep. Sci. Technol.* **43** (2008) 286 (https://dx.doi.org/10.1080/01496390701787438)
10. D. M. Krstić, W. Höflinger, A. K. Koris, G. N. Vatai, *Sep. Purif. Technol.* **57** (2007) 134 (https://dx.doi.org/10.1016/j.seppur.2007.03.023)
11. S. Popović, M. Karadžić, J. Cakl, *J. Clean. Prod.* **231** (2019) 320 (https://dx.doi.org/10.1016/j.jclepro.2019.05.184)
12. B. Bellhouse, G. Costigan, K. Abhinava, A. Merry, *Sep. Purif. Technol.* **22**–**23** (2001) 89 (https://dx.doi.org/10.1016/S1383-5866(00)00145-3)
13. H. Y. Tsai, A. Huang, J. F. Soesanto, Y. L. Luo, T. Y. Hsu, C. H. Chen, K. J. Hwang, C. D. Ho, K. L. Tung, *J. Memb. Sci.* **573** (2019) 647 (https://dx.doi.org/10.1016/j.memsci.2018.11.081)
14. S. Armbruster, O. Cheong, J. Lölsberg, S. Popovic, S. Yüce, M. Wessling, *J. Memb. Sci.* **554** (2018) 156 (https://dx.doi.org/10.1016/j.memsci.2018.02.015)
15. Ž. R. Lazić, *Design of Experiments in Chemical Engineering*, Wiley-VCH Verlag GmbH & Co. KGaA, Weinheim, 2004
16. M. C. Martí-Calatayud, M. C. Vincent-Vela, S. Álvarez-Blanco, J. Lora-García, E. Bergantiños-Rodríguez, *Chem. Eng. J.* **156** (2010) 337 (https://dx.doi.org/10.1016/j.cej.2009.10.031)
17. Gaspar, P. Tekic, A. Koris, A. Krisztina, S. Popovic, G. Vatai, *Hem. Ind.* **69** (2015) 713 (https://dx.doi.org/10.2298/HEMIND140312001G)
18. M. Leu, A. Marciniak, J. Chamberland, Y. Pouliot, L. Bazinet, A. Doyen, *J. Dairy Sci.* **100** (2017) 7071 (https://dx.doi.org/10.3168/jds.2017-12774).

Journal of the Serbian Chemical Society
JSCS-info@shd.org.rs • www.shd.org.rs/JSCS
J. Serb. Chem. Soc. 85 (12) S572–S574 (2020) *Supplementary material*

SUPPLEMENTARY MATERIAL TO

Enhancement of ultrafiltration of milk proteins by application of twisted tapes: A sensitivity analysis using a response surface methodology

SVETLANA S. POPOVIĆ[1]*, MIRELA D. ILIČIĆ[1] and IGOR L. GÁSPÁR[2]

[1]*Faculty of Technology Novi Sad, University of Novi Sad, Boulevard cara Lazara 1, Novi Sad, Serbia and* [2]*Szent István University, Faculty of Food Science, Food Engineering Department, H-1118. Budapest, Menesi st. 4, Hungary*

J. Serb. Chem. Soc. 85 (12) (2020) 1629–1642

TABLE S-I. Box–Behnken design and responses

Run	*c* mass % (X_1)	*CFR* L min^{-1} (X_2)	*AR* (X_3)	*TMP* kPa (X_4)	J_{NTP*} L m^{-2} h^{-1}	J_{TT} L m^{-2} h^{-1}	*FI* / % (Y_1)	*E* kW h m^{-3} (Y_2)
1	2.0	1.0	2.5	100.0	10.4	31.0	198	0.30
2	3.0	1.0	2.5	100.0	8.2	27.7	238	0.33
3	2.0	3.0	2.5	100.0	30.9	80.3	160	1.58
4	3.0	3.0	2.5	100.0	19.2	63.1	229	2.01
5	2.5	2.0	1.0	50.0	15.1	60.3	299	1.06
6	2.5	2.0	4.0	50.0	15.1	37.0	145	0.99
7	2.5	2.0	1.0	150.0	15.1	59.1	269	1.08
8	2.5	2.0	4.0	150.0	15.1	48.3	202	0.76
9	2.5	2.0	2.5	100.0	15.8	53.2	237	0.84
10	2.0	2.0	2.5	50.0	17.4	55.3	218	0.81
11	3.0	2.0	2.5	50.0	13.9	42.8	208	1.04
12	2.0	2.0	2.5	150.0	18.7	59.4	218	0.75
13	3.0	2.0	2.5	150.0	12.3	45.5	270	0.98
14	2.5	1.0	1.0	100.0	9.1	34.6	280	0.36
15	2.5	3.0	1.0	100.0	23.9	88.4	270	2.00
16	2.5	1.0	4.0	100.0	9.1	21.6	137	0.32
17	2.5	3.0	4.0	100.0	23.9	57.0	138	1.78
18	2.5	2.0	2.5	100.0	15.8	47.1	198	0.95
19	2.0	2.0	1.0	100.0	18.8	68.8	266	0.93
20	3.0	2.0	1.0	100.0	13.0	51.5	296	1.24
21	2.0	2.0	4.0	100.0	18.8	42.9	128	0.85
22	3.0	2.0	4.0	100.0	13.0	33.2	155	1.01
23	2.5	1.0	2.5	50.0	9.5	27.9	194	0.33

* Corresponding author. E-mail: svetlana.popovic@uns.ac.rs

24	2.5	3.0	2.5	50.0	22.7	71.3	214	1.78
25	2.5	1.0	2.5	150.0	8.8	26.2	198	0.35
26	2.5	3.0	2.5	150.0	23.8	74.5	212	1.70
27	2.5	2.0	2.5	100.0	15.8	52.4	232	0.85

* NTP without promoter

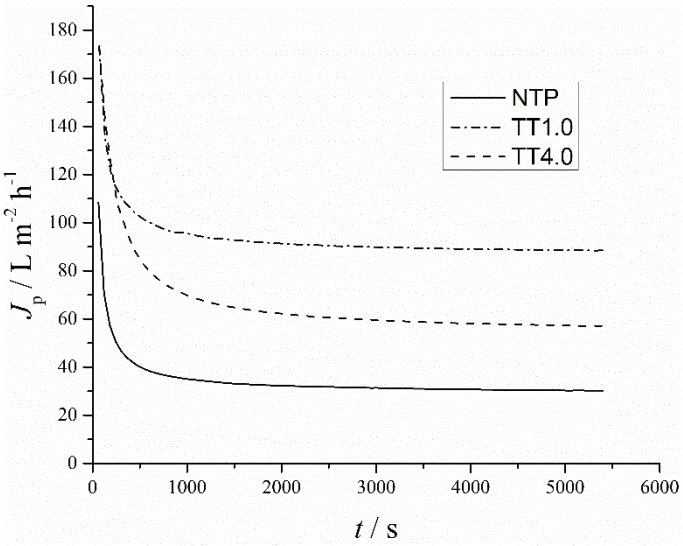

Fig. S-1. Flux dependency in time for the operation without promoter, NTP, and with twisted tapes of two aspect ratios, 1.0 and 4.0; 2.5 mass % concentration of proteins, cross-flow rate of 3 L min^{-1} and transmembrane pressure of 100 kPa.

MATHEMATICAL MODELS USED FOR FITTING THE EXPERIMENTAL DATA:

$$FI = 416.1 - 5.5\,c + 28\,CFR - 68.1\,AR - 2.5\,TMP - 9.37\,c^2 - 16.9\,CFR^2 - \\ - AR^2 - 0.002\,TMP^2 - 14.5c\,CFR - c\,AR + 0.62c\,TMP + 1.83\,CFR\,AR - \\ - 0.03\,CFR\,TMP - 0.29\,AR\,TMP - 0.03\,CFR\,TMP - 0.29\,AR\,TMP \quad \text{(S-1)}$$

$$E = 0.695 - 0.52c - 0.24\,CFR - 0.05\,AR - 0.003\,TMP - 0.15\,c^2 + \\ + 0.15\,CFR^2 + 0.042\,AR^2 + 0.2\,c \cdot CFR - 0.05\,c\,AR - 0.00006\,c\,TMP - \\ - 0.03\,CFR\,AR - 0.0005\,CFR\,TMP + 0.0008\,AR\,TMP \quad \text{(S-2)}$$

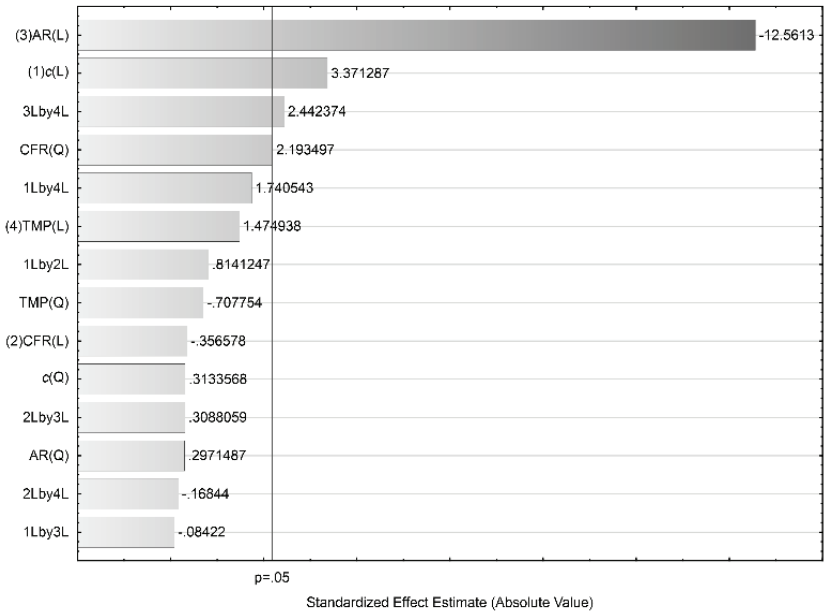

Fig. S-2. Pareto chart of standardized effects for flux improvement ((L) –linear; (Q) – quadratic).

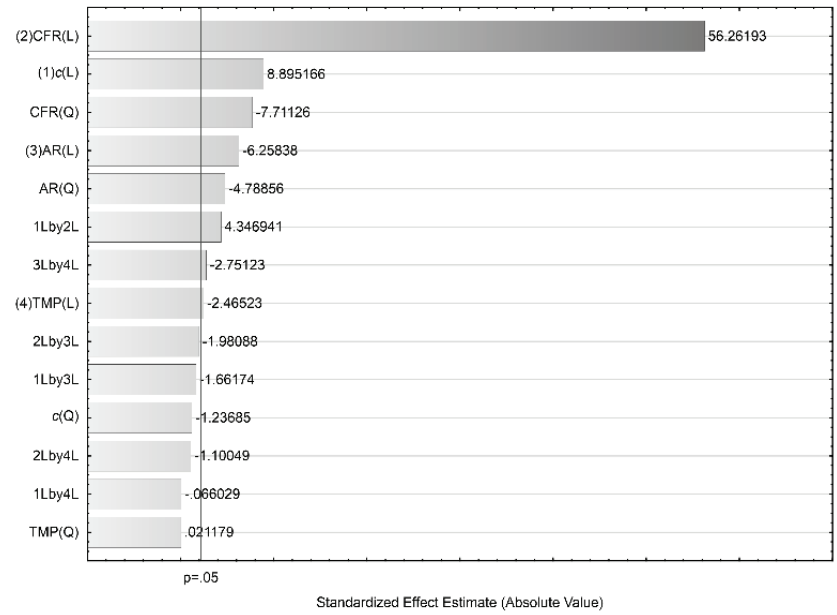

Fig. S-3. Pareto chart of standardized effects for specific energy consumption ((L) –linear; (Q) – quadratic).

Journal of the Serbian Chemical Society
JSCS-info@shd.org.rs • www.shd.org.rs/JSCS
J. Serb. Chem. Soc. 85 (12) 1643–1655 (2020)
JSCS–5399
UDC 547.914+546.33'131:544.77.052.21:628.316.12
Original scientific paper

The purification of natural coagulant extracted from common bean on IRA 958 Cl anion exchange resin

JELENA M. PRODANOVIĆ*, MARINA B. ŠĆIBAN#, DRAGANA V. KUKIĆ, VESNA M. VASIĆ, NEVENA T. BLAGOJEV and MIRJANA G. ANTOV#

Faculty of Technology Novi Sad, University of Novi Sad, Blvd. Cara Lazara 1, 21000 Novi Sad, Serbia

(Received 11 March, revised 24 May, accepted 26 May 2020)

Abstract: Natural coagulants are of organic nature and can increase the organic load of treated water and thus, they require purification in order to remove compounds that do not have coagulation activity. In this work, natural coagulant was extracted from 50 g L^{-1} of ground common bean with 0.5 mol L^{-1} NaCl. Proteins from this crude extract were precipitated by addition of ammonium sulphate. After the precipitation, separation and resolution of proteins, further purification was performed using the anion-exchange resin Amberlite IRA 958 Cl in a batch process. Partially purified coagulant eluted with 2 mol L^{-1} NaCl solution achieved the highest coagulation activity of 53.3 % at a dose of 1 mL L^{-1} although it contained the lowest amount of proteins, but a slightly lower coagulation activity of 49.8 % was achieved at more than 5 times lower dosage of the same fraction. The organic load in treated water when the purified fraction was applied as coagulant was almost 4 times lower than in case of the crude extract as coagulant.

Keywords: proteins; coagulation activity; water clarification; organic load.

INTRODUCTION

In the era of evident and fast environmental degradation, the usage of green and sustainable technologies are in line with global efforts for nature and life preservation and water quality protection, which is one of the environmental aspects concerning not only scientists and environmentalists but all humans. The usage of natural coagulants extracted from different sources, such as plants, animals and microorganisms, in water and wastewater treatment, though not a completely new idea, is a promising technique considering environmental and health protection.

* Corresponding author. E-mail: jejap@uns.ac.rs
# Serbian Chemical Society member.
https://doi.org/10.2298/JSC200311031P

Application of natural coagulants dates back centuries, but it was limited to household water treatment mainly in developing countries. In the past few decades, they have attracted the attention of researchers around the world due to their advantages over conventional coagulants and flocculants (*i.e.* salts of alum and iron). Since the 60's of the last century, many studies that drew attention to the potential harmful health influence (Alzheimer's and Parkinson's diseases, carcinogenic and neurotoxic effects) of residues of alum and synthetic organic flocculants in treated water were published.[1–2] Additionally, epidemiological and clinical investigations showed that an increased content of iron in the body is linked with increased risk of cancer, vascular diseases and neurological disorders.[3,4] Beside the potential adverse health effects, the remaining alum and iron sludges are hazardous to the environment and so cannot be disposed of into the surroundings while, on the other hand, high concentrations of metals complicate their further biological treatment. In addition, the alum sludges are acidic, gelatinous, and difficult to dewater and to dispose of in the environment, and the lowering of pH of treated water and increase in conductivity are additional disadvantages of alum coagulants.[5] Natural coagulants do not present a health threat in general. They are obtained from renewable sources and the sludges remaining after their application can be added to feed or fertilizers, or biologically treated.

The main drawback of the application natural coagulants is an increase in organic matter content in treated water. Organic matter can cause colour and an unpleasant odour of water, may lead to increased microbial growth and will react with chlorine or other disinfectants giving toxic and carcinogenic by-products during the disinfection process at the water treatment plant. This problem can be addressed by purification of the coagulant, which can be accomplished by different techniques.[6–9] The importance of purification of natural coagulants is reflected through novel papers dealing with this subject.[10–13]

The most investigated plant in terms of the preparation of natural coagulants is the tropical plant *Moringa oleifera*.[5–7,14–17] During previous research, the potential of common bean, as a widely grown, cheap and easily available source of natural coagulants in the region of the Balkan, as well as Europe, was investigated and its crude seed extract was confirmed as an effective coagulant.[18–22]

The present paper deals with the purification of the crude extract of common bean seed on IRA 958 Cl anion exchange resin the aim of removing compounds that did not possess coagulation activity.

EXPERIMENTAL

Extraction of active component

To obtain the natural coagulant, common bean (*P. vulgaris*) seeds were ground and sieved through 0.4 mm sieve. The smaller fraction, 50 g L^{-1}, was suspended in 0.5 mol L^{-1} NaCl. The suspension was stirred 10 min using a magnetic stirrer in order to extract the active

coagulant, and then filtered through filter paper Macherey–Nagel MN 651/120 to obtain a crude extract.

Precipitation of active component

Proteins extracted from common bean seed were further processed by precipitation and dialysis. The crude extract was saturated to 80 % by adding $(NH_4)_2SO_4$ and centrifuged at 3000 rpm for 10 min. The precipitate was dissolved in 0.01 mol L^{-1} phosphate buffer (pH 7) and dialysed overnight at 4 °C against Millipore water in a dialysis bag with a molecular cut-off of 12–14 kDa.

Optimization of resin binding conditions and elution of active component

Prior to further purification of the active component, the kinetics of protein binding to the anion exchange resin (the optimal binding time), the optimal resin/protein solution ratio, the influence of initial protein concentration, buffer ionic strength and pH on the binding efficiency were examined. The optimization of binding conditions was conducted using a dialysed extract, obtained according to the above-explained procedure, in batch ion-exchange experiments with Amberlite^{TM} IRA 958 Cl (Rohm and Haas) as the matrix. Amberlite^{TM} IRA 958 Cl is a macroreticular strong base anion exchange resin having quaternary ammonium functionality in a crosslinked acrylic polymer matrix. Its shipping weight is 720 g L^{-1} and its total exchange capacity is ≥ 0.80 eq L^{-1} (Cl^- form). The choice of the optimal binding conditions was made by measuring the amount of bound protein (q):

$$q = (C_0 - C)/m \quad (1)$$

where q is the amount of bound protein, mg protein mL^{-1} of resin, C_0 is the initial protein concentration in the protein solution, mg mL^{-1}, C is the protein concentration in solution in equilibrium, mg mL^{-1} and m / mL is the amount of the resin added in 1 mL of protein solution. The protein concentrations were measured according to Bradford[23] with bovine serum albumin as the standard.

Another parameter used for selection of optimal binding conditions was the binding efficiency (E):

$$E\ /\ \% = 100(C_0 - C)/C_0 \quad (2)$$

After optimization of the binding conditions, the kinetics of elution was examined when the optimal elution time was determined. NaCl (0.5 mol L^{-1}) was mixed with resin at a 1:1 ratio. Samples of 0.1 mL during 60 min were taken and analyzed for their protein content.

Purification of the active component

The binding of the active component was performed in a batch mode at the previously determined optimal binding conditions. The dialysed extract was diluted to achieve a defined initial protein concentration and mixed with Amberlite^{TM} IRA 958 Cl. Thereafter, the residual solution of protein was removed, and resin was washed for 15 min with 0.01 mol L^{-1} phosphate buffer (pH 7) at a resin/buffer ratio 1:1. The flushing buffer was removed. After binding, different concentrations (0.5, 1, 1.5 and 2 mol L^{-1}) of NaCl solution were applied in consecutive order during 20 min for each solution and at a resin/NaCl solution ratio 1:1 to accomplish elution of the active components. Coagulation activity of obtained eluates was examined by jar tests in model water.

Model water

The coagulation activity of partially purified natural coagulant was assessed by the jar test using synthetic turbid water. First, kaolin was ground in a ceramic mortar and sieved

through 0.4 mm sieve. The smaller fraction was used to prepare a 10 g L^{-1} suspension in tap water. The suspension was stirred for 60 min on a magnetic stirrer to achieve uniform dispersion of the kaolin particles, and left for 24 h in order to achieve complete hydration of the kaolin. Model water was prepared just before performing the coagulation tests, by adding this 1 % kaolin suspension to tap water to obtain water with an initial turbidity of 35 NTU (nephelometric turbidity units).

Coagulation test

Coagulation activities were assessed by jar tests in a jar tester VELP FC6S using model water of initial turbidity 35 NTU. The pH value of the model water was adjusted to 9 by addition of 33 % NaOH, in accordance with previous investigations.[18,24] The jar tests were performed by addition of different amounts of eluates to 200 mL of model water. After fast stirring at 200 rpm for 1 min in order to disperse the coagulant, it was continued with slower stirring at 60 rpm for 30 min in order to promote the flocculation of the kaolin particles present in the model water, and then the systems were left for 1 h for sedimentation. As the blank, the same coagulation test was conducted but with no coagulant. After sedimentation for 1 h, the residual turbidity was determined in the upper clarified liquid using a WTW Turb 550/550IR turbidimeter and the coagulation activity was calculated:

$$CA, \% = 100(T_b - T_s)/T_b \quad (3)$$

where T_b and T_s are the turbidity of the blank and the sample, respectively.

Analytical methods

The turbidity was measured using a turbidimeter (WTW TURB 550/550 IR) and it was expressed in nephelometric turbidity units. The permanganate demand was determined in an acid medium according to the Kübel–Tiemann method.[25]

Statistical analysis

All analyses were run in triplicate and the results were expressed as means ± standard deviation (*SD*). Mean values were considered significantly different at $p < 0.05$ confidence level, after performance of the one-way ANOVA statistical analysis followed by Tukey's test.

RESULTS AND DISCUSSION

According to literature data, proteins are compounds from plant material that possess coagulation ability.[6–7,26] Thus, the coagulation active components in the current study were precipitated by ammonium sulphate, dialysed, and dialysed extract was used for further purification.

Optimization of the binding conditions

As the first step of binding optimization, the kinetics of proteins binding to the anion exchange resin was studied at room temperature. The dialysed extract was diluted with 0.01 mol L^{-1} phosphate buffer (pH 7) to achieve an initial protein concentration of 0.401 and 0.239 mg mL^{-1}. The resin was equilibrated with 0.01 mol L^{-1} phosphate buffer (pH 7) for 15 min. The diluted dialysed solutions were added to the resin at a resin/solution ratio of 1:1 and the mixtures were stirred at 100 rpm. Samples (0.1 mL) of the solution were collected in certain inter-

vals for 120 min and analyzed for their protein content. The amounts of bound protein (q) were calculated and results are presented in Fig. 1.

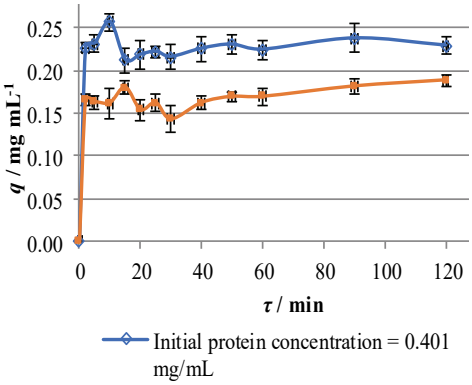

Fig. 1. Adsorption kinetics of the dialysed extract from common bean seed by the anion exchange resin Amberlite^{TM} IRA 958 Cl at 10 mmol L^{-1} phosphate buffer, pH 7.

As could be seen from Fig. 1, the rate of protein adsorption was high at the beginning of the adsorption. The highest binding efficiency was achieved in the first 25 min of the binding process and thereafter, the process became unstable. Hence, 15 min was chosen as the binding time for the following experiments. The results of the performed statistical analysis suggested that there was significant difference in the binding efficiencies in protein solutions of different initial protein concentrations. For a binding time of 15 min, in the protein solution of higher initial protein concentration, a binding efficiency of 52.82 % was attained, while in protein solution of lower initial protein concentration, a higher binding efficiency, 75.12 %, was achieved.

The estimate of the optimum volume of resin required for adsorption and purification of protein extracted from common bean was based on the experiments conducted with constant amount of resin but varying the volumes of dialysed extract. The dialysed extract was diluted with 0.01 mol L^{-1} phosphate buffer (pH 7) to obtain a protein solution with initial protein concentration of 0.260 mg mL^{-1}. It was afterwards mixed with resin for 15 min at 100 rpm and after that analyzed for protein content. Based on obtained data, binding efficiencies were calculated. The results of these experiments are shown in Fig. 2.

The results revealed that increasing the volume of the protein solution led to a decrease in the percentage of adsorbed protein, and a resin/protein solution ratio of 1:0.5 gave the highest binding efficiency, when 88.46 % of protein was adsorbed. This ratio was applied in the succeeding experiments.

The effect of initial protein concentration in the protein solution on the binding efficiency and the amount of bound protein was also investigated. The dialysed extract was diluted with 0.01 mol L^{-1} phosphate buffer (pH 7) to obtain protein solutions with different initial protein concentrations. These solutions were

mixed with matrix for 15 minutes at 100 rpm and matrix/solution ratio 1:0.5. After separation, protein content in liquid phase was measured and the binding efficiency and amount of bound protein were calculated. The obtained results are shown in Fig. 3.

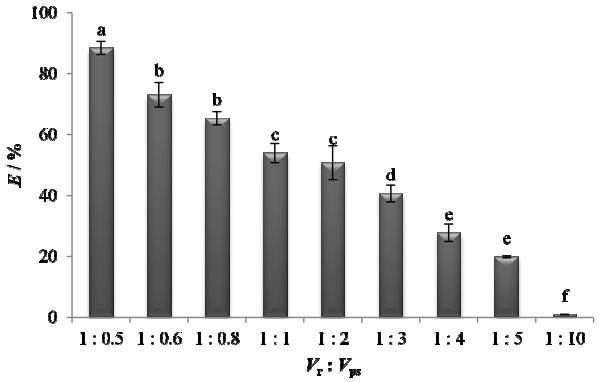

Fig. 2. The influence of resin/protein solution ratio (V_r:V_{ps}) on the binding of proteins on the anion exchange resin Amberlite^{TM} IRA 958 Cl at 10 mmol L^{-1} phosphate buffer, pH 7; the different letters indicate significant differences between the samples ($p < 0.05$).

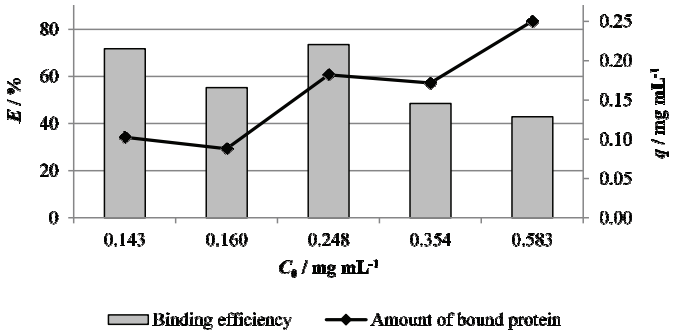

Fig. 3. The effect of initial protein concentration on binding efficiency and amount of bound proteins on the Amberlite^{TM} IRA 958 Cl anion exchange resin at 10 mmol L^{-1} phosphate buffer, pH 7.

According to results presented in Fig. 3, the highest binding efficiency was attained when initial protein concentration was 0.248 mg mL^{-1}. At higher initial protein concentrations, the amount of bound protein increased and achieved the highest value at an initial protein concentration of 0.583 mg mL^{-1}. However, the binding efficiency was significantly lower at higher initial protein concentrations, *i.e.*, more unbound proteins remained in solution.

The effect of ionic strength of the buffer on the adsorption was investigated by measuring the binding efficiency of proteins to the matrix in phosphate buffer within the concentration range 10–100 mmol L^{-1} at pH 7. The initial protein con-

centration in solution was adjusted to 0.260 mg mL^{-1}. The obtained protein solutions were mixed with the matrix for 15 min at 100 rpm and a matrix/protein solution ratio of 1:0.5. The results are presented at Fig. 4. An increase in the ionic strength of the buffer from 0.01 to 0.05 mol L^{-1} did not significantly affect the adsorption of proteins. However, at buffer ionic strength 0.1 mol L^{-1}, the amount of adsorbed protein decreased. This could be explained by the competition for adsorption sites at the matrix between protein ions and buffer ions, which increases when buffer ions are present in higher concentrations.[27] The highest binding efficiency was observed with 0.05 mol L^{-1} buffer, but it was just slightly higher than the one obtained with 0.01 mol L^{-1} buffer, which is economically better. Hence, 0.01 mol L^{-1} phosphate buffer was chosen for further work.

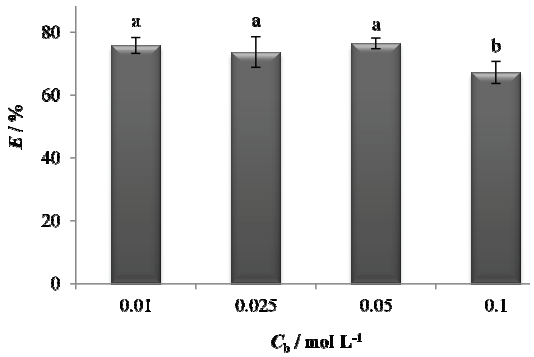

Fig. 4. The effect of phosphate buffer concentration (C_b) on the adsorption of proteins extracted from common bean on the anion exchange resin Amberlite™ IRA 958 Cl at pH 7; different letters indicate significant differences between the samples ($p < 0.05$).

According to previous research (data not shown),[8] the isoelectric point (p*I*) of the dialysed extract obtained from common bean is between pH 4 and 5.5. Thus, the effect of the pH of the buffer on the amount of bound proteins from dialysed extract on the anion exchange resin was studied within the pH range 7––9. In order to find the optimal pH of the buffer for the adsorption, the dialysed extract was diluted in universal McIlvaine buffer having pH from 7 to 9 with an increment pH increase of 0.5. The initial protein concentration was around 0.260 mg mL^{-1}. The matrix and the protein solution were mixed in a ratio 1:0.5 for 15 min at 100 rpm. The results (Fig. 5) revealed that the maximum of protein adsorption was achieved at pH 7 and 7.5. Considering this, further experiments were

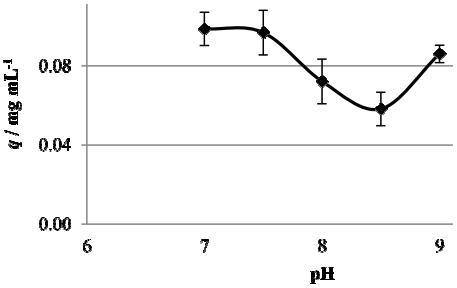

Fig. 5. The effect of the buffer pH on the adsorption of proteins extracted from common bean on the anion exchange resin Amberlite™ IRA 958 Cl.

conducted at pH 7. Statistical analysis showed significant difference between the protein adsorptions at pH 8 and 8.5 in comparison to that achieved at other pH values.

Optimization of the elution

Following optimization of binding conditions and prior to purification of active component, optimization of elution was performed. The dialysed extract was diluted with 10 mmol L^{-1} phosphate buffer (pH 7) to obtain a protein solution with an initial protein concentration of 0.262 mg mL^{-1}. The protein solution was added to Amberlite^{TM} IRA 958 Cl resin, which had previously been equilibrated in 10 mmol L^{-1} phosphate buffer (pH 7). The resin/protein solution ratio was 1:0.5 and the system was mixed for 15 min at 100 rpm. After completion of the adsorption, the remaining protein solution was drained and the matrix was washed with 10 mmol L^{-1} phosphate buffer (pH 7). The elution was performed with 0.5 mol L^{-1} NaCl solution at a 1:1 resin/solution ratio. The kinetics of elution were monitored during 60 min. Solution samples of 0.1 mL were collected in certain time intervals and analysed for their protein content. From the obtained results, presented in Fig. 6, an optimal elution time of 20 min was determined.

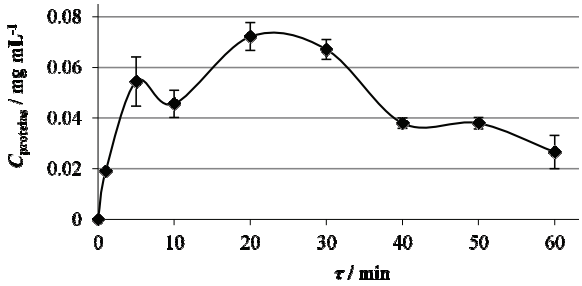

Fig. 6. Kinetics of the elution of proteins from common bean seed on anion exchange resin Amberlite^{TM} IRA 958 Cl with 10 mmol L^{-1} phosphate buffer, pH 7.

According to ANOVA, there were significant ($p < 0.05$ confidence level) differences in protein contents in fractions obtained during the first 40 min of elution of proteins from common bean seed from anion exchange resin Amberlite TM IRA 958 Cl. However, the performed statistical analysis suggested that there were insignificant differences between proteins contents of samples collected after 40 min.

Purification of active component and coagulation study

Dialysed extract was diluted with 10 mmol L^{-1} phosphate buffer (pH 7) to obtain a protein solution with an initial protein concentration of 0.261 mg mL^{-1}. The protein solution was added to Amberlite^{TM} IRA 958 Cl anion exchange resin, which had previously been equilibrated with 10 mmol L^{-1} phosphate buf-

fer (pH 7), and the binding was performed under the previously determined optimal conditions. The amount of adsorbed proteins was 0.230 mg mL^{-1}, *i.e.*, a binding efficiency of 88.35 % was achieved. After washing with 10 mmol L^{-1} phosphate buffer (pH 7) at 100 rpm and resin/buffer ratio of 1:1 during 15 min, elution was performed by step gradient of NaCl during 20 min for each step and at a resin/NaCl solution ratio 1:1. In this way, four fractions were obtained, the protein contents of which were determined (Fig. 7).

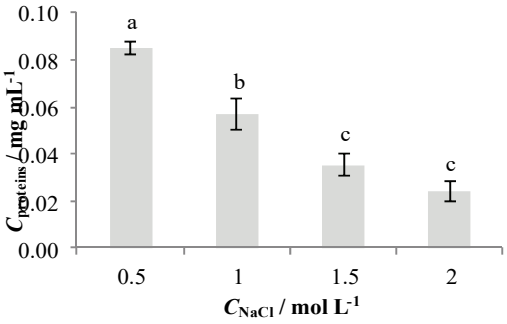

Fig. 7. Protein contents in fractions obtained by elution of bound common bean proteins from the anion exchange resin Amberlite^{TM} IRA 958 Cl in step gradient of NaCl solutions; different letters indicate significant differences between samples ($p < 0.05$).

With increasing concentration of the NaCl solution, the protein content of the fractions decreased. An elution efficiency of 87.37 % was achieved, *i.e.*, 12.63 % of the proteins remained bound to the resin.

In order to determine whether there was a correlation between the concentrations of the proteins in the fractions and their coagulation ability, fractions were examined as coagulants in coagulation tests. The main aim of coagulation/ /flocculation process is turbidity removal and thus, the coagulation activities of the fractions were estimated in synthetic turbid water of initial turbidity 35 NTU at pH 9. The results of the coagulation tests of the fractions in relation to applied coagulant dose are shown in Fig. 8.

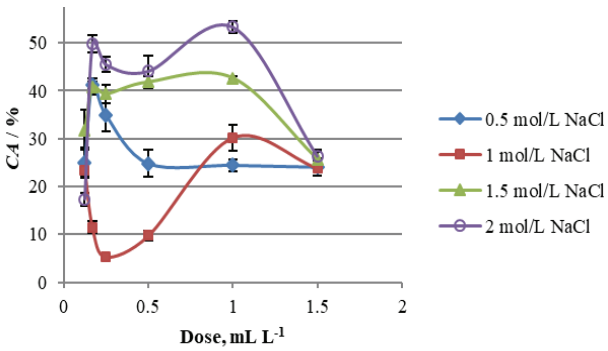

Fig. 8. Coagulation activity of the fractions purified on anion exchange resin Amberlite TM IRA 958 Cl at different doses.

Significant differences in coagulation behaviour of the fractions obtained by elution with different NaCl concentrations were confirmed by ANOVA statistical analysis.

Although it contained the lowest amount of proteins, the fraction obtained by elution with 2 mol L^{-1} NaCl showed the best coagulation ability. The fraction obtained with 1.5 mol L^{-1} NaCl showed similar behaviour to the fraction obtained with 2 mol L^{-1} NaCl, which imposes that they contained proteins of similar characteristics considering coagulation, but with lower coagulation activities. The highest coagulation activity of the fraction obtained with 2 mol L^{-1} NaCl was 53.3 % at an applied dose 1 mL L^{-1}, but only a slightly lower coagulation activity of 49.8 % was achieved at more than 5 times lower dosage (0.17 mL L^{-1}) of this fraction. Thus, it could be considered as optimal one. Calculated based on proteins concentration, the optimal coagulation dose was 0.0041 mg L^{-1}.

In a previous investigation[8] when Amberlite^{TM} IRA 900 Cl was used for purification of coagulant from common bean in the continual mode, the highest coagulation activity of 72.3 % was obtained at dose of purified fraction 0.081 mg L^{-1}. When compared to the results from that study, the optimal dose of the fraction obtained by purification on Amberlite^{TM} IRA 958 Cl was almost 20 times lower than the dose of fraction obtained by purification on Amberlite^{TM} IRA 900 Cl, and when calculated on the basis of proteins that were added in the model water, the coagulation activity obtained with optimal dose in the present research was almost 14 times higher than that of the purified fraction obtained on Amberlite^{TM} IRA 900 Cl.

Baptista *et al.*[10] fractionated protein coagulants from *Moringa oleifera* seed based on their solubility in different extraction systems. According to their results, fraction obtained by extraction with 0.5 mol L^{-1} NaCl that corresponded to globulin (II)[10] showed turbidity removal of about 30 % in surface water the initial turbidity of which was 102.42 NTU. As the authors claimed, the presented removal value was similar to the analysis control (without addition of *Moringa oleifera*), meaning that it was inherent to the decanting process through gravity of particles and not due to an effective action of the coagulant tested. However, fractions obtained by water extraction showed high turbidity removal ranging from 79–89 %. The higher coagulation activities of these fractions compared to those of the fractions obtained in this work could be attributed to the fact that the initial turbidity of the treated water in the paper of Baptista *et al.*[10] was almost 1.5 times greater than that of the model water used in experiments presented in the present paper. Literature data show that natural coagulants achieve higher efficiency of particles removal in more turbid waters[28–31]. Moreover, the applied dosage of the fractions in the paper of Baptista *et al.*[10] was more than three thousand time higher than optimal dosage achieved in the present work.

Organic matter in the water before and after coagulation tests with common bean crude extract and the fraction obtained with 2 mol L^{-1} NaCl at the optimal

doses was assessed to determine the increase in organic load. The results revealed that the crude extract and purified fraction had increased organic matter content in treated water by 68 and 19 %, respectively. This was in accordance with the low protein content in the tested fraction, but it could also be explained by the absence of other organic compounds in purified fraction.

CONCLUSIONS

Evaluation of fractions obtained by purification of common bean seed crude extract on Amberlite^{TM} IRA 958 Cl anion exchange resin for their suitability for model water clarification revealed that they were efficient. The highest coagulation activity of 53.3 % was achieved by the fraction obtained with 2 mol L^{-1} NaCl at a dose of 1 mL L^{-1}. The optimal dose of the fraction obtained by purification on Amberlite^{TM} IRA 958 Cl was almost 20 times lower than the optimal dose of the fraction obtained by purification on Amberlite^{TM} IRA 900 Cl, while its coagulation activity was almost 14 times higher.

Acknowledgements. This work was supported by the Ministry of Education, Science and Technological Development of the Republic of Serbia (Grant No. 451-03-68/2020-14/200134) and Provincial Secretariat for Higher Education and Scientific Research, Province of Vojvodina, Republic of Serbia (Grant No. 142-451-2166/2019-01/02).

ИЗВОД

ПРЕЧИШЋАВАЊЕ ПРИРОДНОГ КОАГУЛАНТА ИЗ СЕМЕНА ПАСУЉА НА АНЈОНСКОМ МЕЊАЧУ ЈОНА IRA 958 CL

ЈЕЛЕНА М. ПРОДАНОВИЋ, МАРИНА Б. ШЋИБАН, ДРАГАНА В. КУКИЋ, ВЕСНА М. ВАСИЋ, НЕВЕНА Т. БЛАГОЈЕВ и МИРЈАНА Г. АНТОВ

Технолошки факултет Нови Сад, Универзитет у Новом Саду, Бул. Цара Лазара 1, 21000 Нови Сад

Природни коагуланти представљају органска једињења и могу повећати садржај органских материја у третираној води, те их је стога потребно пречистити како би се уклониле материје које немају коагулациону способност. У овом раду је природни коагулант екстрахован са 0,5 mol L^{-1} раствором NaCl из 50 g L^{-1} самлевеног семена пасуља. Протеини из сировог екстракта су исталожени додавањем амонијум-сулфата. Након таложења, одвајања талога и поновног растварања протеина, даље пречишћавање је изведено на анјонској јоноизмењивачкој смоли Amberlite IRA 958 Cl у шаржном поступку. Делимично пречишћени коагулант који је добијен елуирањем са 2 mol L^{-1} раствором NaCl је показао највећу коагулациону активност од 53,3 % при дози од 1 mL L^{-1} иако је та фракција садржала најмању концентрацију протеина. Незнатно нижу коагулациону активност од 49,8 % је иста фракција постигла при 5 пута нижој дози. Повећање садржаја органских материја у обрађеној води је било око 4 пута ниже у случају примене ове пречишћене фракције као коагуланта у поређењу са сировим екстрактом.

(Примљено 11. марта, ревидирано 24. маја, прихваћено 26. маја 2020)

REFERENCES

1. S. C. Bondy, *Neurotoxicology* **31** (2010) 575 (https://doi.org/10.1016/j.neuro.2010.05.009)

2. V. Chico Galdo, C. Massart, L. Jin, V. Vanvooren, P. Caillet-Fauquet, G. Andry, P. Lothaire, D. Dequanter, M. Friedman, J. Van Sande, *Mol. Cell. Endocrinol*. **257**–**258** (2006) 6 (https://doi.org/10.1016/j.mce.2006.06.003)
3. D. Berg, M. Gerlach, M. B. H. Youdim, K. L. Double, L. Zecca, P. Riederer, G. Becker, *J. Neurochem*. **79** (2001) 225 (https://doi.org/10.1046/j.1471-4159.2001.00608.x)
4. V. R. M. Chandrasekaran, I. Muthaiya, P.-C. Huang, M.-Y. Liu, *Water Res.* **4** (2010) 5823 (https://doi.org/10.1016/j.watres.2010.06.063)
5. A. Ndabigengesere, K. S. Narasiah, *Water Res*. **32** (1998) 781 (https://doi.org/10.1016/S0043-1354(97)00295-9)
6. K. A. Ghebremichael, K. R. Gunaratna, H. Henriksson, H. Brumer, G. Dalhammar, *Water Res.* **39** (2005) 2338 (https://doi.org/10.1016/j.watres.2005.04.012)
7. K. A. Ghebremichael, K. R. Gunaratna, G. Dalhammar, *Appl. Microbiol. Biotechnol.* **70** (2006) 526 (https://doi.org/10.1007/s00253-005-0130-7)
8. M. G. Antov, M. B. Šćiban, N. J. Petrović, *Bioresour. Technol.* **101** (2010) 2167 (https://doi.org/10.1016/j.biortech.2009.11.020)
9. M. G. Antov, M. B. Šćiban, J. M. Prodanović, *Ecol. Eng*. **49** (2012) 48 (https://doi.org/10.1016/j.ecoleng.2012.08.015)
10. A. T. A. Baptista, M. O. Silva, R. G. Gomes, R. Bergamasco, M. F. Vieira, A. M. S. Vieira, *Sep. Purif. Technol.* **180** (2017) 114 (https://doi.org/10.1016/j.seppur.2017.02.040)
11. S. M. Dezfooli, V. N. Uversky, M. Saleem, F. S. Baharudin, S. M. S. Hitam, R. T. Bachmann, *Process Biochem.* **51** (2016) 1085 (https://doi.org/10.1016/j.procbio.2016.04.021)
12. A. T. A. Baptista, P. F. Coldebella, P. H. F. Cardines, R. G. Gomes, M. F. Vieira, R. Bergamasco, A. M. S. Vieira, *Chem. Eng. J.* **276** (2015) 166 (https://doi.org/10.1016/j.cej.2015.04.045)
13. A. S. Taiwo, K. Adenike, O. Aderonke, *Heliyon* **6** (2020) (https://doi.org/10.1016/j.heliyon.2020.e03335)
14. M. Rosmawanie, R. Mohamed, A. Al-Gheethi, F. Pahazri, M. K. Amir-Hashim, M. Z. Nur-Shaylinda, *J. Environ. Chem. Eng.* **6** (2018) 2417 (https://doi.org/10.1016/j.jece.2018.03.035)
15. F. P. Camacho, V. S. Sousa, R. Bergamasco, M. R. Teixeira, *Chem. Eng. J.* **313** (2017) 226 (https://doi.org/10.1016/j.cej.2016.12.031)
16. E. Vunain, E. F. Masoamphambe, P. M. G. Mpeketula, M. Monjerezi, A. Etale, *J. Environ. Chem. Eng.* **7** (2019) 103118 (https://doi.org/10.1016/j.jece.2019.103118)
17. D. L. Villaseñor-Basulto, P. D. Astudillo-Sánchez, J. del Real-Olvera, E. R. Bandala, *J. Water Process Eng.* **23** (2018) 151 (https://doi.org/10.1016/j.jwpe.2018.03.017)
18. M. Šćiban, M. Klašnja, J. Stojimirović, *Acta Periodica Technol.* **36** (2005) 81 (http://www.doiserbia.nb.rs/img/doi/1450-7188/2005/1450-71880536081S.pdf)
19. M. B. Šćiban, M. A. Vasić, J. M. Prodanović, M. G. Antov, M. T. Klašnja, *Acta Periodica Technol.* **41** (2010) 141 (http://www.doiserbia.nb.rs/img/doi/1450-7188/2010/1450-71881041141S.pdf)
20. J. M. Prodanović, M. B. Šćiban, M. G. Antov, J. M. Dodić, *Romanian Biotechnol. Lett*. **16** (2011) 6638
21. J. M. Prodanović, M. B. Šćiban, M. G. Antov, D. V. Kukić, V. M. Vasić, *Acta Periodica Technol.* **46** (2015) 77 (http://www.doiserbia.nb.rs/img/doi/1450-7188/2015/1450-71881546077P.pdf)

22. V. M. Vasić, J. M. Prodanović, D. V. Kukić, M. B. Šćiban, M. G. Antov, D. Ž. Ivetić, *Desalin. Water Treat*. **51** (2013) 437 (https://doi.org/10.1080/19443994.2012.714525)
23. M. M. Bradford, *Anal. Biochem.* **72** (1976) 248 (https://doi.org/10.1016/0003-2697(76)90527-3)
24. T. Okuda, A. U. Baes, W. Nishijima, M. Okada, *Water Res.* **35** (2001) 405 (https://doi.org/10.1016/S0043-1354(00)00290-6)
25. R. Feliks, S. Škunca-Milovanović, *Voda za piće. Standardne metode za ispitivanje higijenske ispravnosti*, Savezni zavod za zdravstvenu zaštitu & NIP Privredni pregled, Blgrade, 1990, p.p. 134–136 (in Serbian)
26. C.-Y. Yin, *Process Biochem.* **45** (2010) 1437 (https://doi.org/10.1016/j.procbio.2010.05.030)
27. R. Scopes, *Protein Purification*, 3rd ed., Springer, New York, 1994
28. K. Ghebremichael, J. Abaliwano, G. Amy, *J. Water Supply Res. Technol. AQUA* **58** (2009) 267 (https://doi.org/10.2166/aqua.2009.060)
29. T. Nkurunziza, J. B. Nduwayezu, E. N. Banadda, I. Nhapi, *Water Sci. Technol*. **59** (2009) 1551 (https://doi.org/10.2166/wst.2009.155)
30. M. Pritchard, T. Mkandawire, A. Edmondson, J. G. O'Neill, G. Kululanga, *Phys. Chem. Earth* **34** (2009) 799 (https://doi.org/10.1016/j.pce.2009.07.001)
31. M. Pritchard, T. Craven, T. Mkandawire, A. S. Edmondson, J. G. O'Neill, *Phys. Chem. Earth* **35** (2010) 791 (https://doi.org/10.1016/j.pce.2010.07.020).

Journal of the Serbian Chemical Society
JSCS@tmf.bg.ac.rs • www.shd.org.rs/JSCS
J. Serb. Chem. Soc. 85 (12) 1657–1666 (2020)

Contents of Volume 85

NUMBER 1

NUMBER 2

NUMBER 3

NUMBER 4

NUMBER 5

Journal of the Serbian Chemical Society
JSCS-info@shd.org.rs • www.shd.org.rs/JSCS
J. Serb. Chem. Soc. *85* (12) 1667–1673 (2020)

Author Index

Subject Index of Vol. **85** and List of Referees in 2020 are given in the electronic form at the Internet address of the Journal of the Serbian Chemical Society: http://www.shd.org.rs/JSCS

End of Volume 85.

Journal of the Serbian Chemical Society
JSCS-info@shd.org.rs • www.shd.org.rs/JSCS
Volume *85* (2020)

Subject index

Journal of the Serbian Chemical Society
JSCS-info@shd.org.rs • www.shd.org.rs/JSCS
Volume *84* (2020)

2020 List of Referees

Editorial Board of the Journal is grateful to the following referees for reviewing the manuscripts published during 2020:

Mohammad Abid, *Department of Chemical Engineering, University of Technology, P.O. Box 18310, Baghdad, Iraq*
Danica Agbaba, *Department of Pharmaceutical Chemistry, Faculty of Pharmacy, University of Belgrade, Serbia*
Tanweer Ahmad, *College of Natural and Computational Science, Madda Walabu University, Bale-Robe, Ethiopia*
Vladimir Ajdačić, *Faculty of Chemistry, University of Belgrade, Serbia*
Jovana Ajduković, *Faculty of Sciences, University of Novi Sad, Serbia*
Filip Andrić, *Faculty of Chemistry, University of Belgrade, Serbia*
Jasmina Anojčić, *Faculty of Science, University of Novi Sad, Serbia*
Ofélia Anjos, *Instituto Politécnico de Castelo Branco, Castelo Branco, Portugal*
Bratislav Antić, *Institute of Nuclear Sciences Vinča, Belgrade, Serbia*
Mališa Antić, *Faculty of Agriculture, University of Belgrade, Serbia*
Ozgur Arar, *Department of Chemistry, Ege University, İzmir, Turkey*
Jelena Arsenijević, *Faculty of Pharmacy, Department of Pharmacognosy University of Belgrade, Serbia*
Muhammad Arshad, *University of Veterinary and Animal Sciences Lahore, Jhang, Pakistan*
Mahmut Aslani, *Institue of Nuclear Sciences, Nuclear Technology Department, Ege University, Izmir, Turkey*
Darko Ašanin, *Faculty of Science, University of Kragujevac, Serbia*
Jelena Avdalović, *Institute of Chemistry, Technology and Metallurgy, University of Belgrade, Serbia*
Marija Babić, *Innovation Center of the Faculty of Technology and Metallurgy, University of Belgrade, Serbia*
Divna Bajić, *Faculty of Technology and Metallurgy, University of Belgrade, Serbia*
Robert Baker, *School of Chemistry, University of Dublin, Trinity College, Dublin, Ireland*
Vladimir Beškoski, *Faculty of Chemistry, University of Belgrade, Serbia*
Nabil Bouarra, *Center of Scientific and Technical Research in Physicochemical Analyzes (CRAPC), Tipaza, Algeria*
Danica Brzić, *Faculty of Technology and Metallurgy, University of Belgrade, Serbia*
Roxana Bugoi, *Horia Hulubei National Institute for Nuclear Physics and Engineering, Măgurele, Romania*
Xin Che, *Shandong University, P. R. China*
Viviana Consonni, *Department of Earth and Environmental Sciences, Università degli Studi di Milano-Bicocca, Milano, Italy*

Branislav Jović, *Faculty of Sciences, Department of Chemistry, Biochemistry and Environmental Protection, University of Novi Sad, Serbia*
Ivan Juranić, *Faculty of Chemistry, University of Belgrade, Serbia*
Ioannis Konstantinos Karabagias, *Department of Chemistry, University of Ioannina, Greece*
Oxana Kazakova, *Ufa Institute of Chemistry, Russian Academy of Sciences, Ufa, Russian Federation*
Vesna Kilibarda, *Posoning Control Centre, Military Medical Academy, Belgrade, Serbia*
Arun Kodoth, *Mangalore University, Karnataka, India*
Juraj Kóňa, *Slovak Academy of Sciences, Bratislava, Slovak Republic*
Mirjana Kostić, *Faculty of Technology and Metallurgy, University of Belgrade, Serbia*
Tatjana Kop, *Institute of Chemistry, Technology and Metallurgy - Department of Chemistry, University of Belgrade, Serbia*
Matjaž Kristl, *Faculty of Chemistry and Chemical Engineering, University of Maribor, Maribor, Slovenia*
Uroš Lačnjevac, *Institute for Multidisciplinary Research, University of Belgrade, Serbia*
Ping Li, *School of Chemistry and Chemical Engineering, Qufu Normal University, Qufu, China*
Snežana Maletić, *Faculty of Sciences, University of Novi Sad, Serbia*
Dragan Manojlović, *Faculty of Chemistry, University of Belgrade, Serbia*
Sanja Marinović, *Institute of Chemistry, Technology and Metallurgy, University of Belgrade, Serbia*
Smilja Marković, *Institute of Technical Sciences of the Serbian Academy of Sciences and Arts, Belgrade, Serbia*
Zoran Marković, *State University of Novi Pazar, Serbia*
Verka Meško, *International Balkan University, Skopje, North Macedonia*
Nevena Mihailović, *Institute for the Application of Nuclear Energy, University of Belgrade, Serbia*
Jelena Miladinović, *Faculty of Technology and Metallurgy, University of Belgrade, Serbia*
Miloš Milčić, *Faculty of Chemistry, University of Belgrade, Serbia*
Srđan Miletić, *Faculty of Chemistry, University of Belgrade, Serbia*
Dušan Milivojević, *Institute of Molecular Genetics and Genetic Engineering, University of Belgrade, Serbia*
Slobodan Milosavljević, *Faculty of Chemistry, University of Belgrade, Serbia*
Djenana Miodragovic, *Chemistry of Life Processes Institute, Northwestern University, Evanston, IL, USA*
Svetlana Momchilova, *Institute of Organic Chemistry, Centre of Phytochemistry, Bulgarian Academy of Sciences, Sofia, Bulgaria*
Aleksandra Nastasović, *Institute of Chemistry, Tehnology and Metallurgy, University of Belgrade, Serbia*
Olgica Nedić, *Institute for the Application of Nuclear Energy, University of Belgrade, Serbia*
Jovan Nedeljković, *Institute of Nuclear Sciences Vinča, Belgrade, Serbia*
Eva Németh-Zámboriné, *Faculty of Horticultural Science, Szent István University, Budapest, Hungary*
Nikola Nikačević, *Faculty of Technology and Metallurgy, University of Belgrade, Serbia*
Jasmina Nikolić, *Faculty of Technology and Metallurgy, University of Belgrade, Serbia*
Katarina Nikolić, *Faculty of Chemistry, University of Belgrade, Serbia*
Tanja Nikolić, *Academy of Professional Studies South Serbia, Leskovac, Serbia*
Jasmina Novaković, *Apotex Inc, Toronto, Ontario, Canada*
Miroslav Novaković, *Institute of Chemistry, Tehnology and Metallurgy, University of Belgrade, Serbia*

Vladimir Šukalović, *Institute of Chemistry, Technology and Metallurgy - Department of Chemistry, University of Belgrade, Serbia*
Maja Šumar Ristović, *Faculty of Chemistry, University of Belgrade, Serbia*
Gordana Tasić, *Faculty of Pharmacy, University of Belgrade, Serbia*
Vele Tešević, *Faculty of Chemistry, University of Belgrade, Serbia*
Jelena Trifković, -*Faculty of Chemistry, University of Belgrade, Serbia*
Dragica Trivić, *Faculty of Chemistry, University of Belgrade, Serbia*
Milena Trmčić, *Inovation Center of Faculty of Chemistry, University of Belgrade, Serbia*
Aleksandra Tubić, *Faculty of Sciences, University of Novi Sad, Serbia*
Pablo Ulloa, *Instituto de Investigaciones Agropecuarias, Inia, Chile*
Đorđe Veljović, *Faculty of Technology and Metallurgy, University of Belgrade, Serbia*
Monu Verma, *Department of Environmental Engineering, University of Seoul, Seoul, Republic of Korea*
Tanja Vidaković-Koch, *Max Planck Institute for Dynamics of Complex Technical Systems, Magdeburg, Germany*
Željko Vitnik, *Department of Chemistry, Institute of Chemistry, Technology and Metallurgy, University of Belgrade, Serbia*
Sandra Vojnović, *Institute of Molecular Genetics and Genetic Engineering, University of Belgrade, Serbia*
Vesna Vučić, *Institute for Medical Research, University of Belgrade, Serbia*
Ljubodrag Vujisić, *Faculty of Chemistry, University of Belgrade, Serbia*
Radojka Vujasin, *Vinča Institute of Nuclear Sciences, Belgrade, Serbia*
Milica Vujković, *Faculty of Physical Chemistry, University of Belgrade, Serbia*
Malcolm Watson, *Faculty of Sciences, University of Novi Sad, Serbia*
Saeed Yousefinejad, *Shiraz University of Medical Sciences, Iran*
Aleksandra Zarubica, *Department of Chemistry, Faculty of Science and Mathematics, University of Niš, Serbia*
Matija Zlatar, *Institute of Chemistry, Technology and Metallurgy, University of Belgrade, Serbia*
Mario Zlatović, *Faculty of Chemistry, University of Belgrade, Serbia*
Emila Živković, *Faculty of Technology and Metallurgy, University of Belgrade, Serbia*